

**Active Antimicrobial Food Packaging using Biological Potential from  
Malaysian Medicinal Plants**

Raja Nur Asila Binti Raja Mazlan

Submitted in accordance with the requirements for the degree of  
Doctor of Philosophy

The University of Leeds  
School of Food Science and Nutrition

October, 2025

The candidate confirms that the work submitted is her own and that appropriate credit has been given where reference has been made to the work of others.

This copy has been supplied on the understanding that it is copyright material and that no quotation from the thesis may be published without proper acknowledgement

The right of Raja Nur Asila Binti Raja Mazlan to be identified as Author of this work has been asserted by her in accordance with the Copyright, Designs and Patents Act 1988

© 2025 The University of Leeds and Raja Nur Asila Binti Raja Mazlan

## Acknowledgements

Alhamdulillah for making this dream come true!

First and foremost, I would like to express my deepest gratitude to my supervisory committee members, Prof. Lisa Marshall, Dr. Evi Paximada, and Dr. Melvin Holmes. Their unwavering guidance, support, and encouragement over the past four years have been invaluable. Without their mentorship and steadfast belief in my work, this thesis would not have been possible.

I extend my heartfelt appreciation to my husband, Harithah, for being my unwavering pillar of emotional support throughout this challenging journey. His trust in me and his willingness to embrace this new path in a foreign place, far from our family, friends, and comfort zone have meant the world to me. My deepest gratitude also goes to my family, especially my mother, Aliah and extended family members, whose constant prayers and boundless encouragement have kept me grounded and motivated every step of the way. I believe this journey would not have been as vibrant without my university mates, who made every step more colourful and bearable. We shared our struggles, celebrated our small victories, and lifted each other during difficult times. My deepest thanks go to Faridatul Ain, Hadfizah, Hazwani, Dini, Kubra, Cidem, Andrea, Ella, Fatimah, Ruixian, Puteri, Maryam, Hani, Lena and many more friends whom I couldn't name here but whose support will always be remembered.

To the staff members of the School of Food Science and Nutrition, whether laboratory staff or administrative support, thank you for ensuring my work ran smoothly in the labs and for assisting with administrative matters. A special thanks to Miles, Sara, Natalie, Joanna, Neil, Ian, Catherine, George, Gita, Katelyn, and Matthew for their dedication and support. Finally, I would like to take this opportunity to express my deepest appreciation to my financial sponsor, Majlis Amanah Rakyat (MARA), for providing the financial support that made this PhD journey possible over the past 4 years. I also acknowledge the use of ChatGPT-5.0 (Open AI, <https://chatgpt.com/>) and QuillBot Premium (Learneo Inc., <https://quillbot.com/>) in the proof-reading of the thesis before submission. I confirm that the proof-reading undertaken by ChatGPT and QuillBot was in accordance with the Postgraduate Researcher Proof-reading Policy.

## Abstract

Despite extensive research on medicinal plants, many remain underexplored. Therefore, the aim of this study was to investigate the potential of underutilised Malaysian medicinal plants of *Colubrina asiatica*, *Garcinia atroviridis*, and *Gnetum gnemon* as antimicrobial agents in biobased and biodegradable zein film. The research focused on their application as wrapping film, utilising raw beef as a food sample to represent typical microbial risks in foods, such as food contamination by *Escherichia coli*, *Listeria monocytogenes*, and *Salmonella*. Electrospinning was used to produce zein-based films. A comparative assessment of biological activities of the plant extracts was first performed. The extraction of *C. asiatica*, *G. atroviridis*, and *G. gnemon* using ethanol-to-water ratios of 0:100, 25:75, 50:50, 75:25 and 100:0 and two extraction methods of solvent extraction (S) and microwave-assisted extraction (MAE) yielded *C. asiatica* extract (CAE), *G. atroviridis* extract (GATE), and *G. gnemon* extract (GGE). The findings highlighted that the ethanol ratio influenced extraction yield and bioactivities more significantly than the extraction method. GATE exhibited the highest yield but showed the lowest total phenolic content, 2,2-diphenyl-1-picrylhydrazyl (DPPH) and ferric reducing antioxidant power (FRAP) activities. Antimicrobial testing at 50 mg/mL showed that GATE50-S/M had stronger antibacterial activity, while CAE50-M exhibited higher antifungal activity. A significant correlation was found between the total phenolic content of CAE and antioxidant activities ( $p < 0.05$ ). Novel zein-based films, Ze-CAE, Ze-GATE, and Ze-GGE were successfully produced using electrospinning, utilising zein as the primary polymer and incorporating 5% (w/w) of the selected extracts. An evaluation of their properties showed that Ze-GGE films had significantly greater fibre diameter and thickness compared to the other films ( $p < 0.05$ ). All films displayed a water contact angle between 20° and 35° (hydrophilic surface), with encapsulation efficiency exceeding 90%. The attenuated total reflectance-Fourier transform infrared spectroscopy (ATR-FTIR) spectra confirmed successful encapsulation of CAE, GATE, and GGE into zein films without structural modification and highlighted hydrogen bonding between zein and the plant extracts. Ze-GATE was the most thermally stable among all films. In a soil burial test, all films exhibited the indicator of a rapid biodegradation process. All the beef samples wrapped with the zein-based films, particularly Ze-GATE and Ze-GGE, exhibited reduced bacterial growth over a five-day storage period, indicating a higher antibacterial activity compared to the tested commercial film. However, the hydrophilic characteristics of films present a limitation for beef wrapping, highlighting the need for further research. The outcomes of this research contribute to the knowledge for the development of active antimicrobial

films developed from biobased and biodegradable materials, aiming to reduce the reliance on plastic packaging and offering a sustainable alternative.

## Table of Contents

<b>Acknowledgements</b> .....	<b>iii</b>
<b>Abstract</b> .....	<b>iv</b>
<b>Table of Contents</b> .....	<b>vi</b>
<b>List of Tables</b> .....	<b>ix</b>
<b>List of Figures</b> .....	<b>xi</b>
<b>List of Abbreviations</b> .....	<b>xviii</b>
<b>Chapter 1 Introduction</b> .....	<b>1</b>
1.1 Background of study.....	1
1.2 Literature review .....	5
1.2.1 Medicinal plants .....	5
1.2.2 Secondary metabolites .....	5
1.2.3 Malaysian medicinal plants .....	10
1.2.4 Extraction of medicinal plants .....	22
1.2.5 Microorganisms in nature .....	33
1.2.6 Food Packaging .....	40
1.3 Aim and objectives .....	50
1.3.1 Aim of research.....	50
1.3.2 Research questions and research objectives .....	50
1.4 Outline of thesis.....	52
<b>Chapter 2 Materials and Methodology</b> .....	<b>54</b>
2.1 Materials and reagents .....	54
2.2 Sample collection .....	55
2.3 Extraction of medicinal plants.....	55
2.3.1 Preparation of plant extract.....	56
2.4 Biological activity of extracts.....	56
2.4.1 Total phenolic content.....	56
2.4.2 Antioxidant assay.....	57
2.4.3 Antimicrobial activity assay .....	58
2.5 Development of zein-based films .....	63
2.5.1 Preparation of electrospinning solution.....	63
2.5.2 Viscosity measurement.....	64
2.5.3 Electrospinning .....	64
2.6 Assessing zein-based films properties .....	65
2.6.1 Scanning electron microscope (SEM) .....	65
2.6.2 Film thickness .....	66
2.6.3 Encapsulation efficiency .....	66
2.6.4 Water contact angle .....	67
2.6.5 Attenuated total reflectance - Fourier transform infrared spectroscopy (ATR - FTIR).....	68
2.6.6 Thermal properties.....	68

2.6.7	Biodegradation study .....	68
2.7	Storage study .....	68
2.7.1	Microbiological analysis .....	69
2.7.2	Water activity ( $a_w$ ) .....	70
2.7.3	Colour analysis .....	70
2.8	Statistical analysis .....	70
2.9	Overview of the workflow.....	71
<b>Chapter 3</b>	<b>Extraction and Biological Activity.....</b>	<b>72</b>
3.1	Introduction.....	72
3.2	Aim of the chapter .....	72
3.3	Results and Discussion .....	73
3.3.1	Extraction yields.....	73
3.3.2	Total Phenolic Content .....	79
3.3.3	Antioxidant Activity.....	84
3.3.4	Correlation of total phenolic content and antioxidant activity.....	96
3.3.5	Antimicrobial activity .....	99
3.4	Conclusion.....	111
<b>Chapter 4</b>	<b>Development of Zein-Based Films .....</b>	<b>113</b>
4.1	Introduction.....	113
4.2	Aim of the chapter .....	114
4.3	Results and Discussion .....	115
4.3.1	Preparation of electrospinning solution and viscosity measurement.....	115
4.3.2	Electrospinning of zein-based films .....	120
4.3.3	Scanning electron microscopy (SEM).....	124
4.3.4	Film thickness .....	132
4.3.5	Encapsulation efficiency .....	134
4.3.6	Water contact angle ( $\theta$ ).....	137
4.3.7	Attenuated total reflectance-Fourier transform infrared spectroscopy (ATR-FTIR).....	141
4.3.8	Thermal properties.....	149
4.3.9	Biodegradation study .....	157
4.4	Conclusion.....	161
<b>Chapter 5</b>	<b>Storage Study of Zein-Based Films on Beef.....</b>	<b>162</b>
5.1	Introduction.....	162
5.2	Aim of the chapter .....	165
5.3	Results and Discussion .....	166
5.3.1	Microbiological activity analysis .....	168
5.3.2	Water activity ( $a_w$ ) .....	174
5.3.3	Colour analysis .....	179
5.4	Conclusion.....	190

<b>Chapter 6</b>	<b>General Discussion .....</b>	<b>192</b>
6.1	Summary of the research .....	192
6.2	Discussion points and contribution of the thesis .....	193
6.2.1	Effect of different ethanol ratios and extraction methods on yield and biological activities .....	193
6.2.2	Comparison of the biological activities of CAE, GATE, and GGE and their potential as active antimicrobial agents .....	195
6.2.3	Electrospinning as a novel approach to develop zein-based films incorporated with CAE, GATE, and GGE .....	197
6.2.4	The quality of beef stored with newly developed zein-based films .....	199
6.3	Research limitations .....	201
6.4	Future directions .....	203
6.5	Conclusion .....	206
	<b>List of References .....</b>	<b>207</b>
	<b>Appendix A Supplementary Materials .....</b>	<b>248</b>

## List of Tables

Table 1.1 Classification of three Malaysian medicinal plants species.....	11
Table 1.2 Phytochemical constituents and biological activity of <i>C. asiatica</i> .....	13
Table 1.3 Phytochemical constituents and biological activity of <i>G. atroviridis</i> ...	16
Table 1.4 Phytochemical constituents and biological activity of <i>G. gnemon</i> . ....	20
Table 1.5 Common extraction solvent and its physicochemical properties.....	23
Table 1.6 Common foodborne pathogens found in food commodities that were responsible for the outbreak.....	35
Table 1.7 Food spoilage microorganisms in food commodities, adapted from (Wessner et al., 2020, p. 590). ....	38
Table 2.1 List of materials and reagents. ....	54
Table 2.2 Medium preparation for antimicrobial testing. ....	60
Table 2.3 Microbial strains and growth medium.....	60
Table 2.4 Electrospinning parameters for zein-based films. ....	65
Table 3.1 Yields of CAE, GATE, and GGE using different extraction methods and ethanol ratios.....	75
Table 3.2 Total phenolic content of CAE, GATE, and GGE using different extraction methods and ethanol ratios. ....	80
Table 3.3 Antioxidant activity of CAE, GATE, and GGE using different extraction methods and ethanol ratios: DPPH. ....	86
Table 3.4 Antioxidant activity of CAE, GATE, and GGE using different extraction methods and ethanol ratios: FRAP. ....	91
Table 3.5 Correlation between total phenolic content and DPPH and FRAP....	98
Table 3.6 DDA and MIC/MBC of 10 mg/mL extracts against <i>B. cereus</i> .....	100
Table 3.7 DDA of 50 mg/mL extracts against foodborne pathogens and spoilage microorganisms. ....	105
Table 3.8 MIC and MBC/MFC of 50 mg/mL plant extracts against foodborne pathogens and spoilage microorganisms.....	108
Table 4.1 The abbreviation for zein-based films. ....	115
Table 4.2 Solution viscosity and characterisation of zein-based films. ....	117
Table 4.3 TGA profile of zein-based films at the temperature between 30 and 600 °C. ....	150
Table 4.4 Physical appearance of Neat zein, Ze-CAE, Ze-GATE, and Ze-GGE films before and after soil burial test conducted for 12 days. ....	158
Table 5.1 Bacterial growth observed on beef wrapped with different packaging films of Neat zein, Ze-CAE, Ze-GATE, Ze-GGE and commercial films. ....	169

Table 5.2 Water activity of beef wrapped with different packaging films of Neat zein, Ze-CAE, Ze-GATE, Ze-GGE and commercial films.....	174
Table 5.3 Colour of beef wrapped with different packaging films of Neat zein, Ze-CAE, Ze-GATE, Ze-GGE and commercial films: ( $L^*$ ).....	180
Table 5.4 Colour of beef wrapped with different packaging films of Neat zein, Ze-CAE, Ze-GATE, Ze-GGE and commercial films: ( $a^*$ ).....	183
Table 5.5 Colour of beef wrapped with different packaging films of Neat zein, Ze-CAE, Ze-GATE, Ze-GGE and commercial films: ( $b^*$ ).....	187
Table 6.1 The influence of ethanol ratio and extraction method. ....	194
Table 6.2 The rank of biological activity of the plant extract.....	196

## List of Figures

Figure 1.1 The examples of therapeutic compounds from alkaloids group; morphine, coniine, and cocaine.....	6
Figure 1.2 Basic skeleton of phenol with aromatic ring and hydroxyl (-OH) group and the examples of phenolic compounds of kaempferol, vanillin, resveratrol, and coumarin.....	7
Figure 1.3 The five-carbon (isoprene) units based on isopentane skeleton of terpenoids and the examples of terpenoids; linalool and limonene....	8
Figure 1.4 <i>Colubrina asiatica</i> plant (left), freshly collected leaves (middle), leaf individual size (right).....	12
Figure 1.5 <i>Garcinia atroviridis</i> tree (left), fresh unripe fruits (middle), cut and sun-dried slice (right).....	15
Figure 1.6 <i>Gnetum gnemon</i> tree (left), mature leaves with unripe fruit (middle), individual size (right).....	19
Figure 1.7 Solvent extraction process for grounded plant materials using a suitable solvent to produce crude plant extracts, created with (Biorender.com).....	24
Figure 1.8 Schematic diagram of Soxhlet extraction apparatus consists of a solvent flask, an extraction thimble, and a condenser.....	26
Figure 1.9 Main components for microwave-assisted extraction: (a) a closed system consists of an extraction vessels, a turntable, a closed chamber, reflectors, and a microwave source, (b) an open system with primary components of a focused microwave source, an extraction vessel, and a water condenser. ....	28
Figure 1.10 Different UAE setups (a) ultrasonic bath, (b) ultrasonic horn. ....	29
Figure 1.11 Schematic diagram of ASE system utilising high temperatures and pressures.....	31
Figure 1.12 A schematic diagram of SFE comprises a high-pressure pump and an extraction cell.....	32
Figure 1.13 Visual appearance of zein powder obtained from the commercial supplier and the polypeptide backbone of zein consists of amide group (-NH-), carbonyl group (C=O), amino acid side chain (R) with m representing the number of repeating amino acid units in the zein polypeptide chain (Magoshi et al., 1992; Forato et al., 1998; Mohammed-Ziegler and Billes, 2002; Sun et al., 2023, p.2). ....	43
Figure 1.14 Biodegradable and active film preparation via (a) solvent casting by spreading the solution onto a mould, (b) extrusion where the solid biopolymer materials are heated, converted into a melt, extruded through a nozzle, and cooled into a film. ....	45

Figure 1.15 Basic electrospinning set-up comprises of a solution reservoir with a spinneret, a grounded metallic collector, and a high-voltage power supply ranging from 1 to 30 kV, created with (Biorender.com). .....	46
Figure 2.1 SEM sample preparation where the films were mounted on the stub. ....	66
Figure 2.2 A commercial film purchased from a supermarket was used as a comparison to the zein-based films in evaluating their effectiveness at reducing the growth of foodborne pathogens and spoilage microorganisms in beef. ....	69
Figure 2.3 Flowchart of research methodology. ....	71
Figure 3.1 Percentage of extraction yield (%) of (a) CAE, (b) GATE, (c) GGE using different extraction methods; solvent and microwave assisted extraction (MAE) and varying ethanol ratios (0, 25, 50, 75, and 100 ethanol).....	76
Figure 3.2 Gallic acid standard curve for total phenolic content determination using gallic acid concentration between 0.04 and 0.31 mg/mL. ....	79
Figure 3.3 Total phenolic content (mg GAE/g) of (a) CAE, (b) GATE, and (c) GGE using different extraction methods; solvent and microwave assisted extraction (MAE) and varying ethanol ratios (0, 25, 50, 75, and 100 ethanol). ....	81
Figure 3.4 Percentage of DPPH inhibition of CAE using different extraction methods; solvent and microwave assisted extraction (MAE) and varying ethanol ratios (0, 25, 50, 75, and 100 ethanol). ....	86
Figure 3.5 Percentage of DPPH inhibition of GATE using different extraction methods; solvent and microwave assisted extraction (MAE) and varying ethanol ratios (0, 25, 50, 75, and 100 ethanol). ....	87
Figure 3.6 Percentage of DPPH inhibition of GGE using different extraction methods; solvent and microwave assisted extraction (MAE) and varying ethanol ratios (0, 25, 50, 75, and 100 ethanol). ....	87
Figure 3.7 Trolox standard curve for FRAP determination using Trolox at concentration between 0.016 to 0.50 $\mu$ M. ....	90
Figure 3.8 FRAP value ( $\mu$ M TE/g DW) of CAE using different extraction methods; solvent and microwave assisted extraction (MAE) and varying ethanol ratios (0, 25, 50, 75, and 100 ethanol). ....	92
Figure 3.9 FRAP value ( $\mu$ M TE/g DW) of GATE using different extraction methods; solvent and microwave assisted extraction (MAE) and varying ethanol ratios (0, 25, 50, 75, and 100 ethanol). ....	92
Figure 3.10 FRAP value ( $\mu$ M TE/g DW) of GGE using different extraction methods; solvent and microwave assisted extraction (MAE) and varying ethanol ratios (0, 25, 50, 75, and 100 ethanol). ....	93

Figure 3.11 Significant Pearson’s correlation of CAE between total phenolic content and (a) percentage of DPPH inhibition ( $r = 0.498$ ), and (b) FRAP value ( $r = 0.526$ ).....	98
Figure 3.12 Representative photos of (a) diameter of inhibition zone (red arrow) of 10 mg/mL CAE50-S and CAE75-S extracts tested against <i>B. cereus</i> using Mueller Hinton agar plate following 24 hours incubation at $37\pm 2$ °C, (b) no diameter of inhibition zone of 10 mg/mL CAE50-S and CAE75-S extracts tested against <i>S. aureus</i> using Mueller-Hinton agar plate following 24 hours incubation at $37\pm 2$ °C. The yellow zone around the disc is the colour of the plant extract infused into the disc. ....	99
Figure 3.13 Representative MBC plates of GATE100-M (left) and CHX (right) against <i>B. cereus</i> using Mueller Hinton agar media following 24 hours incubation at $37\pm 2$ °C with MBC values of 1.25 mg/mL and 0.031 mg/mL, respectively.....	102
Figure 3.14 Diameter of inhibition zone (red arrow) of (a) 50 mg/mL GATE50 extracts tested against <i>B. cereus</i> using Mueller Hinton agar plate following 24 hours incubation at $37\pm 2$ °C, (b) CAE50 extracts tested against <i>C. albicans</i> using Sabouraud dextrose agar plate following 48 hours incubation at $37\pm 2$ °C. The yellow zone around the disc is the colour of the plant extract infused into the disc. ....	105
Figure 3.15 Representative MFC plate of CAE50-M (MFC: 0.78 mg/mL) against <i>C. albicans</i> using Sabouraud dextrose agar media (left) and MBC plate of GATE50-M (MBC: 3.13 mg/mL) against <i>B. cereus</i> using Mueller Hinton agar media (right) after 48 and 24 hours of incubation periods, respectively.....	107
Figure 4.1 Zein solutions of Neat zein (yellowish, orange-coloured solution), Ze-CAE (brownish solution), Ze-GATE (yellowish, orange-coloured solution), and Ze-GGE (dark green solution). ....	117
Figure 4.2 Log viscosity (Pa.s) of Neat zein, Ze-CAE, Ze-GATE, and Ze-GGE with respect to shear rate from 0.1 to 100 $s^{-1}$ at 25 °C, with data points represent a single measurement. ....	118
Figure 4.3 (a) Electrospinning set-up for zein-based films production comprises of a solution reservoir with a spinneret, a grounded metallic collector, and a high-voltage power supply, (b) The example of electrospun zein-based film deposited onto the collector using the solution flow rate of 1.0 mL/h, voltage at 15-17 kV, with distance to collector set at 15 cm and performed at $21\pm 2$ °C with relative humidity of $40\pm 5\%$ and the collector size of 12 x 12 cm. ....	121

Figure 4.4 Visual appearance of zein-based films (a) Neat zein, (b) Ze-CAE, (c) Ze-GATE, (d) Ze-GGE, with an additional granular-like appearance on the surfaces of Ze-GATE and Ze-GGE. ....	122
Figure 4.5 Comparison of SEM micrographs of films at 5000X magnification.	124
Figure 4.6 SEM micrograph of Neat zein at 5000X magnification showing fibres with flat ribbon-like morphology and bend formation. ....	125
Figure 4.7 Histogram showing the average fibre diameter distribution based on 100 randomly selected fibres from the SEM micrograph of Neat zein. ....	126
Figure 4.8 The average fibre diameter ( $\mu\text{m}$ ) between Neat zein, Ze-CAE, Ze-GATE and Ze-GGE films. ....	126
Figure 4.9 SEM micrograph of Ze-CAE at 5000X magnification showing fibres with flat ribbon-like morphology along with strings and branches formation. ....	127
Figure 4.10 Toroid observed in Ze-CAE fibres at 2000X magnification. ....	128
Figure 4.11 Histogram showing the average fibre diameter distribution based on 100 randomly selected fibres from the SEM micrograph of Ze-CAE. ....	128
Figure 4.12 SEM micrograph of Ze-GATE at 5000X magnification showing fibres with flat ribbon-like morphology and bend formation. ....	129
Figure 4.13 Histogram showing the average fibre diameter distribution based on 100 randomly selected fibres from the SEM micrograph of Ze-GATE. ....	130
Figure 4.14 SEM micrograph of Ze-GGE at 5000X magnification showing flat ribbon-like morphology and strings formation. ....	131
Figure 4.15 Histogram showing the average fibre diameter distribution based on 100 randomly selected fibres from the SEM micrograph of Ze-GGE. ....	131
Figure 4.16 The film thickness ( $\mu\text{m}$ ) of Neat zein, Ze-CAE, Ze-GATE and Ze-GGE films. ....	133
Figure 4.17 Encapsulation efficiency (%) of Ze-CAE, Ze-GATE, and Ze-GGE films. ....	136
Figure 4.18 The $\alpha$ -zein structure that comprises of glutamine-rich bridges that connect the linear stacks of rod-shaped helical repeat units of zein. ....	136
Figure 4.19 Measurement of water contact angle by sessile drop method at $20\pm 2$ °C using drop shape tensiometer with 3 $\mu\text{L}$ of water droplet deposited on the surface of the film (20 x 40 mm). ....	138
Figure 4.20 The water contact angle (°) of Neat zein, Ze-CAE, Ze-GATE, and Ze-GGE films. The figures above the bar graph shows the different	

shapes of water droplet observed after 2 seconds of exposure to films; contact angle of  $33.26 \pm 10.37^\circ$  for Neat zein,  $28.04 \pm 6.11^\circ$  for Ze-CAE,  $22.74 \pm 6.55^\circ$  for Ze-GATE, and  $23.18 \pm 6.79^\circ$  for Ze-GGE.

..... 139

Figure 4.21 FTIR spectrum for Neat zein at the range of 4000 to 400  $\text{cm}^{-1}$ . Diverse absorption bands related to zein are evidenced such as Amide A (N-H: 3291  $\text{cm}^{-1}$ ), methyl ( $\text{CH}_3$ ) and methylene ( $\text{CH}_2$ ) aliphatic groups (C-H: 2955  $\text{cm}^{-1}$ ), Amide I (C=O: 1653  $\text{cm}^{-1}$ ), Amide II (C-N & N-H: 1540  $\text{cm}^{-1}$ ), Amide III (C-N: 1450 & 1240  $\text{cm}^{-1}$ )..... 142

Figure 4.22 Comparison of FTIR spectra between Neat zein film, Ze-CAE film and CAE extract at the range of 4000 to 400  $\text{cm}^{-1}$ . Absorption bands related to CAE extract are phenolics (O-H: 3244  $\text{cm}^{-1}$ ), aliphatic groups (C-H: 2926  $\text{cm}^{-1}$ ), flavonoids (C=C & C=O: 1583  $\text{cm}^{-1}$ ), methyl group (C-H: 1389  $\text{cm}^{-1}$ ), tannins or phenolic structures (C-O: 1249  $\text{cm}^{-1}$ ), aromatic groups (C-H: 1039 & 772  $\text{cm}^{-1}$ ). Absorption bands related to Ze-CAE showed similar major bands to Neat zein with several band shifting, including (N-H overlapping with O-H: 3291  $\rightarrow$  3282  $\text{cm}^{-1}$ ), (C-H: 2955  $\rightarrow$  2932  $\text{cm}^{-1}$ ), (C-N: 1450  $\rightarrow$  1447  $\text{cm}^{-1}$ , 1240  $\rightarrow$  1237  $\text{cm}^{-1}$ ). The disappearance of bands of 1389, 1039, and 772  $\text{cm}^{-1}$  from CAE extract in the Ze-CAE spectrum might be attributed to the lower concentration of CAE incorporated into the Ze-CAE film, resulting in reduced signal intensity. .... 144

Figure 4.23 Comparison of FTIR spectra between Neat zein film, Ze-GATE film, and GATE extract at the range of 4000 to 400  $\text{cm}^{-1}$ . Absorption bands related to GATE extract are (O-H: 3226  $\text{cm}^{-1}$ ), (C-H: 2928  $\text{cm}^{-1}$ ), (C=O & C=C: 1585  $\text{cm}^{-1}$ ), (C-H: 1384  $\text{cm}^{-1}$ ), (C-O: 1253  $\text{cm}^{-1}$ ), (C-H: 1036, 813, & 775  $\text{cm}^{-1}$ ). Absorption bands related to Ze-GATE showed similar major bands to Neat zein with several band shifting, including (N-H & O-H: 3291  $\rightarrow$  3296  $\text{cm}^{-1}$ ), (C-H: 2955  $\rightarrow$  2957  $\text{cm}^{-1}$ ), (N-H & C-N: 1540  $\rightarrow$  1538  $\text{cm}^{-1}$ ), (C-N: 1450  $\rightarrow$  1443  $\text{cm}^{-1}$ ). The disappearance of bands of 1036, 813, and 775  $\text{cm}^{-1}$  from GATE extract in the Ze-GATE spectrum might be attributed to the lower concentration of GATE incorporated into the Ze-GATE film, resulting in reduced signal intensity. .... 146

Figure 4.24 Comparison of FTIR spectra between Neat zein film, Ze-GGE film, and GGE extract at the range of 4000 to 400  $\text{cm}^{-1}$ . Absorption bands related to GGE extract are phenolics (O-H: 3233  $\text{cm}^{-1}$ ), methyl & methylene aliphatic groups (C-H: 2926  $\text{cm}^{-1}$ ), carboxylic acid/ alkene (C=O/C=C: 1587  $\text{cm}^{-1}$ ), methyl group (C-H: 1389  $\text{cm}^{-1}$ ), phenolics (C-O: 1246  $\text{cm}^{-1}$ ), aromatic groups (C-H: 1039, 811, & 772  $\text{cm}^{-1}$ ).

Absorption bands related to Ze-GGE showed similar major bands to Neat zein with several band shifting, including (N-H & O-H: 3291→3285 cm <sup>-1</sup> ), (C-H: 2955→2957 cm <sup>-1</sup> ), (C=O: 1653→1650 cm <sup>-1</sup> ), (N-H & C-N: 1540→1533 cm <sup>-1</sup> ), (C-N: 1450→1447 cm <sup>-1</sup> ). The disappearance of bands of 1039, 811, and 772 cm <sup>-1</sup> from GGE extract in the Ze-GGE spectrum might be attributed to the lower concentration of GGE incorporated into the Ze-GGE film, resulting in reduced signal intensity.....	148
Figure 4.25 Comparison of (a) TGA and (b) DTG curves for zein-based films. ....	151
Figure 4.26 TGA/DTG curve of Neat zein showing four-stage decomposition process with maximum decomposition rate temperature at 318.33 °C. ....	152
Figure 4.27 TGA/DTG curves of (a) Ze-CAE showing five-stage decomposition process with maximum decomposition rate temperature at 308.17 °C, (b) Ze-GATE showing five-stage decomposition process with maximum decomposition rate temperature at 319 °C, and (c) Ze-GGE showing four-stage decomposition process with maximum decomposition rate temperature at 305.17 °C.....	154
Figure 5.1 Representative photo of beef (left) wrapped with commercial film and (right) zein-based films on day 0 of storage. ....	164
Figure 5.2 (a) Different beef samples utilised; British beef rump steak and British beef fillet steak, (b) the beef was cut to 5.0±1.0 g, approximately 2.3 x 2.3 cm in surface dimensions.....	168
Figure 5.3 Bacterial growth observed on beef wrapped with different packaging films of Neat zein, Ze-CAE, Ze-GATE, Ze-GGE and commercial films during five days of storage at 4 °C. The red dotted line represents the microbial safety threshold for chilled beef, set at log 6.0 CFU/g. ...	170
Figure 5.4 Water activity of beef wrapped with different packaging films of Neat zein, Ze-CAE, Ze-GATE, Ze-GGE and commercial films during five days of storage.....	175
Figure 5.5 Lightness ( <i>L</i> <sup>*</sup> ) of beef wrapped with different packaging films of Neat zein, Ze-CAE, Ze-GATE, Ze-GGE and commercial films.....	181
Figure 5.6 Red/green opponent colours ( <i>a</i> <sup>*</sup> ) of beef wrapped with different packaging films of Neat zein, Ze-CAE, Ze-GATE, Ze-GGE and commercial films.....	184
Figure 5.7 The comparison of beef colours over a five-day storage period using different films of Neat zein, Ze-CAE, Ze-GATE, Ze-GGE, and commercial films. The beef colour gradually progressed from a bright	

red colour, with a moist and tender appearance (Day 0), to the darker colour, stale, and dry appearance (Day 5). .....	185
Figure 5.8 Yellow/blue opponent colours ( $b^*$ ) of beef wrapped with different packaging films of Neat zein, Ze-CAE, Ze-GATE, Ze-GGE and commercial films.....	188

## List of Abbreviations

ABTS	2,2'-azinobis-(3-ethylbenzothiazoline-6-sulfonic acid
AEE	Aqueous enzymatic extraction
AFM	Atomic force microscopy
AR	Analytical reagent
ASE	Accelerated solvent extraction
ASTM	American Society for Testing and Materials
ATCC	American Type Culture Collection
ATR	Attenuated total reflectance
BHI	Brain heart infusion
BHT	Butylated hydroxytoluene
CAE	<i>Colubrina asiatica</i> extract
CDC	Centers for Disease Control and Prevention
CFU	Colony forming unit
CHX	Chlorhexidine
CLSI	Clinical & Laboratory Standards Institute
CPE	Cold-pressing oil extraction
CSA	Cajaninstilbene acid
DDA	Disc diffusion assay
DEHP	Di-(2-ethylhexyl)phthalate
DMSO	Dimethyl sulfoxide
DNA	Deoxyribonucleic acid
DPPH	2,2-diphenyl-1-picrylhydrazyl
DSC	Differential scanning calorimetry
DTG	Derivative thermogravimetry
DW	Dry weight
EAB	Elongation at break
FAO	Hydroxyl
FCC	Food contact chemicals
FDA	Food and Drug Administration
FFS	Film-forming solution
FRAP	Ferric reducing antioxidant power
FRIM	Forest Research Institute Malaysia
FSA	Food Safety Authority
FT	Fourier transform
FTC	Ferric thiocyanate
FTIR	Fourier transform infrared spectroscopy
GAE	Gallic acid equivalent
GAL	<i>Garcinia atroviridis</i> leaf extract

GATE	<i>G. atroviridis</i> extract
GCMS	Gas Chromatography Mass Spectrometry
GGE	<i>G. gnemon</i> extract
GRAS	Generally recognized as safe
HCA	Hydroxycitric acid
HCl	Hydrochloric acid
HDPE	High-density polyethylene
HO•	Hydroxyl radical
HPLC	High performance liquid chromatography
IC <sub>50</sub>	Half-maximal inhibitory concentration
ICID	International Commission on Irrigation and Drainage
ID	Inner diameter
IFN	Interferon
IL	Interleukin
IR	Infrared
ISO	International Organization for Standardization
IUCN	International Union for Conservation of Nature
LD	Lethal dose
LDPE	Low-density polyethylene
LEO	<i>Laurus nobilis</i> essential oil
MAE	Microwave-assisted extraction
MAP	Modified atmosphere packaging
MBC	Minimum bactericidal concentration
MFC	Minimum fungicidal concentration
MHA	Mueller Hinton agar
MHB	Mueller Hinton broth
MIC	Minimum inhibitory concentration
MOH	Ministry of Health
MRI	Magnetic resonance imaging
NCCLS	National Committee for Clinical Laboratory Standards
NMR	Nuclear magnetic resonance
NRCS	Natural Resources Conservation Service
OD	Outer diameter
OH	Hydroxyl
ORAC	Oxygen radical absorption capacity
PBAT	Poly(butylene adipate-terephthalate)
PBS	Phosphate buffered saline
PCA	Plate count agar
PDA	Potato dextrose agar
PDB	Potato dextrose broth

PE	Polyethylene
PEG	Polyethylene glycol
PET	Polyethylene terephthalate
PI	Pinostrobin
PP	Polypropylene
PS	Polystyrene
PSE	Pressurised solvent extraction
PUFA	Polyunsaturated fatty acid
PVC	Polyvinyl chloride
RE	Reflux extraction
REO	<i>Rosmarinus officinalis</i> essential oil
RH	Relative humidity
RO	Research objective
ROO•	Peroxyl radical
ROS	Reactive oxygen species
RQ	Research question
SAXS	Small-angle X-ray scattering
SC-CO <sub>2</sub>	Supercritical carbon dioxide extraction
SDA	Sabouraud dextrose agar
SDB	Sabouraud dextrose broth
SEM	Scanning electron microscope
SFE	Supercritical fluid extraction
TBA	Thiobarbituric acid
TE	Trolox equivalent
TGA	Thermogravimetric analysis
TPTZ	2,4,6-Tripyridyl-s-triazine
TS	Tensile strength
UAE	Ultrasound-assisted extraction
USDA	United States Department of Agriculture
UV-Vis	Ultraviolet-visible
WHO	World Health Organization
WVP	Water vapour permeability
WVTR	Water vapour transmission rate
XRD	X-ray diffraction
YM	Young's modulus

# Chapter 1

## Introduction

### 1.1 Background of study

Food safety and food quality are widely discussed issues, and for many years, numerous food-related incidents have been addressed in mainstream media, with the extensively publicised topics are food contamination and food spoilage. Food contamination occurs when harmful substances, such as foreign particles or hazardous materials, infiltrate food products. These contaminants may be introduced at various stages of the food production process, from initial handling and processing to later stages, including distribution and consumption by the end user. Contaminants can lead to food spoilage, transforming edible food into waste and, in more severe cases, posing significant health risks to consumers (Liu, A. et al., 2018). Food contaminants that are present in food come from different sources, including heavy metals, halogenated organic compounds, antibiotic resistance genes carried by foodborne pathogens and livestock bacteria as well as contaminants derived from the pathogens themselves (Thakali and MacRae, 2021). Of the many different types of food contaminants present, contamination caused by foodborne pathogens such as *Salmonella* spp., *Staphylococcus aureus* and *Escherichia coli* are the most widespread, being found in various types of food, such as meat, dairy products, eggs, and vegetables (Linscott, 2011; Bintsis, 2017).

On a global scale, the World Health Organization (WHO) estimates that governments in low- and middle-income countries lose approximately USD 110 billion annually in terms of productivity and medical expenses due to unsafe food consumption (WHO, 2024b). Furthermore, approximately £9 billion was lost in 2018 in the United Kingdom due to the foodborne illness resulting from contaminated foods with foodborne pathogens (Daniel et al., 2020). In addition, it is estimated that *Salmonella* accounts for about 1.35 million infections, 26,500 hospitalisations, and 420 deaths in the US every year. Likewise, multistate outbreaks of *E. coli* infections in the US have been reported, involving fresh produce, meat products, frozen and ready-to-eat food products (CDC, 2021a; CDC, 2021b). Malaysia is no exception when it comes to the challenges posed by public health concerns. A recent study highlights that acute diarrhoea has emerged as a significant public health issue in the country, with over 13.5 million cases reported annually. Foodborne bacterial pathogens are identified as the

leading cause of diarrhoea, contributing to prolonged illness, increased patient mortality rates, and a substantial economic burden on Malaysia (Cheesman et al., 2023). Another set of data provided by the Ministry of Health (MOH) of Malaysia showed the incidence rate of food and waterborne illness over the course of ten years, from 2004 to 2013, with food poisoning having the highest incident rate compared to other illnesses such as cholera, dysentery, typhoid, and hepatitis A (Ministry of Health, 2014, cited in Abdul-Mutalib et al., 2015, p. 898). In addition, a recent report by the Ministry of Health Malaysia revealed an increase in the number of food poisoning episodes from 496 episodes in 2023 to 707 episodes in 2024 (Ministry of Health, 2024). A current report from Food and Agriculture Organization (FAO) estimates that \$400 billion per year is wasted due to food loss between harvesting and up to retail stage, which accounts for 14% of the world's food supply (FAO, 2019). These findings are alarming since the issues of foodborne pathogens, food spoilage, and food loss are often intertwined and have an impact on individuals as well as the economy, environment, and society.

To address the challenges posed by foodborne pathogens and food spoilage, various food preservation and packaging techniques have been developed to preserve the organoleptic properties of food, increase their shelf life, and maintain their quality. In food preservation, preservatives are typically added in small quantities, measured in parts per million (ppm) or by weight, usually ranging from 1 to 3%. Common preservatives include sodium benzoate, potassium sorbate, and sulphur dioxide (Garcia-Garcia and Searle, 2016). Traditionally, food packaging has been used to protect food from contamination and spoilage, facilitate transportation and storage processes, and provide uniform measurement of contents and commonly referred to as passive packaging (Hine, 1995, cited in Robertson, G., 2013a, p. 2). Common food packaging materials include polyethylene terephthalate (PET), polyvinyl chloride (PVC), polypropylene (PP), low-density polyethylene (LDPE), high-density polyethylene (HDPE), and polystyrene (PS) (Marsh and Bugusu, 2007). Among these, LDPE is commonly used for film packaging or cling wrap, particularly for perishable foods, such as fresh produce, meat, and poultry. These foods, with a shelf life of several days to three weeks, are highly prone to contamination (Robertson, G., 2013a; Marsh and Bugusu, 2007). However, concerns are emerging regarding the prolonged use of polyethylene (PE)-based packaging, particularly due to the migration of food contact chemicals (FCCs) from PE materials into food. Among the most detected FCCs are non-authorized substances, such as phthalates and metal antioxidants. Phthalates, often used as plasticisers, are known as endocrine-disrupting chemicals, raising significant safety concerns due to their

potential health impacts, such as endocrine and reproductive dysregulation, as well as respiratory problems like allergies and asthma (Jaakkola and Knight, 2008; Liu, J. et al., 2018; Zhang, Y.-J. et al., 2021; Gerassimidou et al., 2023). Furthermore, the widespread use of plastic packaging has long been linked to the generation of significant plastic waste, which contributes to the accumulation of debris in landfills and ocean pollution. This pollution poses serious threats to marine life, disrupting ecosystems and endangering numerous species (Thompson et al., 2009). A study by Jambeck et al. (2015) revealed that out of 192 countries, China ranked first in mismanaged plastic waste, contributing 27.7% of the global total. Malaysia, with 2.9%, also ranked among the highest in Southeast Asia. According to a 2018 report, plastic waste made up 13.2% of Malaysia's total waste, making it the second-largest waste category after food waste, which accounted for 44.5% (Poverty-Pollution-Persecution, 2019).

Over the years, with technological advancements, more sophisticated packaging materials have been developed, including a shift from the traditional functions of packaging materials to more diverse functions. Packaging now carries more broad classification such as the introduction of intelligent and active packaging, with the latter has been extensively researched (Robertson, G., 2013a). Intelligent packaging incorporates external or internal indicators into the packaging materials to provide information about the package history and/or food quality. In contrast, active packaging involves the intentional incorporation of active substances into or onto packaging materials to improve product quality and safety (Robertson, G., 2013b). According to the definition provided by the European FAIR-project CT 98-4170, active packaging is a type of packaging that changes the condition of the packaging to extend shelf-life or improve safety or sensory properties while maintaining the quality of the food (Vermeiren et al., 1999). Further details regarding the various classifications of packaging will be discussed in Section 1.2.6. Active packaging especially those developed from biobased and biodegradable materials promises great potential and offer hope for a more sustainable future where the dependency on the plastic as a sole packaging material could be reduced. Thus, ongoing research into sustainable bioplastic packaging with minimal chemical use is crucial for reducing plastic waste, preventing contamination, and extending shelf life.

Recent research has focused on the utilisation of biobased and biodegradable materials, including polysaccharides and proteins, as primary packaging options, providing sustainable alternatives. Natural active substances are frequently integrated into packaging material formulations to improve particular properties. For instance, Kavooosi et al. (2014) utilised solvent casting to produce gelatine

films, incorporating essential oils derived from *Zataria multiflora* (Shirazi thyme). The films demonstrated significant antioxidant properties and were effective against both Gram-positive and Gram-negative bacteria, indicating their potential as active antioxidant and antimicrobial packaging materials. More recent research on the development of antimicrobial packaging from sustainable materials includes the fabrication of zein film incorporated with thyme essential oil for strawberry quality preservation. The findings revealed that the addition of thyme essential oil successfully reduced bacterial, fungal, and yeast growth on strawberries stored at  $4\pm 0.5$  °C and  $85\pm 5\%$  relative humidity (RH) for 15 day, compared with the control (strawberries packed in PET containers without film) and with zein film without thyme essential oil (Ansarifar and Moradinezhad, 2021). In line with these developments, this present study focuses on exploring the potential of three underutilised Malaysian medicinal plants extracts of *Garcinia atroviridis* ('asam gelugor'), *Colubrina asiatica* ('peria pantai'), and *Gnetum gnemon* ('belinjau') as antimicrobial agents in zein film, specifically for use as wrapping film, with raw beef used as a representative food sample.

## **1.2 Literature review**

### **1.2.1 Medicinal plants**

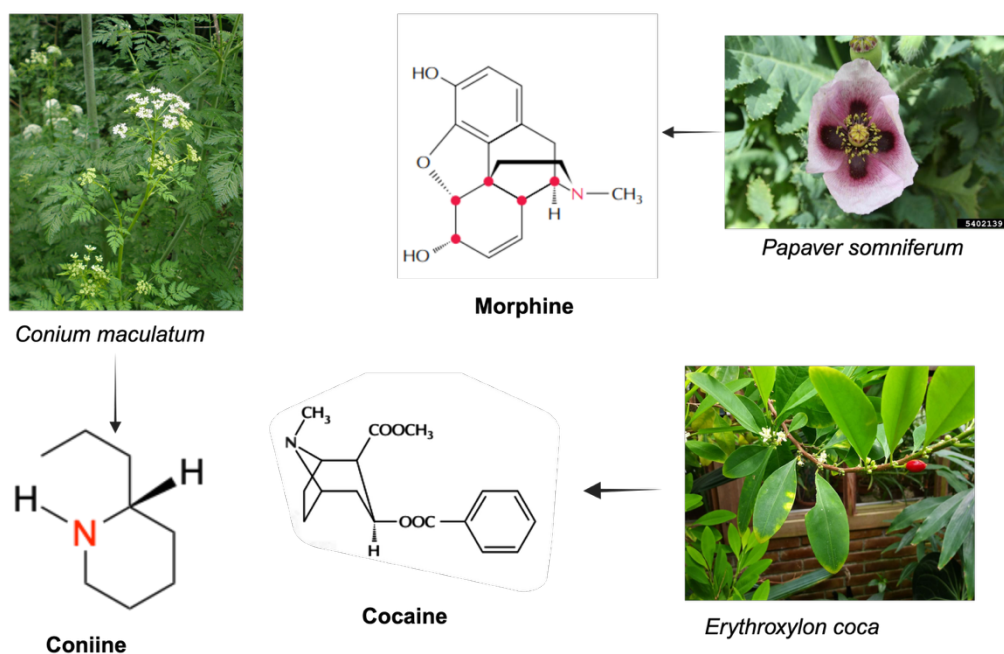
Natural products are biologically derived molecules obtained from naturally occurring organisms, without human synthetic modification (Croteau et al., 2000). Plants are a major source of these products, consisting of both primary and secondary metabolites. Primary metabolites, such as carbohydrates, amino acids, proteins, and lipids, are essential for fundamental cellular functions like growth and development (Salam et al., 2023). In contrast, secondary metabolites, including alkaloids, terpenoids, and phenolic compounds, are not directly involved in growth and development but play a key role in helping plants respond to various environmental conditions, and contribute to their colours, fragrances, and flavours (Croteau et al., 2000; Reshi et al., 2023). Plants rich in secondary metabolites with therapeutic potential are often referred to as medicinal plants (Anand et al., 2019).

The utilisation of medicinal plants is dated from centuries ago since folklore traditionally used them to treat diseases. Globally, it is estimated that approximately 80% of the population depend on the plants as traditional medicines with developed countries such as USA continuously developing plant-derived drugs (Farnsworth et al., 1985). According to a report by Allkin (2017), at least 28,187 plant species have been documented for medicinal use. With the increasing global use of medicinal plants and the rising demand for plant-based ingredients, potentials and concerns regarding the traditional use of these plants continue to emerge. These concerns primarily involve the risk of toxicity, as their safety and efficacy are often not verified, well documented or regulated (Zhang, J. et al., 2015). As a result, modern-day researchers aim to study the potential of secondary metabolites from medicinal plants, not only to establish scientific knowledge but also to determine safe dosages for human consumption, whether for drug development or other applications.

### **1.2.2 Secondary metabolites**

Plant secondary metabolites are broadly classified into three major groups based on their chemical structures: alkaloids, phenolic compounds, and terpenoids (Croteau et al., 2000). Alkaloids are organic compounds that contain at least one nitrogen atom within a heterocyclic ring and are recognised for their pharmacological activity. These compounds are characterised by a distinct bitter taste, which serves to protect plants from herbivores and microbes, as well as playing a role in germination (Croteau et al., 2000; Teoh, 2015). Alkaloids are

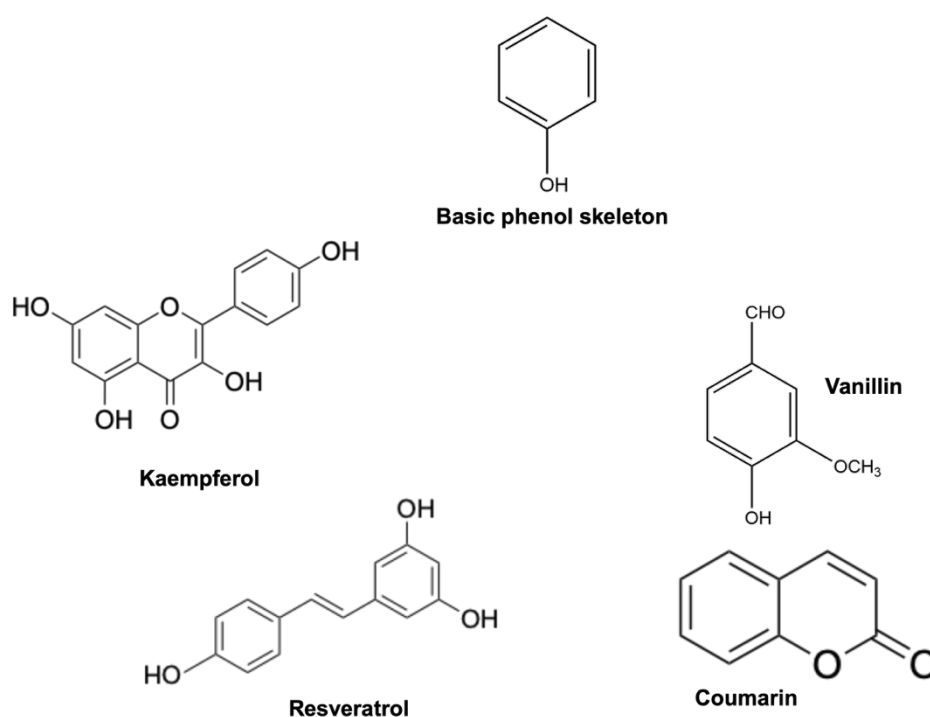
further classified as true alkaloids (pyrrole, pyrrolidine, pyridine, piperidine, quinoline, isoquinoline, indolizidine, tropane, indole, imidazole), protoalkaloids, and pseudoalkaloids (Gutierrez-Grijalva et al., 2020). The first synthesised alkaloid, coniine, derived from *Conium maculatum*, is highly toxic and can cause paralysis of the nervous system (Figure 1.1). Due to their bioactive nature, alkaloids have been extensively studied for their therapeutic properties, leading to the development of various pharmaceutical agents. For instance, morphine, extracted from the opium poppy (*Papaver somniferum*), is widely used as a narcotic analgesic (Figure 1.1). Similarly, cocaine, obtained from *Erythroxylon coca*, functions as a topical anaesthetic, a potent central nervous system stimulant, and an adrenergic blocking agent (beta-blocker) which is responsible for blood vessel dilation, reduced blood pressure, and slows heart rate (Figure 1.1). However, the misuse and abuse of these compounds pose significant dangers when used without proper medical supervision or prescribed dosages (Croteau et al., 2000; Vardanyan and Hruby, 2016).



**Figure 1.1** The examples of therapeutic compounds from alkaloids group; morphine, coniine, and cocaine. Adapted from (Croteau et al., 2000; Ingram, 2011; Oommen, 2018; Universiteit-Leiden, 2024)

In addition to alkaloids, phenolic compounds are also one of the important secondary metabolites, consisting of an aromatic ring with one or more hydroxyl (-OH) group (Figure 1.2). Phenolics are ubiquitous in the plant kingdom and are

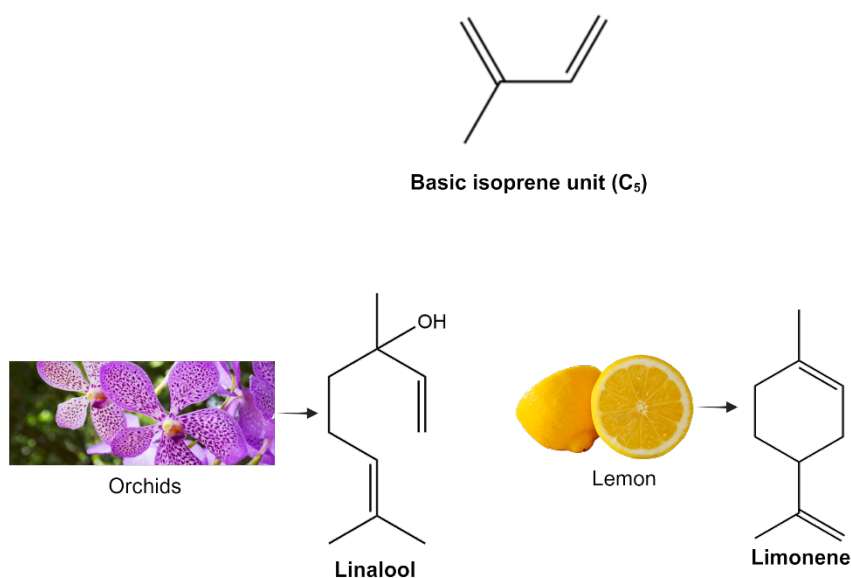
further subdivided into coumarins, flavonoids, lignans, simple phenolics, stilbenes, and tannins (Croteau et al., 2000). These compounds serve a broad range of functions in plants. For instance, the flavonoid subclass anthocyanins are responsible for various colour pigmentations in fruits and flowers, and these pigments can also mimic insects (Croteau et al., 2000; Teoh, 2015). Additionally, lignans contribute to defence against external pathogens or act as antioxidants. Other groups of phenolics such as coumarins, stilbenes, and tannins protect plants by deterring pathogens, serving as feeding deterrents due to its distinct astringency taste of the seed, acting as heartwood protectants, and inhibiting seed germination. Examples of commonly found phenolics are depicted in Figure 1.2. For instance, vanillin, a primary extract from vanilla beans, is well-known for contributing to the vanilla flavour. Another example, resveratrol, is a widely studied compound renowned for its antioxidant properties. From a pharmacological perspective, phenolics are highly valued for their antioxidant, antimicrobial, anti-inflammatory, anticancer, and cardiovascular protective activities (Croteau et al., 2000; Teoh, 2015).



**Figure 1.2** Basic skeleton of phenol with aromatic ring and hydroxyl (-OH) group and the examples of phenolic compounds of kaempferol, vanillin, resveratrol, and coumarin.

Adapted from (Croteau et al., 2000)

Terpenoids are another group of plant secondary metabolites and are the most abundant, which constitute both volatile and non-volatile compounds that are responsible for the aromatic scent in plants (Teoh, 2015). These compounds are characterised by a structural foundation of five-carbon units called isoprene units (Figure 1.3). Based on the number of isoprene units, terpenoids are further categorised into hemiterpenes ( $C_5$ ), monoterpenes ( $C_{10}$ ), sesquiterpenes ( $C_{15}$ ), diterpenes ( $C_{20}$ ), sesterterpenes ( $C_{25}$ ), triterpenes ( $C_{30}$ ), and polyterpenes ( $>C_{30}$ ) (Croteau et al., 2000; Teoh, 2015). An example of a well-known monoterpene is linalool, which contributes to the fragrance of orchids (Croteau et al., 2000; Kaiser, 1993, cited in Teoh, 2015, p. 61). Another example is limonene, a compound produced by citrus fruits that imparts their characteristic zesty aroma and flavour (Figure 1.3). Other notable terpenoids include camphor, costunolide, myrcene, artemisinin, and taxol. These compounds serve various ecological functions, such as acting as insect repellents, mammalian antifeedants, and pollinator attractants (Croteau et al., 2000). The primary applications of terpenoids are in the cosmetics (e.g., essential oil components of peppermint and spearmint are produced by secondary enzymatic transformations of limonene) and pharmaceutical industries (e.g., glycyrrhizin, a triterpenoid saponin to treat respiratory symptoms), where they are valued for their aromatic and functional properties (Croteau et al., 2000; Bailly and Vergoten, 2020; Frank et al., 2021).



**Figure 1.3** The five-carbon (isoprene) units based on isopentane skeleton of terpenoids and the examples of terpenoids; linalool and limonene. Adapted from (Croteau et al., 2000; The-Habitat, 2023; Villareal, 2024)

### **1.2.2.1 Secondary metabolites: mechanism of action**

Plant secondary metabolites exert their effects through specific mechanisms of action targeting cells. Although the precise mechanisms of action for these compounds are not yet fully elucidated, a general conceptual framework has been established. It is recognised that different classes of secondary metabolites often exhibit synergistic effects, while also potentially acting cooperatively within the same class (Bakkali et al., 2006). Broadly, three primary mechanisms of action have been proposed: activation of apoptosis and/or necrosis leading to cell death, induction of cell cycle arrest, and disruption of essential organelle functions (Sharifi-Rad et al., 2017). For instance, Jeon et al. (2015) demonstrated that esculetin, a coumarin-derived compound, suppressed cancer cell proliferation by inducing apoptosis in the HMM G361 cell line.

Furthermore, mechanisms of action specific to different classes of secondary metabolites have also been proposed. For example, alkaloids are believed to exert their effects by inhibiting cell proliferation through the action of topoisomerase enzymes, which delay DNA replication and ultimately lead to cell death (Anwar et al., 2020). For phenolics, the mechanisms of action are typically compound-specific. Curcumin, for instance, demonstrates its activity through reactive oxygen species (ROS) scavenging, modulation of signalling pathways, induction of apoptosis, and regulation of the tumour microenvironment. Similarly, resveratrol modulates various signalling pathways associated with the initiation, progression, and metastasis of cancer. Terpenoids, primarily act by altering and suppressing signalling pathways involved in cancer cell progression. They also induce apoptosis and cause cell cycle arrest, further contributing to their anticancer effects (Majrashi et al., 2023). As for volatile compounds from terpenoids, the lipophilic nature and low molecular weight enhance their ability to penetrate the bacterial cell wall and cytoplasmic membrane, ultimately leading to cellular damage (Sharifi-Rad et al., 2017).

The previous sections focused on how secondary metabolites interact with human cells, highlighting their potential in advancing cancer therapies through the application of plant-derived compounds. Shifting the focus to their role as antimicrobial agents, it is equally important to investigate how these metabolites combat bacterial cells and the mechanisms underlying their effects. Two principal mechanisms underpin the antimicrobial activity of secondary metabolites: interference with bacterial synthesis and function, and the ability to overcome conventional mechanisms of antibacterial resistance. These mechanisms target various structural and functional components of bacterial cells, including the ribosome, cell membrane, DNA, and cell wall. The first mechanism involves

disruption of bacterial protein biosynthesis by targeting ribosomal subunits, interference with the peptidoglycan layer in the cell wall, inhibition of nucleic acid synthesis by suppressing enzymes responsible for DNA replication, and damage to the bacterial cell membrane (Maxwell, 1997; Walsh, 2003; Schneider and Sahl, 2010; Khameneh et al., 2019). The second mechanism focuses on strategies such as efflux pump inhibition, structural modifications of porins, degradation of antibacterial agents, antibiotic modification, and alterations of the bacterial target site (Khameneh et al., 2019).

### 1.2.3 Malaysian medicinal plants

Malaysia, located in Southeast Asia, is characterised by a tropical climate with high humidity and temperature ranging from 21 to 32 °C year-round (ICID, 2024). The country covers a land area of 329,758 km<sup>2</sup>, accounting for only about 0.2% of the global land mass (Shahrul, 2023; ICID, 2024). Despite its relatively small size, Malaysia's climate offers ideal conditions for nurturing a rich diversity of natural flora, including having various types of forests such as dipterocarp, peat swamp and mangroves forests (Shahrul, 2023). Although Malaysia boasts a wealth of plant diversity, scientific research on its plant species, particularly medicinal plants, remains limited. Of the approximately 12,500 plant species found in the country, only 1,200 have been documented for their medicinal properties, accounting for just 9.6% of the total (Ramlan, 2003, cited in Tan, T.Y.C. et al., 2020, p. 1). Data also shows that of these 15,000 vascular plant species, 2,700 are endemic to Malaysia, while 12,300 are shared with other countries (Shahrul, 2023). This highlights Malaysia's rich and unique plant diversity, much of which remains underexplored for its potential.

Commonly used medicinal plants in Malaysia include *Curcuma domestica* (turmeric), *Centella asiatica* ('pegaga'), *Eurycoma longifolia* ('Tongkat ali'), *Kaempferia galanga* ('cekur'), and *Orthosiphon grandiflorus* ('misai kucing') (Shahrul, 2023). While these plants have been extensively researched for their various biological activities, three underutilised species of *G. atroviridis* ('asam gelugor'), *C. asiatica* ('peria pantai'), and *G. gnemon* ('belinjau') are less frequently mentioned in the literature of Malaysian medicinal plants, particularly the latter two. In this context, research on the active extracts from these plants is in its infancy, and more research should be conducted to increase the visibility of these plants' potential. Therefore, one of the objectives of the present study was to investigate the extraction efficiency, analysis of phenolic content, and biological activities of *C. asiatica*, *G. atroviridis*, and *G. gnemon*.

The classification for these three plants species is shown in Table 1.1, with further information elaborated in Sections 1.2.3.1 to 1.2.3.3.

**Table 1.1** Classification of three Malaysian medicinal plants species.

Hierarchy	<i>Colubrina asiatica</i>	<i>Garcinia atroviridis</i>	<i>Gnetum gnemon</i>
<b>Kingdom</b>	Plantae	Plantae	Plantae
<b>Subkingdom</b>	Tracheobionta	-	Tracheobionta
<b>Superdivision</b>	Spermatophyta	-	Spermatophyta
<b>Division</b>	Magnoliophyta	Streptophyta	Gnetophyta
<b>Class</b>	Magnoliopsida	Equisetopsida	Gnetopsida
<b>Order</b>	Rhamnales	Malpighiales	Gnetales
<b>Family</b>	Rhamnaceae	Clusiaceae	Gnetaceae
<b>Genus</b>	<i>Colubrina</i>	<i>Garcinia</i>	<i>Gnetum</i>
<b>Scientific name</b>	<i>Colubrina asiatica</i> (L.) Brongn	<i>Garcinia atroviridis</i> Griff. ex T. Anderson	<i>Gnetum gnemon</i> var. <i>gnemon</i> L.
<b>Common local name</b>	'peria pantai'	'asam gelugor'	'belinjau', 'congkak'

Adapted from: (Royal-Botanic-Gardens-Kew, 2023; USDA-NRCS, 2024a; USDA-NRCS, 2024b)

### 1.2.3.1 *Colubrina asiatica*

*Colubrina asiatica* also known as latherleaf, Asian snakewood, or 'peria pantai', is a sprawling shrub plant commonly found near the coastal area in Africa (e.g. Mozambique, Kenya, Madagascar), Asia (e.g. China, India, Malaysia, Indonesia, Singapore, Thailand) and Tropical Australia as well as Pacific Islands (USDA-NRCS, 2024a). The plant can grow up to 5 metres tall, featuring drooping branches and wavy-edged leaves that range from 3.7 to 8.0 cm in length. Its yellow flowers bloom year-round, typically emerging in the leaf axils. These small flowers measure about 3.8 mm in width and 5 mm in length (Flora-Fauna-Web, 2023).

The plant is predominantly used for soap substitutes, dental care, bleaching and cleaning mats, fish poison, and alleviating inflammation (Richardson et al., 2000, Uphoff et al., 2001, cited in Desai and Gaikwad, 2014, p. 282). Research on *C. asiatica* has revealed that it contains essential oils and phenolic compounds, which are responsible for various biological activities, including antioxidant, antimicrobial, antimycobacterial (mycobacterial species includes *Mycobacterium tuberculosis* which responsible for tuberculosis and *Mycobacterium leprae* that causes leprosy), antimalarial, and cytotoxic properties (Ma et al., 2007; Desai and Gaikwad, 2014; Desai et al., 2015; Sangsopha et al., 2018). Figure 1.4 showcases an image of *C. asiatica*, accompanied by detailed information on its phytochemical constituents and biological activities, which are outlined in Table 1.2.



**Figure 1.4** *Colubrina asiatica* plant (left), freshly collected leaves (middle), leaf individual size (right).

**Table 1.2** Phytochemical constituents and biological activity of *C. asiatica*.

Plant part	Class	Phytochemical	Biological activity	Reference
Leaf	Essential oils	dodecamethylcyclohexasiloxane ( <b>1</b> ), tetradecamethylcycloheptasiloxane ( <b>2</b> ), $\alpha$ -cubebene ( <b>3</b> ), 2,4-dimethylhexane ( <b>4</b> ), 6,6-methylenebicyclo[3.1.1]heptane ( <b>5</b> ), cadina-1(10),4-diene ( <b>6</b> ), hexadecamethylcyclooctasiloxane ( <b>7</b> ), octamethylcyclo-tetrasiloxane ( <b>8</b> ), isocaryophyllene ( <b>9</b> ), dehydro-N-[4,5-methylenedioxy-2-nitrobenzylidene]-tyramine ( <b>10</b> )	antioxidant, antimicrobial	(Desai and Gaikwad, 2014)
	Glycosides	3''-O-acetylcolubrin ( <b>11</b> ), 3'',2''-O-diacetylcolubrin ( <b>12</b> ), 3''-O-acetyl-6''-O-trans-crotonylcolubrin ( <b>13</b> ), colubrin ( <b>14</b> ), rutin ( <b>15</b> ), kaempferol 3-O-rutinoside ( <b>16</b> )	(-)	(Lee, S.-S. et al., 2000)
	Phenolic	quercetin-3-O-rhamnoside ( <b>17</b> ), kaempferol-3-O-glucoside ( <b>18</b> ), kaempferol-3-O-rutinoside ( <b>16</b> )	(-)	(Mat-Ali, 2008)
Stem	Triterpene acids	ceanothic acid ( <b>19</b> ), granulosic acid ( <b>20</b> ), zizyberenalic acid ( <b>21</b> ), colubrinic acid ( <b>22</b> ), alipholic acid ( <b>23</b> ), betulinic acid ( <b>24</b> )	( <b>21*</b> ) cytotoxicity against KB and NCI-H187 cells, antimalarial, ( <b>23*</b> ) cytotoxicity against KB, NCI-H187, and MCF-7 cells, antimycobacterial, ( <b>24*</b> ) cytotoxicity against KB, and NCI-H187 cells	(Sangsopha et al., 2018)
	Steroids	stigmast-5-en-7-one ( <b>25</b> ), ang6 $\beta$ -hydroxystigmast-4-en-3-one ( <b>26</b> ), stigmast-4-ene-3,6-dione ( <b>27</b> ), ergosterol peroxide ( <b>28</b> ), $\beta$ -sitosterol ( <b>29</b> )	( <b>28*</b> ) cytotoxicity against KB and NCI-H187 cells, antimalarial	(Sangsopha et al., 2018)

Phytochemical numbered in bold: phytochemicals extracted/ identified/ isolated from the respective study

Phytochemical marked with asterisk: biological activity tested with the phytochemical, (-) no data

**Table 1.2** continued

Plant part	Class	Phytochemical	Biological activity	Reference
Stem	Benzoic acid derivative	2-hydroxy-5-methoxybenzoic acid ( <b>30</b> )	inactive & (-)	(Sangsopha et al., 2018)
	Phenylalanine derivative	(-)-auranamide ( <b>31</b> ), D-phenylalanine, <i>N</i> -benzoyl-(2 <i>R</i> )-2-(acetlamino)-3-phenylpropyl ester ( <b>32</b> )	( <b>31</b> *) cytotoxicity against KB, and NCI-H187 cells	(Sangsopha et al., 2018)
	Sesquiterpenoid	isointermedeol ( <b>33</b> )	inactive & (-)	(Sangsopha et al., 2018)
	Glycoside	3''- <i>O</i> -acetylcolubrin ( <b>11</b> )	inactive & (-)	(Sangsopha et al., 2018)
Root	Triterpenoids	3,7- <i>O,O</i> -dibenzoyl ceanothic acid methylester ( <b>34</b> ), 3- <i>O</i> -acetyl-7- <i>O</i> -benzoyl ceanothic acid methylester ( <b>35</b> ), squalene ( <b>36</b> )	( <b>34</b> *) cytotoxicity against KB, and NCI-H187 cells, antimalarial, ( <b>35</b> *) cytotoxicity against KB, and NCI-H187 cells, antimalarial, antimycobacterial	(Sangsopha et al., 2020)
	Glycosides	3''- <i>O</i> -acetylcolubrin ( <b>11</b> ), 3'',2''- <i>O</i> -diacetylcolubrin ( <b>12</b> )	( <b>11</b> * and <b>12</b> *) cytotoxicity against KB, and MCF-7 cells	(Sangsopha et al., 2020)
	Triterpene acids	ceanothic acid ( <b>19</b> ), zizyberenic acid ( <b>21</b> ), alphitolic acid ( <b>23</b> ), betulinic acid ( <b>24</b> ), 24-hydroxyceanothic acid ( <b>37</b> )	(-)	(Sangsopha et al., 2020)
	Phytosterols	$\beta$ -sitosterol-3- <i>O</i> -glucoside ( <b>38</b> )	inactive & (-)	(Sangsopha et al., 2020)

Phytochemical numbered in bold: phytochemicals extracted/ identified/ isolated from the respective study

Phytochemical marked with asterisk: biological activity tested with the phytochemical, (-) no data

### 1.2.3.2 *Garcinia atroviridis*

*Garcinia atroviridis*, commonly known as ‘asam gelugor’ in Malaysia and Indonesia and ‘Som Khaek’ in Thailand, is a perennial tree endemic to Southeast Asia, particularly found in countries such as Malaysia, Myanmar, Thailand, and parts of India (Kosin et al., 1998; Shahid et al., 2023). The tree grows up to 25–27 metres tall and has oblong leaves. Its fruit is characterised by deep ridges, large petals, and sepals (Figure 1.5). Initially green when unripe, the fruit transitions to a bright yellow hue upon ripening and can reach up to 10 cm in diameter (Chew and Lim, 2018; Shahid et al., 2022).

Sun-dried fruits are commonly used in culinary applications, appreciated for their sour flavour, which enhances the taste of various dishes. Young leaves are also sometimes consumed raw as a salad. The fruit and leaves of *G. atroviridis* are widely valued in traditional medicine, reputed to help lower blood cholesterol levels, treat infections, coughs, and digestive issues (Al-Mansoub et al., 2014; Tan, W.-N. et al., 2019). The plant’s distinct sour taste is attributed to its high content of organic acids, with hydroxycitric acid (HCA) being one of the primary phytoconstituents in *G. atroviridis* (Jena et al., 2002). Phytochemical studies have shown that *G. atroviridis* and its bioactive compounds exhibit a wide range of biological activities, including antioxidant, antimicrobial, antibacterial, anti-inflammatory, antihyperlipidemic, antiobesity, antihypercholesterolemic, anti-tumor-promoting, and cytotoxic effects (Mackeen et al., 2000; Al-Mansoub et al., 2014; Hamidon et al., 2017; Milanda et al., 2019). Figure 1.5 features an image of the *G. atroviridis* tree and fruits, while Table 1.3 provides comprehensive details on its phytochemical constituents and associated biological activities.



**Figure 1.5** *Garcinia atroviridis* tree (left), fresh unripe fruits (middle), cut and sun-dried slice (right).

**Table 1.3** Phytochemical constituents and biological activity of *G. atroviridis*.

Plant part	Class	Phytochemical	Biological activity	Reference
Fruit	Organic acid	hydroxycitric acid (HCA) ( <b>1</b> ), tartaric acid ( <b>2</b> ), ascorbic acid ( <b>3</b> ), malic acid ( <b>4</b> )	antioxidant, antiobesity, not toxic: LD <sub>50</sub> : 2000 mg/kg	(Lim et al., 2020)
	Acid derivatives	2-(butoxycarbonylmethyl)-3-butoxycarbonyl-2-hydroxy-3-propanolide ( <b>5</b> )	antioxidant, antiobesity, not toxic: LD <sub>50</sub> : 2000 mg/kg	(Lim et al., 2020)
	Sesquiterpenoids	$\beta$ -caryophyllene alcohol ( <b>6</b> ), ginsenosol ( <b>7</b> ), (1S,2S,5S,8S)-4,4,8-trimethyltricyclo[6.3.1.0]dodecan-2-ol ( <b>8</b> )	( <b>6*</b> , <b>7*</b> , and <b>8*</b> ) antibacterial, anti-inflammatory	(Tan, W.-N. et al., 2013)
	Acid derivatives	2-(butoxycarbonylmethyl)-3-butoxycarbonyl-2-hydroxy-3-propanolide ( <b>5</b> ), 1',1''-dibutyl methyl hydroxycitrate ( <b>9</b> )	( <b>5*</b> and <b>9*</b> ) antifungal	(Mackeen et al., 2002)
	Coumarin derivative	7-hydroxy-4-methyl-8-nitro-2H-chromen-2-one ( <b>10</b> )	antifungal	(Mokhtar et al., 2018)
	Quinone	6-Nitro-1,4-naphthoquinone ( <b>11</b> )	(-)	(Mokhtar et al., 2018)
	Benzofuran	4-Nitrofuro[2,3-b][1]benzofuran ( <b>12</b> )	(-)	(Mokhtar et al., 2018)
	Organic acid	HCA ( <b>1</b> ), citric acid ( <b>13</b> ), oxalosuccinic acid ( <b>14</b> )	antioxidant, antidiabetic, cytotoxicity against L6 cells	(Shahid et al., 2023)
	Prenylated acyl phloroglucinol	colupone ( <b>15</b> )	(-)	(Shahid et al., 2023)
	Fatty acid amide	palmitic amide ( <b>16</b> ), linoleamide ( <b>17</b> )	(-)	(Shahid et al., 2023)
Aromatic ether	2,4-dinitro-1-(3-nitrophenoxy)benzene ( <b>18</b> )	(-)	(Shahid et al., 2023)	
Fatty acid	2,3-dihydroxycyclopentaneundecanoic acid ( <b>19</b> )	(-)	(Shahid et al., 2023)	

Phytochemical numbered in bold: phytochemicals extracted/ identified/ isolated from the respective study

Phytochemical marked with asterisk: biological activity tested with the phytochemical, (-) no data

**Table 1.3** continued

Plant part	Class	Phytochemical	Biological activity	Reference
Fruit	Piperidine alkaloid	ammodendrine ( <b>20</b> )	(-)	(Shahid et al., 2023)
	Tricarboxylic acids	oxaloglutarate ( <b>21</b> ), monoglyceride citrate ( <b>22</b> ), homoisocitrate ( <b>23</b> )	(-)	(Shahid et al., 2023)
	Terpenoid	cassaidine ( <b>24</b> ), persicaxanthin ( <b>25</b> )	(-)	(Shahid et al., 2023)
	Phenolic lactone	3-butylidene-7-hydroxyphthalide ( <b>26</b> )	(-)	(Shahid et al., 2023)
	Thymidine monophosphate	thymidine 3,5-cyclic monophosphate ( <b>27</b> )	(-)	(Shahid et al., 2023)
	Tetralins	emmotin A ( <b>28</b> )	(-)	(Shahid et al., 2023)
	Glycerophospho-ethanolamines	PE(17:0/0:0) ( <b>29</b> )	(-)	(Shahid et al., 2023)
Leaf	Essential oils	( <i>E</i> )- $\beta$ -farnesene ( <b>30</b> ), $\beta$ -caryophyllene ( <b>31</b> )	cytotoxicity against MCF-7 cells	(Tan, W.-N. et al., 2018)
	Xanthone	garcinexanthone F ( <b>32</b> ), morellin dimethyl acetal ( <b>33</b> ), maclurin ( <b>34</b> ), nigrolineaxanthone A ( <b>35</b> ), bannaxanthone A ( <b>36</b> ), garcimangosone B ( <b>37</b> ), nigrolineaxanthone P ( <b>38</b> ), scortechinones Q ( <b>39</b> ), scortechinone V ( <b>40</b> ), scortechinones C ( <b>41</b> ), moreollic acid ( <b>42</b> ), gambogin ( <b>43</b> )	antioxidant, anti-heat stress	(Chuaijit et al., 2024)
	Flavones	dulcinoside ( <b>44</b> )	(-)	(Chuaijit et al., 2024)
	Phloroglucinols	vismiaphenone C ( <b>45</b> ), garcinielliptone R ( <b>46</b> )	(-)	(Chuaijit et al., 2024)
	Polyprenylated cyclic polyketides	guttiferone K ( <b>47</b> ), oxy-guttiferone K2 ( <b>48</b> )	(-)	(Chuaijit et al., 2024)

Phytochemical numbered in bold: phytochemicals extracted/ identified/ isolated from the respective study

Phytochemical marked with asterisk: biological activity tested with the phytochemical, (-) no data

**Table 1.3** continued

Plant part	Class	Phytochemical	Biological activity	Reference
Root	Prenylated compounds	atrovirinone ( <b>49</b> ), atrovirisidone ( <b>50</b> )	( <b>49</b> *) antimicrobial, cytotoxicity against HeLa cells, ( <b>50</b> ) antimicrobial	(Permana et al., 2001)
	Prenylated hydroquinone	4-methylhydroatrovirinone ( <b>51</b> ), morelloflavone ( <b>52</b> ), fukugiside ( <b>53</b> ), 14- <i>cis</i> -docosenoic acid ( <b>54</b> )	(-)	(Permana et al., 2003)
	Prenylated depsidone	atrovirisidone ( <b>50</b> ), atrovirisidone B ( <b>55</b> ), naringenin ( <b>56</b> ), 3,8"-binaringenin ( <b>57</b> )	( <b>50</b> *, <b>55</b> *, <b>56</b> *, and <b>57</b> ) cytotoxicity against MCF-7 cells, ( <b>50</b> *, <b>55</b> *, and <b>56</b> *) cytotoxicity against DU-145 cells, ( <b>50</b> *, <b>55</b> *, and <b>57</b> ) cytotoxicity against H-460 cells	(Permana et al., 2005)
Stem bark	Triflavanone	garcineflavanone A ( <b>58</b> )	anti-cholinesterase	(Tan, W.-N. et al., 2014)
	Biflavonol	garcineflavonol A ( <b>59</b> )	anti-cholinesterase	(Tan, W.-N. et al., 2014)
	Xanthone	atroviridin ( <b>60</b> )	(-)	(Kosin et al., 1998)
	Essential oils	palmitoleic acid ( <b>61</b> ), palmitic acid ( <b>62</b> )	cytotoxicity against MCF-7 cells	(Tan, W.-N. et al., 2018)
	Xanthone	garcinexanthone G ( <b>63</b> ), stigmasta-5,22-dien-3 $\beta$ -ol ( <b>64</b> ), stigmasta-5,22-dien-3- <i>O</i> - $\beta$ -glucopyranoside ( <b>65</b> ), 3 $\beta$ -acetoxy-11 $\alpha$ ,12 $\alpha$ -epoxyoleanan-28,13 $\beta$ -olide ( <b>66</b> ), 2,6-dimethoxy- <i>p</i> -benzoquinone ( <b>67</b> ), 1,3,5-trihydroxy-2-methoxyxanthone-9-one ( <b>68</b> ), 1,3,7-trihydroxyxanthone ( <b>69</b> )	antioxidant	(Tan, W.-N. et al., 2016)
	Flavonol	kaempferol ( <b>70</b> ), quercetin ( <b>71</b> )	antioxidant	(Tan, W.-N. et al., 2016)

Phytochemical numbered in bold: phytochemicals extracted/ identified/ isolated from the respective study

Phytochemical marked with asterisk: biological activity tested with the phytochemical, (-) no data

### 1.2.3.3 *Gnetum gnemon*

*Gnetum gnemon*, commonly known as 'belinjau' or 'congak' in Malaysia and Indonesia, belongs to the Gnetaceae family and is widespread in Southeast Asia, including Indonesia, Malaysia, Thailand, the Philippines, and the western Pacific islands (Barua et al., 2015). Four varieties have been identified: *G. gnemon* var. *brunonianum* (Griff.) Markgr., *G. gnemon* var. *griffithii* (Parl.) Markgr., *G. gnemon* var. *gnemon*, and *G. gnemon* var. *tenerum*. Of these, only *G. gnemon* var. *gnemon* grows as a tree, while the others are woody shrubs (Barua et al., 2015; Anisong et al., 2022). The *G. gnemon* tree can reach heights of 10 to 15 metres, featuring dark green, ovate-oblong, or elliptic leaves measuring 4 to 7 cm in width and 10 to 20 cm in length. Its fruit, ellipsoid to globose depending on variety, measures 1 to 3 cm (Figure 1.6). During ripening, the fruit transitions from green to yellow, orange, and finally red at full maturity (Kato, E. et al., 2009; Barua et al., 2015).

Traditionally, *G. gnemon* has been used as a food source, with its young leaves incorporated into cooking and its ripened fruits processed into crackers. Numerous studies have explored the plant's potential biological activities, including antioxidant properties, DNA damage prevention, pancreatic lipase inhibition, pancreatic  $\alpha$ -amylase inhibition, antimicrobial effects, and antiplasmodial activity (Kato, E. et al., 2009; Santoso et al., 2010; Wazir et al., 2011; Barua et al., 2015; Dutta et al., 2018). Table 1.4 provides an overview of its phytochemical constituents along with the biological activities.



**Figure 1.6** *Gnetum gnemon* tree (left), mature leaves with unripe fruit (middle), individual size (right).

**Table 1.4** Phytochemical constituents and biological activity of *G. gnemon*.

Plant part	Class	Phytochemical	Biological activity	Reference
Fruit/ Seeds	Stilbenoids	gnetin L ( <b>1</b> ), gnetin C ( <b>2</b> ), gnemonoside A ( <b>3</b> ), gnemonoside C ( <b>4</b> ), gnemonoside D ( <b>5</b> ), resveratrol ( <b>6</b> )	( <b>1*</b> , <b>2*</b> , <b>3*</b> , <b>4*</b> , <b>5*</b> , and <b>6*</b> ) antioxidant, pancreatic lipase inhibition, ( <b>2*</b> , <b>3*</b> , <b>4*</b> , and <b>5*</b> ) pancreatic $\alpha$ -amylase inhibition, ( <b>1*</b> , <b>2*</b> , <b>4*</b> , <b>5*</b> , and <b>6*</b> ) antimicrobial	(Kato, E. et al., 2009)
	Stilbenoids	gnetin C ( <b>2</b> ), gnemonoside D ( <b>5</b> ), resveratrol ( <b>6</b> ), isorhapontigenin ( <b>7</b> ), gnetin E ( <b>8</b> ), gnemonoside L ( <b>9</b> ), gnemonoside M ( <b>10</b> )	( <b>2*</b> and <b>10*</b> ) enhance Th1 cytokines; IL-2 & IFN- $\gamma$ production in Peyer's Patch cells	(Kato, H. et al., 2011)
	Stilbenoids	gnetin L ( <b>1</b> ), gnetin C ( <b>2</b> ), gnemonoside A ( <b>3</b> ), gnemonoside C ( <b>4</b> ), gnemonoside D ( <b>5</b> ), resveratrol ( <b>6</b> )	( <b>1*</b> , <b>2*</b> , <b>3*</b> , <b>4*</b> , <b>5*</b> and <b>6*</b> ) suppress multiple angiogenesis-related endothelial cells functions and/or tumor angiogenesis	(Kunimasa et al., 2011)
	Stilbenoids	gnetin C ( <b>2</b> ), gnemonoside A ( <b>3</b> ), gnemonoside D ( <b>5</b> ), <i>trans</i> -resveratrol ( <b>6</b> )	( <b>6*</b> ) inhibited endothelial senescence	(Ota et al., 2013)
Leaf	Monoacyl-glycerols	2,3-dihydroxypropyl icosanoate ( <b>11</b> )	( <b>11*</b> ) antiplasmodial, cytotoxicity against L6 and HeLa cells	(Dutta et al., 2018)
	Monounsaturated fatty acid	oleic acid ( <b>12</b> )	( <b>12*</b> ) antiplasmodial, cytotoxicity against L6 and HeLa cells	(Dutta et al., 2018)
	Triterpene	ursolic acid ( <b>13</b> )	( <b>13*</b> ) antiplasmodial, cytotoxicity against L6 and HeLa cells	(Dutta et al., 2018)
	Phenylheptanoid	gnetumal ( <b>14</b> )	( <b>14*</b> ) tyrosinase inhibitory activity	(Le, T.H. et al., 2021)
	Diterpene	callyspinol ( <b>15</b> ), cassipourol ( <b>16</b> )	inactive	(Le, T.H. et al., 2021)

Phytochemical numbered in bold: phytochemicals extracted/ identified/ isolated from the respective study

Phytochemical marked with asterisk: biological activity tested with the phytochemical, (-) no data

**Table 1.4** continued

Plant part	Class	Phytochemical	Biological activity	Reference
Leaf	Sesquiterpenoids	(+)-dehydrovomifoliol ( <b>17</b> )	inactive	(Le, T.H. et al., 2021)
	Phenolic acid	<i>p</i> -coumaric acid ( <b>18</b> ), ferulic acid ( <b>19</b> )	<b>(18*)</b> tyrosinase inhibitory activity	(Le, T.H. et al., 2021)
	Diterpene alcohol	phytol ( <b>20</b> )	antibacterial activity	(Trisha et al., 2024)
	Fatty acid	cis,cis,cis-7-10-13-hexadecatrienal ( <b>21</b> )	(-)	(Trisha et al., 2024)
	Tocopherol	vitamin E ( <b>22</b> )	(-)	(Trisha et al., 2024)
Stem bark	Phenolics	3,4-dimethoxy-chlorogenic acid ( <b>23</b> ), resveratrol ( <b>6</b> ), 3-methoxyresveratrol ( <b>24</b> )	antioxidant, UV-B protection test	(Atun et al., 2007)
Root	Stilbene derivatives	gnemonol K ( <b>25</b> ), gnemonol L ( <b>26</b> ), gnemonol M ( <b>27</b> ), gnemonoside K ( <b>28</b> )	<b>(25*</b> and <b>26*</b> ) antioxidant	(Iliya et al., 2003)
	Stilbenoids	resveratrol ( <b>6</b> ), isorhapontigenin ( <b>7</b> ), (-)- $\epsilon$ -viniferin ( <b>29</b> ), gnetol ( <b>30</b> ), gnetifolin E ( <b>31</b> ), gnetifolin K ( <b>32</b> ), isorhapontigenin-3-O- $\beta$ -D-glucopyranoside ( <b>33</b> ), latifolol ( <b>34</b> ), gnemonoside A ( <b>3</b> ), gnemonoside B ( <b>35</b> ), gnemonoside F ( <b>36</b> )	<b>(6*</b> , <b>7*</b> , <b>29*</b> , <b>30*</b> , and <b>34*</b> ) antioxidant	(Iliya et al., 2003)
	Lignan	(+)-lirioresinol B ( <b>37</b> )	inactive	(Iliya et al., 2003)

Phytochemical numbered in bold: phytochemicals extracted/ identified/ isolated from the respective study

Phytochemical marked with asterisk: biological activity tested with the phytochemical, (-) no data

#### **1.2.4 Extraction of medicinal plants**

Extraction is a crucial step in recovering and isolating phytoconstituents from plants, where soluble components are separated from insoluble counterpart (Handa, 2008; Azwanida, 2015). Various plant parts, including fruits, seeds, stems, bark, leaves, roots, and flowers, can be used for extraction. Prior to extraction, plant samples are typically dried using methods such as sun-drying, air-drying, oven-drying, or microwave-drying to preserve and prepare the material (Azwanida, 2015). Generally, the extraction process begins with pulverizing the dried plant material into a fine powder to break down cell structures, making the phytochemicals more accessible to the extraction solvent. After pulverization, the preferred extraction method is applied, followed by filtration to separate the extracted substances from the plant material. A vacuum evaporator is then used to concentrate the extracts, which are subsequently dried at room temperature to remove residual solvents. The resulting crude extract, which may appear as an impure liquid, semisolid, or powder, typically contains a complex mixture of plant metabolites such as phenolics, alkaloids, and terpenoids (Handa, 2008; Azwanida, 2015).

Several factors must be considered when conducting plant extraction, including the method, solvent type, extraction time, solvent-to-sample ratio, and temperature. Among these, optimising the extraction method and selecting an appropriate solvent are particularly critical for isolating specific bioactive compounds (Sarker and Nahar, 2012). A variety of extraction methods are now available, ranging from traditional techniques like solvent and Soxhlet extraction to more advanced and innovative methods such as microwave-assisted extraction (MAE), ultrasound-assisted extraction (UAE), accelerated solvent extraction (ASE), and supercritical fluid extraction (SFE). Detailed descriptions of each of these methods are provided in Sections 1.2.4.1 to 1.2.4.6.

The choice of extraction solvent is essential to the efficiency of the extraction process. Solvents are generally categorised based on polarity: polar solvents (such as water, ethanol, methanol, and ethyl acetate), and nonpolar solvents (such as hexane, pentane, and heptane) (Sarker and Nahar, 2012). In many cases, combinations of solvents or solvent-water mixtures in various ratios are also employed to improve extraction outcomes. Typically, polar solvents are used to extract polar metabolites, while nonpolar solvents target nonpolar compounds. Moreover, solvent toxicity must be carefully evaluated when selecting solvents for extraction, especially for applications where extracts are intended for therapeutic, food, or cosmetic use, to ensure compliance with health and

environmental safety standards (Seidel, 2012). Table 1.5 details the commonly used extraction solvents with their polarity index and other physicochemical properties such as boiling point, viscosity, and dielectric constant. The information regarding these properties is crucial, as it directly influences the extraction efficiency and allows the recovery of targeted phytoconstituents. For example, higher polarity index solvents such as methanol, ethanol, and water are more efficient in the extraction of polyphenols and flavonoids, whereas lower polarity index solvents are better suited for the extraction of nonpolar compounds such as terpenoids and essential oils (Cacace and Mazza, 2003; Dai and Mumper, 2010).

**Table 1.5** Common extraction solvent and its physicochemical properties.

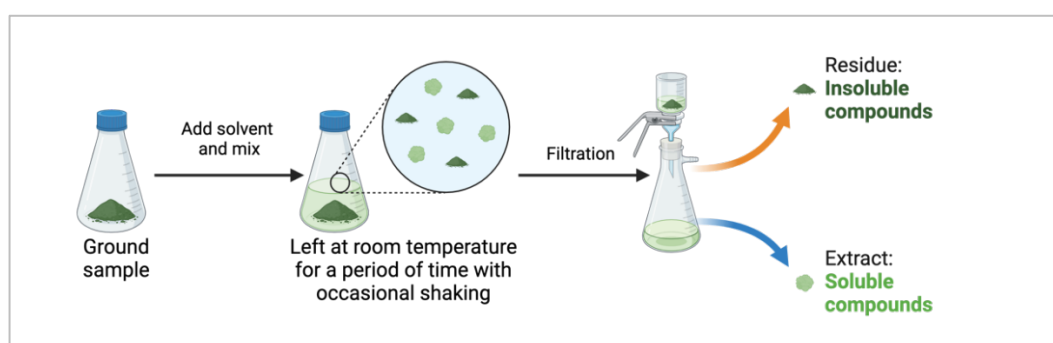
<b>Solvent</b>	<b>Molecular formula</b>	<b>Polarity index</b>	<b>Boiling point (°C)</b>	<b>Viscosity 20 °C (cP)</b>	<b>Dielectric constant</b>
Hexane	C <sub>6</sub> H <sub>14</sub>	0.0	69	0.33	1.88
Dichloromethane	CH <sub>2</sub> Cl <sub>2</sub>	3.1	41	0.44	8.93
Chloroform	CHCl <sub>3</sub>	4.1	61	0.57	4.81
Ethyl acetate	C <sub>4</sub> H <sub>8</sub> O <sub>2</sub>	4.4	77	0.45	6.02
Acetone	C <sub>3</sub> H <sub>6</sub> O	5.1	56	0.32	20.7
Methanol	CH <sub>4</sub> O	5.1	65	0.60	32.7
Ethanol	C <sub>2</sub> H <sub>6</sub> O	5.2	78	1.20	24.5
Water	H <sub>2</sub> O	9.0	100	1.00	80.1

Adapted from: (Seidel, 2012; Louisiana-State-University, 2024)

### 1.2.4.1 Solvent extraction

Solvent extraction is one of the conventional techniques to extract bioactive constituents from plant materials and it is performed by placing powdered plant materials in a clean container and mixed with the solvent of choice. The mixture is allowed to sit at room temperature for two to seven days, with frequent agitation (Figure 1.7). As the extraction process works by molecular diffusion in a static system, occasional shaking facilitates diffusion and provides an even distribution of the concentrated mixtures. A closed container is used to avoid evaporation of the extraction solvent during the extraction course, which avoids batch to batch variation. Solvent extraction is commonly preferred method for extraction because of the feasibility of the process, and it is less costly (Handa, 2008). In addition, this method is suitable for the extraction of thermolabile compounds. However, several limitations of solvent extraction include long extraction times, using high volume of extraction solvent and low recovery of yield (Bitwell et al., 2023).

Many studies have compared conventional extraction methods such as solvent extraction with more advanced techniques. For instance, Kong, Y. et al. (2010) examined the yield of cajaninstilbene acid (CSA) and pinostrobin (PI) from pigeonpea leaves using solvent extraction, MAE, UAE, and reflux extraction (RE) with ethanol concentrations of 70%, 80%, and 90%. Their findings showed that solvent extraction produced significantly lower yields of both compounds than the other methods for all ethanol concentrations ( $n = 3$ ,  $p < 0.05$ ). Notably, solvent extraction required the longest extraction time and lower extraction temperature (12 hours, 25 °C) compared to MAE (0.5–30 minutes, 65 °C), UAE (60 minutes, 65 °C), and RE (60 minutes, 65 °C).



**Figure 1.7** Solvent extraction process for grounded plant materials using a suitable solvent to produce crude plant extracts, created with (Biorender.com).

#### 1.2.4.2 Soxhlet extraction

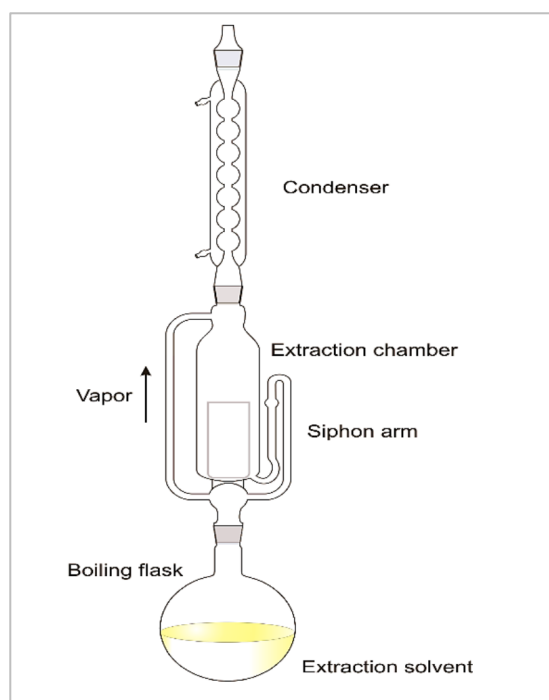
In addition to solvent extraction, Soxhlet extraction is another widely used conventional technique, originally developed for extracting fats and oils from plant materials (Peanparkdee and Iwamoto, 2019). Over time, its application has expanded significantly and now includes the extraction of various bioactive compounds such as sterols, lignin, and carotenoids (Saini and Keum, 2018; Qin et al., 2023).

The Soxhlet apparatus consists of three main components: a solvent flask, an extraction thimble, and a condenser (Figure 1.8). The Soxhlet extraction process begins when a solvent in the bottom flask is heated by a heating mantle. As the solvent heats, it vaporises and rises through the apparatus to the condenser, where it cools and condenses back into liquid form. This condensed solvent then drips onto the sample in the extraction chamber, dissolving target compounds. Once the solvent level in the extraction chamber reaches the siphon arm, the solution, now containing extracted compounds, flows back into the flask (Azwanida, 2015; Ghenabzia et al., 2023).

This process repeats in a continuous cycle, maintaining regular contact between the solvent and the sample, and thus optimising the extraction of compounds from the sample material. This method is straightforward, using relatively inexpensive equipment and does not require any filtration. However, Soxhlet extraction requires long extraction time and large volumes of solvent, which can increase costs and environmental impact. Additionally, the heat involved in the process makes it unsuitable for heat-sensitive compounds, as they may degrade under prolonged exposure. Furthermore, no agitation could be introduced during the extraction process (Luque de Castro and Garcia-Ayuso, 1998). In summary, Soxhlet extraction remains a reliable and efficient method for solid-liquid extractions, particularly for compounds stable under heat. However, limitations such as high solvent usage and thermal stress on delicate compounds have spurred research into alternative extraction methods aimed at improving sustainability and efficiency.

A previous study by Raghu and Velayudhannair (2023) investigated two extraction methods (Soxhlet extraction and solvent extraction) and two extraction solvents (methanol and ethanol) on the yield of *Stevia rebaudiana* leaves. The findings reported that the extraction of 20 g of powdered leaf in 200 mL of ethanol using Soxhlet extraction at 60 °C yielded higher percentage of extract ( $23.87 \pm 0.72\%$ ) compared to solvent extraction ( $7.13 \pm 0.09\%$ ) (20 g powdered leaf in 100 mL ethanol). Further analysis of total phenolic content, total flavonoid

content, tannin content, carbohydrate, and protein showed that solvent extraction extract exhibited significantly higher activity than Soxhlet extract ( $n = 3, p < 0.05$ ). For instance, the total phenolic content in solvent extraction extract was  $61.69 \pm 1.53$  mg/g, compared to  $45.25 \pm 1.49$  mg/g in Soxhlet extract, possibly due to the heat applied during Soxhlet extraction, which may degrade thermolabile bioactive compounds (Raghu and Velayudhannair, 2023). Similarly, Shi et al. (2025) examined methods for extracting camellia oil using cold-pressing oil extraction (CPE), Soxhlet extraction, aqueous enzymatic extraction (AEE), and supercritical carbon dioxide extraction (SC-CO<sub>2</sub>). Based on the data, Soxhlet extraction using 18 g of dried powder camellia seeds and petroleum ether as a solvent produced the highest lipid yield ( $41.02 \pm 2.34\%$ ), while AEE had the lowest ( $19.27 \pm 0.57\%$ ) ( $n = 3, p < 0.05$ ). However, Soxhlet extraction resulted in the lowest  $\alpha$ -tocopherol content ( $242.95 \pm 42.48$  mg/kg) while, SC-CO<sub>2</sub> resulted in the highest ( $375.24 \pm 48.27$  mg/kg) ( $n = 3, p < 0.05$ ). In this study, Soxhlet extraction was conducted at 30 to 60 °C, while CPE involved no heat, and AEE and SC-CO<sub>2</sub> operated at temperatures up to 50 °C. This suggests that high temperatures in Soxhlet extraction may reduce certain bioactive compounds, such as  $\alpha$ -tocopherol.



**Figure 1.8** Schematic diagram of Soxhlet extraction apparatus consists of a solvent flask, an extraction thimble, and a condenser. Adapted from (Ghenabzia et al., 2023, p. 475)

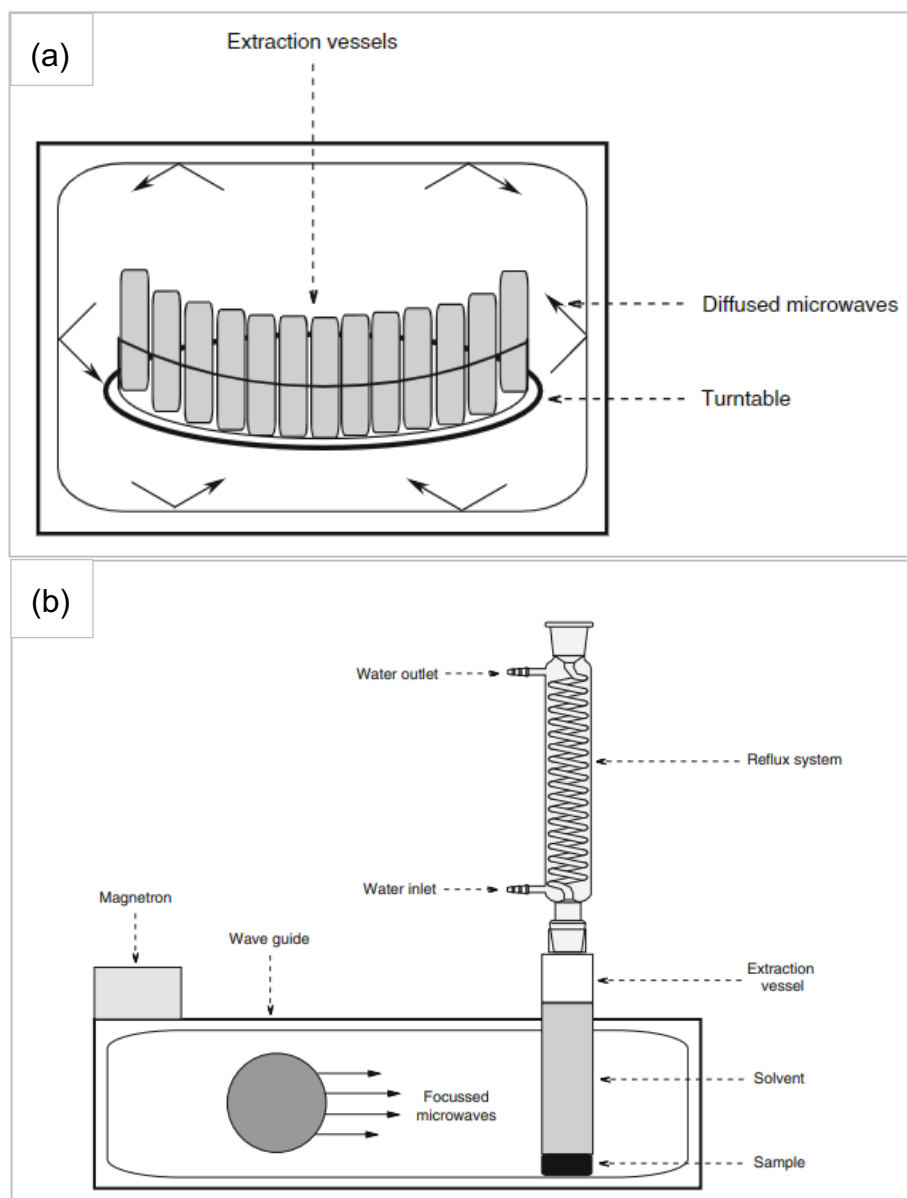
#### **1.2.4.3 Microwave-assisted extraction (MAE)**

Microwave-assisted extraction (MAE) has emerged as a modern extraction technique that combines microwave heating with conventional solvent extraction. Microwaves, which are electromagnetic waves with frequencies between 0.3 and 300 GHz, interact with polar materials and solvents to induce ion migration. This interaction generates localised heating of surface materials, followed by heat transfer through conduction. Additionally, the rotation of molecular dipoles disrupts hydrogen bonds, enhances ion migration, and improves solvent penetration into plant materials (Camel, 2001; Kaufmann and Christen, 2002; Azwanida, 2015). Compared to conventional extraction methods, MAE requires a shorter extraction time and less solvent while offering a higher extraction yield (Delazar et al., 2012).

MAE systems are broadly classified into closed/pressurised and open/focused systems. A closed system typically consists of five main components: extraction vessels, a turntable, a closed chamber, reflectors, and a microwave source (Figure 1.9a). In this system, samples and solvents are enclosed in extraction vessels, where the mixture is heated to a controlled temperature using microwave energy. The closed design enables precise control of extraction parameters, allows simultaneous processing of multiple samples, and is more suitable for volatile compounds (Camel, 2001; Delazar et al., 2012). In an open system, the primary components include a focused microwave source, an extraction vessel, and a water condenser (Figure 1.9b). Only the solvent and sample parts are exposed directly to microwave irradiation within the extraction vessel. Open systems are advantageous for their ability to accommodate larger sample sizes and safer operation at atmospheric pressure. However, extraction temperature is dependent on the solvent's boiling point at an atmospheric pressure (Delazar et al., 2012).

Numerous studies have been conducted to optimise MAE operating conditions such as solvent-to-sample ratio, microwave power, irradiation time, vessel type, and extraction temperature. For instance, Rezaei, S. et al. (2013) applied MAE for extracting polyphenolic compounds from apple pomace, comparing two ethanol-water ratios (65:35, 35:65), three solvent-to-sample ratios (10:1, 20:1, and 30:1), and three different power levels of microwave (90, 180, and 360 W). The results indicated that the optimal conditions for extracting polyphenolic compounds were a 65:35 ethanol-water ratio, a solvent-to-sample ratio of 20:1, and a microwave power of 90 W. More recently, Shang et al. (2020) investigated the effect of various microwave extraction conditions on the antioxidant activity of

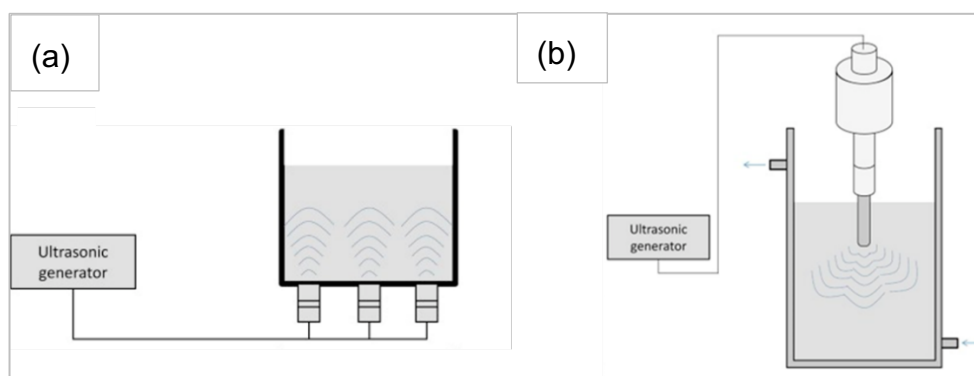
sweet tea (*Lithocarpus polystachyus* Rehd.). The study found that the optimal conditions were at an ethanol concentration of 58.43%, a solvent-to-sample ratio of 35.39:1 mL/g, an irradiation time of 25.26 minutes, a microwave power of 600 W, and an extraction temperature of 50 °C. Given the diversity of extraction parameters reported in the literature, the choice of MAE conditions should be tailored to the specific target compounds and plant materials under study.



**Figure 1.9** Main components for microwave-assisted extraction: (a) a closed system consists of an extraction vessels, a turntable, a closed chamber, reflectors, and a microwave source, (b) an open system with primary components of a focused microwave source, an extraction vessel, and a water condenser. Adapted from (Delazar et al., 2012, p. 93)

#### 1.2.4.4 Ultrasound-assisted extraction (UAE)

Ultrasound-Assisted Extraction (UAE) is a modern extraction technique that utilises ultrasound energy at frequencies exceeding 20 kHz. Figure 1.10 (a-b) illustrates typical setups of ultrasonic equipment. The UAE method operates through three primary mechanisms: thermal, mechanical, and cavitation effects, with cavitation being the most dominant (Tiwari, 2015; Shen et al., 2023). The thermal effect occurs as the medium absorbs ultrasonic energy and releases it as heat (Qiu et al., 2020). The mechanical effect arises from particle vibrations caused by ultrasound, which enhance particle motion and accelerate mass transfer (Wen et al., 2018). Cavitation occurs when ultrasound waves create pressure changes in a liquid, by forming tiny bubbles that grow and collapse. This bubble implosion generates energy critical for the extraction process. UAE offers several advantages, including higher extraction efficiency, shorter extraction times, lower extraction temperatures, reduced solvent usage, and the flexibility to work with solvents and target compounds regardless of polarity. UAE has some drawbacks, including noise from the ultrasonic equipment and the formation of free radicals when extraction occurs above 20 kHz (Handa, 2008; Shen et al., 2023). Chahyadi and Elfahmi (2020) investigated the influence of extraction methods of solvent extraction, boiling, reflux, UAE, and MAE on rutin yield of cassava leaves. The study demonstrated that 2.5 g of cassava leaves extracted using UAE at 50 °C with frequency of 40 kHz achieved the highest extraction efficiency for rutin, reaching 99%, compared to other methods such as microwave-assisted extraction (MAE: 94%), reflux (90%), boiling (83%), and solvent extraction (65%). Similarly, a study by Li et al. (2004), using scanning electron microscopy (SEM), observed that applying UAE for 30 minutes to 3 hours led to the rupture of cell walls in ground soybean flakes, facilitating the release of intracellular components. This process is attributed to the cavitation effect induced by UAE.

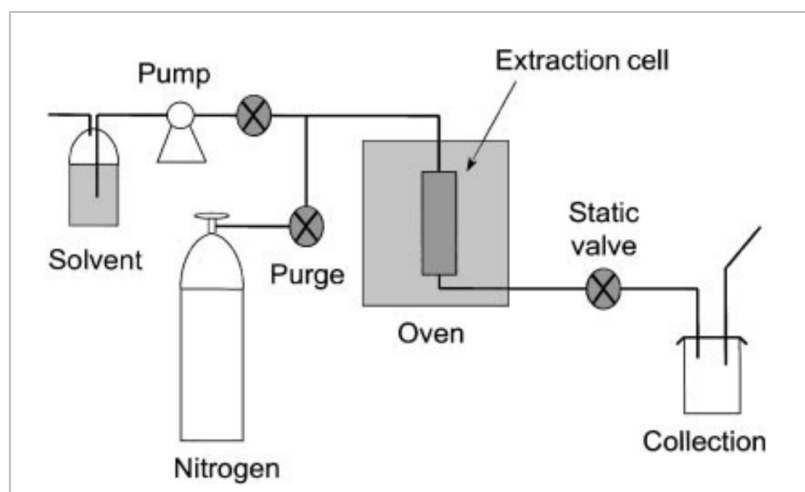


**Figure 1.10** Different UAE setups (a) ultrasonic bath, (b) ultrasonic horn. Adapted from (Tiwari, 2015, p.104)

#### 1.2.4.5 Accelerated solvent extraction (ASE)

Accelerated solvent extraction (ASE), also known as pressurised solvent extraction (PSE), is a technique that employs solvent at elevated temperatures and pressures to enhance extraction kinetics (Kaufmann and Christen, 2002). In this method, the sample is commonly placed in a stainless-steel cell, filled with solvent, and heated to 50 to 200 °C under pressures of 500 to 3000 psi. Excess pressure is controlled by a static valve, with vented solvent collected separately. The sample undergoes a static extraction phase (5 to 10 minutes), followed by rinsing with fresh solvent to clean the sample and tubing. Finally, residual solvent is purged using compressed gas (e.g., nitrogen), and the combined extract and rinse solvent is collected in a vial (Richter et al., 1996; Kaufmann and Christen, 2002). A schematic diagram of ASE is shown in Figure 1.11. ASE is favoured for its short extraction time, reduced solvent usage, and improved analyte solubility and mass transfer. However, its limitations include unsuitability for extracting thermolabile compounds, as high temperatures may compromise their structure and functionality (Richter et al., 1996; Ajila et al., 2011).

A recent study by Fortier et al. (2019) extracted cotton fibre wax using two extraction methods of ASE (4 g cotton in 100 mL ethanol under nitrogen at 150 psi for 1 hour at 140 °C) and Soxhlet extraction (10 g cotton in 250 mL ethanol for 6 hours at 65 °C). Compared to Soxhlet extraction, ASE achieved a lower wax yield ( $0.626 \pm 0.130\%$  vs.  $0.708 \pm 0.102\%$ ,  $n = 36$ ,  $p < 0.05$ ) but causes less fibre surface damage, with smaller SEM-observed defects (1–5  $\mu\text{m}$  vs. 15–25  $\mu\text{m}$ ). In another study, solvent extraction, MAE, UAE, and ASE were performed, and the recovery of polyphenols from citrus peels was compared. The results showed that ASE performed at 120 °C and 1500 psi for 5 minutes with 3 static cycles produced lower total phenolic content values and oxygen radical absorption capacity (ORAC) values compared to MAE, UAE, and solvent extraction methods ( $n = 3$ ,  $p < 0.05$ ). This reduction is likely due to the combined effects of oxidation during the extraction process and interactions between phenolic and non-phenolic compounds (e.g., sugar, fatty acids), which can degrade or alter the phenolic compounds and hinder accurate detection during analysis (Nayak et al., 2015a). Based on the findings, ASE produced lower yield, TPC, and ORAC values, however it caused less damage to cotton fibre, probably due to the shorter extraction time compared to Soxhlet. These findings underscore a key limitation of the ASE method, as a higher extraction temperature likely reduces the extraction yield and the biological activities.



**Figure 1.11** Schematic diagram of ASE system utilising high temperatures and pressures.

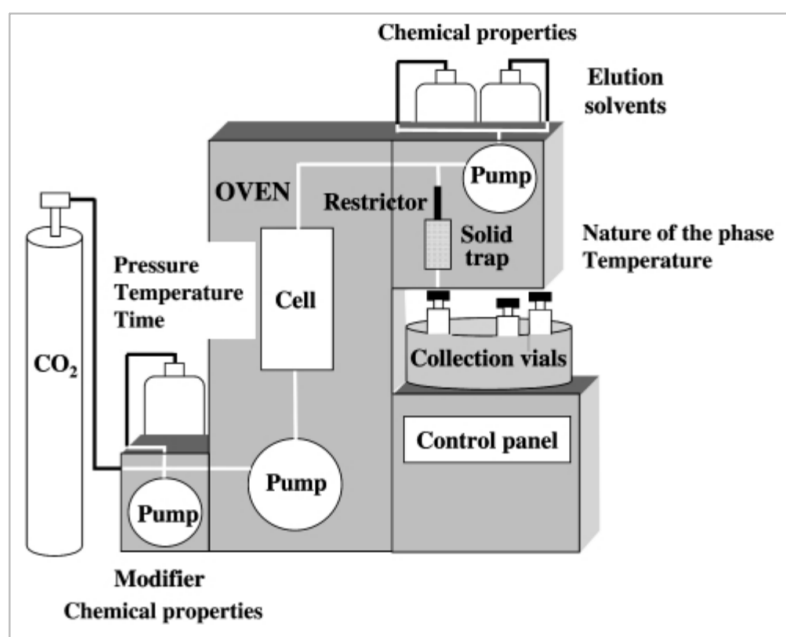
Adapted from (Richter et al., 1996, p. 1034)

#### 1.2.4.6 Supercritical fluid extraction (SFE)

A supercritical fluid is a homogeneous fluid formed at temperatures and pressures exceeding its critical point (Nahar and Sarker, 2012). In supercritical fluid extraction (SFE), supercritical fluids, most commonly carbon dioxide ( $\text{CO}_2$ ) are used as the extraction medium instead of traditional organic solvents. A standard SFE system comprises a high-pressure pump and an extraction cell (Figure 1.12). The fluid, often combined with an organic solvent or modifier, is delivered into the extraction cell to enhance the efficiency of the process. At the restrictor's outlet, depressurised fluid allows analytes to be trapped in an organic solvent or on a solid-phase cartridge, from which they are eluted with a small solvent volume (2 to 5 mL). The choice of trapping conditions such as solvent, solid phase, and temperature is crucial for efficient recovery of extract (Camel, 2001). SFE using  $\text{CO}_2$  offers notable advantages, including its nontoxic nature, high selectivity, absence of harmful residues, and simplified solvent recovery. However, it also has limitations. As  $\text{CO}_2$  is nonpolar, the extraction process is more effective for nonpolar compounds. When modifiers are added to enable the extraction of polar compounds, challenges arise, including alterations to the critical pressure and temperature values. Additionally, optimisation becomes complex and labour-intensive, and the equipment incurs higher operational costs (Camel, 2001; Nahar and Sarker, 2012).

SFE has been extensively used for the extraction of essential oils, valorisation of by-products as well as for the extraction of many other natural products. For example, carotenoids have been successfully extracted from mango peel using SFE under optimal parameters: 25 MPa pressure, 15% w/w ethanol as a modifier,

and a temperature of 60 °C. This process yielded 1.9 mg of all-*trans*-β-carotene equivalents per gram of dried mango peel. Notably, the extract demonstrated strong antioxidant properties by inhibiting lipid oxidation in sunflower oil, suggesting its potential application as a natural antioxidant additive (Sanchez-Camargo et al., 2019). In another study, Conde-Hernandez et al. (2017) compared SFE with hydro distillation and steam distillation for extracting rosemary essential oils. Analysis using Gas Chromatography-Mass Spectrometry (GC-MS) revealed that SFE produced a greater yield of essential oils, with camphor, β-caryophyllene, and eucalyptol as the predominant components. Furthermore, oils extracted via SFE exhibited superior antioxidant activity compared to those obtained through traditional methods. These findings highlight the advantages of SFE for extracting essential oils and other nonpolar compounds, offering both higher efficiency and enhanced extract quality. Nevertheless, this method is only effective for extracting nonpolar compounds, which underscores its limitation in extracting polar compounds.



**Figure 1.12** A schematic diagram of SFE comprises a high-pressure pump and an extraction cell.  
Adapted from (Camel, 2001, p. 1183)

### 1.2.5 Microorganisms in nature

Microorganisms, often referred to as microbes, are organisms that are too small to be observed with the naked eye, making them microscopic in nature. They are ubiquitous in the environment and exist in diverse forms, including unicellular (single-celled), multicellular, or complex organisms. Microbes inhabit a wide range of environments, including soil, water, air, and even extreme conditions. The classification of microbes encompasses algae, archaea, bacteria, fungi, protozoa, multicellular animal parasites, and viruses (LibreTexts, 2024). While all these groups have garnered significant interest from researchers worldwide, this study focuses specifically on bacterial and fungal species.

Bacteria exhibit various shapes, including spherical, rod-shaped, curved rods, and spiral forms, with sizes typically ranging from 0.5 to 5  $\mu\text{m}$  in diameter. They are commonly differentiated using the Gram staining method, which classifies them as either Gram-positive or Gram-negative. Gram-positive bacteria possess a thick (~40 nm) peptidoglycan cell wall that stains purple under a microscope, whereas Gram-negative bacteria have a thinner (~2 nm) peptidoglycan layer surrounded by an outer membrane, appearing pink under the microscope (Wessner et al., 2020). Both Gram-positive and Gram-negative bacteria include beneficial and pathogenic species. For instance, beneficial lactic acid bacteria, such as *Lactobacillus bulgaricus* and *Streptococcus thermophilus*, play an essential role in the food industry as starter cultures in yogurt production (Ayivi and Ibrahim, 2022). Conversely, pathogenic bacteria have caused millions of infections globally, resulting in numerous hospitalisations over the years (Wessner et al., 2020).

Fungi are heterotrophic organisms that derive energy by utilising organic compounds. Unlike bacteria, fungi possess a cell wall composed of chitin, which provides structural support and integrity. Like bacteria, fungi are widely distributed in nature and include both beneficial and pathogenic species. Beneficial fungi, such as *Penicillium* species and *Saccharomyces cerevisiae*, play significant roles in various industries. *Penicillium* is instrumental in the production of the antibiotic penicillin, while *S. cerevisiae* is widely used in baking and fermentation processes (Wessner et al., 2020). Further details regarding pathogenic bacteria and fungi are discussed in Section 1.2.5.1.

### 1.2.5.1 Pathogenic bacteria and fungi in food

Foodborne pathogens encompass bacteria, viruses, parasites, or toxic chemicals present in food, which, when ingested, can lead to foodborne illnesses (WHO, 2024c). These illnesses are broadly categorised into foodborne intoxications and foodborne infections. Foodborne infections occur when individuals consume the live organisms, whereas foodborne intoxications result from ingesting toxins produced by microorganisms, even in the absence of the organisms themselves (Wessner et al., 2020). Symptoms of foodborne illnesses range from mild, such as diarrhoea, nausea, and vomiting, to severe, including life-threatening complications. Severe cases occur when foodborne pathogens multiply in the intestines and release harmful toxins or chemicals into the human body. Globally, over 200 foodborne diseases have been documented to date (Linscott, 2011; Wessner et al., 2020). Bacteria are responsible for approximately two-thirds of foodborne disease outbreaks globally, with *Salmonella* spp., *Staphylococcus aureus* and *Escherichia coli* being the most common pathogens. Other significant bacterial pathogens include *Bacillus cereus*, *Campylobacter jejuni*, *Clostridium botulinum*, *Clostridium perfringens*, *Listeria monocytogenes*, and *Shigella* spp. (Bintsis, 2017). Besides bacteria, viruses (e.g., norovirus, astrovirus, rotavirus) and protozoans (e.g., *Giardia duodenalis*, *Cryptosporidium* spp.) are also the major causes of foodborne illnesses. Table 1.6 presents the common examples of bacteria foodborne pathogens.

**Table 1.6** Common foodborne pathogens found in food commodities that were responsible for the outbreak.

<b>Bacteria</b>	<b>Description</b>	<b>Common sources of contamination</b>	<b>Example of outbreak</b>	<b>Source</b>
<i>Bacillus cereus</i>	Gram-positive, rod-shaped, motile, spore forming, facultative aerobic	Meat and poultry, vegetables, milk and milk products, fried and cooked rice, pasta salad, noodles	In August 1990, 485 individuals in Thailand were ill with symptoms of nausea, vomiting, and abdominal pain caused by <i>B. cereus</i> toxin in cream-filled eclairs.	(Thaikruea et al., 1995; Bintsis, 2017)
<i>Campylobacter</i> spp.	Gram-negative, spiral shaped, motile, microaerophilic	Raw or undercooked poultry, meat, unpasteurised milk, or cross contamination from other foods	In May 2012, 44 people fell ill from undercooked chicken liver pate in Sweden, positive for <i>Campylobacter</i> spp.	(Bintsis, 2017; Lahti et al., 2017; Abebe et al., 2020)
<i>Clostridium botulinum</i>	Gram-positive, rod-shaped, motile, spore-forming, anaerobic	Honey, fish, meat, vegetables, infant and canned foods	In March 2006, 209 botulism cases were reported in Thailand linked to contaminated home-canned bamboo shoots.	(Ungchusak et al., 2007; Bintsis, 2017)
<i>Clostridium perfringens</i>	Gram-positive, rod-shaped, nonmotile, spore-forming, anaerobic	Beef, poultry, pork	In June 2012, <i>C. perfringens</i> outbreak was reported in England for 15 care home residents due to consumption of mince and vegetable pie and/or gravy.	(Acheson et al., 2016; Bintsis, 2017)
<i>Escherichia coli</i>	Gram-negative, rod-shaped, motile, non-spore forming, facultative anaerobic	Fresh produce, undercooked ground meat	In May 2011, 4075 cases of Shiga-toxin producing <i>E. coli</i> (O104:H4) were reported in Germany and 15 other countries.	(Abebe et al., 2020; WHO, 2024a)

**Table 1.6 Continued**

<b>Bacteria</b>	<b>Description</b>	<b>Common sources of contamination</b>	<b>Example of outbreak</b>	<b>Source</b>
<i>Listeria monocytogenes</i>	Gram-positive, rod-shaped, motile, non-spore forming, facultative anaerobic	Uncooked meats and vegetables, deli meat, ready-to-eat meat products, soft cheeses, cold smoked fishery products	In 2011 (August - October), 147 people were ill after consumed contaminated cantaloupe with 33 of deaths reported.	(McCollum et al., 2013; Abebe et al., 2020; WHO, 2024d)
<i>Salmonella</i> spp.	Gram-negative, rod-shaped, non-spore forming, relatively anaerobic	Eggs, meat, poultry	In 2012 (January - July), 425 <i>Salmonella</i> spp. cases linked to frozen raw yellowfin tuna were reported in Washington, D.C., USA, resulting in 55 hospitalizations.	(CDC, 2012; Abebe et al., 2020)
<i>Shigella</i> spp.	Gram-negative, rod-shaped, non-motile, non-spore forming, facultative anaerobic	Milk, salads, chicken, shellfish, fresh produce	In August 1998, 21 of 65 Minnesota football players developed shigellosis after consuming cold sandwiches prepared during a flight.	(Hedberg et al., 1992; Bintsis, 2017)
<i>Staphylococcus aureus</i>	Gram-positive, sphere-shaped (cocci), non-motile, facultative anaerobic	Ground beef, pork sausage, ground turkey, oysters, shrimp, cream pies, milk, delicatessen salads	In October 2018, food poisoning involving 352 primary school children in Ninh Binh Province, Vietnam after having lunch (chicken floss) at the school canteen.	(Bintsis, 2017; Abebe et al., 2020; Le, H.H.T. et al., 2021)
<i>Vibrio</i> spp.	Gram-negative, straight or curved rods, non-spore forming, motile, facultative anaerobic	Raw or undercooked oysters, crabs, prawns, scallops, seaweed, clams	From 2010 – 2014, 71 outbreaks were reported in China, resulting 933 illnesses and 117 hospitalisations due to <i>Vibrio parahaemolyticus</i>	(Bintsis, 2017; Chen, J. et al., 2017)

In addition to food contamination caused by foodborne pathogens, foods can also undergo spoilage that leads to quality deterioration. Food spoilage refers to the decline in food quality and safety, resulting in changes in texture, taste, or appearance, rendering it unsuitable or unsafe for consumption. Spoilage can result from various factors, including physical, chemical, and microbial influences such as exposure to air, temperature fluctuations, and the growth of bacteria, fungi (moulds and yeast). While not all spoilage poses a direct health risk, it still leads to the loss of valuable food resources (Amit et al., 2017). Perishable and semi-perishable foods like fresh vegetables, fruits, and meats are particularly prone to spoilage due to their high water activity ( $a_w$ ). The  $a_w$  of foods generally ranges from 0.20 to 0.99, with lower values found in very dry foods and higher values observed in moist, fresh foods (FSA-Ireland, 2022). Water activity above 0.91 provides an ideal condition for microbial growth, and most fresh foods have an  $a_w$  between 0.96 and 0.99. Moulds are more prevalent in fruits due to their lower pH, which moulds tolerate better than bacteria. Conversely, vegetables, with a nearly neutral pH, typically experience bacterial spoilage, as bacteria outcompete fungi in such conditions (Wessner et al., 2020). Fungal and moulds spoilage in food is often identified by visual growth on the surface, the formation of metabolites causing off-odours and flavours, and changes in colour or texture. Common spoilage microorganisms include *Candida* spp., *Penicillium* spp., *Aspergillus* spp., *Cladosporium*, *Pseudomonas*, *E. coli*, and *Campylobacter* (Ledenbach and Marshall, 2009; Garnier et al., 2017). Table 1.7 further details the common occurrence of food spoilage with associated microorganisms.

**Table 1.7** Food spoilage microorganisms in food commodities, adapted from (Wessner et al., 2020, p. 590).

Food	Microbial substrates	Spoilage reactions	Effects of spoilage	Common spoilage organisms
Fruits, vegetables	Pectin	Hydrolysis	Soft rot, loss of fruit structure	Bacteria: <i>Erwinia</i> , <i>Pseudomonas</i> , <i>Corynebacterium</i>
	Sugars	Fermentations	Souring, acidification	Fungi: <i>Aspergillus</i> , <i>Botrytis</i> , <i>Rhizopus</i> , <i>Penicillium</i> , <i>Alternaria</i> , various yeasts
Fresh meat, poultry, seafood	Proteins	Proteolysis, deamination	Bitterness, souring, bad odour, sliminess	Bacteria: <i>Acinetobacter</i> , <i>Aeromonas</i> , <i>Campylobacter</i> , <i>Escherichia</i> , <i>Listeria</i> , <i>Micrococcus</i> , <i>Pseudomonas</i> , <i>Salmonella</i>
	Carbohydrates	Hydrolysis, fermentations	Souring, acidification	Fungi: <i>Candida</i> , <i>Cladosporium</i> , <i>Mucor</i> , <i>Penicillium</i> , <i>Rhizopus</i> , <i>Rhodotorula</i> , <i>Sporotrichium</i>
Milk	Lactose	Hydrolysis, fermentations	Souring, clumping	Bacteria: lactic acid bacteria (including <i>Streptococcus</i> , <i>Leuconostoc</i> , <i>Lactococcus</i> , <i>Lactobacillus</i> ), <i>Pseudomonas</i> , <i>Proteus</i>
	Proteins (casein)	Proteolysis, deamination	Bitterness, souring, foul odour, sliminess	Fungi: <i>Candida</i> , <i>Geotrichum</i>

The impact of foodborne pathogens and food spoilage microorganisms poses a significant challenge to the food industry, with the potential to strain healthcare systems and disrupt the normal function in the society, such as increase in the hospital cost due to inpatients and outpatients visit, loss of earnings, and work reorganisation cost to the employer due to employee sick absence (Daniel et al., 2020). Furthermore, food contamination caused by these microorganisms contributes to substantial food loss throughout the supply chain, ultimately leading to food waste (FAO, 2019). This exacerbates issues related to food security, creating additional challenges. To address these issues, various preventive and control measures have been implemented. These include good manufacturing and hygiene practices, reducing the water activity ( $a_w$ ) of foods through freeze-drying, controlling temperature by refrigeration or pasteurisation, adding preservatives, irradiating food by exposing the food to electron beams, X-rays or gamma rays, and employing advanced packaging methods (Garnier et al., 2017; Wessner et al., 2020; Food Standard Agency, 2022). With regard to advanced packaging methods, numerous reports demonstrated the critical role of active antimicrobial packaging, especially through the incorporation of substances derived from plants in inhibiting foodborne pathogens (Sung et al., 2013; Nur Amila Najwa et al., 2020; Valizadeh et al., 2024). Investigation into antimicrobial activities and potential uses of the plant extracts in packaging materials has regained momentum over the past few years. Therefore, one of the significances of this research is that it can advance the understanding on the antimicrobial properties of active plant extracts from *C. asiatica*, *G. atroviridis*, and *G. gnemon* against foodborne pathogens and spoilage microorganisms prior to their use as packaging materials. Further details on the packaging are discussed in the next section, Section 1.2.6.

### 1.2.6 Food Packaging

According to the Department of Environment, Food and Rural Affairs (DEFRA), (2010), packaging is defined as any materials of products in different forms used to serve the purposes such as containment, protection, handling, delivery and preservation of goods from the producer to the end user (Department of Environment, Food and Rural Affairs, 2010, cited in Dobson and Yadav, 2012, p.3). Food packaging can be broadly classified into three types: passive, intelligent, and active packaging. Passive packaging is the conventional food packaging application with the aim of protecting the food from air and moisture without interaction with the food materials. Passive packaging materials could be either plastic, boxes, or cans (Nicoletti and Serrone, 2017). Food manufacturers predominantly use plastic packaging to display their products at retail stores, especially for fresh produce and meat products since the usage of those types of packaging is accustomed to a low cost, being thin, lightweight, and durable, whilst the transparent characteristics of the plastic allow the consumer to visually inspect the quality of products (Eldesouky et al., 2015).

However, prolonged use of traditional/passive plastic packaging has become unfavourable to the environment since plastic is a non-biodegradable resource and has remained in the environment for many years. In addition, plastic poses a threat to human health due to the risk of hazardous chemical substances leaking from the packaging material such as bisphenol A and di-(2-ethylhexyl)phthalate (DEHP) (North and Halden, 2013). In addition, the ocean has become the illegal dumping ground of plastic waste that extremely endangers marine life with the likelihood of ingestion, suffocation, and entanglement of the plastic by marine species (IUCN, 2024). With recent technological advancements, more research has been conducted to address the challenges arising from the use of plastic by developing sustainable alternatives to replace conventional plastic packaging. As a result, materials derived from natural (e.g., plants and animals) and food-grade sources are becoming viable options.

The development variety of packaging materials including the intelligent and active packaging has been of great interest to researchers and manufacturers. Intelligent packaging is defined as “packaging that contains an external or internal indicator to provide information about aspects of the history of the package and/or the quality of the food” (Robertson, G., 2013b, p. 402). Active packaging is a food packaging technology where active substances are intentionally incorporated into or onto the packaging materials to improve product quality and safety. Currently, several types of widely accepted active packaging which includes antimicrobial,

oxygen absorbers, carbon dioxide emitters and absorbers, moisture regulators, and flavour releasers and absorbers (Robertson, G., 2013b). The specific role of active packaging varies depending on its type and function. For instance, oxygen absorbers, as the name suggests, remove residual oxygen from food packages. These are typically used in the form of porous sachets containing iron powder, which reacts with oxygen to form iron oxide (Ozdemir and Floros, 2004). On the other hand, antimicrobial packaging employs the incorporation of active antimicrobial substances (e.g. organic acids and their salts, fungicides, enzymes, plant extracts) into the food packaging materials, and it can be directly incorporated into the packaging materials or introduced by means of surface attachment or coating (Robertson, G., 2013b). The use of antimicrobial packaging enables the controlled release of active antimicrobial constituents from the packaging material to the food surface over time. One of the mechanisms of release in active antimicrobial packaging films is polymer swelling caused by the diffusion of water molecules into the polymer matrix. For instance, a slower release rate of antimicrobials achieved when hydrophobic compounds are incorporated, resulting in a slower hydration process as well as reduced diffusion of active agents from the film matrix (Ouattara et al., 2000; Ozdemir and Floros, 2003; Mastromatteo et al., 2010; Arcan and Yemenicioglu, 2013). In addition, active packaging can also be produced through the attachment of amine-terminated bioactive molecules to the polymer matrix via covalent linkages (Barish and Goddard, 2011). This approach has proven to be more effective than direct spraying or dripping, where the active agents rapidly diffuse onto the food surface and are often denatured by interactions with food components (Quintavalla and Vicini, 2002).

#### **1.2.6.1 Biodegradable and active antimicrobial film**

Over the past few years, the demand for biobased and biodegradable materials has surged across various sectors of the food packaging industry, particularly in the development of single-use plastics for meat, poultry, and fresh produce's application. According to European Bioplastics (2024), global bioplastic production is projected to grow from 2.47 million tonnes in 2024 to 5.73 million tonnes by 2029. According to American Society for Testing and Materials (ASTM), biobased plastic contains organic carbon from renewable resources, while biodegradable plastics are the plastic that is degradable into smaller fragments through the action of bacteria, fungi, and algae under suitable conditions (Robertson, G., 2013c; Pires et al., 2022). In brief, biodegradation occurs through two main stages. The first stage, depolymerisation/ chain cleavage, involves breaking down long polymer chains into smaller oligomeric

fragments. The second stage, mineralisation, occurs within cells, where these fragments are further transformed into biomass, minerals, salts, water, and gases. Several factors affect the biodegradation process, including environmental conditions, the material's chemical structure, crystallinity, and molecular weight. While not all biobased packaging materials are biodegradable, most materials derived from plants and animals are considered both biobased and biodegradable (Robertson, G., 2013c).

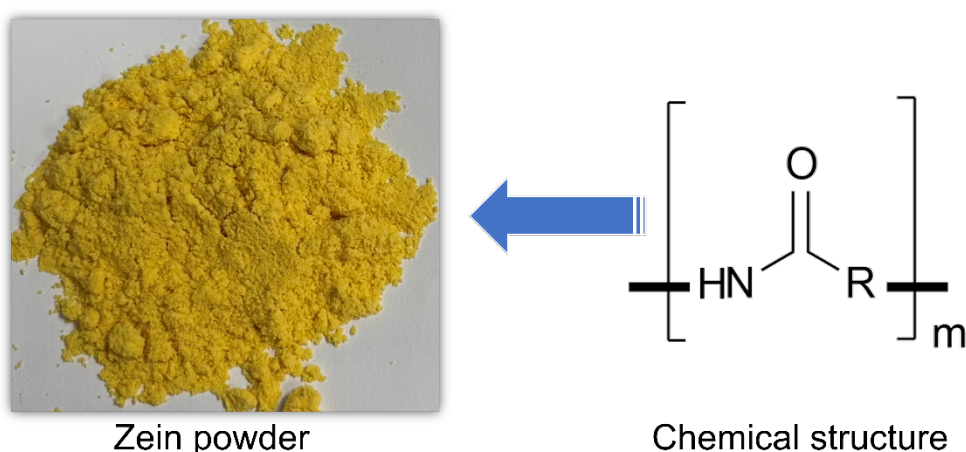
In the context of producing active antimicrobial film packaging from biodegradable resources, primary materials such as polysaccharides and proteins have garnered significant interest. Polysaccharides are complex carbohydrates composed of monosaccharide units linked by glycosidic bonds. They exist in various forms, including starch, cellulose, hemicellulose, chitosan, and gums. The use of polysaccharides as biobased and biodegradable films has attracted considerable attention due to their numerous advantageous properties. These include their abundance in nature, non-toxic, low cost, excellent film-forming capabilities, and strong mechanical and gas barrier properties. Additionally, polysaccharide-based films serve as effective barriers against oil and lipids, making them highly suitable for sustainable packaging applications (Robertson, G., 2013c). However, polysaccharide-based films also have drawbacks, such as lower water resistance and weaker water vapor barrier properties compared to conventional plastic films (Yang, L. and Paulson, 2000).

Films developed from animal- and plant-based proteins, such as collagen, gelatine, wheat gluten, zein (derived from corn), soy protein, whey protein, and casein, also offer valuable properties. Protein-based films are known for their good mechanical and optical characteristics, as well as their strong barrier properties against oxygen, carbon dioxide, aromas, and lipids. However, they tend to exhibit high water vapour permeability. To enhance the performance of biodegradable films, additives such as plasticisers, emulsifiers, antimicrobials, and antioxidants are often incorporated (Robertson, G., 2013c). Since this present study focuses on developing biobased and biodegradable films from zein with the addition of antimicrobial agents, the following section, Section 1.2.6.2 will provide a detailed discussion of zein as a film packaging material and explore the incorporation of antimicrobial agents on its properties.

#### **1.2.6.2 Zein as film packaging**

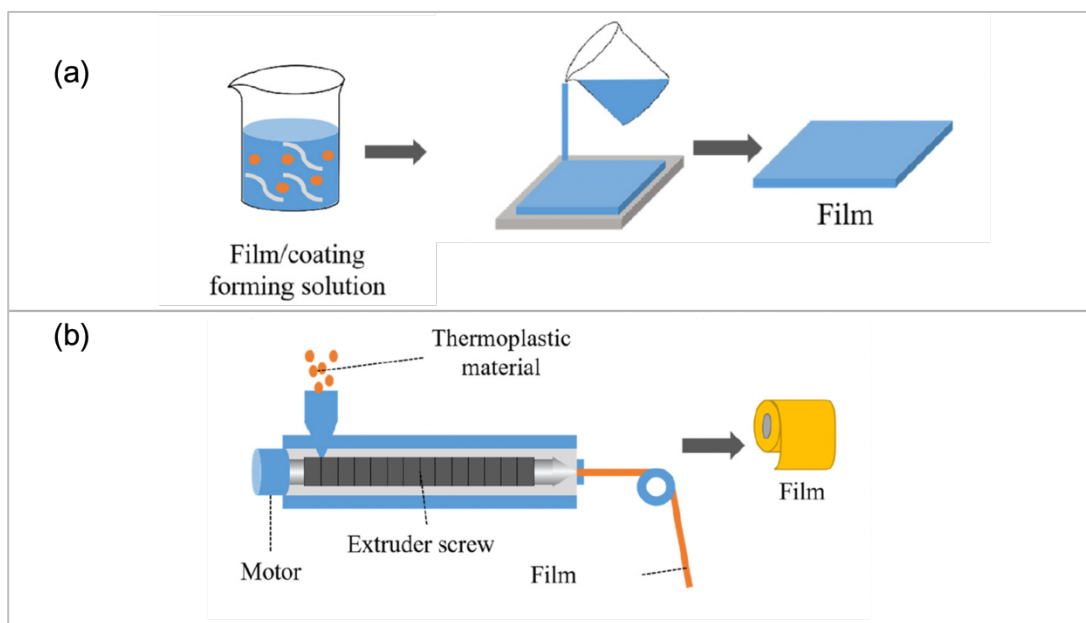
The corn wet milling industry operates by separating corn kernels into their primary components, starch, and various by-products. One significant by-product

of this process is corn gluten meal, which is primarily used as feed for animals and poultry. Corn gluten meal can be further processed to extract zein (Figure 1.13), a class of prolamins that constitutes 65–68% of the total protein content in corn gluten meal (Neumann et al., 1984, Hardwick and Glatz, 1989, cited in Zheng et al., 2014, p. 496). Zein is categorised into four distinct classes according to their solubility and sequence homology:  $\alpha$ -zein,  $\beta$ -zein,  $\gamma$ -zein, and  $\delta$ -zein. The first three classes account for 75-80%, 10-15%, and 10-15% of the total zein, respectively. The majority of the commercially available zein is composed of  $\alpha$ -zein and a minor proportion of  $\beta$ -zein and  $\gamma$ -zein (Wilson, 1991; Woo et al., 2001).  $\delta$ -zein constitutes of only a small fraction of the overall zein content (Esen, 1987). Zein consists of non-polar amino acids such as leucine, proline, and alanine, which contribute to its natural insolubility in water. However, it is deficient in essential amino acids like lysine and tryptophan, which are crucial for human nutrition (Shukla and Cheryan, 2001; Sharif et al., 2019). It is hydrophobic in nature but soluble in alcohol, with a molecular weight ranging from 10 to 27 kDa (Wilson, 1991, cited in Anderson and Lamsa, 2011, p. 160). The U.S. Food and Drug Administration (FDA) has classified zein as a generally recognized as safe (GRAS) product (FDA, 2024). The utilisation of zein spans various industries, including food, packaging, pharmaceuticals, cosmetics, coating agents, and adhesives. In the context of food packaging, zein's properties such as being non-toxic, hydrophobic, good biocompatibility, and having excellent film-forming capabilities make it particularly valuable as primary packaging material (Shukla and Cheryan, 2001; Corradini et al., 2014).



**Figure 1.13** Visual appearance of zein powder obtained from the commercial supplier and the polypeptide backbone of zein consists of amide group (-NH-), carbonyl group (C=O), amino acid side chain (R) with  $m$  representing the number of repeating amino acid units in the zein polypeptide chain (Magoshi et al., 1992; Forato et al., 1998; Mohammed-Ziegler and Billes, 2002; Sun et al., 2023, p.2).

Currently, several methods are employed to produce zein films and other biobased, biodegradable polymers, including solvent casting, extrusion, and electrospinning. Solvent casting, regarded as a conventional method for preparing zein films, is commonly performed at the laboratory scale. This method typically involves preparing a biopolymer solution, spreading the solution onto a mould, and then allowing it to dry (Figure 1.14a) (Rhim et al., 2006; Ribeiro et al., 2021). The advantages of solvent casting include its simplicity, low cost, and the absence of heating, which makes it suitable for thermolabile components. However, it has notable drawbacks, such as its unsuitability for mass production and the risk of wrinkling or tearing during the peeling process of the film (Dhumal and Sarkar, 2018; Suhag et al., 2020; Wang, Q. et al., 2022). On the other hand, extrusion is a widely used method for producing film packaging, including zein films, at an industrial scale. In general, solid biopolymer materials and additives are heated above their glass transition temperature, converted into a melt, mixed, extruded through a nozzle, and then cooled into a film (Figure 1.14b) (Wang, Q. et al., 2022). Extrusion offers several advantages, including short processing times, no solvent use, and ease of handling high-viscosity polymers. It also allows for better control of feed residence time (an extrusion parameter that determines the amount of time polymer melt spends inside the extruder from feeding to exit) and mixing efficiency. However, the method has some disadvantages, such as higher initial and maintenance costs, and is limited to biopolymers that can withstand high temperatures ranging from 70 to 500 °C depending on the processing conditions (Altomare and Ghossi, 1986; van Duin et al., 2001; Liu, H. et al., 2009; Suhag et al., 2020; Wang, Q. et al., 2022).

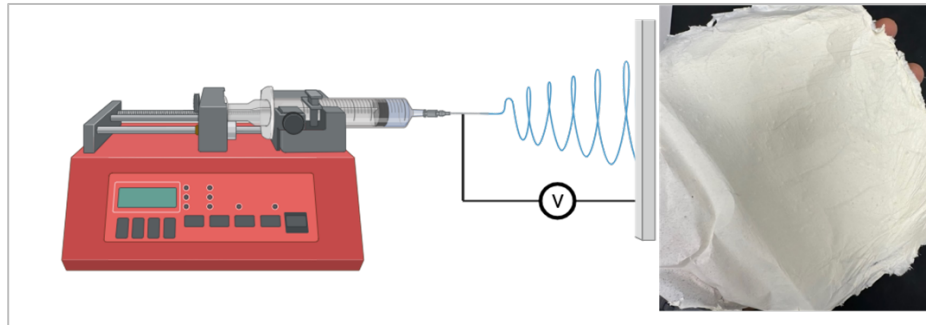


**Figure 1.14** Biodegradable and active film preparation via (a) solvent casting by spreading the solution onto a mould, (b) extrusion where the solid biopolymer materials are heated, converted into a melt, extruded through a nozzle, and cooled into a film.

Adapted from (Wang, Q. et al., 2022, p. 6)

Electrospinning is a film production technology capable of creating films with fibre diameters ranging from nanoscale to microscale. Its growing application in film packaging is driven by its flexibility, cost-effectiveness, non-thermal process, high encapsulation, and its ability to produce materials with a high surface-to-volume ratio and customisable morphology (Anu Bhushani and Anandharamakrishnan, 2014). A basic electrospinning setup comprises three main components: a solution reservoir with a spinneret, a grounded metallic collector, and a high-voltage power supply ranging from 1 to 30 kV (Figure 1.15) (Kriegel et al., 2008; Kong, L. and Ziegler, 2014). To produce nanofibers, a polymer solution is pumped through a needle under suitable voltage, forming a charged droplet that elongates into a Taylor cone at the needle tip. Electrostatic forces then overcome surface tension, ejecting the solution as a jet that stretches and deposits nanofibers onto the collector (Doshi and Reneker, 1995; Andradý, 2008). Initially, the jet formation from the Taylor cone follows a straight path; however, due to electrohydrodynamic instability, the jet begins to whip rapidly before being deposited onto the collector (Reneker and Chun, 1996, cited in Rezaei, A. et al., 2015, p. 270). The formation of fibres during electrospinning is influenced by various factors, including process parameters (e.g., applied voltage, solution flow rate, and spinning distance), solution properties (e.g., polymer concentration, viscosity, molecular weight, surface tension, and conductivity), and environmental conditions such as ambient temperature. Typically, the applied voltage ranges from 10 to 21 kV, with a solution flow rate of 0.6 to 3 mL/h and a

spinning distance of 10 to 15 cm from the collector (Andrady, 2008; Rezaei, A. et al., 2015).



**Figure 1.15** Basic electrospinning set-up comprises of a solution reservoir with a spinneret, a grounded metallic collector, and a high-voltage power supply ranging from 1 to 30 kV, created with (Biorender.com).

Biodegradable and active packaging films must meet specific standards and requirements due to their direct use in contact with food. These requirements include acceptable sensory attributes, stability in biochemical, physicochemical, and microbial properties, the absence of toxic components, simple production methods, and cost-effectiveness of both raw materials and manufacturing processes (Debeaufort et al., 1998; Murrieta-Martinez et al., 2018). Additionally, the selection and formulation of packaging film materials must consider their physical, mechanical, and barrier properties (Murrieta-Martinez et al., 2018; Ribeiro et al., 2021). Physical properties are commonly evaluated through measurements like thickness, scanning electron microscopy (SEM), Fourier-transform infrared spectroscopy (FTIR), X-ray diffraction (XRD), thermogravimetric analysis (TGA), and differential scanning calorimetry (DSC). These methods provide valuable information on the film's thickness, surface characteristics, morphology, and thermal behaviour. According to ASTM standards, plastic films should not exceed a thickness of 0.25 mm, while biodegradable and edible films are typically less than 0.3 mm (ASTM, 2010; Senturk Parreidt et al., 2018). Information on mechanical properties, such as the maximum force the film can withstand when it is pulled, the change in length of a film when subjected to tensile force, and an index of the stiffness of thin plastic sheeting are represented by tensile strength, elongation at break (EAB), and Young's modulus (YM) values, respectively. Information on these values are critical in order to maintain food quality during handling and storage within the supply chain (ASTM, 2010; Murrieta-Martinez et al., 2018). These properties are often tested using ASTM Standard D882 (ASTM, 2010). Barrier properties, such as water vapour permeability, gas permeability, and light transmittance, play a critical role in determining the shelf life of food products. These properties assess

the interaction of water, gases, and light with packaging materials, which are primary contributors to the physical and chemical degradation of food (Miller and Krochta, 1997; Germain, 1997, cited in Siracusa et al., 2008, p. 636). In summary, an ideal film packaging film must effectively protect the product, enhance shelf life, ensure safety, and align with sustainability goals while maintaining economic feasibility.

Extensive literature is available demonstrating the potential of zein as an active packaging. For instance, zein films incorporating spent coffee grounds extracts were prepared using a solvent casting technique with glycerol as a plasticiser. The study revealed that incorporating up to 45% spent coffee grounds extract yielded films with acceptable mechanical properties suitable for packaging. The films demonstrated a tensile strength of  $14.21 \pm 3.99$  MPa, EAB of  $0.58 \pm 0.15\%$ , and YM of  $2128.25 \pm 661.24$  MPa, showcasing their potential as sustainable active packaging materials (Drago et al., 2022). While there is no universal standard for tensile strength, EAB, and YM values for biodegradable films, a compilation of data for other types of polymers from agar-based films showed a tensile strength range between 0.11 and 100 MPa, EAB between 0.8 and 200%, and YM between 0.03 and 4150 MPa. In addition, these values could be improved by modifying parameters such as the use of plasticiser, adjusting film thickness, addition of crosslinking agents, and the incorporation of ingredients such as plant extracts (Mostafavi and Zaeim, 2020; Hernandez et al., 2022). A previous study also showed that zein fibres loaded with carvacrol essential oil, produced through electrospinning, exhibited antifungal efficacy by inhibiting 99.6% of mould and fungal growth on wheat bread stored at 25 °C for seven days (Altan et al., 2018). Furthermore, zein films enriched with thyme essential oil, also produced via electrospinning, demonstrated effectiveness in cold storage applications for strawberries. These films reduced weight loss and preserved the anthocyanin content, firmness, and colour of strawberries over a 15-day storage period (Ansarifar and Moradinezhad, 2022). Considering the potential of zein as primary polymer for developing active, biobased and biodegradable packaging materials, it is essential to emphasise further research to enhance its visibility to a broader audience. To date, there has been little to no study conducted on the use of zein and *C. asiatica*/*G. atroviridis*/*G. gnemon* extracts as packaging film employing the electrospinning method. A few studies reported the addition of *G. atroviridis* extract for a film production via solvent casting, and to the best of the author's knowledge, no such studies have been conducted on the other two plants. Therefore, the significance of this research is that it can provide a reference point for the use of these extracts in the development of film packaging and enhance

the knowledge of other researchers of the potential of the plant extracts in food packaging applications.

### **1.2.6.3 Deterioration of food**

Foods can generally be classified into three categories based on their shelf life: perishable, semi-perishable, and non-perishable foods. Perishable foods, such as fresh produce, meat, and poultry, typically have a  $a_w$  above 0.99. Since most bacteria require a minimum  $a_w$  of 0.91 for growth, these foods provide an ideal environment for microbial activity, leading to deterioration and spoilage. Semi-perishable foods, including nuts and potatoes, spoil more slowly than perishable foods but still require proper storage to prolong their shelf life. In contrast, non-perishable foods, such as flour, sugar, and dried beans, remain stable over long storage periods due to their low  $a_w$ , generally around 0.2, which makes them less susceptible to microbial growth and spoilage (Wessner et al., 2020). In all food categories, packaging plays a pivotal role in extending shelf life by minimising exposure to factors that contribute to deterioration. Effective food packaging helps preserve product safety, quality, and nutritional integrity throughout storage and distribution.

Food packaging serves as a protective barrier between food products and their internal and external environments during processing and storage. Without this barrier, food is susceptible to various changes that result in deterioration. The deterioration process is influenced by enzymatic, microbiological, and chemical reactions. In terms of enzymatic reactions, temperature plays a critical role. Lower temperatures in packaged food help slow down enzyme activity, thereby extending shelf life. Additionally,  $a_w$  is closely linked to the rate of enzyme activity, as enzyme activity depends on the amount of water available, and low levels of water can severely restrict enzymatic reactions, therefore controlling  $a_w$  can further inhibit these reactions. Moreover, modifying the packaging environment, particularly the level of oxygen ( $O_2$ ) within the package is also important because many enzyme-catalysed reactions are oxygen-dependent. Microbiological changes are closely related to the presence of microorganisms, with  $a_w$  playing a pivotal role in their growth and activity. For chemical reactions, several processes contribute to food deterioration, including non-enzymatic browning, lipid oxidation, protein denaturation, and protein hydrolysis. The use of specific type of packaging materials with the ability to reduce the food deterioration process due to enzymatic, microbiological and chemical factors can help mitigate these reactions and reduce the rate of deterioration in foods. Food deterioration

negatively affects key attributes such as texture, flavour, colour, appearance, and nutritional value (Robertson, G., 2013d).

Hu et al. (2023) developed allicin-zein (Al-Ze) composite nanoparticle gelatine films and examined the changes in the colour of fresh beef stored at 4 °C during 12 days of storage. The study found that the colour was influenced by the type of films applied, and the addition of allicin in the films effectively delayed the decline of red/green ( $a^*$ ), and yellow/blue ( $b^*$ ) colour of beef. The brightness of beef samples was maintained, indicating the films' potential in reducing deterioration during storage ( $n = 3$ ,  $p < 0.05$ ). Research on the quality of meat, especially beef, continues to attract attention because beef is a highly perishable food with high nutritional value. It is recognised as a rich source of essential nutrients, including protein and micronutrients such as vitamins B6 and B12, zinc, magnesium, selenium, and iron (Williams, 2007). Additionally, beef is a highly perishable food that deteriorates rapidly due to microbial growth. The high susceptibility to spoilage renders it as an ideal example for evaluating the effectiveness of the developed films. Consequently, demonstrating the effectiveness of film in preserving beef may suggest its potential use for other foods, including poultry, fish, fruits, and bakery products. Moreover, deterioration in the quality of beef due to microbial growth is regarded as a food safety issue, as the outbreak often leads to foodborne illness and even death. For instance, the analysed data from USDA showed 129 outbreaks originated from meat and poultry from 2007 to 2012, with approximately 80% of the outbreaks linked to beef (Robertson, K. et al., 2016). Therefore, maintaining the quality of perishable foods, particularly beef, is important in preventing the deterioration process. Recognising the crucial role of packaging materials in preserving foods as well as the high value of beef, this study aimed to evaluate the efficacy of newly developed antimicrobial zein-based films in preserving the quality of raw beef, including the potential to inhibit the growth of foodborne pathogens on raw beef wrapped and stored under chilled conditions.

## 1.3 Aim and objectives

### 1.3.1 Aim of research

The aim of this study is to evaluate the biological potential of extracts from *C. asiatica*, *G. atroviridis*, and *G. gnemon* as active antimicrobial agents for incorporation into biodegradable and biobased zein film, intended for use as antimicrobial wrapping film, with raw beef selected as a food sample representing typical microbial risks in foods.

### 1.3.2 Research questions and research objectives

The research questions (RQ) and research objectives (RO) of this study are:

- RQ1: How do different extraction methods, specifically solvent extraction and microwave-assisted extraction (MAE), along with varying ethanol-to-water ratios (0, 25, 50, 75 and 100), impact the extraction yield and biological activities of plant extracts from *C. asiatica*, *G. atroviridis*, and *G. gnemon*?
- RO1: This study aims to investigate and compare the effects of two extraction methods: solvent extraction and microwave-assisted extraction (MAE) on the yield and biological activities of *C. asiatica*, *G. atroviridis*, and *G. gnemon* extracts. Specifically, it will assess the total phenolic content, antioxidant, and antimicrobial properties of the extracts. The research will also examine how different ethanol ratios of 0, 25, 50, 75 and 100 impact the extraction efficiency and bioactivity. The goal is to identify the optimal extraction conditions that maximise both yield and bioactivity, and ultimately understanding the effective extraction methods for these medicinal plants.
- RQ2: What is the potential for incorporating extracts from *C. asiatica*, *G. atroviridis*, and *G. gnemon* into biodegradable zein-based packaging films, and how do their bioactive properties contribute to the functional characteristics of these films?
- RO2: The objective of this study is to explore the potential of *C. asiatica*, *G. atroviridis*, and *G. gnemon* extracts in the development of biodegradable zein-based films. The properties of the produced films will be evaluated such as thickness, surface morphology, encapsulation efficiency, thermal properties, and biodegradability of the films. This approach aims to create sustainable, functional

packaging that meets the demands for food preservation while reducing environmental impact.

RQ3: How effective are biodegradable and antimicrobial zein-based films in inhibiting the growth of foodborne pathogens and spoilage microorganisms and maintaining the safety and quality of raw beef?

RO3: The objective of this research is to evaluate the efficacy of biodegradable and antimicrobial zein-based films in inhibiting the growth of foodborne pathogens and spoilage microorganisms on raw beef wrapped with the films and stored under chilled conditions, by assessing the microbiological activity, water activity ( $a_w$ ), and colour, and impact on the quality and safety of the raw beef.

## 1.4 Outline of thesis

This study examined the biological properties of three Malaysian medicinal plants extracts and evaluated their potential for the development of active antimicrobial packaging materials, with a focus on their effectiveness in wrapping raw beef. This thesis presents an analysis and summary of the data, organised into six main chapters as outlined below:

This thesis starts with **Chapter 1**, which has been outlined in the previous sections, providing the general background of the study, followed by a literature review covering an extensive review of medicinal plants and secondary metabolites, various extraction methods, the presence of microorganisms in food, food packaging, and an overview of the deterioration process in food.

**Chapter 2** details the materials and methodologies used in this research. The first part of the study detailed the protocols for extraction of Malaysian medicinal plants and evaluation of biological activities. The second part elaborates on the development of active antimicrobial zein-based films using electrospinning and the characterisation of these films, including the measurement of films' thickness, surface morphology, encapsulation efficiency, thermal properties, as well as the investigation into the biodegradability of the films. The third part examines how these films perform during storage of raw beef, determined through the assessment of microbial activity via total plate count method, water activity ( $a_w$ ), and colour analysis.

**Chapter 3** presents the results and discussion of the different extraction methods and the evaluation of those extracts for total phenolic content, antioxidant, and antimicrobial potential, along with the impact of different extraction methods and ethanol ratios on yield and bioactivities. This chapter also assesses the correlation between the total phenolic content and antioxidant activity.

**Chapter 4** discusses the development of zein-based films, using zein as the primary material and incorporating selected plant extracts. It also reviews the properties of these films through various testing methods. Additionally, this chapter also explores the biodegradability potential of developed films.

**Chapter 5** covers the effects of zein-based films on the quality and safety of raw beef stored in a chiller for five days, based on microbiological, water activity ( $a_w$ ) and colour analysis.

**Chapter 6** highlights the general discussion in relation with the findings obtained in Chapters 3 to 5, summarises the main results, outlines the research limitations and the directions for future research, before the overall conclusion of study.

## Chapter 2 Materials and Methodology

### 2.1 Materials and reagents

The use of materials and reagents is divided into three sections based on the work done: extraction and evaluation of biological activity, development of active antimicrobial zein-based films, and storage study. The details of materials and reagents are outlined in Table 2.1, while the use of specific instruments and apparatus is detailed in each experimental procedure.

**Table 2.1** List of materials and reagents.

Section	Material/reagent – Manufacturer/supplier
1. Extraction and evaluation of biological activity	<ul style="list-style-type: none"> <li>• Acetic acid - Sigma-Aldrich, USA</li> <li>• Amphotericin B - Cayman Chemical Company, USA</li> <li>• Brain heart infusion (BHI) agar - Remel, USA</li> <li>• Brain heart infusion (BHI) broth - VWR International, Belgium</li> <li>• Chlorhexidine 99.5% - Sigma-Aldrich, USA</li> <li>• DMSO 99+% - Thermo Fisher Scientific, UK</li> <li>• DPPH - Santa Cruz Biotechnology Inc., USA</li> <li>• Ethanol AR 99.8% - VWR Chemicals, France</li> <li>• Ferric chloride anhydrous - Sigma-Aldrich, USA</li> <li>• Folin-Ciocalteu's reagent - VWR Chemicals, France</li> <li>• Gallic acid - Cayman Chemical Company, USA</li> <li>• Glycerol - Thermo Fisher Scientific, UK</li> <li>• Hydrochloric acid AR 1.18, ~37%, 12.1M - Fisher Scientific, UK</li> <li>• Mueller-Hinton agar (MHA) - BD Difco, USA</li> <li>• Mueller-Hinton broth (MHB) - Oxoid, UK</li> <li>• Paper disc 6mm – VWR International, UK</li> <li>• Phosphate buffer saline - Sigma-Aldrich, USA</li> <li>• Sabouraud dextrose agar (SDA) - Oxoid, UK</li> <li>• Sabouraud dextrose broth (SDB) - BD Difco, USA</li> <li>• Sodium acetate anhydrous - Fluorochem Limited, UK</li> <li>• Sodium carbonate - Fisher Scientific, UK</li> <li>• Sodium chloride - Oxoid, UK</li> <li>• Sodium hydroxide - Sigma-Aldrich, USA</li> <li>• Trolox - ACROS Organics, USA</li> <li>• Whatman filter paper No. 2 - Whatman International Ltd, England</li> <li>• 2,4,6-Tripyridyl-s-triazine (TPTZ) - Santa Cruz Biotechnology Inc., USA</li> <li>• 9 cm diameter petri plate - Fisher Scientific, UK</li> <li>• 96-well flat-bottom microtiter plate - Fisher Scientific, UK</li> <li>• 96-well U-bottom microtiter plate - Fisher Scientific, UK</li> </ul>

**Table 2.1** Continued

<b>Part</b>	<b>Material/reagent – Manufacturer/supplier</b>
2. Development of zein-based films	<ul style="list-style-type: none"><li>• Ethanol AR 99.8% - VWR Chemicals, France</li><li>• BD Emerald 10 mL syringe - BD, Spain</li><li>• Glycerol - Thermo Fisher Scientific, UK</li><li>• Hamilton needle 17 G - Fisher Scientific, UK</li><li>• Zein - Sigma-Aldrich, USA</li></ul>
3. Storage study	<ul style="list-style-type: none"><li>• 0.85% sodium chloride - Oxoid, UK</li><li>• Plate count agar (PCA) - VWR International, Belgium</li></ul>

## 2.2 Sample collection

Three Malaysian medicinal plants were selected: *C. asiatica* ('peria pantai'), *G. atroviridis* ('asam gelugor'), and *G. gnemon* ('belinjau'). Fresh leaves of *C. asiatica* and *G. gnemon* were collected from Kampung Bukit Berangan, Terengganu, Malaysia, in December 2020, while dried fruits of *G. atroviridis* were purchased from a local market in Terengganu, Malaysia. Terengganu is a tropical region with an annual precipitation of 2911 mm and an average temperature of 26.1 °C (Abdullahi et al., 2014). The selection of *C. asiatica* leaves and *G. atroviridis* fruits was based on their primary use in culinary and medicinal applications, while *G. gnemon* leaves were chosen due to their availability. Among the three plant materials, only the fruits of *G. atroviridis* are seasonal. The plant samples were collected in December 2020 mainly based on logistical convenience. As a result, the growth stage of the plants at the time of collection was not determined, and it could not be confirmed whether all three plants were at the same stage of growth. After collection and purchase, the samples were oven dried for three days at 60 °C at the Technology Herbal Centre, Forest Research Institute Malaysia (FRIM), Kuala Lumpur, Malaysia. Samples were identified by a research officer, Dr. Fadzureena Jamaludin from the Natural Products Division, FRIM, and subsequently stored at -20 °C in the Food Technology Laboratory at the School of Food Science and Nutrition, University of Leeds until further use.

## 2.3 Extraction of medicinal plants

Two different extraction methods, solvent extraction, and microwave-assisted extraction (MAE) were conducted for the plant extracts. For solvent extraction, dried plant materials (5 g) were ground and extracted using different ethanol-to-water ratios (0:100, 25:75, 50:50, 75:25, and 100:0) in a total volume of 40 mL for 48 hours at room temperature with occasional shaking (Rukayadi et al., 2013).

Microwave-assisted extraction was conducted using a closed MAE system. To perform MAE, dried ground plant material (5 g) was placed in an Xpress vessel within a microwave digestion system MARS 6, using an output power of 3150 W and frequency 2455 MHz (CEM, USA). Extraction was conducted for 30 min at 50 °C with medium stirrer speed, using the same ethanol-to-water ratios as in solvent extraction (0:100, 25:75, 50:50, 75:25, and 100:0) and a sample-to-solvent ratio of 16:1. The extracts were filtered with Whatman filter paper No. 2 with a vacuum pump, concentrated using a rotary evaporator (Heidolph VV2011, Germany) and centrifugal evaporator (GeneVac EZ-2<sup>plus</sup>, USA) at 40 °C, and freeze-dried to remove any remaining water (freeze-drying is a process in which water is removed by sublimation, transitioning from the solid state to the vapour state, eliminating the liquid state, thereby preserving the biological, nutritional, and organoleptic properties of food/ plant material) (Rezaei, S. et al., 2013; Nowak and Jakubczyk, 2020). The extraction procedure from grounding the dried plants to freeze-drying process was repeated three times. The extracts were stored in sealed bottles at 4 °C. The yield percentage was calculated using Equation 2.1.

$$\text{Yield of extract (\%)} = [m_{\text{final}} (\text{g}) / m_{\text{initial}} (\text{g})] \times 100\% \quad (\text{Eq. 2.1})$$

where,  $m_{\text{final}}$  is the mass of plant extract after freeze-dried,  $m_{\text{initial}}$  is the mass of dried plants.

### 2.3.1 Preparation of plant extract

Plant extracts with a concentration of 10 mg/mL or 1% (w/v) equivalence were used, unless stated otherwise. To make a 10 mg/mL concentration of extract, 10 mg of each extract are dissolved in 1 mL of the respective solvent and vortexed to obtain a homogenous solution. All plant extracts were freshly prepared prior to starting an experiment (Zainin et al., 2013).

## 2.4 Biological activity of extracts

### 2.4.1 Total phenolic content

The antioxidant ability of plants is often associated with phenolic compounds; hence, a preliminary assay of total phenolic content is an important step in assessing the biological activity of the plants (Al-Mansoub et al., 2014; Tan, W.-N. et al., 2019). In this study, *C. asiatica* extract (CAE), *G. atroviridis* extract (GATE) and *G. gnemon* extract (GGE) were subjected to a total phenolic content assay to determine the effect of different ethanol ratios and extraction methods

on the total phenolic content. The reagents essential to the experiment such as gallic acid, Folin-Ciocalteu's reagent and sodium carbonate were prepared prior to the experiment.

The total phenolic content of various extracts was determined using the Folin-Ciocalteu method (Singleton et al., 1999). Extracts (10 mg/mL) and gallic acid standard (0.04 to 0.31 mg/mL) were prepared. In a 96-well flat-bottom plate, 10  $\mu$ L of each extract or standard was mixed with 40  $\mu$ L of 10% (v/v) Folin-Ciocalteu's reagent, shaken thoroughly and left at room temperature for 5 minutes. Then, 150  $\mu$ L of 4% (w/v) sodium carbonate was added, mixed, and allowed to stand for 30 minutes in the dark. Absorbance was measured at 765 nm using a microplate reader (TECAN Spark 10M, Austria). A standard curve for gallic acid was constructed and total phenolic content was expressed as milligrams of gallic acid equivalent per gram of extract (mg GAE/g extract). The experiment was performed in triplicate.

## **2.4.2 Antioxidant assay**

Various scientific methods have been developed to measure antioxidant activity in plants. In this study, the antioxidant capacity of CAE, GATE, and GGE of different extraction methods and ethanol ratios was evaluated using 2,2-diphenyl-1-picrylhydrazyl (DPPH) and ferric reducing antioxidant power (FRAP) methods. The reagents required such as gallic acid, Trolox, DPPH and FRAP solution were prepared prior to the experiment.

### **2.4.2.1 2,2-diphenyl-1-picrylhydrazyl (DPPH) assay**

The DPPH assay was performed to evaluate antioxidant activity in accordance with the methods by Thaipong et al. (2006) with slight modifications. Extracts (5 mg/mL) and gallic acid (1000  $\mu$ g/mL) were prepared. The 96-well flat-bottom plate was filled with 18  $\mu$ L of the plant extracts/ gallic acid, followed by the addition of 180  $\mu$ L of DPPH solution (0.1 mM). The mixture was mixed and allowed to stand in the dark for 30 minutes at room temperature. The absorbance at 517 nm was measured with a microplate reader (TECAN Spark 10M, Austria) with triplicate measurements. The scavenging ability of the samples was evaluated using the percentage of DPPH inhibition (%), calculated using Equation 2.2.

$$\text{DPPH Inhibition (\%)} = [(A_0 - A_s) / A_0] \times 100\% \quad (\text{Eq. 2.2})$$

where,  $A_0$  is the absorbance of the negative control,  $A_s$  is the absorbance of samples and DPPH.

#### **2.4.2.2 Ferric reducing antioxidant power (FRAP) assay**

The FRAP assay was performed according to a previously described protocol with slight modifications (Benzie and Strain, 1999). Extracts (10 mg/mL) and Trolox as a standard (0.016 to 0.50  $\mu$ M) were prepared. Acetate buffer solution (300 mM, pH 3.6) was prepared by weighing 160 mg of sodium acetate and further dissolved in 100 mL of 0.28M acetic acid, and the pH was adjusted by using sodium hydroxide (NaOH) or hydrochloric acid (HCl). 2,4,6-Tripyridyl-s-triazine (TPTZ) solution (5 mM) was prepared by dissolving 156 mg of TPTZ in 100 mL of 40 mM HCl. Ferric chloride ( $\text{FeCl}_3$ ) solution (20 mM) was prepared by dissolving 135 mg of ferric chloride anhydrous in 25 mL of distilled water. Briefly, the FRAP reagent was freshly prepared by mixing acetate buffer, TPTZ solution, and ferric chloride solution at a ratio of 10:1:1 (v/v/v). In a 96-well flat-bottom microtiter plate, 180  $\mu$ L of FRAP reagent and 6  $\mu$ L of plant extract/ Trolox were mixed and incubated for 15 minutes at 37 °C (Thermo Scientific Heratherm Incubator, UK). The absorbance at 593 nm was determined with a microplate reader (TECAN Spark 10M, Austria), and the standard calibration curve was constructed using Trolox. The data were presented as FRAP values ( $\mu$ M TE/g dry weight). All measurements were made in triplicate.

#### **2.4.3 Antimicrobial activity assay**

The antimicrobial properties of CAE, GATE, and GGE were assessed using antimicrobial susceptibility testing, which included disc diffusion assay (DDA), minimum inhibitory concentration (MIC), and minimum bactericidal/fungicidal concentration (MBC/MFC) assays. The DDA served as an initial screening method to evaluate the antimicrobial activity of plant extracts against selected bacterial and yeast species. Based on the DDA results, MIC and MBC/MFC assays were conducted to determine the minimum concentration of an antimicrobial agent required to inhibit microbial growth (MIC) and to kill at least 99% of microorganisms (MBC/MFC), as described by Rukayadi et al. (2013). Plant extracts from CAE, GATE, and GGE were tested at concentrations of 10 mg/mL and 50 mg/mL, alongside positive controls (0.1% (v/v) chlorhexidine (CHX) for bacteria, and 0.1% (v/v) and 5% (v/v) amphotericin B for yeast) and negative controls (10% (v/v) DMSO). Freshly prepared growth media, bacterial and fungal suspensions, and plant extract solutions were used. All media preparation and microbial handling were conducted under aseptic conditions within a Class II Biosafety Cabinet.

#### **2.4.3.1 Plant extracts' preparation**

CAE, GATE, and GGE were utilised in this study at concentrations of 10 mg/mL and 50 mg/mL. The preparation of the 10 mg/mL extract followed the same procedure described in Section 2.3.1, with 10% DMSO serving as the solvent. For the 50 mg/mL concentration, 50 mg of each extract was dissolved in 10% DMSO (Zainin et al., 2013).

#### **2.4.3.2 Preparation of positive and negative test control**

In this study, CHX was used as a positive control for the susceptibility test against foodborne bacteria. A stock solution of CHX was prepared by dissolving 10 mg of CHX powder in 1 mL of distilled water to make up a concentration of 1% (w/v). A volume of 100  $\mu$ L is taken from the stock solution and further diluted with 900  $\mu$ L of distilled water to make a final concentration of 0.1% (v/v) of CHX. The final concentration of 0.1% (v/v) CHX was used in the antibacterial susceptibility test. Amphotericin B was used as a positive control for the antifungal susceptibility test, and similar preparation protocols as for CHX were carried out to obtain 0.1% (v/v) of amphotericin B. For the preparation of 5% (v/v) amphotericin B, 50 mg of amphotericin B was dissolved in 1 mL of distilled water (Rukayadi and Hwang, 2007; Zainin et al., 2013).

For a negative control, a 10% (v/v) DMSO solution was prepared by dissolving 10 mL of DMSO (99.9%) in 90 mL of distilled water. The 10% (v/v) DMSO concentration demonstrated that it did not kill the microorganisms tested in the study carried out by Zainin et al. (2013).

#### **2.4.3.3 Preparation of growth media**

The preparation of agar and broth was carried out in accordance with the manufacturer's instructions. Briefly, a predetermined amount of media powder was weighed and dissolved in distilled water and autoclaved at a specific temperature and time. The preparation details are summarised in Table 2.2.

**Table 2.2** Medium preparation for antimicrobial testing.

Type of media	Preparation procedure			
	Media powder (g)	Deionised water (L)	Autoclave temperature (°C)	Time (min)
Brain Heart Infusion (BHI) agar	52	1.0	121	15
Brain Heart Infusion (BHI) broth	37	1.0	121	15
Mueller Hinton agar (MHA)	38	1.0	121	15
Mueller Hinton broth (MHB)	21	1.0	121	15
Sabouraud dextrose agar (SDA)	65	1.0	121	15
Sabouraud dextrose broth (SDB)	30	1.0	121	15

#### 2.4.3.4 Microbial strains

Six strains of microorganisms were purchased from LGC Standards Limited, UK. The bacterial and fungal strains were selected as representative foodborne pathogens and food spoilage microorganisms commonly found in food commodities and responsible for foodborne outbreaks and spoilage, as discussed in Section 1.2.5.1. Further information on the strains is tabulated in Table 2.3.

**Table 2.3** Microbial strains and growth medium.

Microbial strains	Source	Growth medium
<i>Bacillus cereus</i>	ATCC 14579	Mueller Hinton (MH)
<i>Escherichia coli</i>	ATCC 25922	Mueller Hinton (MH)
<i>Listeria monocytogenes</i>	ATCC 19111	Brain Heart Infusion (BHI)
<i>Salmonella spp.</i>	ATCC 14028	Mueller Hinton (MH)
<i>Staphylococcus aureus</i>	ATCC 25923	Mueller Hinton (MH)
<i>Candida albicans</i>	ATCC 14053	Sabouraud dextrose (SD)

ATCC: American Type Collection Culture (Rockville, MD, USA)

Bacteria and yeast strains were provided in freeze-dried form within stoppered serum vials (Preceptrol cultures). The propagation of these microorganisms was carried out following the protocols outlined in the *Reviving Freeze-Dried Microorganisms Instructional Guide* (ATCC, 2021). In brief for bacteria, the Preceptrol culture vial was opened in accordance with the provided instructions. A total of 5 mL of MH/BHI broth was added to a test tube, and 500 µL of this broth

was withdrawn to rehydrate the bacterial pellet. The resulting suspension was then transferred back to the test tube and mixed thoroughly. A few drops of the bacterial suspension were streaked onto MH/BHI agar plates and incubated for 24 hours at  $37\pm 2$  °C. To ensure viability, the bacteria were subcultured twice before preparing the inoculum for antimicrobial susceptibility testing. For the yeast strain, 500  $\mu$ L of sterile water was used to rehydrate the pellet, and the suspension was transferred into a test tube containing 5 mL of sterile water. The suspension was allowed to stand at room temperature for a few hours before being transferred to SDA/SDB medium. The yeast cultures were incubated at  $37\pm 2$  °C for 48 hours. Similar to the bacteria, the yeast strain was subcultured twice before inoculum preparation for antimicrobial susceptibility testing (ATCC, 2021).

Bacteria/yeast cultures maintained on agar plate can be stored at 4 °C for a few weeks before use. Prior to initiating a new subculture, all stored plates were visually inspected to ensure there was no sign of contamination. Only plates that showed no contamination were streaked onto fresh agar plates for subculture. The newly subcultured plates were then incubated for 24/48 hours (bacteria/fungi), and the resulting growth was examined again to confirm the absence of contamination before proceeding with subsequent experimental procedures. For long-term storage of bacteria and yeast, glycerol stock was prepared by mixing 0.5 mL of overnight culture with 0.5 mL of 50% (v/v) sterile glycerol, vortexed, and stored at -80 °C (Addgene, 2021). All glycerol stock and agar plate cultures were stored accordingly in the Microbiology Laboratory at the School of Food Science and Nutrition, University of Leeds.

#### **2.4.3.5 Inoculum preparation**

The inoculation of bacteria was performed in accordance with the CLSI reference standard M02-A11 using growth method. In brief, bacteria were grown on MH/BHI agar for 24 hours at  $37\pm 2$  °C. The cultured plate was then taken out, and using inoculation loop, three to five well-isolated colonies of bacteria were propagated in 5 mL MH/BHI broth. The broth culture was further incubated at  $37\pm 2$  °C for two to six hours. The turbidity of the bacterial suspension was measured using a spectrophotometer at 625 nm and adjusted with broth/saline medium until it achieved the turbidity equivalent to 0.5 McFarland standard (absorbance 0.08 to 0.13), which resulted in a suspension containing approximately  $10^6$  -  $10^8$  CFU/mL bacteria (CLSI, 2012a). In addition, the inoculation of yeast was performed in accordance with the NCCLS reference standard M44-A. In brief, yeast was grown on SDA for 48 hours at  $37\pm 2$  °C. The cultured plate was then taken out, and three

to five well-isolated colonies of yeast were propagated in 5 mL SDB. The SDB culture was further vortexed for 15 seconds. The turbidity of the yeast suspension was measured using a spectrophotometer at 625 nm and adjusted with broth/saline medium until it achieved the turbidity equivalent to 0.5 McFarland standard (absorbance between 0.08 to 0.13), which resulted in a suspension containing approximately  $10^6$  -  $10^8$  CFU/mL yeast (NCCLS, 2004).

#### **2.4.3.6 Disc diffusion assay**

The disc diffusion assay (DDA) was conducted in accordance with the methods recommended by the CLSI/NCCLS against bacteria and yeast. Briefly, a sterile cotton swab was dipped and rotated several times in the freshly prepared inoculum broth, MHB/BHI/SDB, with a standardised inoculum of  $10^6$  -  $10^8$  CFU/mL. Then, the cotton swab was firmly pressed against the wall of the tube to remove excess liquid. Subsequently, the cotton swab was streaked onto an entire MHA/BHI/SDA plate, and the process was repeated twice, with each time the plate being rotated approximately  $60^\circ$  to ensure even inoculum distribution. 6 mm-diameter sterile paper discs were placed on inoculated agar plates. Each of the paper discs was infused with 25  $\mu$ L of extract (10 mg/mL/ 50 mg/mL). For the positive control, 0.1% (v/v) CHX (bacteria) and 5% (v/v) amphotericin B (yeast) were used, while DMSO at a 10% (v/v) concentration was used for the negative control. The plates were labelled accordingly and incubated at  $37\pm 2$  °C for 24 hours (bacteria) and 48 hours (yeast). The results were collected based on a triplicate measurement of the diameter of the zone of inhibition and recorded in millimetres (mm) (NCCLS, 2004; CLSI, 2012a).

#### **2.4.3.7 Determination of minimum inhibitory concentration (MIC) and minimum bactericidal/fungicidal concentration (MBC/ MFC)**

The MIC and MBC/MFC of the extracts were determined using the broth microdilution method following CLSI protocols M07-A9. A 96-well U-bottom microtiter plate was utilised, with an inoculum suspension adjusted to  $10^5$  CFU/mL. The first column contained 100  $\mu$ L of MHB/BHI/SDB as a negative control, and the second column contained 100  $\mu$ L of bacterial/yeast suspension as a positive control. Columns three to twelve were pre-filled with 100  $\mu$ L of bacterial/yeast suspension. A two-fold microdilution of the plant extracts (100  $\mu$ L) was performed from column twelve to column three. Similarly, CHX and amphotericin B were diluted from 0.50 mg/mL to 0.001 mg/mL. Plates were incubated at  $37\pm 2$  °C for 24 hours (bacteria) and 48 hours (yeast). MBC/MFC was determined by subculturing 10  $\mu$ L from each MIC well onto MHA/BHI/SDA

plates, followed by incubation at  $37\pm 2$  °C for 24 hours (bacteria) and 48 hours (yeast) (CLSI, 2012b).

## **2.5 Development of zein-based films**

Active antimicrobial zein-based films incorporating CAE, GATE, and GGE were developed to evaluate the antimicrobial potential of these plant extracts. Zein powder, obtained from Sigma-Aldrich, served as the primary biopolymer, with the selected antimicrobial extracts added to the zein polymer solution. The process of developing these active films involved three key steps. First, zein and zein-loaded antimicrobial solutions were prepared. Next, the viscosity of the polymer solution was tested to assess its suitability for electrospinning. Finally, the electrospinning process was carried out to produce the films. The detailed procedures are described in the following sections.

### **2.5.1 Preparation of electrospinning solution**

Preliminary tests were conducted using zein solutions at concentrations of 16%, 20%, 25%, and 30%, prepared using 75% ethanol as a solvent to identify the optimal concentration for electrospinning. Based on viscosity measurements, visual inspection of film morphology, and SEM analysis, a 30% (w/v) zein solution was selected for further experimentation. Due to a malfunction in the electrospinning machine at the University of Leeds, two different electrospinning solution preparations were employed. The solutions intended for production of films for characterisation tests were prepared by the author. Briefly, to prepare the 30% (w/v) zein solution, 6 g of zein powder was dissolved in 20 mL of a 75% (v/v) aqueous ethanol solution and stirred for 2 hours at 21 °C. Plant extracts (CAE, GATE, and GGE) were then incorporated at a concentration of 5% (w/w) relative to the zein content and stirred until a homogeneous solution was achieved. The control solution, which did not contain plant extracts, was designated as Neat zein, while solutions containing 5% (w/w) of CAE, GATE and GGE were labelled as Ze-CAE, Ze-GATE and Ze-GGE, respectively (Salevic et al., 2022).

The solutions intended for production of films for storage study were prepared by SKE Research Equipment (Italy), and slight variations occurred. The preparation of Ze-CAE solution involved heating a 5% (w/w) CAE extract to 80 °C in a water bath, then adding it to a 30% (w/v) zein solution and stirring for 1 hour at 21 °C. The Ze-GGE solution was stirred in an ultrasonic bath for 24 hours at 21 °C to ensure homogeneity. The Ze-GATE solution preparation followed the original protocol.

### **2.5.2 Viscosity measurement**

The determination of a suitable viscosity for a polymer solution is essential, as it determines the suitability for electrospinning and would affect the fibre diameter and morphology (Demir et al., 2002; Zong et al., 2002). The viscosity of zein and zein-loaded plant extract solutions was analysed to investigate their flow behaviour using a rheometer (Netzsch Kinexus Lab+, Malaysia). Approximately 2 mL of each electrospinning solution was carefully placed into a cone and plate geometry setup (PL65 C0052 SS and CP2/60 SC006 SS). The experiment was conducted at a controlled temperature of 25 °C, with shear rates ranging from 0.1 s<sup>-1</sup> to 100 s<sup>-1</sup>, and 10 measurements were recorded per decade. The obtained shear rate and viscosity data were used to construct flow curves for the zein and zein-loaded plant extract solutions (Sokhal et al., 2019).

### **2.5.3 Electrospinning**

Due to a malfunction in the electrospinning machine at the University of Leeds, slightly different electrospinning parameters were employed for the production of the films. The slight variations in the parameters could be due to the nature of electrospinning machine, where the voltage and flow rate need to be regularly adjusted to ensure the production of smooth film, without any droplet on the collector. The films used for characterisation studies were electrospun by the author, while those intended for storage study was sourced from a company (SKE Research Equipment, Italy). In brief, zein-based fibres were produced using an electrospinning system (SKE-Research-Equipment, Italy). A 10 mL plastic syringe, equipped with a metallic needle (17 G, ID: 1.0 mm, OD: 1.47 mm), was utilised for electrospinning Neat zein/Ze-CAE/Ze-GATE/Ze-GGE solutions. The syringe was mounted on a single-channel syringe pump, and the electrospinning process was conducted in a horizontal setup. Detailed parameters for the procedure are provided in Table 2.4. The process was carried out within a fume hood, and the electrospun fibres were collected and stored at room temperature for further analysis (Salevic et al., 2022).

**Table 2.4** Electrospinning parameters for zein-based films.

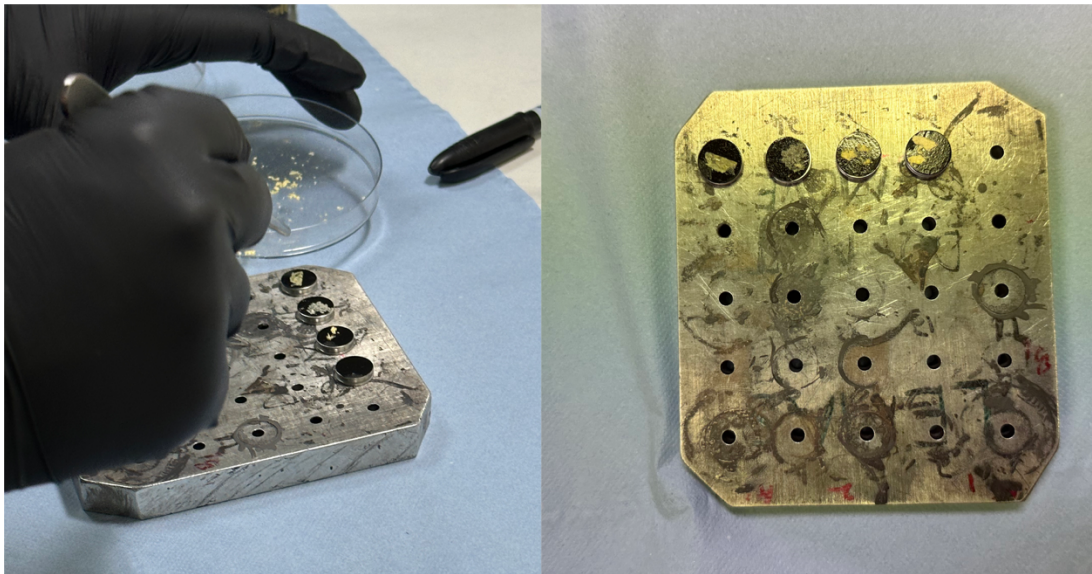
Parameters	Films: physical properties	Films: storage study Ze- CAE	Films: storage study Ze- GATE	Films: storage study Ze- GGE
Total amount of solution (mL)	6	6	6	6
Solution flow rate (mL/h)	1.0	0.9	0.9	0.6
Voltage (kV)	15 to 17	+12, -4	+12, -4	+16, -16
Distance (cm)	15	15	15	15
Relative humidity (%)	40±5	40±5	40±5	40±5
Temperature (°C)	21±2	21±2	21±2	21±2
Collector size (cm)	12 x 12	12 x 12	12 x 12	12 x 12

## 2.6 Assessing zein-based films properties

The electrospun films were examined under a scanning electron microscope (SEM) to observe the films' morphology. To study the physical properties, the films were subjected to several tests, such as measurements of thickness, encapsulation efficiency, water contact angle, ATR-FTIR, thermal analysis and a biodegradation study.

### 2.6.1 Scanning electron microscope (SEM)

The surface morphology of electrospun fibres was analysed using a SEM (Carl Zeiss EVO MA15, UK). Prior to imaging, samples were mounted onto SEM stubs and sputter-coated with a thin layer of conductive gold-palladium (Figure 2.1). Imaging was performed at an operating voltage of 20 kV under vacuum conditions. Observations were conducted at magnifications of 500X, 1000X, 2000X, and 5000X. The average fibre diameter was determined by measuring 100 randomly selected fibres from each sample using ImageJ (National Institute of Health, USA) and OriginPro softwares (OriginLab, USA) (Salevic et al., 2022).



**Figure 2.1** SEM sample preparation where the films were mounted on the stub.

### **2.6.2 Film thickness**

Films thickness was measured to ensure the robustness of the packaging, and the functionality of the films incorporated with CAE, GATE, and GGE. The conditioned films thickness was measured using a digital micrometre (Mitutoyo, Japan) with accuracy of 0.001 mm. Five random measurements of each film were taken, and the thickness was measured by calculating the average values of the films (Nazari et al., 2019).

### **2.6.3 Encapsulation efficiency**

The incorporation of CAE, GATE, and GGE into zein film via electrospinning is a novel approach, thus, the determination of the maximum wavelength of these three extracts is crucial. Firstly, the experimental procedure was designed by measuring the maximum wavelength of the plant extracts by spectrophotometer between 200 and 800 nm wavelength, which covers both UV and Vis regions. The selection of these regions is based on their capacity to absorb light from biologically relevant molecules (Cockell and Knowland, 1999; Saxena and Saxena, 2012; Dankowska and Kowalewski, 2019; Saha et al., 2020). The UV-Vis absorbance quantification is the preferred approach compared to other methods such as mass spectrometry, <sup>1</sup>H nuclear magnetic resonance (NMR), and time-resolved small-angle X-ray scattering (SAXS) due to the feasibility of the procedure, high repeatability, and low variability in measurements (Minelli et al., 2022; Marques and Segundo, 2024). Secondly, a calibration curve for the extracts was established. Finally, the encapsulation efficiency test was conducted

to determine the percentage of extracts successfully incorporated into the zein fibres.

To determine the maximum wavelength of plant extracts, a 10 mg/mL solution of CAE50-S was prepared by dissolving 10 mg of extract in 50% aqueous ethanol, followed by vortex. Same procedure was repeated for GATE100-M, GGE50-M, and zein using 100%, 50%, and 75% aqueous ethanol, respectively. Ten-fold dilution of the extracts was performed thrice for all extracts. The peaks were measured using a UV-Vis spectrophotometer (SPECORD 250 Analytik Jena AG, Germany) with the measurement mode set to spectra for the wavelength recorded between 200 to 800 nm. Maximum wavelength for CAE, GATE, GGE, and zein were observed at 267, 322, 666, and 444 nm respectively. The calibration curves of plant extracts were constructed from the absorbance values obtained (Yao et al., 2016).

The encapsulation efficiency of films was determined using absorbance method described in previous literature with slight modifications (Rind et al., 2010; Drago et al., 2022). Five milligrams of films (Ze-CAE, Ze-GATE, Ze-GGE) was added to 5 mL solvent (75% ethanol) and dissolved by continuous shaking until the films were completely solubilised and no visible fragments remained. The spectrophotometric analysis was conducted at pre-determined wavelength, and the actual extract concentration was determined from a calibration curve. For the preparation of blank test, 5 mg of Neat zein was dissolved in 75% ethanol and the absorbance of the blank test has been subtracted to the samples' absorbance. The test was conducted in triplicate, and the encapsulation efficiency is calculated using the formula bellow:

$$\begin{aligned} & \text{Encapsulation efficiency (\%)} \\ & = \frac{\text{Total extract concentration} - \text{Free extract concentration}}{\text{Total extract concentration}} \times 100\% \end{aligned} \quad (\text{Eq. 2.3})$$

#### **2.6.4 Water contact angle**

The determination of surface wettability of zein-based films was analysed by measuring the water contact angle at a temperature of 20±2 °C using a drop shape tensiometer (OCA 25, Germany) and the sessile drop method. A 3 µL droplet of Milli-Q water was deposited on the surface of the films (20 x 40 mm), and the droplet's image was captured using a digital camera. Three film samples were utilised for each sample type, and the contact angle was determined using ImageJ software (Yang, Y. et al., 2020).

### **2.6.5 Attenuated total reflectance - Fourier transform infrared spectroscopy (ATR - FTIR)**

The chemical interactions of functional groups in zein-based films were assessed through ATR-FTIR spectroscopy (Bruker, Germany) within a wavenumber range of 4000 to 400  $\text{cm}^{-1}$ . Measurements were performed at a spectral resolution of 4  $\text{cm}^{-1}$ , averaging 16 scans per sample. The data were processed and analysed using OriginPro software (OriginLab, USA) (Ansarifar and Moradinezhad, 2021).

### **2.6.6 Thermal properties**

Thermogravimetric analysis (TGA) was performed to evaluate the thermal stability of zein-based films utilising TGA/DSC1 STAR System (Mettler Toledo, USA). A sample weighing approximately 10 mg was prepared, and the experimental parameters were established with a temperature range of 30 to 600  $^{\circ}\text{C}$ , utilising a heating rate of 10  $^{\circ}\text{C}/\text{min}$  in a nitrogen atmosphere at a flow rate of 50  $\text{mL}/\text{min}$ . Data analysis was conducted using OriginPro software (OriginLab, USA) (Yang, Y. et al., 2020).

### **2.6.7 Biodegradation study**

Biodegradation test of zein-based films was performed using soil burial test to measure biodegradability of the films. The films were cut into 20 x 50 mm and were buried in a topsoil (Westland, UK) at a depth of 10 cm at  $20\pm 2$   $^{\circ}\text{C}$ . The films samples were retrieved at five-day intervals and subjected to drying in an oven at 50  $^{\circ}\text{C}$  for 24 hours. The percentage of weight loss was determined (Equation 2.4), and biodegradation graph was constructed. Triplicate measurement was performed for each film sample (di Franco et al., 2004).

$$\text{Weight loss (\%)} = \frac{\text{Initial film weight} - \text{Final film weight}}{\text{Initial film weight}} \times 100\% \quad (\text{Eq. 2.4})$$

## **2.7 Storage study**

Zein-based films were developed and subjected to various physical tests to evaluate their properties. To explore their potential application as packaging materials, these films, incorporated with CAE, GATE, and GGE, were utilised for beef packaging and stored under refrigeration. Their effectiveness in inhibiting microbial growth was assessed, alongside an evaluation of beef quality through water activity ( $a_w$ ), and colour analysis. A comparison of these parameters with a

commercial wrapping film purchased from a supermarket (Buffalo cling film, China) was also performed (Figure 2.2). To ensure the sterility and stability of the films, preliminary studies were conducted in which the films were stored at room temperature, 4 °C, and -20 °C for one month. During this period, the films were visually inspected for any signs of contamination or degradation (data not shown). After confirming that no contamination or degradation occurred during storage, the subsequent experiments of storage study were carried out. A comprehensive description of the methodology is provided in Sections 2.71 to 2.73.



**Figure 2.2** A commercial film purchased from a supermarket was used as a comparison to the zein-based films in evaluating their effectiveness at reducing the growth of foodborne pathogens and spoilage microorganisms in beef.

### 2.7.1 Microbiological analysis

Raw beef (British beef rump steak/ British beef fillet steak) was purchased from a supermarket in Leeds, UK. Each sample (25.0 g) was pre-cut to  $5.0 \pm 1.0$  g (approximately 2.3 x 2.3 cm in surface dimensions) on day 0 and wrapped with commercial and zein-based films in a food-grade plastic tray. The wrapped samples were stored in a refrigerator at 4 °C for a duration of five days. Microbiological analysis was conducted daily, starting from day 0. A piece of the beef sample ( $5.0 \pm 1.0$  g) was collected under aseptic conditions (all handling was performed inside a biological safety cabinet using sterilised instruments to avoid contamination), homogenised with 45 mL of sterilised saline solution (0.85% NaCl) using a stomacher machine (Seward 400 Circulator, UK) for 9 minutes, and prepared for microbial analysis.

For analysis, 1 mL from the homogenised solution was pipetted and ten-fold serial dilutions were prepared using the saline solution to achieve dilution levels of  $10^{-1}$ ,  $10^{-2}$ ,  $10^{-3}$ , and  $10^{-4}$ . The diluted samples (0.1 mL) were plated on plate count agar. The plates were then incubated at  $37 \pm 2$  °C for 12 to 24 hours for bacterial growth. The bacterial load was quantified by counting the total colonies on each plate and expressed as log CFU/g of beef. All experiments were performed in duplicate. Plate count agar is a general purpose culture media used for the determination of the total count of aerobic bacteria and agar media was prepared

by dissolving 23.5 g of media powder in 1 L of deionised water and autoclaved for 15 minutes at 121 °C (Rollini et al., 2016; Merck, 2019).

### **2.7.2 Water activity ( $a_w$ )**

The water activity of stored beef wrapped with different packaging materials was monitored daily, including day 0 using a water activity device (Rotronic Hygrolab, Switzerland). For each measurement,  $5.0 \pm 1.0$  g of the beef sample was placed in the device. Each test was carried out in duplicate (Rotronic, 2011).

### **2.7.3 Colour analysis**

A colorimeter (PCE Instruments PCE-CSM 4, UK) was used to measure the colour of beef surface wrapped in different packaging materials, with measurements taken daily over a period of 5 days. The lightness ( $L^*$ ), red/green opponent colours ( $a^*$ ), and yellow/blue opponent colours ( $b^*$ ) were recorded for two replicates of each packaging type, using beef samples of  $5.0 \pm 1.0$  g (Arezoo et al., 2020).

## **2.8 Statistical analysis**

Data analysis was performed using Minitab (Version 22.1.0.0), and R software (Version 2022.07.1). Results are expressed as the mean  $\pm$  standard deviation (SD) of three replicates, unless otherwise stated. Statistical differences between samples were assessed using analysis of variance (ANOVA), post-hoc t-test and using general linear models utilising relevant factors and variables available. Model assumptions were tested to ensure that the models could be appropriately applied e.g. normally distributed and homoscedasticity assumptions in the case of the linear models. Post-hoc Tukey's pairwise comparisons were performed to identify differences between treatment means. In Chapter 3, Tukey's test was used to compare different extraction methods and ethanol ratios in terms of extraction yield, total phenolic content, antioxidant and antimicrobial activities. In Chapter 4, comparisons were conducted among film types to assess the average fibre diameter, film thickness, percentage of encapsulation efficiency, and water contact angle values. In Chapter 5, both type of films and days of storage were compared with respect to microbiological activity, water activity ( $a_w$ ), and beef colour parameters. In addition, Pearson correlation coefficients were also calculated in Chapter 3 to evaluate the relationship between total phenolic content and antioxidant activity. A p-value of less than 0.05 ( $p < 0.05$ ) was reported as statistically significant and adopted for all tests.

## 2.9 Overview of the workflow

The overview of the workflow, encompassing the extraction of medicinal plants, investigation of their biological activities, development of active antimicrobial and biodegradable packaging materials, and subsequent storage studies, is schematically presented in Figure 2.3.

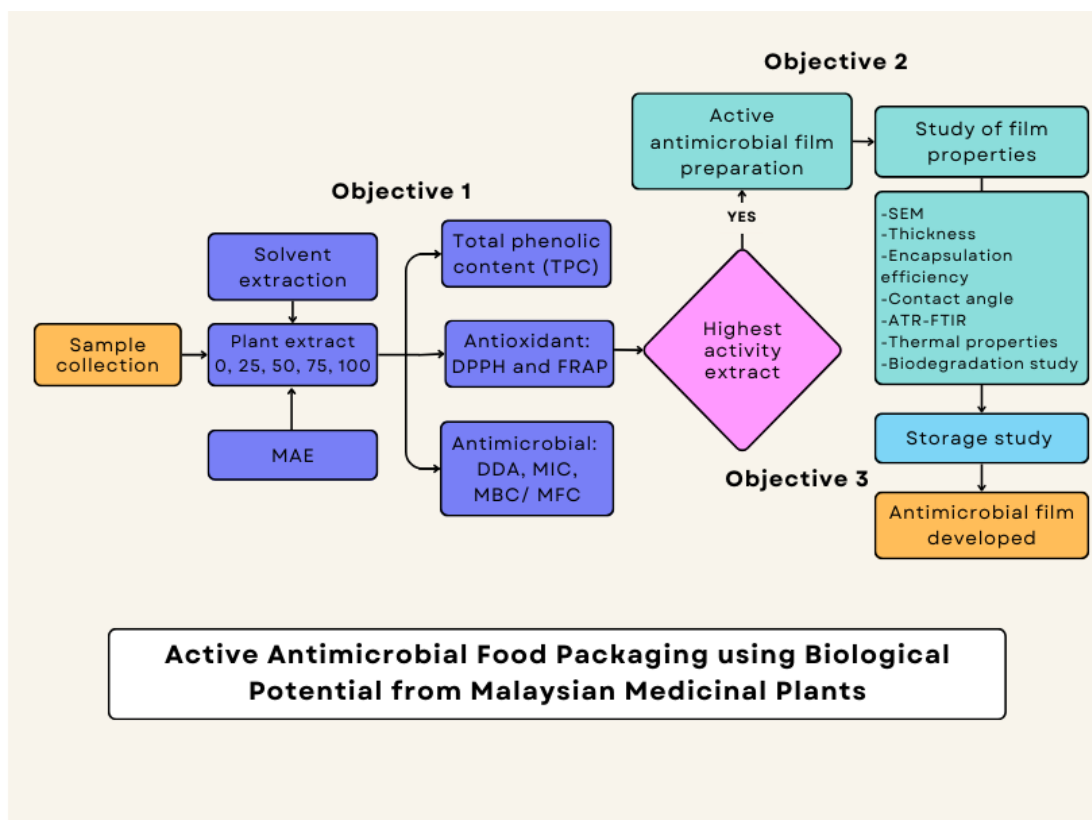


Figure 2.3 Flowchart of research methodology.

## **Chapter 3**

### **Extraction and Biological Activity**

#### **3.1 Introduction**

According to a report from the Royal Botanic Gardens, Kew, UK, in 2017 only approximately 7.5% of medicinal plants had been identified from a total number of 400,000 plant species globally (Allkin, 2017). Medicinal plants are composed of phytoconstituents of various biochemical groups, the most important of which are alkaloids, phenolics, and terpenoids (Croteau et al., 2000). Phenolic content is often associated with antioxidant activities and measured with assays such as 2,2-diphenyl-1-picrylhydrazyl (DPPH), ferric reducing antioxidant power (FRAP), and hydrogen peroxide scavenging activity (Wong et al., 2006). Thus, measuring phenolic content is crucial for obtaining an initial assessment of plant biological activities.

In context of medicinal plants from Malaysia, considerable research on the extraction and biological activities of *C. asiatica*, *G. atroviridis*, and *G. gnemon* has been conducted, however, to the best of author's knowledge, no study has evaluated the biological activities of these three plant extracts (*C. asiatica*, *G. atroviridis*, and *G. gnemon*) using different extraction methods and ethanol ratios. This study is primarily focussed on two extraction methods and five ethanol-to-water ratios, followed by the evaluation of their biological activities in terms of total phenolic content, antioxidant activity of DPPH and FRAP, and antimicrobial activity against foodborne pathogens and spoilage microorganisms.

#### **3.2 Aim of the chapter**

The aim of this chapter was to investigate and compare the effects of different extraction methods, namely solvent extraction and microwave-assisted extraction (MAE), on the extraction yields and biological activities of *C. asiatica* extract (CAE), *G. atroviridis* extract (GATE), and *G. gnemon* extract (GGE). The analysis focused on assessing total phenolic content, antioxidant activities, and antimicrobial potential. Additionally, the chapter examined the impact of varying ethanol-to-water ratios (0, 25, 50, 75, and 100) on extraction efficiency and bioactivity. By identifying optimal extraction conditions that maximise yield and biological activity, this chapter contributes to the development of effective extraction protocols for these medicinal plants.

### 3.3 Results and Discussion

#### 3.3.1 Extraction yields

The leaves of *C. asiatica*, *G. gnemon*, and the fruits of *G. atroviridis* were extracted by means of solvent extraction and MAE by using five ethanol-to-water ratios (v/v) (0:100, 25:75, 50:50, 75:25, and 100:0), abbreviated as 0, 25, 50, 75, and 100, respectively, with (S) for solvent extraction and (M) for MAE. In terms of rationale for selection of plant parts, *C. asiatica* leaves and *G. atroviridis* fruits were chosen because they are the primary plant parts traditionally used for culinary or medicinal purposes, while *G. gnemon* leaves were selected due to their availability. Although the fruits of *G. gnemon* are also commonly investigated for their biological activities, they are seasonal. As a result, harvesting the fruits in December 2020 was impractical, which justified the preference for using the leaves. The utilisation of five ethanol ratios can be rationalised by considering the inherent diversity of phytoconstituents, which encompass compounds of different polarity. Each ethanol ratio selectively attracts compounds based on their polarity, therefore, the use of varying ethanol ratios will optimise the extraction of diverse phytoconstituents (Do et al., 2014). Meanwhile, ethanol was selected since it is primarily safe for food and human consumption. In the context of extraction methods selection, solvent extraction is a conventional technique characterised by its simplicity and its cost-effectiveness. Conversely, MAE, a more recent technological advancement, was chosen for its ability to reduce extraction time and enhance yield efficiency, attributed to the application of heat during the extraction process (Rezaei, S. et al., 2013). The selection of optimal parameters for MAE, including extraction times, solvent-to-sample ratio, and microwave temperature, were determined based on previous literature (Chan et al., 2011; Rezaei, S. et al., 2013; Mahardika and Roanisca, 2020; Shang et al., 2020).

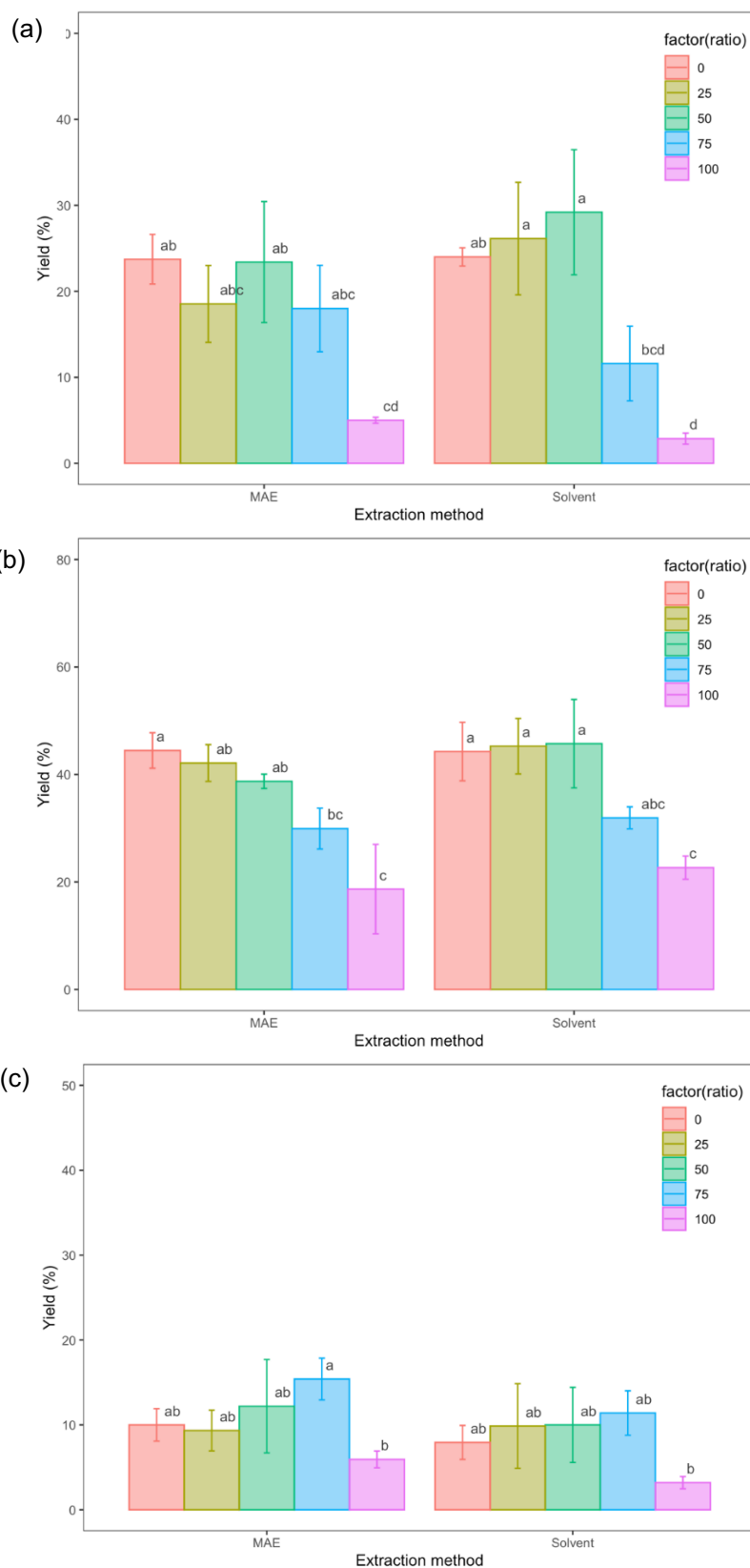
The percentage of extraction yields of CAE, GATE, and GGE from 5.0 g of raw material varied significantly, with a decreasing trend observed as the ethanol ratio increased (Table 3.1 and Figure 3.1). The morphological characteristics, including colour and form, of CAE, GATE, and GGE are presented in Appendix A Supplementary Material 1(a-c). Statistical analysis of general linear model revealed that there was a statistically significant difference in extraction yield when different ethanol ratios were used in the respective plant extracts ( $p < 0.05$ ). Conversely, there was no significant difference in the extraction yields when different methods were used for extraction ( $p > 0.05$ ). For *C. asiatica*, the highest yield was observed with CAE50-S ( $29.20 \pm 7.27\%$ ), and the yield was not significantly different from other CAE, except for those obtained from CAE75-S

(11.60±4.34%), CAE100-S (2.87±0.64%), and CAE100-M (5.00±0.35%) ( $p < 0.05$ ). Similarly, GATE50-S (45.70±8.24%) exhibited a significantly higher yield in *G. atroviridis* compared to GATE75-M (29.90±3.81%), GATE100-S (22.70±2.16%), and GATE100-M (18.70±8.33%) ( $p < 0.05$ ), but it was not significantly different from GATE0-S, GATE0-M, GATE25-S, GATE25-M, GATE50-M, and GATE75-S ( $p > 0.05$ ). For *G. gnemon*, GGE75-M achieved the highest yield (15.40±2.46%), which was not significantly different from other GGE apart from GGE100-S (3.20±0.72%) and GGE100-M (5.93±0.99%) ( $p < 0.05$ ). Based on the data, GATE50-S showed approximately 1.6x and 3.0x higher extraction yields compared to CAE50-S and GGE75-M, respectively. A possible explanation for this is that GATE, derived from fruit, is naturally rich in organic acid, particularly hydroxycitric acid (HCA) and simple sugars. These compounds contain hydroxyl groups, which exhibit high polarity and can be effectively extracted using polar solvents such as water, ethanol, and their combinations (Lewis, 1969; Jena et al., 2002; Klinchongkon et al., 2022; Shahid et al., 2022). In contrast, CAE and GGE, which were derived from the leaves have been reported to contain higher level of essential oils and fibres, which may be insoluble in polar solvents and possibly hinder the higher recovery of yield (Desai and Gaikwad, 2014; Siripongvutikorn et al., 2023). The data also indicate that using ethanol ratio 100 consistently results in the lowest extraction yields across all plant extracts, suggesting that pure ethanol is not an ideal solvent for optimising extraction efficiency.

**Table 3.1** Yields of CAE, GATE, and GGE using different extraction methods and ethanol ratios.

Ethanol ratio	Percentage of yield (%)					
	CAE		GATE		GGE	
	Solvent extraction	MAE	Solvent extraction	MAE	Solvent extraction	MAE
<b>0</b>	24.00± 1.06 <sup>ab</sup>	23.70± 2.89 <sup>ab</sup>	44.30± 5.44 <sup>a</sup>	44.50± 3.30 <sup>a</sup>	7.93± 2.00 <sup>ab</sup>	10.00± 1.91 <sup>ab</sup>
<b>25</b>	26.10± 6.54 <sup>a</sup>	18.50± 4.47 <sup>abc</sup>	45.30± 5.16 <sup>a</sup>	42.10± 3.42 <sup>ab</sup>	9.87± 4.99 <sup>ab</sup>	9.33± 2.40 <sup>ab</sup>
<b>50</b>	29.20± 7.27 <sup>a</sup>	23.40± 7.03 <sup>ab</sup>	45.70± 8.24 <sup>a</sup>	38.70± 1.33 <sup>ab</sup>	10.00± 4.42 <sup>ab</sup>	12.20± 5.50 <sup>ab</sup>
<b>75</b>	11.60± 4.34 <sup>bcd</sup>	18.00± 5.02 <sup>abc</sup>	31.90± 2.04 <sup>abc</sup>	29.90± 3.81 <sup>bc</sup>	11.40± 2.62 <sup>ab</sup>	15.40± 2.46 <sup>a</sup>
<b>100</b>	2.87± 0.64 <sup>d</sup>	5.00± 0.35 <sup>cd</sup>	22.70± 2.16 <sup>c</sup>	18.70± 8.33 <sup>c</sup>	3.20± 0.72 <sup>b</sup>	5.93± 0.99 <sup>b</sup>

Yield (%) (mean ± SD, n = 3). Means with different superscript letters (a-d) of the same plant extract i.e., same column, are significantly different (Tukey's pairwise comparisons, p < 0.05). CAE: *C. asiatica* extract; GATE: *G. atroviridis* extract; GGE: *G. gnemon* extract; MAE: Microwave-assisted extraction.



**Figure 3.1** Percentage of extraction yield (%) of (a) CAE, (b) GATE, (c) GGE using different extraction methods; solvent and microwave assisted extraction (MAE) and varying ethanol ratios (0, 25, 50, 75, and 100 ethanol). Bar graphs represent the means of extraction yield. Error bars represent the sample standard deviation (mean ± SD, n = 3). Means sharing the same letter indicate that the percentage of extraction yield are not significantly different, while means with different letters indicate a statistically significant difference in extraction yield (Tukey's pairwise comparisons, p < 0.05).

In general, the use of varying ethanol ratios in the extraction of CAE, GATE, and GGE from 0 to 100 affected the extraction yield. In terms of optimising the yield for CAE, GATE, and GGE, water or any lower aqueous ethanol ratio between 0 and 75 is considered a better extraction solvent compared to 100 ethanol. These findings are consistent with prior research, indicating that incorporating water alongside ethanol in the extraction process enhances the extraction yield (Do et al., 2014; Kim and Chin, 2017; Hikmawanti et al., 2021). The literature to date includes studies on the extraction yields of rice paddy herb (*Limnophila aromatica*) using water and different aqueous concentrations of methanol, ethanol, and acetone, and the results demonstrated that the use of aqueous solvents correlated with a higher yield compared to using organic solvent alone (Do et al., 2014). Recent research by Hikmawanti et al. (2021) on sweet leaf (*Sauropus androgynus* (L.) Merr.) has reported that the use of aqueous ethanol (50%) as a solvent result in a higher yield compared to using absolute ethanol. These findings may be justified by the fact that the mixture of water and organic solvent may facilitate the recovery of phytoconstituents that are soluble in water and/or organic solvents (Do et al., 2014; Hikmawanti et al., 2021). In other words, the variation in ethanol-to-water ratios affects ethanol concentration, subsequently altering the physical properties of the solvent, including density, dynamic viscosity, and dielectric constant. The change would lead to modifications in the solubilities of compounds, subsequently affecting yield and biological activity (Frank et al., 1999, cited in Cacace and Mazza, 2003, p. 243). In terms of extraction method, the use of neither solvent nor MAE resulted in a difference of yield in all extracts. A possible explanation for the findings might be due to the nature of phytoconstituents in these plant extracts, which consist of polar and moderately polar compounds. These compounds are soluble in ethanol and aqueous ethanol solvents and can be effectively extracted in normal extraction conditions, and even the heat was involved during the MAE extraction process, the effect on the yield recovery would be very minimal, hence it showed no significant difference in the yield (Lee, S.-S. et al., 2000; Mat-Ali, 2008; Dutta et al., 2018; Mokhtar et al., 2018; Lim et al., 2020).

Based on Table 3.1 and Figure 3.1, some data exhibits considerable variation in yield percentages between replicates, showing high standard deviation values. This variability is likely attributable to instrumental inconsistencies. Specifically, during solvent evaporation using the rotary evaporator, bumping occurred in several extracts, resulting in partial sample loss and contributing to the observed fluctuations in yield. Bumping is characterised by sudden, uncontrolled boiling, which causes portions of the sample to escape from the evaporation flask, leading to sample loss. To minimise this issue in the future, the use of anti-

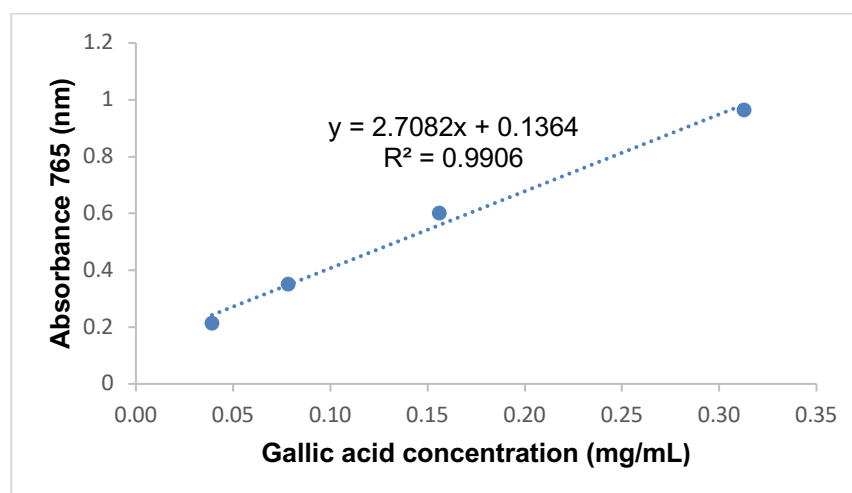
bumping granules is recommended to ensure more stable and controlled evaporation (Tennenhouse, 2017).

In comparison of the percentage of yield with other studies with similar plant species, Irma et al. (2021) reported the yield of *C. asiatica* leaf fraction as 3.16%, 3.77%, and 10.41% when fractionated with n-hexane, ethyl acetate, and methanol, respectively. A separate study documented a yield of  $18.37\pm 0.19\%$  for *C. asiatica* leaf extracted using an aqueous extract (Nik Hairiah et al., 2013). For *G. atroviridis*, the yield percentage of different plant parts of *G. atroviridis* extracted using methanol and aqueous extracts ranged from 2.6% to 35.2% (Al-Mansoub et al., 2014). Additionally, a recent study recorded the yield of *G. atroviridis* leaf extracted sequentially using Soxhlet extraction with petroleum ether, dichloromethane, and absolute ethanol at 18.14% (w/w) (Chuajit et al., 2024). In the case of GGE, the yield for dried endosperms soaked in 50% ethanol was 9.33% (Kato, E. et al., 2009). In another study by Trisha et al. (2024), an extraction yield of *G. gnemon* leaf powder extracted with 95% ethanol was reported at  $11.58\pm 0.38\%$ . Overall, the percentage of yields is influenced by various factors, including differences in plant species and parts, methods of extraction, solvent types, as well as different sampling locations and harvesting seasons (Jamiuddin et al., 2019). Based on the findings, some of the yields obtained from this current study were slightly higher when compared to previous studies, likely due to the use of high polarity solvents of ethanol and water as well as the use of different ratios of ethanol to water, which probably increase the recovery of yields for CAE, GATE, and GGE.

In summary, this study found that ethanol ratio played a more significant role in the extraction yield of CAE, GATE, and GGE compared to the extraction method. The extraction yields for most extracts were optimised when using an ethanol ratio between 0 and 75, regardless of whether solvent extraction or MAE was applied. In contrast, the ethanol ratio of 100 consistently resulted in the lower yield, being the least preferred ratio. Based on these findings, the average percentage of extraction yield followed the ranking order: GATE > CAE > GGE. It is important to note that the results of this section only correspond to the yields of extracts, and they do not represent correlations to the biological activities. To evaluate biological activities, all plant extracts were further subjected to total phenolic content and antioxidant tests of DPPH, FRAP assays and finally antimicrobial tests of disc diffusion, MIC, and MBC/MFC. The details on the biological activities are further discussed in Sections 3.3.2 to 3.3.5.

### 3.3.2 Total Phenolic Content

Phenolic compounds are among ubiquitously available phytoconstituents in plants that are classified as secondary metabolites and acting as defence mechanisms against harmful extrinsic factors (Croteau et al., 2000). Besides, secondary metabolites possess therapeutic properties that are beneficial to humans. For instance, phenolic compounds, which are comprised of aromatic rings with at least one hydroxyl group attached to the structure, have been proven to possess substantial antioxidant properties (Rice-Evans et al., 1996). The total phenolic content assay is a preliminary assay widely used to quantify the phenolic content in plants. The key principle of the total phenolic content assay is the reduction of Folin-Ciocalteu's reagent to molybdenum-tungsten complex in the presence of phenolics, which results in the formation of blue complexes detectable by a spectrophotometer at 765 nm. The intensity of blue formation complexes is proportional to the phenolic concentration in the plants (Singleton et al., 1999). The total phenolic content of CAE, GATE and GGE was determined according to the Folin-Ciocalteu method using gallic acid as a standard (0.04 to 0.31 mg/mL) with a linear equation of  $y = 2.7082x + 0.1364$ ,  $R^2 = 0.9906$  (Figure 3.2).



**Figure 3.2** Gallic acid standard curve for total phenolic content determination using gallic acid concentration between 0.04 and 0.31 mg/mL.

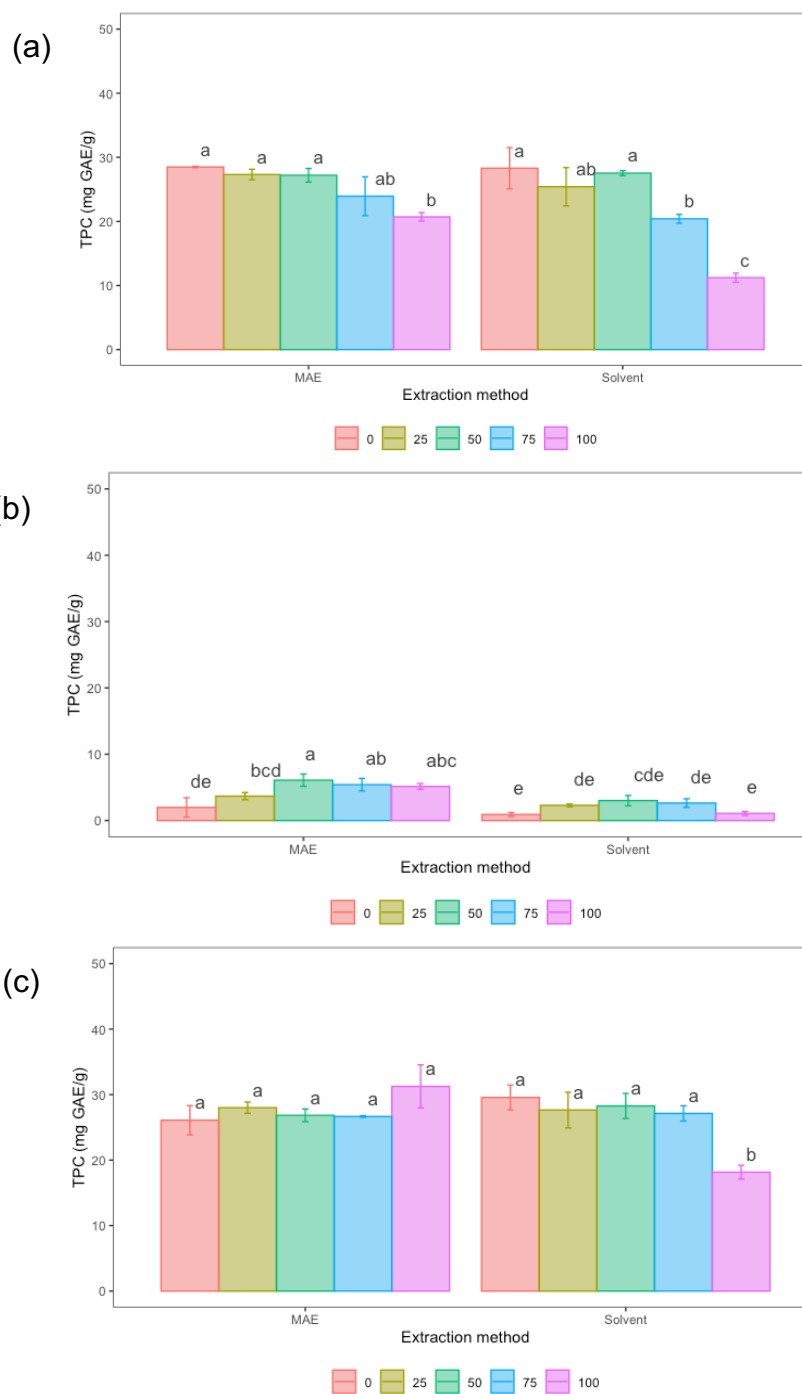
The total phenolic content of 10 mg/mL plant extracts; CAE, GATE and GGE is presented in Table 3.2 and Figure 3.3. Statistical analysis of general linear model indicated that both ethanol ratio and extraction method significantly influenced total phenolic content across all extracts ( $p < 0.05$ ). For *C. asiatica*, the highest total phenolic content was observed in CAE0-M ( $28.48 \pm 0.11$  mg GAE/g), which was significantly higher than that of CAE75-S ( $20.41 \pm 0.69$  mg GAE/g), CAE100-S ( $11.23 \pm 0.71$  mg GAE/g), and CAE100-M ( $20.71 \pm 0.66$  mg GAE/g) ( $p < 0.05$ ),

but was comparable to CAE0-S, CAE25-S, CAE25-M, CAE50-S, CAE50-M, and CAE75-M ( $p > 0.05$ ). For *G. atroviridis*, GATE50-M exhibited the highest total phenolic content ( $6.09 \pm 0.92$  mg GAE/g), comparable to GATE75-M and GATE100-M ( $p > 0.05$ ), and significantly surpassing GATE0-S ( $0.92 \pm 0.30$  mg GAE/g), GATE0-M ( $1.98 \pm 1.46$  mg GAE/g), GATE25-S ( $2.29 \pm 0.21$  mg GAE/g), GATE25-M ( $3.68 \pm 0.54$  mg GAE/g), GATE50-S ( $3.01 \pm 0.78$  mg GAE/g), GATE75-S ( $2.64 \pm 0.64$  mg GAE/g), and GATE100-S ( $1.10 \pm 0.29$  mg GAE/g) ( $p < 0.05$ ). For *G. gnemon*, the highest total phenolic content was recorded in GGE100-M ( $31.25 \pm 3.30$  mg GAE/g). This value was not significantly different from other GGE, except for GGE100-S ( $18.15 \pm 1.05$  mg GAE/g) ( $p < 0.05$ ).

**Table 3.2** Total phenolic content of CAE, GATE, and GGE using different extraction methods and ethanol ratios.

Ethanol ratio	Total phenolic content (mg GAE/g)					
	CAE		GATE		GGE	
	Solvent extraction	MAE	Solvent extraction	MAE	Solvent extraction	MAE
<b>0</b>	$28.30 \pm 3.23^a$	$28.48 \pm 0.11^a$	$0.92 \pm 0.30^e$	$1.98 \pm 1.46^{de}$	$29.57 \pm 1.89^a$	$26.09 \pm 2.23^a$
<b>25</b>	$25.41 \pm 3.00^{ab}$	$27.32 \pm 0.82^a$	$2.29 \pm 0.21^{de}$	$3.68 \pm 0.54^{bcd}$	$27.64 \pm 2.72^a$	$28.00 \pm 0.86^a$
<b>50</b>	$27.53 \pm 0.38^a$	$27.20 \pm 1.06^a$	$3.01 \pm 0.78^{cde}$	$6.09 \pm 0.92^a$	$28.27 \pm 1.91^a$	$26.84 \pm 0.97^a$
<b>75</b>	$20.41 \pm 0.69^b$	$23.93 \pm 3.03^{ab}$	$2.64 \pm 0.64^{de}$	$5.41 \pm 0.95^{ab}$	$27.13 \pm 1.16^a$	$26.66 \pm 0.13^a$
<b>100</b>	$11.23 \pm 0.71^c$	$20.71 \pm 0.66^b$	$1.10 \pm 0.29^e$	$5.15 \pm 0.43^{abc}$	$18.15 \pm 1.05^b$	$31.25 \pm 3.30^a$

Total phenolic content (mg GAE/g) (mean  $\pm$  SD,  $n = 3$ ). Means with different superscript letters (a-e) of the same plant extract i.e., same column, are significantly different (Tukey's pairwise comparisons,  $p < 0.05$ ). CAE: *C. asiatica* extract; GATE: *G. atroviridis* extract; GGE: *G. gnemon* extract; MAE: Microwave-assisted extraction.



**Figure 3.3** Total phenolic content (mg GAE/g) of (a) CAE, (b) GATE, and (c) GGE using different extraction methods; solvent and microwave assisted extraction (MAE) and varying ethanol ratios (0, 25, 50, 75, and 100 ethanol).

Bar graphs represent the means of total phenolic content. Error bars represent the sample standard deviation (mean  $\pm$  SD, n = 3). Means sharing the same letter indicate that the total phenolic content is not significantly different, while means with different letters indicate a statistically significant difference in total phenolic content (Tukey's pairwise comparisons, p < 0.05).

These results demonstrate that total phenolic content varies significantly depending on plant species, ethanol ratio, and extraction method. In this study, CAE exhibited higher phenolic content with ethanol ratios ranging from 0 to 50 using the solvent extraction method, whereas MAE showed higher phenolic content with ethanol ratios between 0 and 75. In contrast, GATE showed significantly higher total phenolic content when using ethanol ratios between 50 and 100, particularly with MAE. This suggests that the phenolic compounds in GATE are influenced by the application of heat during MAE, which facilitates the breakdown of cellular structures, leading to the release of bound phenolics from the cell wall and enhancing polyphenol extraction (Toor and Savage, 2006). For GGE, determining the optimal ethanol ratio for maximising phenolic content was challenging due to the lack of a clear trend in the data. The extracts from all ethanol ratios and extraction methods yielded comparable phenolic content, except for GGE100-S, which deviated from this pattern. Based on these findings, ethanol ratios between 0 and 100 appear suitable when using MAE, whereas for solvent extraction, ethanol ratios between 0 and 75 are more appropriate.

A comparative analysis was conducted to evaluate the total phenolic content across the three plant species. Notably, GATE exhibited significantly lower total phenolic content compared to CAE and GGE, likely due to being derived from the fruit of *G. atroviridis*, a plant part that typically contains lower flavonoid levels than others. Since flavonoids are a key subgroup of phenolic compounds, their lower concentration may contribute to the reduced total phenolic content observed in GATE (Al-Mansoub et al., 2014). This finding aligns with a study by Al-Mansoub et al. (2014), who reported lower phenolic content in the aqueous extract of ripe fruit rind (1.92 µg GAE/mg) compared to leaves (10.86 µg GAE/mg) and stems (8.57 µg GAE/mg). However, other studies have reported higher total phenolic content values for *G. atroviridis* fruit extracts. For instance, Shahid et al. (2023) documented total phenolic contents of 25.1±0.85 mg GAE/g in aqueous extracts. For CAE, Raunsai et al. (2021) reported a high total phenolic content of 128.03±2.41 mg GAE/g dry extract from 1 mg/mL of *C. asiatica* leaves using 96% ethanol as the extraction solvent, while Nik Hairiah et al. (2013) found a comparable total phenolic content of 20.97±0.53 mg GAE/g in an aqueous extract (0.01 g/mL) of *C. asiatica* leaves. A prior work by Shukri et al. (2011) reported a total phenolic content of 105±5.6 mg GAE/kg and 62±2.5 mg GAE/kg for Batch 1 and 2 of *C. asiatica* leaves extracts, respectively. In the case of GGE, Suksanga et al. (2023) reported a total phenolic content of 3548±346.25 µg GAE/g dry weight (DW) for *G. gnemon* leaves extracted with boiled water at 80 °C for 30 minutes. Another investigation recorded total phenolic content of 12.6±5.06 mg

GAE/g and  $15.1 \pm 2.19$  mg GAE/g for *G. gnemon* seed flour extracted with aqueous and ethanol extracts, respectively (Bhat and Yahya, 2014).

These findings indicate considerable variation in total phenolic content across different studies, which may be attributed to differences in processing conditions (temperature during drying, storage duration), concentration of plant extracts, and extraction parameters. For example, the dried *G. atroviridis* sample of this study was obtained from a local market, lacking freshness and specific processing information, compared to the fresh fruit sample obtained from the studies of Shahid et al. (2023), which might explain the higher phenolic content recorded in that study. Additionally, when compared to this current study, Suksanga et al. (2023) reported a lower phenolic content of GGE, probably due to the use of boiled water at 80 °C for extraction, which might degrade the phenolic compounds present in GGE. The effect of heat treatment on the phenolics varied between fruits and vegetables, depending on the stability of phenolic compounds (Nayak et al., 2015b). From the findings, it can be hypothesised that the heat applied during the extraction results in the degradation of phenolics in GGE. Furthermore, differences in phytochemical constituents due to geographical variations may contribute to discrepancies in total phenolic content across plant extracts. The growth of plants at different climate conditions (e.g., temperature, rainfall, drought stress) and soil physicochemical properties (e.g., pH, minerals) will affect the phytochemical content in plants (Kumar et al., 2017; Martins-Noguerol et al., 2023; Prabhudev et al., 2023; Qaderi et al., 2023). In this study, all the plants were obtained from the state of Terengganu, Malaysia, dried in an oven and then transported to the UK for the analysis. Compared to previous studies, the samples were freshly collected and analysed afterwards without an extended storage period. The difference in plants' collection location was also noted, including the collection in different states in Malaysia with different average temperatures and in the different countries of Indonesia and Thailand.

The current findings suggest an inverse relationship between extract yield and total phenolic content, where plant extracts with the highest yield tend to have the lowest total phenolic content, and vice versa. This may be attributed to the presence of other chemical compounds in the extracts that contribute to yield but not to phenolic content. For instance, in the case of GATE, previous investigations on the phytochemical composition of *G. atroviridis* have reported the presence of organic acids (e.g., HCA, tartaric acid, and citric acid), essential oils, terpenoids, and benzofuran, which may contribute to the overall extract yield but not to the phenolic content of GATE (Jena et al., 2002; Tan et al., 2013; Shahid et al., 2023). In summary, different ethanol ratios and extraction methods

influenced total phenolic content. For CAE, a higher phenolic content was achieved with ethanol ratio between 0 and 50 using solvent extraction and 0 to 75 using MAE. GATE showed higher phenolic content with ethanol ratio between 50 and 100, particularly with MAE. For GGE, ethanol ratios of 0 to 100 were suitable when using MAE, whereas the ratios of 0 to 75 were better for solvent extraction. Based on the data, the average level of total phenolic content of all three plant extracts can be ranked in the following order: GGE > CAE > GATE.

### **3.3.3 Antioxidant Activity**

Reactive oxygen species (ROS) are free radicals that contain unstable oxygen molecules and can easily react with other molecules in a cell. Examples of ROS are the hydroxyl radical (HO•), the superoxide radical (O<sub>2</sub>•) and the peroxy radical (ROO•). The accumulation of ROS in cells can induce oxidative damage to lipids, sugars, proteins, and DNA. A myriad of studies has shown that antioxidants can help maintain human health and prevent disease by inhibiting the chain reaction of oxidation and acting as hydrogen donors or acceptors for free radicals, creating more stable radicals (Prenzler et al., 2021). In other words, antioxidants can slow down or prevent oxidation and reduce the harmful effects of reactive species (Halliwell and Gutteridge, 1985). Currently, various techniques for measuring antioxidant activity have been developed since a single antioxidant assay measurement is often insufficient to establish the full antioxidant capacity of extracts. They may differ in terms of measurement, such as spectrometry, chromatography, and electrochemical techniques. Spectrometry techniques such as 2,2'-azinobis-(3-ethylbenzothiazoline-6-sulfonic acid (ABTS), DPPH, FRAP, and oxygen radical absorption capacity (ORAC) are widely used due to the process's feasibility and cost-effectiveness (Munteanu and Apetrei, 2021). Typically, two or more different antioxidant assays are conducted to determine the antioxidant activity of samples (Jamiuddin et al., 2019). In this study, the antioxidant activity determination was performed using DPPH and FRAP assays.

#### **3.3.3.1 2,2-diphenyl-1-picrylhydrazyl (DPPH) assay**

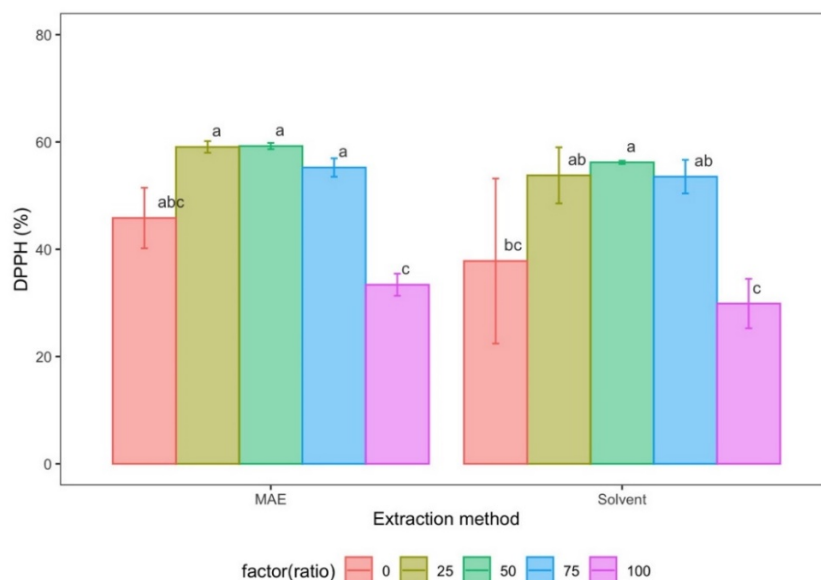
DPPH is a stable free radical, and the assay measures the percentage of DPPH inhibition by the ability of antioxidants to neutralise the radical. This process is indicated by the discoloration of DPPH from deep purple to pale yellow, which is measured spectrophotometrically at 517 nm (Molyneux, 2004). The antioxidant activity of CAE, GATE, and GGE varied across different ethanol ratios and extraction methods, as shown in Table 3.3, and Figures 3.4 to 3.6.

At a concentration of 5 mg/mL, all extracts demonstrated varying degrees of DPPH inhibition. Statistical analyses using general linear model indicated that different ethanol ratios significantly influenced the percentage of DPPH inhibition for CAE, GATE, and GGE, whereas extraction methods had a significant effect only on the DPPH values of GATE ( $p < 0.05$ ). For *C. asiatica*, CAE50-M exhibited the highest inhibition percentage ( $59.20 \pm 0.59\%$ ), but this was not significantly different from other CAE, except for CAE0-S ( $37.80 \pm 15.40\%$ ), CAE100-S ( $29.90 \pm 4.60\%$ ), and CAE100-M ( $33.40 \pm 2.06\%$ ) ( $p < 0.05$ ). For *G. atroviridis*, GATE75-S demonstrated the highest inhibition at  $14.60 \pm 1.64\%$ ). This value was not significantly different from GATE0-S, GATE75-M, GATE100-S, and GATE100-M ( $p > 0.05$ ). However, GATE0-M ( $7.55 \pm 0.57\%$ ), GATE25-S ( $9.32 \pm 0.87\%$ ), GATE25-M ( $7.57 \pm 0.76\%$ ), GATE50-S ( $10.40 \pm 0.81\%$ ), and GATE50-M ( $8.15 \pm 0.78\%$ ) had significantly lower percentages of DPPH inhibition than GATE75-S ( $p < 0.05$ ). For *G. gnemon*, GGE75-S showed the highest inhibition ( $61.00 \pm 1.17\%$ ), which was significantly higher than GGE0-S ( $7.83 \pm 3.30\%$ ), GGE0-M ( $15.50 \pm 2.41\%$ ), GGE25-S ( $43.60 \pm 3.34\%$ ), GGE25-M ( $48.10 \pm 2.49\%$ ), GGE50-M ( $45.70 \pm 2.45\%$ ), GGE100-S ( $36.00 \pm 4.89\%$ ), and GGE100-M ( $39.80 \pm 3.69\%$ ) ( $p < 0.05$ ), while being comparable to GGE50-S and GGE75-M ( $p > 0.05$ ). A standard gallic acid solution at 1000  $\mu\text{g/mL}$  exhibited  $91.84 \pm 0.56\%$  of DPPH inhibition. The findings suggest that ethanol ratio plays a crucial role in optimising DPPH inhibition activity for different plant extracts. Specifically, for CAE, an ethanol ratio of 25 to 75 was preferred when using solvent extraction, while a ratio of 0 to 75 was optimal for MAE. For GATE, ethanol ratios between 75 to 100 using both extraction methods resulted in the higher DPPH inhibition, with ethanol ratio 0 using solvent extraction also being a viable option. For GGE, an ethanol ratio of 50 using solvent extraction and 75 using both solvent extraction and MAE was recommended for achieving higher DPPH inhibition.

**Table 3.3** Antioxidant activity of CAE, GATE, and GGE using different extraction methods and ethanol ratios: DPPH.

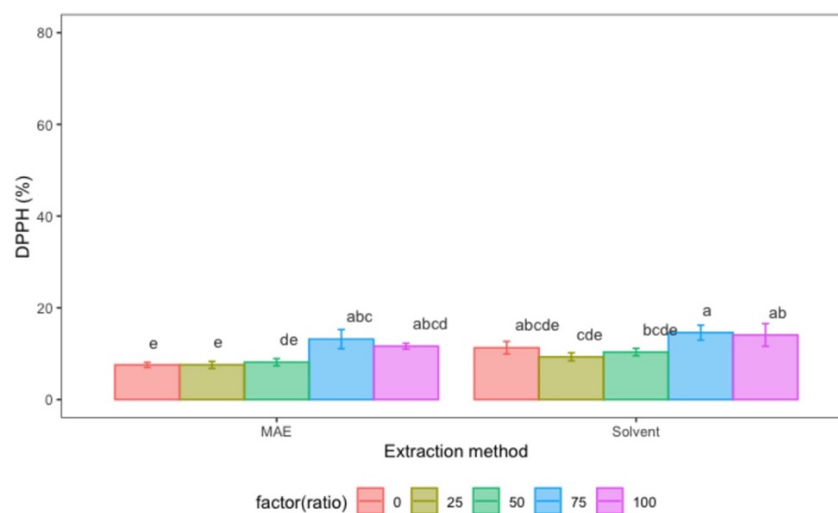
Ethanol ratio	Percentage of DPPH Inhibition (%)					
	CAE		GATE		GGE	
	Solvent extraction	MAE	Solvent extraction	MAE	Solvent extraction	MAE
<b>0</b>	37.80± 15.40 <sup>bc</sup>	45.80± 5.64 <sup>abc</sup>	11.30± 1.37 <sup>abcde</sup>	7.55± 0.57 <sup>e</sup>	7.83± 3.30 <sup>f</sup>	15.50± 2.41 <sup>f</sup>
<b>25</b>	53.80± 5.22 <sup>ab</sup>	59.10± 1.08 <sup>a</sup>	9.32± 0.87 <sup>cde</sup>	7.57± 0.76 <sup>e</sup>	43.60± 3.34 <sup>cde</sup>	48.10± 2.49 <sup>bcd</sup>
<b>50</b>	56.20± 0.30 <sup>a</sup>	59.20± 0.59 <sup>a</sup>	10.40± 0.81 <sup>bcdde</sup>	8.15± 0.78 <sup>de</sup>	53.40± 2.67 <sup>abc</sup>	45.70± 2.45 <sup>cd</sup>
<b>75</b>	53.50± 3.13 <sup>ab</sup>	55.20± 1.72 <sup>a</sup>	14.60± 1.64 <sup>a</sup>	13.20± 2.08 <sup>abc</sup>	61.00± 1.17 <sup>a</sup>	56.60± 5.19 <sup>ab</sup>
<b>100</b>	29.90± 4.60 <sup>c</sup>	33.4± 2.06 <sup>c</sup>	14.10± 2.47 <sup>ab</sup>	11.60± 0.64 <sup>abcd</sup>	36.00± 4.89 <sup>e</sup>	39.80± 3.69 <sup>de</sup>

Percentage of DPPH inhibition (%) (mean ± SD, n = 3). Means with different superscript letters (a-f) of the same plant extract i.e., same column, are significantly different (Tukey's pairwise comparisons, p < 0.05). CAE: *C. asiatica* extract; GATE: *G. atroviridis* extract; GGE: *G. gnemon* extract; MAE: Microwave-assisted extraction.



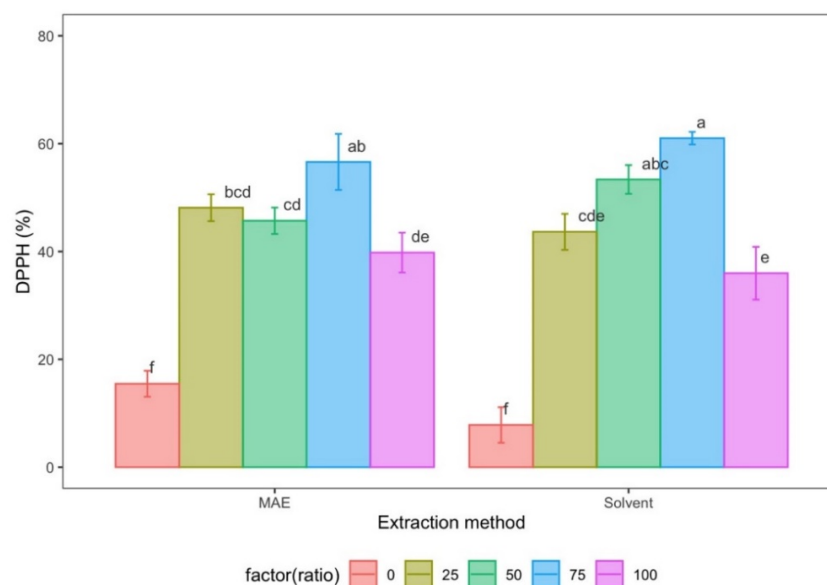
**Figure 3.4** Percentage of DPPH inhibition of CAE using different extraction methods; solvent and microwave assisted extraction (MAE) and varying ethanol ratios (0, 25, 50, 75, and 100 ethanol).

Bar graphs represent the means of percentage of DPPH inhibition. Error bars represent the sample standard deviation (mean ± SD, n = 3). Means sharing the same letter indicate that the percentage of DPPH inhibition is not significantly different, while means with different letters indicate a statistically significant difference in percentage of DPPH inhibition (Tukey's pairwise comparisons, p < 0.05).



**Figure 3.5** Percentage of DPPH inhibition of GATE using different extraction methods; solvent and microwave assisted extraction (MAE) and varying ethanol ratios (0, 25, 50, 75, and 100 ethanol).

Bar graphs represent the means of percentage of DPPH inhibition. Error bars represent the sample standard deviation (mean  $\pm$  SD, n = 3). Means sharing the same letter indicate that the percentage of DPPH inhibition is not significantly different, while means with different letters indicate a statistically significant difference in percentage of DPPH inhibition (Tukey's pairwise comparisons,  $p < 0.05$ ).



**Figure 3.6** Percentage of DPPH inhibition of GGE using different extraction methods; solvent and microwave assisted extraction (MAE) and varying ethanol ratios (0, 25, 50, 75, and 100 ethanol).

Bar graphs represent the means of percentage of DPPH inhibition. Error bars represent the sample standard deviation (mean  $\pm$  SD, n = 3). Means sharing the same letter indicate that the percentage of DPPH inhibition is not significantly different, while means with different letters indicate a statistically significant difference in percentage of DPPH inhibition (Tukey's pairwise comparisons,  $p < 0.05$ ).

The published literature on CAE is limited, making a comprehensive comparison of its biological activity between this study and previous research somewhat challenging. A search for '*Colubrina asiatica*' in the Web of Science and Scopus databases yielded only 14 and 25 results, respectively. The limited reports on the CAE highlight the importance of the current study for the contribution of knowledge on its biological activities. The available data on DPPH scavenging activity was reported by Desai and Gaikwad (2014), which revealed that the aqueous extract of *C. asiatica* leaves exhibited 54.58% and 64.39% DPPH inhibition at extract concentrations of 0.2 mg/mL and 0.4 mg/mL, respectively. Another study by Desai et al. (2015) recorded 36% DPPH inhibition using a 60 µg/mL concentration of *C. asiatica* leaves extracted with boiling water. In comparison, the DPPH inhibition values varied between studies as different extract concentrations and extraction procedures were utilised. The percentage of DPPH inhibition of CAE obtained in this study, particularly with an ethanol ratio of 0 (aqueous extract), were lower than those previously reported. The discrepancies may be due to variations in extraction procedures, as Desai and Gaikwad (2014) performed the extraction process thrice, which might increase the extraction yield of bioactive constituents. Furthermore, Desai et al. (2015) used boiling water for the extraction, likely enhancing the release of bound phenolics and ultimately recovering a higher number of active phytoconstituents (Toor and Savage, 2006).

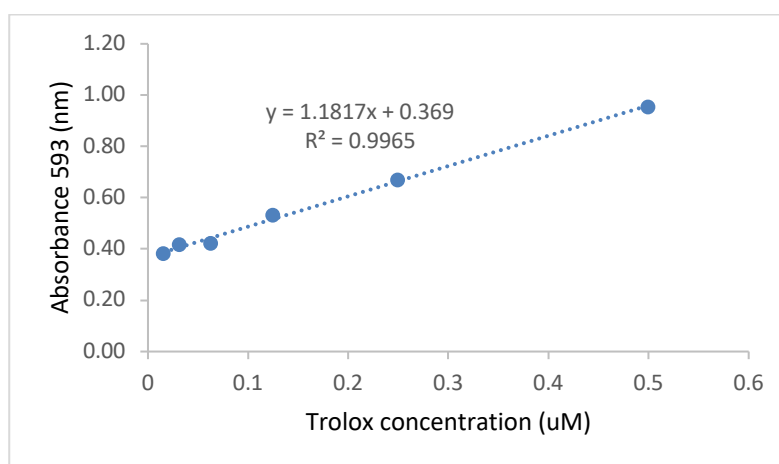
As for GATE, the DPPH inhibition in this present study was relatively lower than those reported by Nursakinah et al. (2012), where an aqueous extract of *G. atroviridis* fruit exhibited 52±0.11% inhibition at concentration of 5 mg/mL. It was noted that their extraction was performed at a higher temperature (60 °C), which may have contributed to the enhanced antioxidant activity. Similarly, Thongkham et al. (2021) reported a much higher DPPH inhibition of 81.30±4.40% using half-ripe *G. atroviridis* fruit (2.5 mg/mL). In addition to fruit, other parts of *G. atroviridis* have also been studied for their antioxidant properties. Al-Mansoub et al. (2014) analysed various plant parts, including leaves, stems, ripe and unripe fruit rinds, and whole fruits (both ripe and unripe, with seeds). Their findings revealed that the ripe fruit rind exhibited the lowest antioxidant activity, as indicated by the highest IC<sub>50</sub> values of 684.17±136.32 µg/mL and 943.08±11.46 µg/mL for methanol and aqueous extract, respectively. Since the present study also utilised ripe fruit, this may explain the lower DPPH inhibition observed. Additionally, Jamila et al. (2020) found that GATE extracted with polar organic solvents, such as ethanol (IC<sub>50</sub>: 5.02 µg/mL) and ethyl acetate (IC<sub>50</sub>: 5.17 µg/mL), demonstrated stronger antioxidant activity. This aligns with the present study's findings, where a 100% ethanol extract of GATE resulted in one of the highest DPPH inhibition

levels. Other than DPPH, other antioxidant assays have been performed on *G. atroviridis*. Mackeen et al. (2000) assessed various plant parts including fruit, stem bark, trunk bark, roots, and leaves using ferric thiocyanate (FTC) and thiobarbituric acid (TBA) assays. Their results demonstrated strong antioxidant activity in all extracts except fruit, with inhibition ranging from 64 to 90% in the FTC assay and 87 to 93% in the TBA assay, values that exceeded those of the commercial antioxidant  $\alpha$ -tocopherol.

In the case of GGE, the DPPH scavenging activity of GGE25 to GGE100 was found to be higher compared to the findings of Wazir et al. (2011). Their study reported inhibition values ranging from  $20.68 \pm 0.24\%$  to  $26.38 \pm 0.13\%$  using five different extraction solvents: methanol, ethanol, hexane, chloroform, and boiling water. However, their study utilised a relatively low concentration ( $300 \mu\text{g/mL}$ ) of *G. gnemon* leaf extracts, which may explain the observed findings. In a separate study, Santoso et al. (2010) investigated the DPPH scavenging activity utilising different *G. gnemon* plant parts. They found that both young and mature leaves exhibited greater DPPH scavenging activity than the seed skin and endosperm in methanolic extracts of *G. gnemon*. A previous study by Kato, E. et al. (2009) identified six stilbenoid compounds extracted from dried *G. gnemon* endosperms using 50% ethanol. Stilbenoids, a class of phenolic compounds known for their strong antioxidant properties, exhibited notable DPPH scavenging activity, as indicated by their  $\text{IC}_{50}$  values. These values were recorded as follows: gnetin L ( $11.1 \pm 1.6 \mu\text{M}$ ), gnetin C ( $10.7 \pm 0.2 \mu\text{M}$ ), gnemonoside A ( $8.3 \pm 0.7 \mu\text{M}$ ), gnemonoside C ( $11.3 \pm 0.1 \mu\text{M}$ ), gnemonoside D ( $9.4 \pm 0.8 \mu\text{M}$ ), and resveratrol ( $13.2 \pm 0.8 \mu\text{M}$ ). All six compounds demonstrated greater scavenging activity compared to the positive controls, ascorbic acid ( $14.1 \pm 0.3 \mu\text{M}$ ) and  $\alpha$ -tocopherol ( $17.1 \pm 1.7 \mu\text{M}$ ), after a five-hour incubation period (Kato, E. et al., 2009). These data indicate that different solvents polarity, extract concentrations, and different plant parts affect the percentage of DPPH inhibition activity, likely due to different phytoconstituents obtained. The findings from this section highlight the potential of antioxidants derived from CAE, GATE, and GGE to inhibit the DPPH radicals. It is, however, important to point out that this antioxidant potential is based on a single measurement of DPPH inhibition, therefore, the other antioxidant measurement method, the FRAP assay was performed to provide a more comprehensive antioxidant profile of the plant extracts, as discussed in the following section.

### 3.3.3.2 Ferric reducing antioxidant power (FRAP) assay

The FRAP assay is based on the reaction where ferric ions ( $\text{Fe}^{3+}$ )-ligand is reduced to ferrous complex ( $\text{Fe}^{2+}$ ) by the action of antioxidants in acidic environments, resulting in an intense navy-blue colour quantified using a spectrophotometer at 593 nm. The absorbance value is directly proportional to the total ferric reducing power of the samples, which reflects the antioxidant potential of the extracts (Benzie and Strain, 1999). A reference standard of Trolox solution with concentrations ranging from 0.016 to 0.50  $\mu\text{M}$  was prepared, and a graph with a linear equation of  $y=1.1817x+ 0.369$ ,  $R^2 = 0.9965$  was constructed, where  $y$  is the absorbance and  $x$  is the Trolox equivalent (TE) concentration ( $\mu\text{M}$ ) (Figure 3.7). The results are expressed as  $\mu\text{M TE/g}$  of dry weight (DW).



**Figure 3.7** Trolox standard curve for FRAP determination using Trolox at concentration between 0.016 to 0.50  $\mu\text{M}$ .

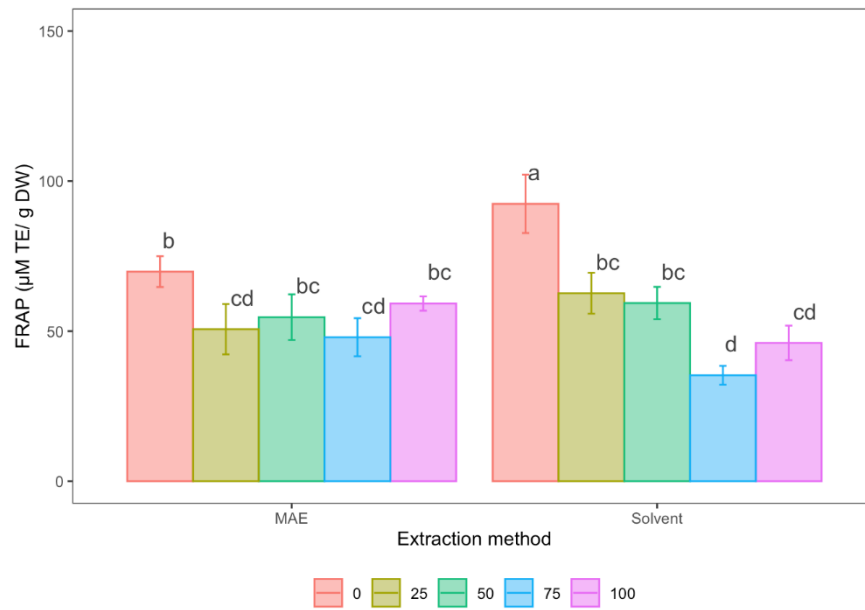
All extracts show some degree of reducing power using the concentration of 10 mg/mL extracts (Table 3.4 and Figures 3.8 to 3.10). The statistical analyses of general linear model suggested that FRAP values were influenced by different ethanol ratios in CAE and GGE ( $p < 0.05$ ) but not in GATE. Additionally, extraction methods significantly impacted FRAP values only in GGE ( $p < 0.05$ ). In terms of specific plant extracts, *C. asiatica* exhibited its highest antioxidant potential in CAE0-S, with a FRAP value of  $92.40 \pm 9.74 \mu\text{M TE/g DW}$ , which was significantly higher than other CAE ( $p < 0.05$ ). For *G. atroviridis*, the highest FRAP value was observed in GATE50-S ( $18.50 \pm 2.19 \mu\text{M TE/g DW}$ ), with similar values recorded in GATE75-S, GATE0-M, and GATE100-M ( $p > 0.05$ ), whereas significantly lower values were recorded in GATE0-S ( $8.23 \pm 0.80 \mu\text{M TE/g DW}$ ), GATE25-S ( $10.60 \pm 1.79 \mu\text{M TE/g DW}$ ), GATE25-M ( $11.20 \pm 1.10 \mu\text{M TE/g DW}$ ), GATE50-M ( $10.10 \pm 1.30 \mu\text{M TE/g DW}$ ), GATE75-M ( $11.10 \pm 1.75 \mu\text{M TE/g DW}$ ), and GATE100-S ( $9.64 \pm 1.75 \mu\text{M TE/g DW}$ ) ( $p < 0.05$ ). In addition, *G. gnemon* exhibited its highest antioxidant activity in GGE0-S, with a FRAP value of

108.00±7.88 µM TE/g DW. This value was statistically comparable to the FRAP values of GGE50-S, GGE100-S, and GGE100-M ( $p > 0.05$ ), and it was significantly higher than GGE0-M (77.40±6.55 µM TE/g DW), GGE25-S (80.10±7.79 µM TE/g DW), GGE25-M (69.40±7.27 µM TE/g DW), GGE50-M (64.90±3.67 µM TE/g DW), GGE75-S (81.80±9.10 µM TE/g DW), and GGE75-M (69.20±6.21 µM TE/g DW) ( $p < 0.05$ ). For *C. asiatica*, solvent extraction with an ethanol ratio of 0 was the most effective in achieving the highest FRAP value. In *G. atroviridis*, extracts obtained through solvent extraction at ethanol ratios of 50 and 75 showed higher FRAP values, while MAE extracts at ethanol ratios of 0 and 100 also yielded comparably higher values. Regarding *G. gnemon*, higher FRAP values were observed in extracts from solvent extraction at ethanol ratios of 0, 50, and 100, as well as from MAE at an ethanol ratio of 100.

**Table 3.4** Antioxidant activity of CAE, GATE, and GGE using different extraction methods and ethanol ratios: FRAP.

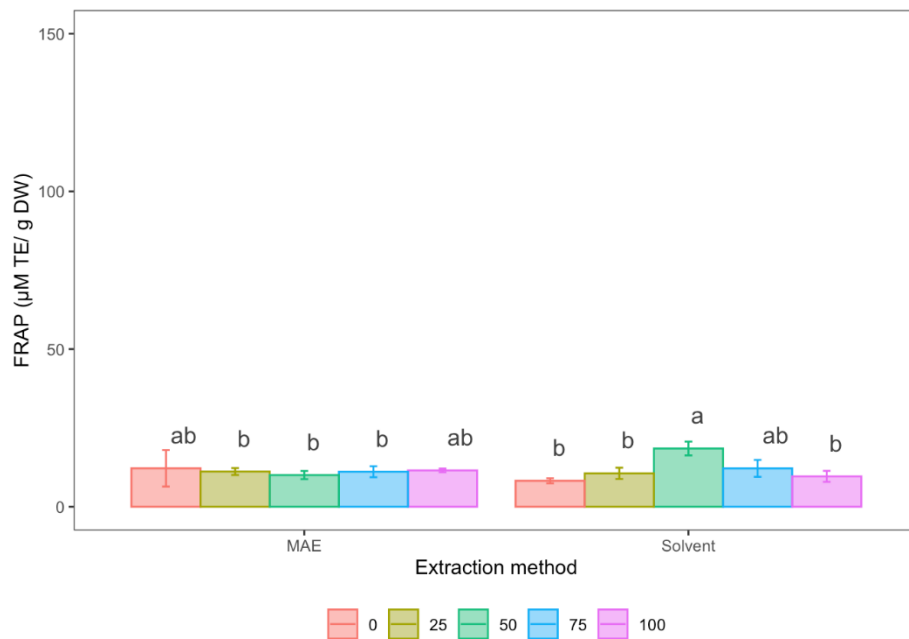
Ethanol ratio	FRAP (µM TE/g DW)					
	CAE		GATE		GGE	
	Solvent extraction	MAE	Solvent extraction	MAE	Solvent extraction	MAE
<b>0</b>	92.40± 9.74 <sup>a</sup>	69.80± 5.13 <sup>b</sup>	8.23± 0.80 <sup>b</sup>	12.20± 5.78 <sup>ab</sup>	108.00± 7.88 <sup>a</sup>	77.40± 6.55 <sup>bcd</sup>
<b>25</b>	62.60± 6.82 <sup>bc</sup>	50.70± 8.39 <sup>cd</sup>	10.60± 1.79 <sup>b</sup>	11.20± 1.10 <sup>b</sup>	80.10± 7.79 <sup>bcd</sup>	69.40± 7.27 <sup>cd</sup>
<b>50</b>	59.40± 5.40 <sup>bc</sup>	54.70± 7.62 <sup>bc</sup>	18.50± 2.19 <sup>a</sup>	10.10± 1.30 <sup>b</sup>	87.10± 8.53 <sup>abc</sup>	64.90± 3.67 <sup>d</sup>
<b>75</b>	35.30± 3.13 <sup>d</sup>	48.00± 6.34 <sup>cd</sup>	12.20± 2.68 <sup>ab</sup>	11.10± 1.75 <sup>b</sup>	81.80± 9.10 <sup>bcd</sup>	69.20± 6.21 <sup>cd</sup>
<b>100</b>	46.10± 5.77 <sup>cd</sup>	59.20± 2.39 <sup>bc</sup>	9.64± 1.75 <sup>b</sup>	11.50± 0.58 <sup>ab</sup>	94.90± 7.26 <sup>ab</sup>	104.00± 8.90 <sup>a</sup>

FRAP (µM TE/g DW) (mean ± SD, n = 3). Means with different superscript letters (a-d) of the same plant extract i.e., same column, are significantly different (Tukey's pairwise comparisons,  $p < 0.05$ ). CAE: *C. asiatica* extract; GATE: *G. atroviridis* extract; GGE: *G. gnemon* extract; MAE: Microwave-assisted extraction.



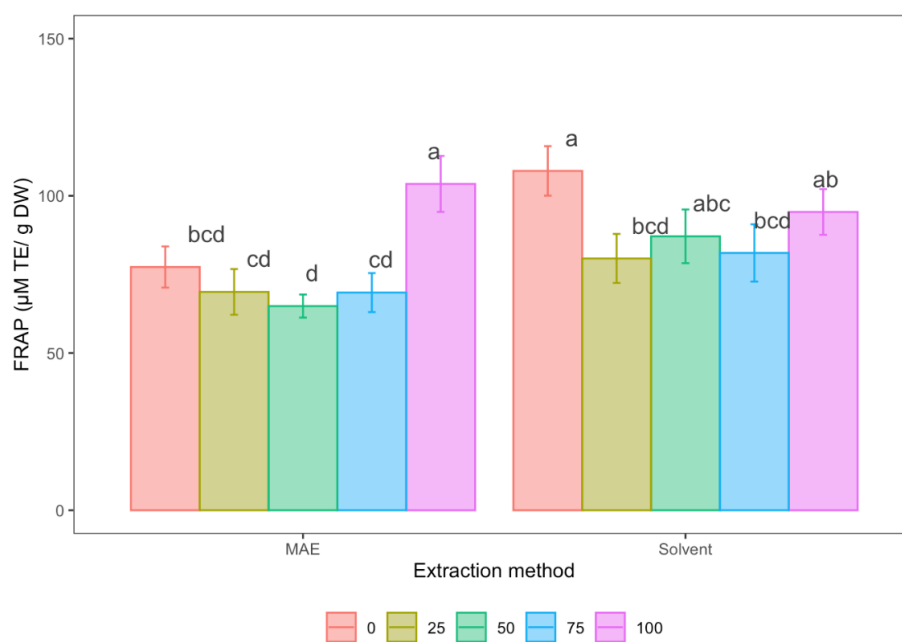
**Figure 3.8** FRAP value ( $\mu\text{M TE/g DW}$ ) of CAE using different extraction methods; solvent and microwave assisted extraction (MAE) and varying ethanol ratios (0, 25, 50, 75, and 100 ethanol).

Bar graphs represent the means of FRAP value. Error bars represent the sample standard deviation (mean  $\pm$  SD,  $n = 3$ ). Means sharing the same letter indicate that the FRAP value is not significantly different, while means with different letters indicate a statistically significant difference in FRAP value (Tukey's pairwise comparisons,  $p < 0.05$ ).



**Figure 3.9** FRAP value ( $\mu\text{M TE/g DW}$ ) of GATE using different extraction methods; solvent and microwave assisted extraction (MAE) and varying ethanol ratios (0, 25, 50, 75, and 100 ethanol).

Bar graphs represent the means of FRAP value. Error bars represent the sample standard deviation (mean  $\pm$  SD,  $n = 3$ ). Means sharing the same letter indicate that the FRAP value is not significantly different, while means with different letters indicate a statistically significant difference in FRAP value (Tukey's pairwise comparisons,  $p < 0.05$ ).



**Figure 3.10** FRAP value ( $\mu\text{M TE/g DW}$ ) of GGE using different extraction methods; solvent and microwave assisted extraction (MAE) and varying ethanol ratios (0, 25, 50, 75, and 100 ethanol).

Bar graphs represent the means of FRAP value. Error bars represent the sample standard deviation (mean  $\pm$  SD,  $n = 3$ ). Means sharing the same letter indicate that the FRAP value is not significantly different, while means with different letters indicate a statistically significant difference in FRAP value (Tukey's pairwise comparisons,  $p < 0.05$ ).

Based on the data, the antioxidant activity of the analysed plant extracts varied between DPPH and FRAP assays. In DPPH inhibition, CAE exhibited the highest antioxidant activity, while in FRAP, GGE ranked first. In contrast, GATE consistently showed the lowest antioxidant activity in both assays. The discrepancy between the results can be attributed to the different phytoconstituents in plant extracts that affect the antioxidant mechanism of action. As discussed earlier in Section 3.3.2, CAE has certain degrees of phenolic content. Phenolics are the group of secondary metabolites that possessed the ideal chemical structures for scavenging activities, as the hydroxyl groups (OH) are prone to donate a hydrogen atom or an electron to a free radical. The extended conjugated aromatic system facilitates the delocalisation of an unpaired electron. Briefly, the phenolic compounds exert their antioxidant activity by acting as free radical acceptors and chain breakers. They interfere with the lipid oxidation as well as the oxidation for other molecules by rapid donation of a hydrogen atom to radicals, which eventually produce relatively stable phenoxy radical intermediates (Dai and Mumper, 2010). In addition, phytoconstituents in GGE, such as terpenoids, might have played a significant role in the higher FRAP values. Terpenoids contain conjugated double bonds which are speculated to be responsible for the antioxidant activity (Wojtunik-Kulesza et al., 2018). Other triterpenoids present in GGE, such as ursolic acid, contain hydroxyl groups that

can donate electrons from antioxidants through a single electron transfer mechanism (Samsonowicz et al., 2021). Other factors such as the DPPH and FRAP solubility, activation energy, redox potential, and stability under varying pH conditions and processing methods might also influence the extent of antioxidant activity (Gil et al., 2002; Sharma and Singh, 2013; Fidrianny et al., 2015).

The available literature on *C. asiatica* highlights its significant reducing power activity, particularly in the aqueous extract of its leaves and stem, which occurs in a dose-dependent manner. A previous study identified ten essential oils, including dodecamethylcyclohexasiloxane, tetradecamethyl-cycloheptasiloxane,  $\alpha$ -cubebene, and 2,4-dimethylhexane, which are the potential contributors to its antioxidant properties (Desai and Gaikwad, 2014). Another study reported that *C. asiatica* extracted with boiling water exhibited higher reducing power activity compared to ascorbic acid, the control (Desai et al., 2015). An earlier study by (Mat-Ali, 2008) measured reducing power based on  $\text{Fe}^{2+}$  concentration (mM) and reported FRAP values of  $0.1 \pm 0.1$  mM and  $0.2 \pm 0.0$  mM for two different *C. asiatica* batches, Batch 1 and 2, respectively.

Previous investigations on the leaves and fruits of *G. atroviridis* using 10% (w/v) aqueous extracts showed that the leaf extract ( $2.24 \pm 0.02$  mmol/L) exhibited significantly higher reducing power activity than the fruit extract (data not included), and comparable to that of the standard antioxidant butylated hydroxytoluene (BHT) ( $2.29 \pm 0.04$  mmol/L) (Nursakinah et al., 2012). Similarly, a study using methanol and aqueous extracts at a concentration of 10 mg/mL found that leaf and stem extracts demonstrated better antioxidant activity than the fruit extract. Additionally, methanol extracts exhibited higher antioxidant activity than aqueous extracts (Al-Mansoub et al., 2014). However, these findings contrast with those of Chew and Lim (2018), who reported comparable antioxidant activity for *G. atroviridis* leaves ( $2.93 \pm 1.33$  mg GAE/g), pericarps ( $0.139 \pm 0.049$  mg GAE/g), and pulps ( $0.589 \pm 0.096$  mg GAE/g) when extracted using 50% ethanol.

The reducing power of *G. gnemon* leaf powder extracted with boiling water at 80 °C was measured at  $1248.14 \pm 115.12$   $\mu\text{g/g}$  DW Trolox equivalent. The study also revealed that antioxidant activity was highest when measured using the ABTS assay, followed by FRAP, with the lowest activity recorded using DPPH, relative to standard antioxidant compounds gallic acid and Trolox (Suksanga et al., 2023). An earlier study by Santoso et al. (2010) suggested that antioxidants in the edible parts of *G. gnemon* (young leaves, mature leaves, seed skin, and endosperm) were predominantly water-soluble, as indicated by higher hydrophilic ORAC activity compared to lipophilic ORAC. Additionally, research by Siswoyo et al.

(2011) isolated two protein fractions from *G. gnemon* seeds which are Gg-AOPI (0.213±0.021 mg vitamin C) and Gg-AOPII (0.150±0.039 mg vitamin C) with antioxidant activity determined by reducing power relative to vitamin C content. Furthermore, (Wazir et al., 2011) reported the reducing power activity of a 300 µg/mL leaf extract in solvents of varying polarity, ranging from 77.70±7.54 to 62.03±1.04%. Based on previous and current findings, *G. gnemon* exhibits antioxidant activity through its ability to donate electrons, as demonstrated by its capacity to reduce ferric ion (Fe<sup>3+</sup>)-ligand to the ferrous (Fe<sup>2+</sup>) complexes.

Overall, the findings from this current study and the previous studies showed diverse ferric reducing power activity, mainly due to differences in extraction parameters, solvents, and concentrations. The variations in reported results in both the present study and previous research were observed. The difference in reporting the antioxidant unit and the use of different standards made it difficult to compare the antioxidant data from the current study and the prior reports. For instance, Mat-Ali, (2008) and Nursakinah et al. (2012) reported the FRAP data in terms of mM Fe<sup>2+</sup> and mmol/L, respectively, whereas the current study used µM TE/g of dry weight as the unit of measurement. Additionally, the existing literature on the biological activities of *C. asiatica*, *G. atroviridis*, and *G. gnemon* primarily focuses on solvent extraction methods for evaluating total phenolic content and antioxidant activities (DPPH and FRAP), with limited emphasis on MAE. Consequently, this study primarily discusses solvent extraction rather than MAE. Expanding data on MAE would enable a more comprehensive comparison of the biological activities of these extracts.

In summary, the antioxidant assays of percentage of DPPH inhibition and FRAP indicated that all three plant extracts of CAE, GATE, and GGE exhibited antioxidant potential, though GATE demonstrated lower activity. The antioxidant activity of DPPH and FRAP was more significantly influenced by the utilisation of extracts with varying ethanol ratios than by different extraction methods. The data on the highest antioxidant activity was diverse in terms of the specific plant extract and type of antioxidant assay. The antioxidant activities of the three plant extracts ranked in the following order based on the overall rankings for DPPH inhibition: CAE > GGE > GATE, and the antioxidant activity based on FRAP followed the order of GGE > CAE > GATE. Further studies, such as antimicrobial activity assessments, would be valuable in exploring their other bioactive potential.

### 3.3.4 Correlation of total phenolic content and antioxidant activity

In this study, Pearson's correlation analysis was conducted to examine the relationship between the total phenolic content of CAE, GATE, and GGE, and their antioxidant activities, as assessed by DPPH and FRAP assays (Table 3.5). A correlation is considered highly positive when  $0.61 \leq r \leq 0.97$  and highly negative when  $-0.61 \leq r \leq -0.97$  (Thaipong et al., 2006; Fidrianny et al., 2015). The findings revealed a significant correlation in CAE between total phenolic content and both DPPH and FRAP (Figures 3.11a and 3.11b, respectively). Specifically, CAE exhibited a moderate positive correlation with DPPH ( $r = 0.498$ ,  $p < 0.05$ ) and FRAP ( $r = 0.526$ ,  $p < 0.05$ ). In contrast, no significant correlations were observed in GATE and GGE. GATE displayed a low negative correlation with DPPH ( $r = -0.156$ ,  $p > 0.05$ ) and a low positive correlation with FRAP ( $r = 0.210$ ,  $p > 0.05$ ). Similarly, GGE showed low positive correlations with both DPPH ( $r = 0.022$ ,  $p > 0.05$ ) and FRAP ( $r = 0.209$ ,  $p > 0.05$ ).

The correlation analysis for CAE revealed that antioxidant activity, as measured by DPPH and FRAP, increased with higher phenolic content, suggesting that phenolic compounds contribute to its antioxidant properties. A previous study identified phenolic compounds in *C. asiatica* leaf including quercetin-3-O-rhamnoside, kaempferol-3-O-glucoside, and kaempferol-3-O-rutinoside, which might contribute to the antioxidant activity in CAE (Mat-Ali, 2008). A similar investigation indicated a notable correlation between total phenolic content and FRAP in two distinct batches of *C. asiatica*, yielding correlation coefficients of -0.950 for Batch 1 (harvested in the rainy season) and 0.945 for Batch 2 (harvested in the dry season) ( $p < 0.001$ ). In contrast to the current study, the previous study reported a stronger positive correlation for Batch 2 ( $r = 0.945$ ) compared to the finding of this study ( $r = 0.526$ ). However, it exhibited a greater negative correlation with Batch 1 ( $r = -0.950$ ). The discrepancy could be due to the variation in factors including sampling location, extraction methods, harvesting season, and post-harvest storage conditions. Various studies have reported that these factors significantly influence the biological activities of plant extracts (Rodriguez-Rojo et al., 2012; Fracassetti et al., 2013; Lu and Luthria, 2014; Kabubii et al., 2023).

Regarding GATE, no significant correlation was found between total phenolic content and antioxidant activities of both DPPH and FRAP. As detailed in Sections 3.3.2 and 3.3.3, this study reported a low total phenolic content, DPPH inhibition, and FRAP activities for GATE. A similar correlation trend was observed in the study by Al-Mansoub et al. (2014), which reported positive correlations

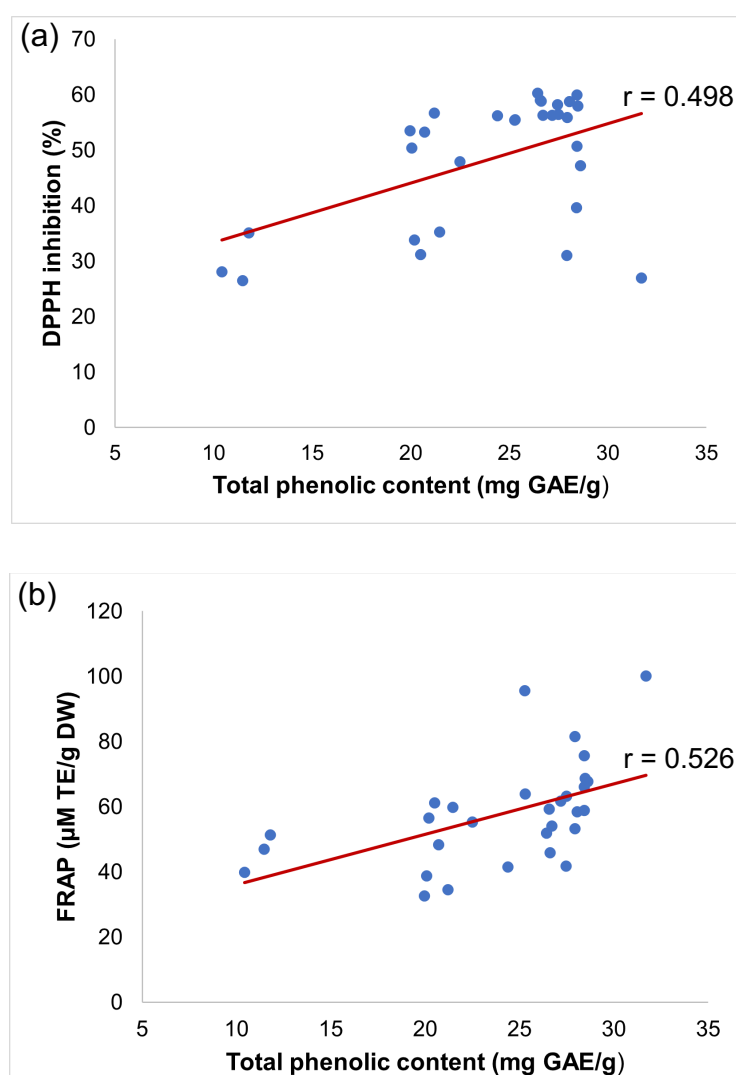
between TPC and FRAP ( $r = 0.729$ ,  $p < 0.01$  for aqueous extract;  $r = 0.840$ ,  $p < 0.01$  for methanol extract), and negative correlations between TPC and DPPH ( $r = -0.807$ ,  $p < 0.01$  for aqueous extract;  $r = -0.593$ ,  $p < 0.01$  for methanol extract). It can be postulated that the strength of correlation may differ among various antioxidant assays, as demonstrated in this study between the DPPH and FRAP assays. The variation can be attributed to differences in the mechanisms of action of antioxidants, indicating that certain phenolic compounds in GATE are more effective in electron transfer reactions in FRAP than in hydrogen atom donation in the DPPH assay (Sharma and Singh, 2013; Foti, 2015; Kiss et al., 2025). The negative correlation is likely attributable to the antioxidant activity resulting from other chemical compounds present in GATE. Previous phytochemical investigation on *G. atroviridis* have reported the presence of other compounds that contributed to the antioxidant activity, including organic acid such as HCA, tartaric acid, and citric acid, with HCA being the predominant acid in the fruit of *G. atroviridis* (Jena et al., 2002). Other compounds, including essential oils, terpenoids, and benzofuran, may also be responsible for the antioxidant activity of GATE (Tan et al., 2013; Shahid et al., 2023). Similar to GATE, GGE exhibited no significant correlation between phenolic content and antioxidant activity. This suggests that phenolic compounds are not the primary contributors to the antioxidant properties of GGE. These findings align with the study by Wazir et al. (2011), which reported very weak correlations between phenolic content and antioxidant activity of DPPH ( $r = 0.0043$ ) and FRAP ( $r = 0.0328$ ). It is likely that the antioxidant activity observed in GGE was due to other classes of bioactive compounds present in the leaf extract, such as diterpene alcohol, monoacylglycerols and triterpenoids (Dutta et al., 2018; Trisha et al., 2024).

In summary, this section revealed the correlation analysis between total phenolic content and antioxidant activity. A significant correlation was identified in CAE, while GATE and GGE demonstrated no significant correlation between total phenolic content and DPPH and FRAP. The strength of these correlations is influenced by various factors, such as the environmental conditions of the plants, variation in extraction methodologies, and the mechanisms of action of bioactive compounds in antioxidant assays.

**Table 3.5** Correlation between total phenolic content and DPPH and FRAP.

Antioxidant assay	Total phenolic content		
	CAE	GATE	GGE
DPPH	0.498*	-0.156 <sup>ns</sup>	0.022 <sup>ns</sup>
FRAP	0.526*	0.210 <sup>ns</sup>	0.209 <sup>ns</sup>

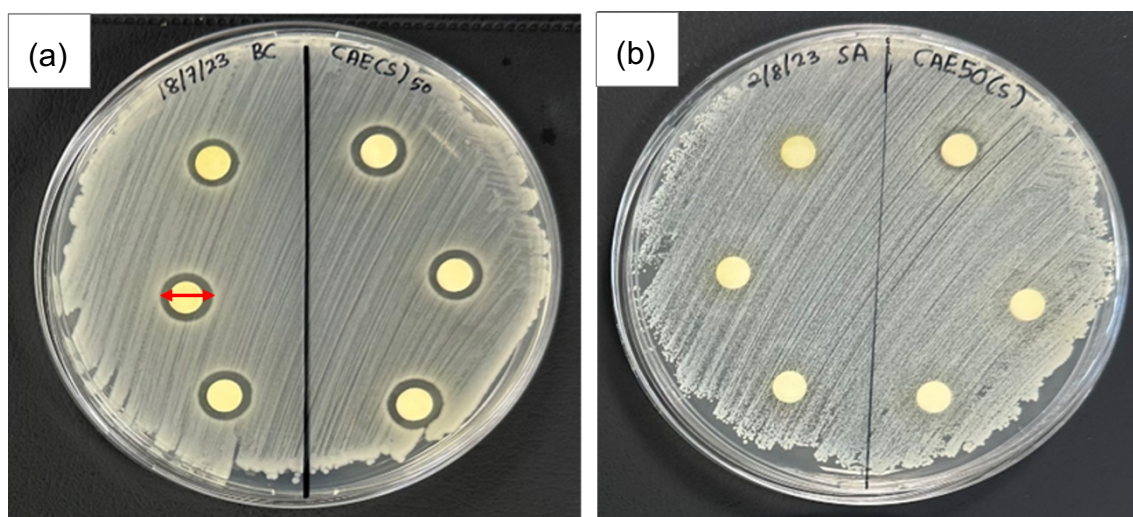
Pearson's correlation analysis was conducted using averaged values of each variable (n = 30). \*, and <sup>ns</sup> indicate; significant at p < 0.05, and non-significant, respectively. CAE: *C. asiatica* extract; GATE: *G. atroviridis* extract; GGE: *G. gnemon* extract



**Figure 3.11** Significant Pearson's correlation of CAE between total phenolic content and (a) percentage of DPPH inhibition ( $r = 0.498$ ), and (b) FRAP value ( $r = 0.526$ ).

### 3.3.5 Antimicrobial activity

The efficacies of CAE, GATE, and GGE (10 mg/mL) against six strains of microorganisms were evaluated using DDA, MIC, and MBC/MFC through a broth microdilution assay. The susceptibility of microorganisms to the extracts in DDA was determined by measuring the clear area on the agar plate, indicating inhibited growth, known as the inhibition zone (Matuschek et al., 2014). According to Table 3.6 and the representative photos in Figures 3.12(a-b), of the six microorganisms tested by DDA, only *B. cereus* was susceptible to the plant extracts, particularly between an ethanol ratio of 50 and 100. *Bacillus cereus*'s growth was not inhibited when ethanol ratios between 0 and 25 were used for both solvent and MAE extracts. The inhibition zone diameters for the extracts ranged from  $7.00\pm 0.00$  to  $10.30\pm 0.76$  mm, and the data were compared with the positive control of 0.1% CHX. Statistical analysis found that the diameter of the inhibition zone of *B. cereus* for all active extracts did not significantly differ from the positive control of their respective extract, with the only exception for the extract of CAE75-M ( $7.83\pm 0.76$  mm) ( $p < 0.05$ ). The data suggests that all tested plant extracts, except for CAE75-M, can inhibit the growth of *B. cereus* similarly to the positive control. All other microorganisms (*E. coli*, *Salmonella*, *S. aureus*, *L. monocytogenes*, and *C. albicans*) were not susceptible to CAE, GATE, and GGE at all ethanol ratios and extraction methods, hence the results were not shown.



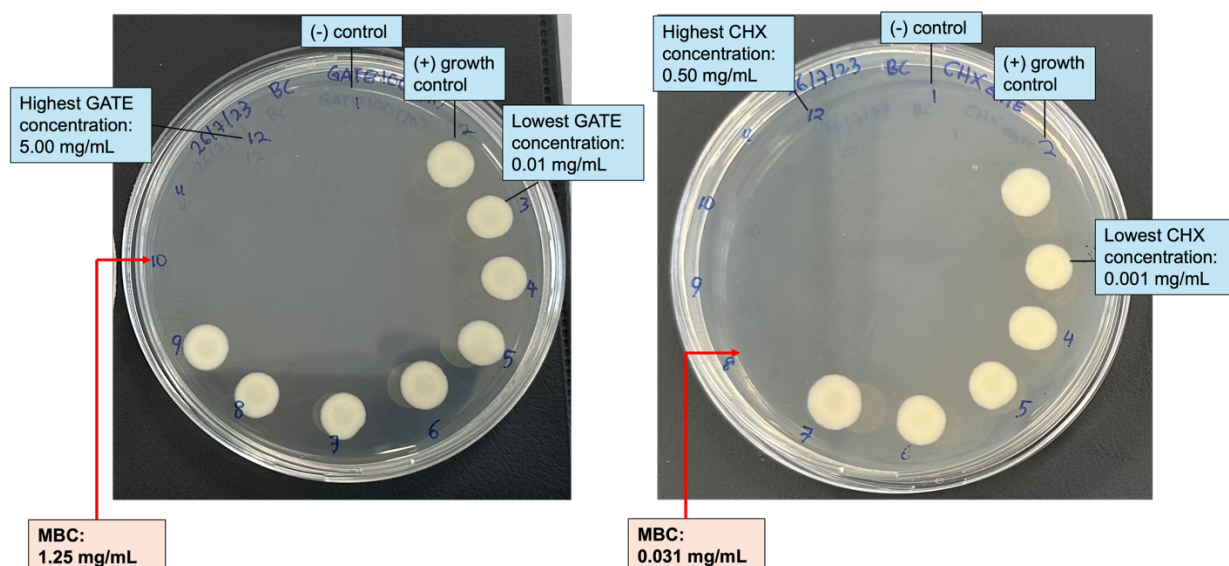
**Figure 3.12** Representative photos of (a) diameter of inhibition zone (red arrow) of 10 mg/mL CAE50-S and CAE75-S extracts tested against *B. cereus* using Mueller Hinton agar plate following 24 hours incubation at  $37\pm 2$  °C, (b) no diameter of inhibition zone of 10 mg/mL CAE50-S and CAE75-S extracts tested against *S. aureus* using Mueller-Hinton agar plate following 24 hours incubation at  $37\pm 2$  °C. The yellow zone around the disc is the colour of the plant extract infused into the disc.

**Table 3.6** DDA and MIC/MBC of 10 mg/mL extracts against *B. cereus*.

Extraction method	Solvent extraction					MAE					(+) control	(-) control
	0	25	50	75	100	0	25	50	75	100	0.1% CHX	10% DMSO
<b>Diameter of inhibition zone (mm)</b>												
CAE	-	-	9.33±0.29 <sup>ab</sup>	9.00±0.00 <sup>ab</sup>	9.00±1.00 <sup>ab</sup>	-	-	8.17±0.29 <sup>ab</sup>	7.83±0.76 <sup>b</sup>	8.50±0.00 <sup>ab</sup>	9.67±0.76 <sup>a</sup>	-
GATE	-	-	7.00±0.00 <sup>a</sup>	7.83±0.76 <sup>a</sup>	7.67±0.58 <sup>a</sup>	-	-	7.33±0.29 <sup>a</sup>	7.00±0.87 <sup>a</sup>	8.17±0.76 <sup>a</sup>	8.67±0.58 <sup>a</sup>	-
GGE	-	-	8.17±0.29 <sup>b</sup>	9.17±0.29 <sup>ab</sup>	9.33±0.29 <sup>ab</sup>	-	-	9.67±0.58 <sup>ab</sup>	9.17±0.76 <sup>ab</sup>	10.30±0.76 <sup>a</sup>	8.83±0.76 <sup>ab</sup>	-
<b>MIC/ MBC (mg/mL)</b>												
CAE	nd	nd	2.50/2.50	5.00/5.00	2.50/2.50	nd	nd	5.00/5.00	5.00/5.00	5.00/5.00	0.008/0.008	-
GATE	nd	nd	2.50/2.50	2.50/2.50	2.50/2.50	nd	nd	2.50/2.50	2.50/2.50	1.25/1.25	0.031/0.031	-
GGE	nd	nd	5.00/5.00	5.00/5.00	0.625/0.625	nd	nd	2.50/2.50	2.50/2.50	2.50/2.50	0.004/0.004	-

Values are the mean ± SD of replications (n=3). Means with different superscript letters (a-b) of the same plant extract are significantly different (Tukey's pairwise comparisons, p < 0.05). (-): no activity, nd: no data. CAE: *C. asiatica* extract; GATE: *G. atroviridis* extract; GGE: *G. gnemon* extract; MAE: Microwave-assisted extraction.

Subsequently, a similar concentration of CAE, GATE, and GGE (10 mg/mL) was utilised to perform MIC and MBC tests to further investigate the antimicrobial potential of the extracts. In this step, MIC and MBC were only performed on *B. cereus* using the extracts with the ethanol ratios that showed an activity in the previous DDA assay (ethanol ratios 50, 75, and 100) (Table 3.6). No MIC and MBC/MFC data obtained for the ethanol ratios of 0 and 25 for *B. cereus* as well as for other microorganisms: *E. coli*, *Salmonella*, *S. aureus*, *L. monocytogenes*, and *C. albicans*. MIC is a minimum plant extract's concentration required to inhibit at least 99% of microorganisms' growth, while MBC/MFC is the minimum concentration required to kill at least 99% of bacteria/fungi (Rukayadi et al., 2013). In other words, a lower MIC, MBC and MFC value indicates better antimicrobial activity. The MIC and MBC values for the tested extracts against *B. cereus* ranged from 0.625 to 5.00 mg/mL (Table 3.6). In the case of *C. asiatica*, both CAE50-S and CAE100-S exhibited the lowest MBC at 2.50 mg/mL. GATE100-M had the lowest MBC for *G. atroviridis* at 1.25 mg/mL, while GGE100-S demonstrated the highest antibacterial activity among all extracts, with an MBC of 0.625 mg/mL. Of the three plant extracts examined, GGE100-S demonstrated the highest potency, requiring only 0.625 mg/mL to achieve a 99% reduction in *B. cereus* growth following 24 hours incubation. It is important to note that positive control for GGE had an MIC/MBC value of 0.004 mg/mL, indicating more potent antibacterial activity compared to GGE100-S. The representative MBC plate photos of GATE100-M and its positive control are shown in Figure 3.13, showing bactericidal activity at 1.25 mg/mL against *B. cereus*. The ranking of antibacterial activity for the plant extracts is as follows: GGE > GATE > CAE.



**Figure 3.13** Representative MBC plates of GATE100-M (left) and CHX (right) against *B. cereus* using Mueller Hinton agar media following 24 hours incubation at  $37\pm 2$  °C with MBC values of 1.25 mg/mL and 0.031 mg/mL, respectively.

Desai et al. (2015) evaluated the essential oils of *C. asiatica* against *E. coli*, *S. aureus*, and *Streptococcus pneumoniae*, reporting inhibition zone diameters of 8, 9, and 10 mm, respectively, while no inhibition was observed for *Pseudomonas aeruginosa*. In comparison to present study, the essential oils obtained by Desai et al. (2015) demonstrated higher efficacy against *E. coli* and *S. aureus*, as no inhibition was observed for either bacterium in this current study. It is possible that using essential oils rather than crude plant extracts (as in this study) improves antimicrobial activity, as the hydrophobic nature of essential oils promotes their integration into lipid cell membranes and mitochondria, resulting in cell wall disruption and increasing permeability (Knobloch et al., 1986, cited in Burt, 2004, p. 239). The leakage of ions and other cellular contents ultimately results in cells' death (Sikkema et al., 1994; Oosterhaven et al., 1995; Gustafson et al., 1998; Helander et al., 1998). Furthermore, components of essential oils, including lipophilic hydrocarbon molecules, can interact with cell proteins in the cytoplasmic membrane by accumulating in the lipid bilayer, thereby disrupting the lipid-protein interactions of bacterial cells (Knobloch et al., 1989; Juven et al., 1994; Sikkema et al., 1995). For *G. atroviridis*, a higher inhibition zone diameter was observed in *G. atroviridis* ethanol extract (10 mg/mL) when tested against seven bacteria (*S. aureus*, *Staphylococcus epidermidis*, *Bacillus subtilis*, *E. coli*, *Salmonella typhimurium*, *Salmonella enteritidis*, and *P. aeruginosa*) and two yeast (*Candida glabrata* and *Candida parapsilosis*) strains. The inhibition zone measured between  $13.00\pm 1.00$  and  $17.40\pm 0.56$  mm (bacteria) and  $7.80\pm 0.20$  and  $15.73\pm 1.15$  mm (yeast) (Basri et al., 2005). These reported values were generally higher than those observed in the present study, probably due to

differences in the source and origin of the microbial strains used, as the previous study utilised a mixed source of strains obtained from ATCC, local clinical isolates, the Department of Biomedical Science laboratory stock (Universiti Kebangsaan Malaysia), and the National Collection of Type Cultures, each of which may differ in susceptibility. Additionally, Basri et al. (2005) did not specify the volume of plant extracts infused to the paper discs, whereas the present study standardised the volume at 25  $\mu$ L. This difference in extract volume may also have contributed to the variation in inhibition zone diameters. A previous investigation on the antimicrobial potential of *G. gnemon* endosperms extracted in 50% ethanol had reported varied MIC values between 250 and 3000  $\mu$ g/mL for the test against *B. subtilis*, *Luconostoc mesenteroides*, *Lactobacillus plantarum*, *E. coli*, *S. cerevisiae*, *Penicillium expansum*, *C. perfringens*, and *Bifidobacterium bifidum* (Kato, E. et al., 2009). A later study found the MIC values between 0.15 and 1.40  $\mu$ g/mL and MBC values between 0.58 and 5.58  $\mu$ g/mL for the seed and peel extracts of *G. gnemon* extracted using ethanol and tested against four bacteria: *B. cereus*, *S. aureus*, *Enterobacter aerogenes*, and *P. aeruginosa* (Parhusip and Sitanggang, 2011). Based on the current and previous findings, diverse diameters of inhibition zones, MIC and MBC were observed among studies, likely due to variations in the plant parts and extracts utilised and the microorganisms tested in each investigation.

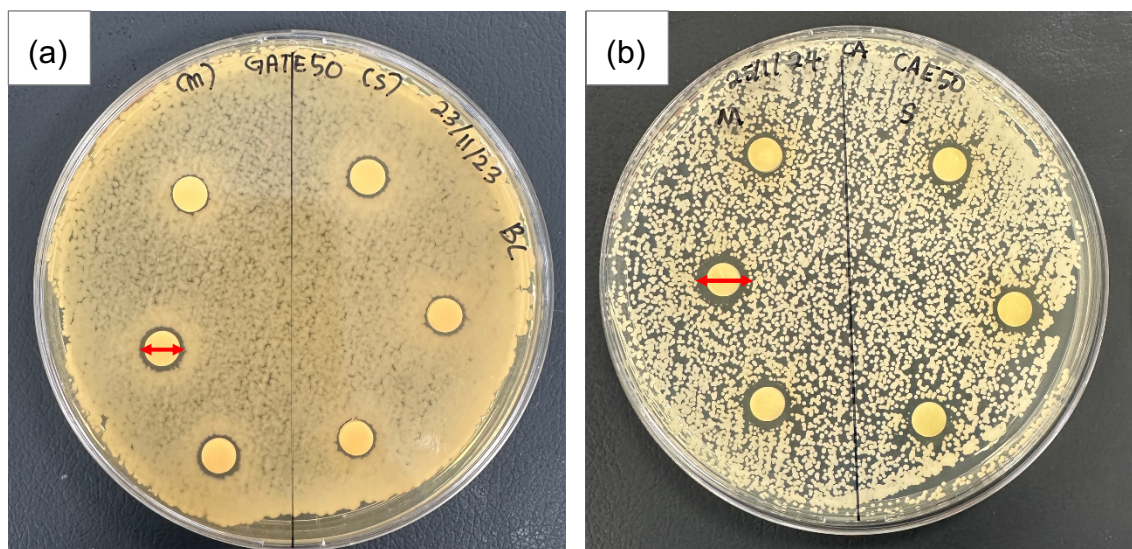
Due to the lack of observed activity against other microorganisms (*E. coli*, *Salmonella*, *S. aureus*, *L. monocytogenes*, and *C. albicans*) at a concentration of 10 mg/mL, new extracts were prepared at a higher concentration of 50 mg/mL, and the assays for DDA, MIC, and MBC/MFC were repeated. In the determination of antimicrobial activity, considering the economic factors related to consumables consumption, experimental materials, as well as the availability of extracts, a single ethanol ratio of 50 was chosen for further testing at a concentration of 50 mg/mL. Furthermore, the analysis of the data indicated comparable inhibition zone diameters for extracts with a 50% ethanol ratio relative to their positive control (Table 3.6). Despite slightly higher MBC values noted for GATE and GGE, the aforementioned factors led to the selection of extracts with a 50% ethanol ratio. The results for DDA with a 50 mg/mL extract are summarised in Table 3.7 and illustrated in Figures 3.14(a-b). Increasing the extract concentration from 10 mg/mL to 50 mg/mL enhanced antimicrobial susceptibility. At the higher concentration, two of the six tested microorganisms, *B. cereus* and *C. albicans* exhibited inhibition zones. However, the inhibitory activity was specific to different extracts: *B. cereus* was only susceptible to GATE50 and *C. albicans* to CAE50. The inhibition zones for *B. cereus* using GATE50-S ( $7.17 \pm 0.29$  mm) and GATE50-M ( $7.33 \pm 0.76$  mm) were significantly lower than 0.1% CHX ( $11.05 \pm 0.50$

mm) ( $p < 0.05$ ). This finding contradicts earlier results at 10 mg/mL, where no significant differences were observed for GATE in comparison to 0.1% CHX. The observed discrepancy may result from DDA limitations, wherein increased extract concentrations slower the diffusion of extract through the disc pores as well as due to the hydrophobic nature of phytoconstituents (Othman et al., 2011). An alternative explanation for this result is that it is due to differences in absorbance values of bacteria during inoculum preparation. An absorbance value between 0.08 and 0.13 is regarded as an equivalent to 0.5 McFarland standard, it can be postulated that a slight variation between the value obtained during the inoculum preparation might result in thicker growth (as seen in the *B. cereus* plate in Figure 3.14a compared to Figure 3.12a), hence reducing the activity of extracts. Nevertheless, the absorbance values obtained for each of the tests were still in the range of 0.08 to 0.13, therefore, it can be suggested that the influence of this factor on the diameter of inhibition zone is rather minimal. The absence of an inhibition zone in 50 mg/mL of CAE and GGE when tested against *B. cereus* may be attributed to similar reasons stated above. Similarly, in the case of *C. albicans*, CAE50-S ( $7.83 \pm 0.29$  mm) and CAE50-M ( $8.00 \pm 0.50$  mm) had significantly lower value compared to 5.0% amphotericin B ( $13.70 \pm 0.29$  mm) ( $p < 0.05$ ).

**Table 3.7** DDA of 50 mg/mL extracts against foodborne pathogens and spoilage microorganisms.

Micro-organisms	Diameter of inhibition zone (mm)							
	Solvent extraction			MAE			(+) control	(-) control
	CAE 50	GATE 50	GGE 50	CAE 50	GATE 50	GGE 50	0.1% CHX	10% DMSO
<i>B. cereus</i>	-	7.17±0.29 <sup>b</sup>	-	-	7.33±0.76 <sup>b</sup>	-	11.50±0.50 <sup>a</sup>	-
<i>E. coli</i>	-	-	-	-	-	-	8.83±0.29	-
<i>S. aureus</i>	-	-	-	-	-	-	12.83±1.15	-
<i>Salmonella</i>	-	-	-	-	-	-	9.50±1.73	-
<i>L. monocytogenes</i>	-	-	-	-	-	-	13.83±0.58	-
<i>C. albicans</i>	7.83±0.29 <sup>b</sup>	-	-	8.00±0.50 <sup>b</sup>	-	-	(*)13.70±0.29 <sup>a</sup>	-

Values are the mean ± SD of replications (n=3). Means with different superscript letters (a-b) of the same microorganisms are significantly different (Tukey's pairwise comparisons,  $p < 0.05$ ) (-): no activity. (\*) Positive control for *C. albicans*: 5.0 % (v/v) Amp. B. CAE: *C. asiatica* extract; GATE: *G. atroviridis* extract; GGE: *G. gnemon* extract; MAE: Microwave-assisted extraction.

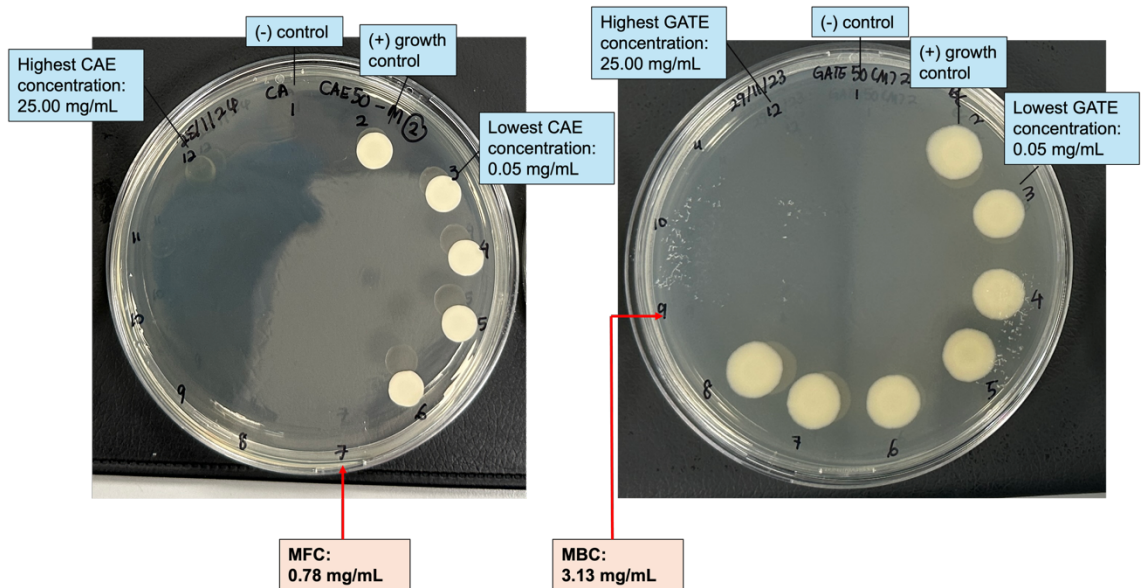


**Figure 3.14** Diameter of inhibition zone (red arrow) of (a) 50 mg/mL GATE50 extracts tested against *B. cereus* using Mueller Hinton agar plate following 24 hours incubation at  $37 \pm 2$  °C, (b) CAE50 extracts tested against *C. albicans* using Sabouraud dextrose agar plate following 48 hours incubation at  $37 \pm 2$  °C. The yellow zone around the disc is the colour of the plant extract infused into the disc.

No inhibition zone activity was observed against other microorganisms, even when CAE, GATE, and GGE were tested at higher concentrations. This can be attributed to the limitations inherent in the DDA method itself. The limitations included factors such as varying diffusion rates, solubility, and evaporation rates of the tested phytoconstituents, which influenced the results of the DDA (King et al., 2008; Bubonja-Sonje et al., 2011). To date, no literature has documented the DDA of CAE at a concentration of 50 mg/mL. However, the leaf fraction of *C. asiatica* at a 40% concentration has been reported to exhibit a higher inhibition zone diameter of  $11.40 \pm 1.20$  mm against *C. albicans* (Irma et al., 2021). Another study reported the inhibition zones for *S. aureus*, *E. coli*, and *C. albicans* at 12 mm, 6.67 mm, and  $\leq 6$  mm, respectively, when utilising GATE extract at a concentration of 50 mg/mL (5%), which contrasts with the findings of this study (Thongkham et al., 2021). In a recent study, a 10% (w/v) concentration of *G. gnemon* leaf extracts demonstrated inhibition zone values of  $12.00 \pm 0.50$  mm for *E. coli* and  $12.50 \pm 0.29$  mm for *S. aureus* (Trisha et al., 2024). The data indicate that variations in inhibition zone values are influenced by myriads of factors such as different source of microbial strains, extraction solvents and concentrations, as well as the use of fractions instead of crude plant extracts.

In addition, the antimicrobial efficacy of the 50 mg/mL extracts was also evaluated using MIC and MBC/MFC assays against similar bacteria and yeast. In contrast to the DDA findings, the data showed that all extracts showed antimicrobial activity via MIC and MBC/MFC for the tested microorganisms, with the exception only for CAE50 when tested against *Salmonella* and GGE50 against *C. albicans* (Table 3.8). Among the extracts, GATE50-S/M consistently showed the highest antibacterial activity, with an MBC of 3.13 mg/mL against *B. cereus* and an MBC of 12.50 mg/mL against the other tested bacterial strains. Meanwhile, CAE50 extracts showed higher antifungal activity compared to other extracts, consistent with the previous DDA data, with CAE50-M demonstrating the strongest antifungal activity, with an MFC of 0.78 mg/mL against *C. albicans*. In comparison, the positive controls exhibited significantly lower MBC/MFC values (0.001 to 0.031 mg/mL for bacteria, 0.002 mg/mL for yeast), indicating superior activity. The MFC and MBC plate photos of CAE50-M and GATE50-M are shown in Figure 3.15, showing fungicidal and bactericidal activities against *C. albicans* and *B. cereus*, respectively. The findings from this current study are consistent with those reported by Thongkham et al. (2021), who observed a similar range of MBC values for the fruit part of GATE, ranging from 3.13 to  $>50.00$  mg/mL, when tested against various bacterial strains (*Streptococcus agalactiae*, *S. aureus*, *Staphylococcus epidermidis*, *Streptococcus intermedius*, *B. subtilis*, *E. coli*). Notably, that study used 95% ethanol as the extraction solvent, whereas the

present study used 50% ethanol. These findings suggest that GATE retains comparable antimicrobial activity even when extracted with a lower ethanol concentration. However, this comparison should be interpreted with caution, as differences in extraction conditions, methodologies, and test organisms could influence the outcomes. In addition, a previous study on *C. asiatica* leaf extract reported antibacterial activity, with MIC values of more than 512 µg/mL against *E. coli* and *S. aureus* (Raunsai et al., 2021). However, comparison with the present study is limited due to the lack of detailed MIC data in that report.



**Figure 3.15** Representative MFC plate of CAE50-M (MFC: 0.78 mg/mL) against *C. albicans* using Sabouraud dextrose agar media (left) and MBC plate of GATE50-M (MBC: 3.13 mg/mL) against *B. cereus* using Mueller Hinton agar media (right) after 48 and 24 hours of incubation periods, respectively.

**Table 3.8** MIC and MBC/MFC of 50 mg/mL plant extracts against foodborne pathogens and spoilage microorganisms.

Microorganisms	MIC/ MBC/ MFC (mg/mL)							
	Solvent extraction			MAE			(+) control	(-) control
	CAE50	GATE50	GGE50	CAE50	GATE50	GGE50	0.1% CHX	10% DMSO
<i>B. cereus</i>	12.50/12.50	3.13/3.13	3.13/3.13	12.50/12.50	3.13/3.13	3.13/3.13	0.03/0.03	-
<i>E. coli</i>	25.00/25.00	6.25/12.50	25.00/25.00	25.00/25.00	6.25/12.50	25.00/25.00	0.001/0.001	-
<i>S. aureus</i>	25.00/25.00	6.25/12.50	25.00/25.00	25.00/25.00	6.25/12.50	25.00/25.00	0.002/0.002	-
<i>Salmonella</i>	-	6.25/12.50	25.00/>25.00	-	6.25/12.50	25.00/>25.00	0.031/0.031	-
<i>L. monocytogenes</i>	25.00/25.00	6.25/12.50	6.25/25.00	25.00/25.00	12.50/12.50	25.00/25.00	0.004/0.004	-
<i>C. albicans</i>	0.78/3.13	25.00/>25.00	-	0.78/0.78	25.00/>25.00	-	*0.001/0.002	-

(-): no activity. (\*) Positive control for *C. albicans*: 0.1 % (v/v) Amp. B. CAE: *C. asiatica* extract; GATE: *G. atroviridis* extract; GGE: *G. gnemon* extract; MAE: Microwave-assisted extraction.

In brief, GGE100-S at a concentration 10 mg/mL exhibited the highest antibacterial activity against *B. cereus* as shown by the lowest MIC and MBC value. For a test at starting concentration of 50 mg/mL, GATE50-S/M demonstrated the highest efficacy against bacteria, while CAE50-M was most effective against fungi. Notably, GATE demonstrated strong antibacterial potential, despite its comparatively low phenolic content and antioxidant activity. This suggests that other bioactive compounds in GATE, such as organic acids (e.g., hydroxycitric acid) likely contribute to its antimicrobial efficacy (Mackeen et al., 2002; Lim et al., 2020). Hydroxycitric acid (HCA), the principal acid present in *G. atroviridis* fruit, may contribute to antimicrobial activity by modulating bacterial metabolic pathways through binding to free iron ions in the medium, thereby limiting bacterial interaction with iron. This interaction may ultimately lead to the disruption in the bacteria cellular pathways (Sumang et al., 2024). In the case of CAE, the antifungal activity is likely due to phenolic compounds from flavonoids such as quercetin-3-O-rhamnoside, kaempferol-3-O-glucoside, and kaempferol-3-O-rutinoside (Mat-Ali, 2008). The mechanism of action of antifungal agents such as flavonoid involves the disruption of the plasma membrane, inhibition of the synthesis of  $\beta$ -glucans and chitin that constitute the fungal cell wall, induction of mitochondrial dysfunction, and the formation of a complex with sterols in the fungal membrane, leading to a loss of membrane integrity (Keukens et al., 1995; Ghannoum and Rice, 1999; Walker and White, 2005; Lagrouh et al., 2017). Additionally, prior research has indicated that saponin obtained from CAE also demonstrate antioxidant and antimicrobial activities, further supporting their role in enhancing antifungal efficacy (Desai and Gaikwad, 2014; Irma et al., 2021). Saponin, which commonly present in CAE exerts antifungal activity by the ability to complex with sterols in fungal membranes which eventually leads to loss of membrane integrity (Keukens et al., 1995). In the case of GGE, previous studies identified diterpene alcohol, monoacylglycerols and triterpenoids from leaf extracts, which may contribute to antibacterial activity (Dutta et al., 2018; Trisha et al., 2024). Phytol, a compound classified as diterpene alcohol, exhibits antibacterial activity by inducing oxidative stress within bacteria cells, which subsequently leads to DNA damage (Lee, W. et al., 2016).

Among the six microorganisms tested, *B. cereus* was the most susceptible (lower MIC/MBC), likely due to its Gram-positive nature that is more permeable to plant extracts. In contrast, Gram-negative bacteria like *Salmonella* and *E. coli* demonstrated higher MIC/MBC values, due to their complex cell wall structure, comprising an outer membrane and peptidoglycan layer, which confers greater intrinsic resistance to plant extracts (Vaara, 1992; Nikaido, 1994; Helander et al.,

1998). To the best of author's knowledge, this is the first report to evaluate the antimicrobial activity of two extract concentrations (10 mg/mL and 50 mg/mL) of CAE, GATE, and GGE against six different microorganisms using both DDA and MIC/MBC/MFC assays. This study, however, possesses certain limitations, such as antifungal activity was assessed against only one fungal strain. Expanding the study to include additional strains would enhance the reliability of the findings. Furthermore, MIC and MBC/MFC assays were not performed for the 10 mg/mL extracts on microorganisms that did not exhibit inhibition zones in the DDA. In summary, for the test at the starting extract concentration of 50 mg/mL, GATE50-S/M demonstrated the strongest antibacterial activity, while CAE50-M showed the highest antifungal activity.

### 3.4 Conclusion

This chapter presents the findings of the effect of utilisation of different ethanol ratios and extraction methods on the yields of CAE, GATE, and GGE. This study also examined the total phenolic content and antioxidant activities, assessed through DPPH and FRAP methods, as well as the impact of varying ethanol ratios and extraction methods on these activities. Additionally, the chapter explored the correlation between total phenolic content and the antioxidant activities, and evaluated the antimicrobial efficacy of CAE, GATE, and GGE against foodborne pathogens and spoilage microorganisms.

Briefly, the findings highlighted that varying ethanol ratios play a greater impact to the extraction yield and biological activities of total phenolic content, DPPH, and FRAP activity for CAE, GATE, and GGE, compared to extraction methods. In the initial part of the study, it was observed that an ethanol ratio between 0 and 50 using both solvent extraction and MAE is preferred to produce higher yields for CAE and GATE. As for GGE, an ethanol ratio between 0 and 75, using both extraction methods, yielded a higher yield. Subsequent analysis of total phenolic content revealed diverse results among plant species and extraction conditions. For CAE, the highest phenolic content was found in extract using ethanol ratio 0 to 50 for solvent extraction and 0 to 75 for MAE. For *G. atroviridis*, MAE extracts with ethanol ratio 50 to 100 had the highest phenolic content. In contrast, *G. gnemon* extracts showed generally comparable phenolic levels, except for GGE100-S. Since phenolic compounds frequently associate with the antioxidant potential of plant extracts, therefore following investigation on the antioxidant potential is performed.

The antioxidant assessment of CAE, GATE, and GGE by DPPH and FRAP assays revealed notable variations in activity, reflecting both the diversity in phytochemical constituents and the different mode of action of antioxidant in specific assay. In the case of CAE, the highest DPPH inhibition achieved with CAE25-S/M to CAE75-S/M as well as CAE0-M. However, as for FRAP assay, the highest FRAP value recorded in CAE0-S. The results emphasise that no single assay can fully characterise the antioxidant capacity of complex plant matrices, as different extracts performed optimally in different assays. The correlation analysis found a significant correlation in CAE between total phenolic content and both DPPH and FRAP, but not for GATE and GGE. In the final section of this chapter, the assessment of antimicrobial potential revealed that at the maximum extract concentration tested (50 mg/mL), GATE50-S/M exhibited the most potent

antibacterial activity, whereas CAE50-M displayed the best antifungal activity. A comprehensive analysis of the plant extracts revealed that GATE achieved the highest extraction yield but had the lowest total phenolic content and antioxidant activity. Thus, it can be inferred that the antimicrobial activity observed in GATE is attributable to a different group of phytochemical constituents in *G. atroviridis*, rather than phenolic compounds. Conversely, it is postulated that the activity of CAE derived from phenolic compounds such as flavonoid and other active phytoconstituents.

These findings from the investigation of biological activities of CAE, GATE, and GGE are critical, as they provide a strong foundation for further research on the application of these extracts. The data were analysed to determine the most suitable active extract for each plant species through a comparative evaluation of their bioactivities and extract availability. For *C. asiatica*, CAE50-S was selected based on higher recovery of yield and total phenolic content with stronger DPPH inhibition. Regarding antimicrobial activity, it demonstrated lower MBC value against *B. cereus* for the test at starting concentration of 10 mg/mL and exhibited antimicrobial activity against five of six tested microorganisms for the test at starting concentration of 50 mg/mL in term of both MIC and MBC/MFC assays. Although CAE50-M recorded a lower MFC for the test at starting concentration of 50 mg/mL, CAE50-S was preferred because it displayed stronger antibacterial activity, including a lower MBC against *B. cereus* for the test at starting concentration of 10 mg/mL. For *G. atroviridis*, GATE50-S, GATE50-M, and GATE100-M consistently displayed higher activities among all *G. atroviridis* extracts. While GATE100-M was not tested at concentration of 50 mg/mL, its inhibition zone diameter at 10 mg/mL was comparable to that of GATE50-S and GATE50-M, and it showed a better MBC value than both. Based on this, GATE100-M was selected for further investigation. In the case of *G. gnemon*, GGE100-S, GGE50-M, GGE75-M, and GGE100-M demonstrated higher activity against *B. cereus* at 10 mg/mL (low MBC values). However, due to extract availability, GGE50-M was chosen for subsequent phase of study.

In conclusion, this chapter provides critical insights into the extraction efficiency, antioxidant potential, and antimicrobial activity of CAE, GATE, and GGE. The findings discovered that CAE, GATE, and GGE possessed some extent of biological activities, and the active extracts of CAE50-S, GATE100-M, and GGE50-M were selected for the development of biodegradable packaging films, utilising zein as the primary packaging material.

## **Chapter 4**

### **Development of Zein-Based Films**

#### **4.1 Introduction**

The utilisation of plastic in food packaging, despite their advantages, has presented many challenges, including land and ocean pollution, as well as the potential leaching of chemicals from plastic into food products (Thompson, R.C. et al., 2009; Gerassimidou et al., 2023). In response, researchers have worked towards creating sustainable alternatives aimed at reducing plastic waste. One type of research involves the development of biodegradable and biobased packaging materials, with an emphasis on the incorporation of active substances to improve the biological activity of packaging. The incorporation of active substances, including bioactive plant extracts, transforms traditional packaging into active packaging. According to the definition by the European FAIR-project CT 98-4170, active packaging is a type of packaging that changes the condition of the packaging to extend shelf-life or improve safety or sensory properties while maintaining the quality of the food (Vermeiren et al., 1999; Robertson, G., 2013b). Recent studies report a growing interest in materials such as starch, cellulose, hemicellulose, chitosan, gums, collagen, gelatine, wheat gluten, zein, soy protein, and whey protein for biodegradable packaging applications (Robertson, G., 2013c).

In this chapter, the active antimicrobial packaging films from biobased and biodegradable sources were developed with zein as the primary packaging material employing electrospinning technology. Zein is a protein by-product derived from the corn wet-milling industry (Neumann et al., 1984; Hardwick and Glatz, 1989, cited in Zheng et al., 2014, p. 496). As previously discussed in Section 1.2.6.2, zein, which is approved by the FDA as generally regarded as safe (GRAS), exhibits favourable film-forming properties, hydrophobicity, and good biocompatibility, rendering it a suitable candidate for primary packaging materials (Shukla and Cheryan, 2001; Corradini et al., 2014; FDA, 2024). Electrospinning is an innovative approach for film production and is gaining more research interest due to its ability to produce thin films with fibre diameters ranging from nanoscale to microscale. Additionally, the method is non-thermal, making it ideal for maintaining the stability of bioactive compounds. Furthermore, the film produced is reported to have high encapsulation efficiency, a high surface-to-volume ratio, and customisable morphology, which are advantageous for integrating bioactive compounds and tailoring their physical, mechanical and barrier properties. The electrospinning approach also does not need the use of

plasticisers, and so is considered a more environmentally friendly formulation of biopolymers (Gonnet et al., 2010; Huang et al., 2010; Luo, Y. et al., 2012; Anu Bhushani and Anandharamakrishnan, 2014; Luis et al., 2019; Qazanfarzadeh et al., 2021).

The plant extracts selected from Chapter 3; CAE50-S, GATE100-M, and GGE50-M were incorporated into zein solution to produce antimicrobial zein-based films. A concentration of 5% (w/w) extract, relative to the zein content, was chosen, as this concentration exhibited higher antimicrobial activity as indicated in the preceding chapter (equivalent to 50 mg/mL of extract in Chapter 3). The incorporation of 5% (w/w) CAE50-S, GATE100-M, and GGE50-M to produce zein biopolymer using electrospinning is considered a novel approach. To date, the production of zein film on a laboratory scale mainly uses a film casting procedure, and there is no prior report on the use of CAE, GATE, and GGE using the electrospinning technique. Thus, this present study highlighted the use of electrospinning in the production of zein-based films from CAE, GATE, and GGE and evaluated their potential functionality in food packaging application.

## **4.2 Aim of the chapter**

The objective of this chapter was to develop novel biodegradable and biobased packaging films from zein by incorporating active plant extracts at 5% (w/w) of CAE50-S, GATE100-M, and GGE50-M. The procedure involved the preparation of zein solutions, followed by the measurement of viscosity, and ultimately the production of zein-based films using the electrospinning technique. Then, scanning electron microscopy (SEM) was employed to determine the average fibre diameter and surface morphology. The thickness of zein-based films was determined, and subsequent characterisation was conducted, including evaluation of thermal properties, attenuated total reflectance-Fourier transform infrared spectroscopy (ATR-FTIR), encapsulation efficiency, and water contact angle. Ultimately, the biodegradability of zein-based films in soil was assessed.

## 4.3 Results and Discussion

In this and subsequent sections, the films are abbreviated as shown in Table 4.1.

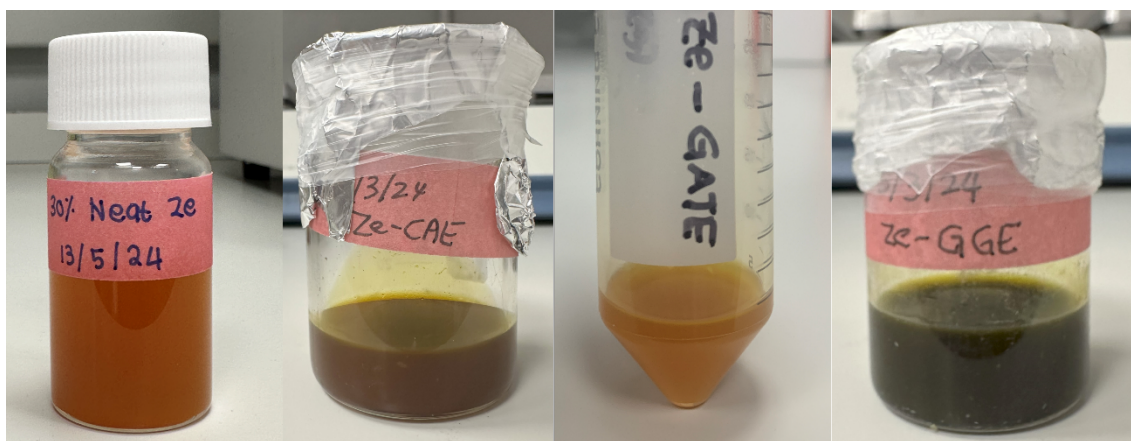
**Table 4.1** The abbreviation for zein-based films.

<b>Film</b>	<b>Description</b>
Neat zein	zein film without the addition of plant extract
Ze-CAE	zein film incorporated with CAE50-S
Ze-GATE	zein film incorporated with GATE100-M
Ze-GGE	zein film incorporated with GGE50-M

### 4.3.1 Preparation of electrospinning solution and viscosity measurement

The viscosity of a polymer solution is significantly influenced by factors such as the nature of the polymer, molecular weight, concentration of solution and temperature (Andrady, 2008). In the present study, zein polymer solutions were prepared by dissolving zein powder in 75% ethanol. The determination of the optimal electrospinning solution concentration was conducted by a preliminary investigation using different zein concentrations from 16% to 30%. The selection was based on viscosity measurement, visual inspection of film morphology and SEM analysis (Appendix A Supplementary Materials 2). From the preliminary data, a zein concentration of 30% was selected for further experiments. This concentration yielded a viscosity in the range of 0.1605 to 0.2586 Pa.s, which is within the ideal range for electrospinning (0.1 to 2.0 Pa.s) and produced bead-free fibres observed under SEM (Fong et al., 1999). The selection of a suitable polymer concentration is essential before the electrospinning process, as this factor influences the fibre diameter and morphology as well as the ability of the solution to be used for electrospinning (Demir et al., 2002; Zong et al., 2002). Electrospinning requires a moderately concentrated polymer solution to facilitate sufficient polymer chain entanglement, which is essential for continuous jet formation (McKee, M. et al., 2004; McKee, M.G. et al., 2005; Shenoy et al., 2005). In a polymer solution with low concentration, the entanglement of polymer chains does not occur, as the chains exist as separate entities, usually resulting in the defect, such as the formation of bead or droplets instead of fibres (McKee, M. et al., 2004; McKee, M.G. et al., 2005; Shenoy et al., 2005; Andrady, 2008). On the other hand, too high polymer concentration is impractical, as it would lead to problems such as needle tip blockage, formation of thick fibres, deposition of fibres on a relatively small area and uneven appearance on the collector plate (Zong et al., 2002; Kameoka et al., 2003; Subbiah et al., 2005).

After the optimal zein polymer concentration was determined, the polymer solutions of Neat zein and zein loaded with 5% (w/w) of Ze-CAE, Ze-GATE and Ze-GGE solutions were prepared. The visual observation on the resulting solutions showed viscous solutions where Neat zein produced a yellowish, orange-coloured solution, while Ze-CAE produced a brownish solution, Ze-GATE produced a yellowish, orange-coloured solution similar to Neat zein and Ze-GGE produced a dark green solution (Figure 4.1). Then, the viscosity was measured at a shear rate between 0.1 and 100.0  $\text{s}^{-1}$ , and the viscosity data and log viscosity graph are presented in Table 4.2 and Figure 4.2. The figure illustrates that all zein solutions exhibit shear thinning behaviour, a type of non-Newtonian flow behaviour where viscosity decreases as the shear rate increases, with the exception of the Neat zein solution (Prentice, 1968; Andradý, 2008). The Neat zein solution was observed to exhibit a Newtonian flow behaviour, where viscosity is linearly related to shear rate. At the start of the test at a shear rate of 0.1  $\text{s}^{-1}$ , the viscosities of the Ze-CAE, Ze-GATE, and Ze-GGE solutions were higher than that of the Neat zein solution, with Ze-GGE solution showing the highest viscosity at 2.753 Pa·s. As the shear rate increased, the viscosity of all zein solutions decreased, becoming almost constant at around 1.0  $\text{s}^{-1}$ . Beyond this point, the viscosity did not significantly change, except for Ze-GATE at 10  $\text{s}^{-1}$ , which showed a minor fluctuation, demonstrated by a slight increase in the viscosity. At a shear rate of 100  $\text{s}^{-1}$ , the viscosities of the zein solutions ranged from 0.1640 Pa·s for Neat zein to 0.1377, 0.1790, and 0.1625 Pa·s for Ze-CAE, Ze-GATE, and Ze-GGE, respectively. Literature has reported that an increase in shear rate leads to a decrease in viscosity due to the disentanglement of polymer chains under shear field (D'Almeida and Dias, 1997). Another study has also reported that at low shear rates, polymer tends to exhibit a sharp decline in viscosity compared to higher shear rates, where the viscosity decreases more gradually due to reduced flow resistance caused by the breaking of aggregates (Karatas and Arslan, 2016).

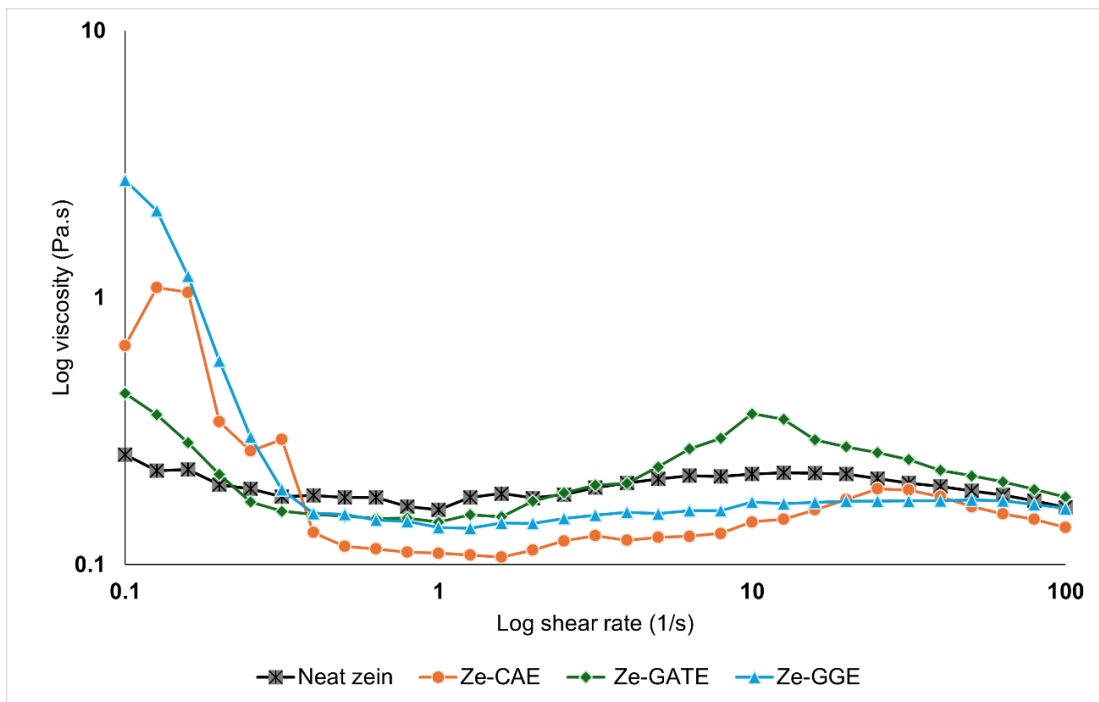


**Figure 4.1** Zein solutions of Neat zein (yellowish, orange-coloured solution), Ze-CAE (brownish solution), Ze-GATE (yellowish, orange-coloured solution), and Ze-GGE (dark green solution).

**Table 4.2** Solution viscosity and characterisation of zein-based films.

Film	Shear viscosity $-100 \text{ s}^{-1}$ (Pa.s)	Average fibre diameter <sup>A</sup> ( $\mu\text{m}$ )	Film thickness <sup>B</sup> ( $\mu\text{m}$ )	Encapsulation efficiency <sup>C</sup> (%)	Water contact angle <sup>D</sup> -2 s ( $^{\circ}$ )
Neat zein	0.1640	$1.02 \pm 0.22^b$	$40.60 \pm 2.51^b$	-	$33.26 \pm 10.37^a$
Ze-CAE	0.1377	$1.07 \pm 0.29^b$	$46.20 \pm 6.69^b$	$99.25 \pm 0.02^b$	$28.04 \pm 6.11^a$
Ze-GATE	0.1790	$1.02 \pm 0.21^b$	$39.20 \pm 4.38^b$	$94.35 \pm 0.00^c$	$22.74 \pm 6.55^a$
Ze-GGE	0.1625	$1.21 \pm 0.25^a$	$73.60 \pm 4.93^a$	$99.97 \pm 0.01^a$	$23.18 \pm 6.79^a$

Values are the mean  $\pm$  SD of replications ( $n = 100^A$ ,  $n = 5^B$ ,  $n = 3^{CD}$ ). Means with different superscript letters (a-c) of the same test are significantly different (Tukey's pairwise comparisons,  $p < 0.05$ ).



**Figure 4.2** Log viscosity (Pa.s) of Neat zein, Ze-CAE, Ze-GATE, and Ze-GGE with respect to shear rate from 0.1 to 100 s<sup>-1</sup> at 25 °C, with data points represent a single measurement.

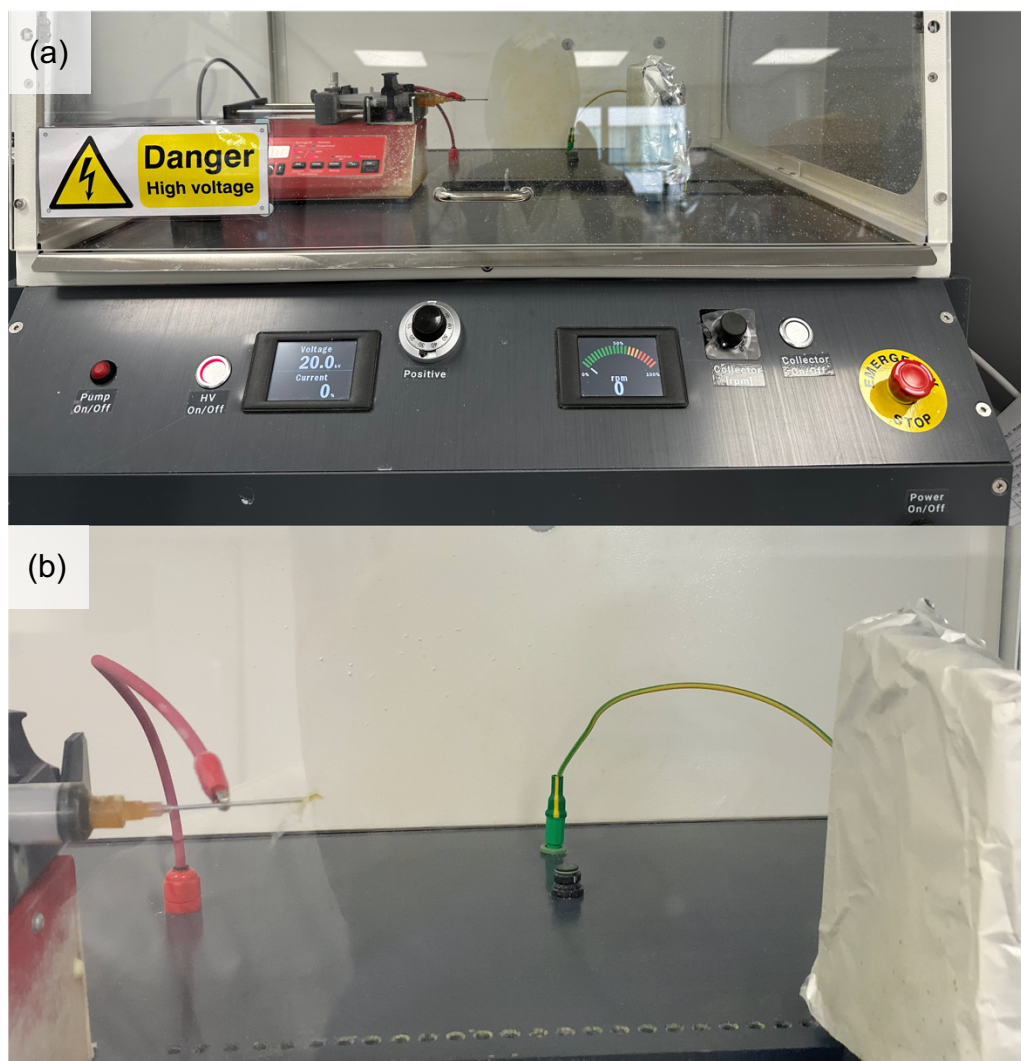
In brief, at shear rate 100 s<sup>-1</sup>, the viscosity of Ze-CAE was slightly lower than the viscosity of Neat zein, with Ze-GATE had a slightly higher viscosity at the same shear rate, and Ze-GGE had almost similar viscosity value with Neat zein. However, no distinct differences in viscosity were observed between Neat zein and zein solutions incorporated with CAE, GATE, and GGE. It is important to note there was no statistical analysis performed on the viscosity data of this study. Overall, the viscosities of all zein solutions were all found to be within the acceptable limits for fibre production by electrospinning, which is between 0.1 and 2.0 Pa.s. The zein polymer solutions exhibited better shear thinning properties at shear rates between 0.1 and 1.0 s<sup>-1</sup> after the addition of CAE, GATE, and GGE. From the data, it can be suggested that the addition of the plant extracts of CAE, GATE, and GGE did not affect the viscosity of the zein polymer solution at a shear rate of 100 s<sup>-1</sup> but improved the shear thinning properties compared to Neat zein solution at a shear rate between 0.1 and 1.0 s<sup>-1</sup>.

Opposed to the findings obtained in this study, the results obtained by Federici et al. (2020) on a 25% (w/w) zein solution with the addition of 2% (w/w) casein, whey protein or rice protein showed a significant increase in viscosity. In the study, the authors stated that the addition of these three co-proteins had a significant effect on the viscosity of the zein polymer solution, with the viscosity of blank zein in 70:30 ethanol/0.1 M NaOH aqueous solution recorded at 0.156±0.004 Pa.s, and

the viscosity after the addition of co-proteins was at  $0.196\pm 0.005$  Pa.s (casein),  $0.179\pm 0.006$  Pa.s (whey protein), and  $0.208\pm 0.005$  Pa.s (rice protein). Another study reported that the addition of two types of essential oils of *Laurus nobilis* essential oil (LEO) and *Rosmarinus officinalis* essential oil (REO) at concentrations of 1%, 5%, and 10% significantly reduced the viscosity of zein solution, except for REO at 1%, which showed no such effect (Goksen et al., 2020). In comparison to the current study, the addition of CAE, GATE, and GGE did not influence the viscosity of the zein polymer solution, indicating that the film-forming solution maintained its rheological properties. This suggests that the incorporation of these plant extracts did not interfere with the film-forming ability of zein. In brief, the findings from the current and the previous studies imply that both the incorporation of various active substances or components and varying concentrations used influence the viscosity of the polymer solution. In general, the order of viscosity of the films at shear rate  $100\text{ s}^{-1}$  tested in this study was Ze-GATE > Neat zein > Ze-GGE > Ze-CAE. The findings from this section highlight the suitability of all zein solutions (Neat zein, Ze-CAE, Ze-GATE, and Ze-GGE) for electrospinning.

### **4.3.2 Electrospinning of zein-based films**

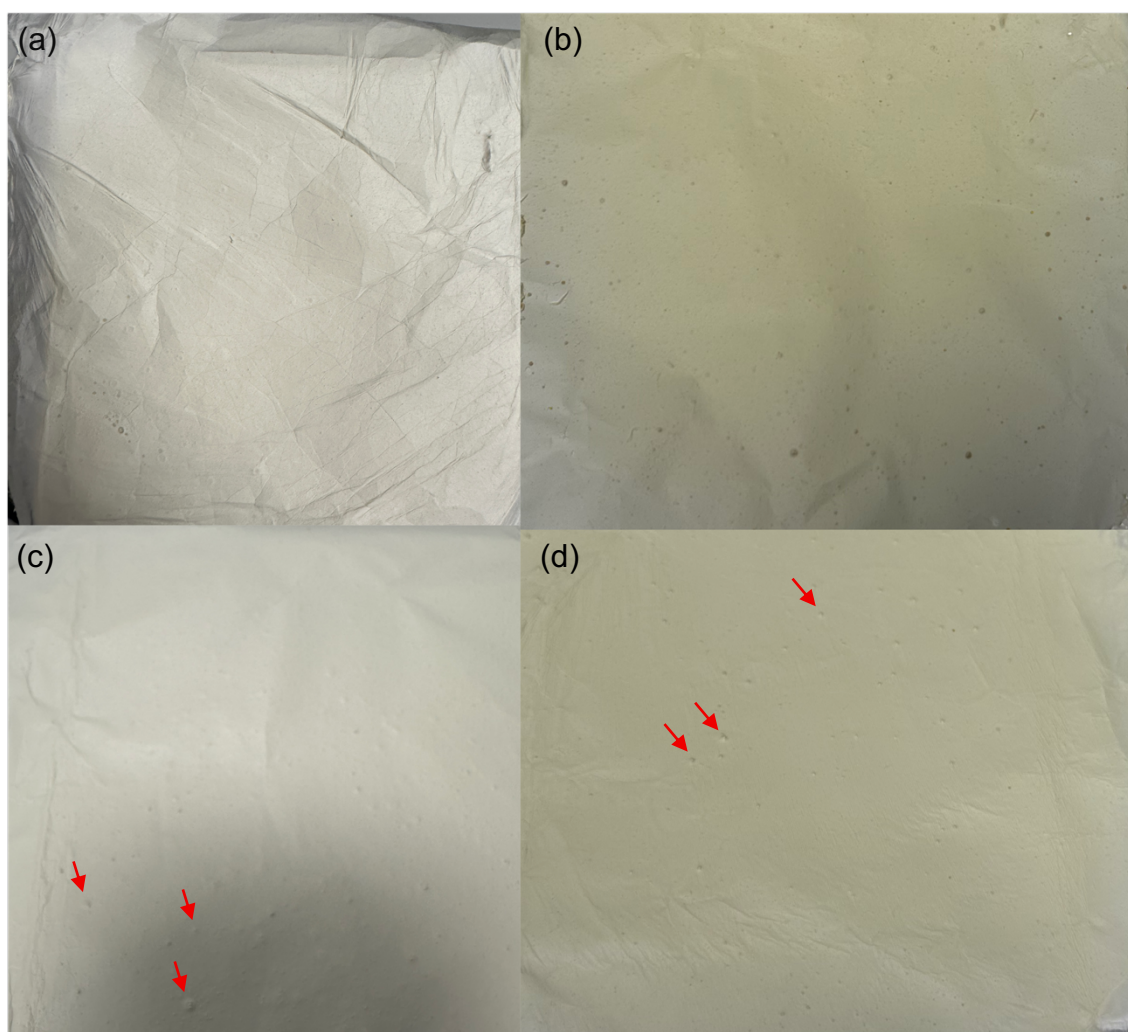
Electrospinning is a process of fibres production using moderately viscous polymer solution and high voltage via interaction of polymer surface tension and applied electric field, with the resultant fibres having average diameter ranging from nanoscale to microscale (Doshi and Reneker, 1995; Andradý, 2008). In this study, Neat zein along with novel biodegradable films of Ze-CAE, Ze-GATE, and Ze-GGE were successfully prepared via electrospinning and prepared from two different sources: the author at the University of Leeds and SKE Research Equipment, Italy. All results in Chapter 4 using the films that were prepared by the author, while the films prepared by SKE Research equipment were used for the storage study in Chapter 5. The typical electrospinning set-up is shown in Figure 4.3(a) and the example of electrospun film deposited onto the collector is shown in Figure 4.3(b).



**Figure 4.3** (a) Electrospinning set-up for zein-based films production comprises of a solution reservoir with a spinneret, a grounded metallic collector, and a high-voltage power supply, (b) The example of electrospun zein-based film deposited onto the collector using the solution flow rate of 1.0 mL/h, voltage at 15-17 kV, with distance to collector set at 15 cm and performed at  $21 \pm 2$  °C with relative humidity of  $40 \pm 5\%$  and the collector size of 12 x 12 cm.

The electrospun films of Neat zein, Ze-CAE, Ze-GATE, and Ze-GGE that were prepared by the author are illustrated in Figures 4.4(a-d). From the figure, all zein-based films appeared visually smooth and thin, opaque, light cream in colour. However, Ze-GATE and Ze-GGE films exhibited an additional granular-like appearance on their surfaces as shown by the arrows in Figures 4.4(c-d). This may be attributed to the droplet formation during interruptions in the electrospinning process. Zein-based electrospinning solutions exhibit high viscosity, and when the machine is paused or temporarily stopped, the solution tend to accumulate at the tip of needle. Upon restarting, the electrostatic field reactivates prior to the formation of a stable Taylor cone, causing droplets to be ejected instead of continuous fibres, as can be observed on Ze-GATE and Ze-GGE films (Doshi and Reneker, 1995; Andradý, 2008). The films were collected

in sizes smaller than 12x12 cm due to their soft edges. The films that were obtained from SKE Research Equipment, Italy, had similar appearances, thus the photos were not shown.



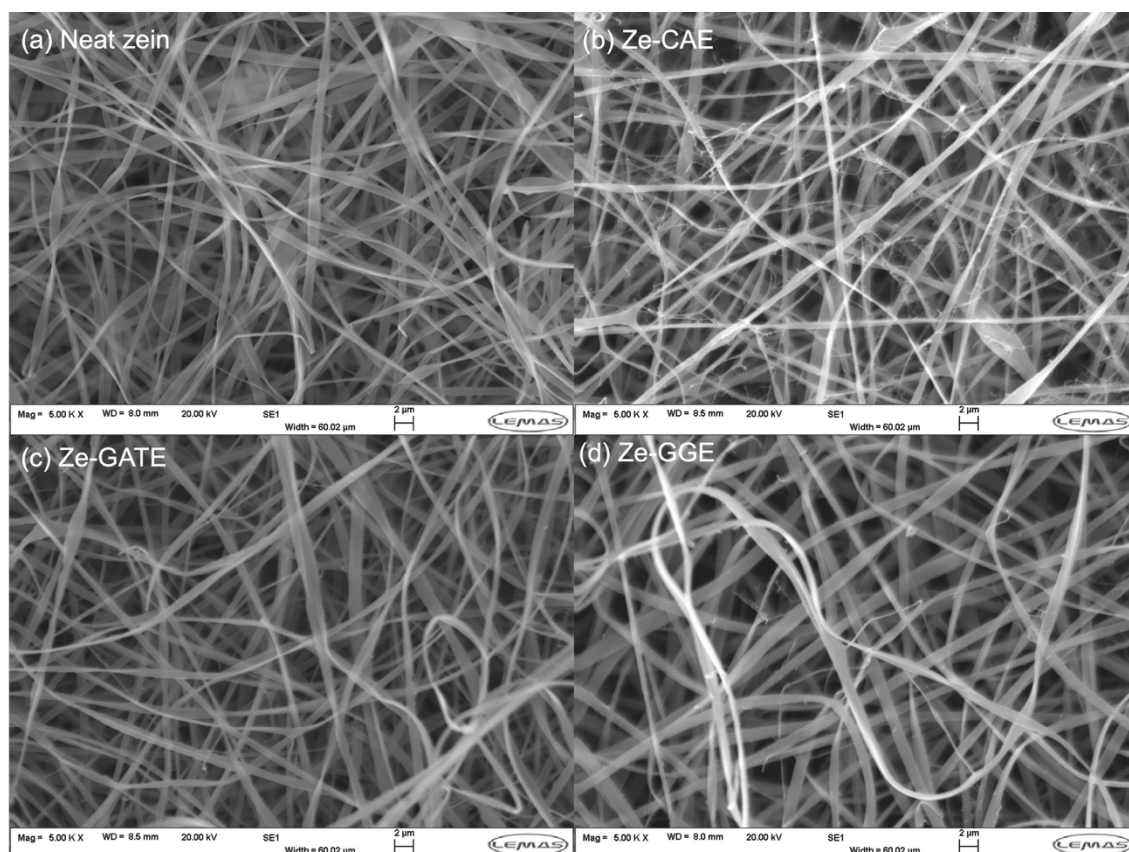
**Figure 4.4** Visual appearance of zein-based films (a) Neat zein, (b) Ze-CAE, (c) Ze-GATE, (d) Ze-GGE, with an additional granular-like appearance on the surfaces of Ze-GATE and Ze-GGE.

In comparison with the current film wrap that is commercially available, it can be observed that the films produced in this present study lack transparency. The opaque films were observed for Neat zein, Ze-CAE, Ze-GATE, and Ze-GGE, which is a normal appearance for electrospun film using zein as a primary polymer material. The opaque appearance results from interconnected pores within the electrospinning membranes, which create numerous air-fibre interfaces where significant reflection and refraction losses occur, ultimately leading to the formation of opaque films (Tang, C. and Liu, 2008). In addition, the light cream colour of films is dominated from the yellow colour of zein, which was used at a concentration of 30% without any plasticiser. Similar results have been reported by a recent study on the multilayer film, which used sage seed gum-gelatin film

as the outer layer and electrospun zein-pomegranate flower extract as the middle layer. They found out that the opacity of the films increased after the addition of electrospun zein-pomegranate flower extract, with the film without the electrospun layer film being almost transparent ( $5.11\pm 0.82$ ), and upon the addition of 20, 40, 60, and 80  $\text{g}\cdot\text{m}^{-2}$  of electrospun zein-pomegranate flower extract, the opacity increased and ranged from  $6.95\pm 0.80$  to  $10.43\pm 1.12$  (Valizadeh et al., 2024). In this study, a plate collector measuring 12x12 cm in size was used, resulting in smaller electrospun films, and several rounds of electrospinning runs were required to produce adequate film samples. The use of a rotating drum collector would produce larger electrospun films (SKE-Research-Equipment, 2020). However, due to the lack of availability of instrumental equipment, the drum collector could not be used, and plate collector was used throughout the experiment. The following investigation on the surface morphology of the films analysed via SEM is detailed in the next section, Section 4.33.

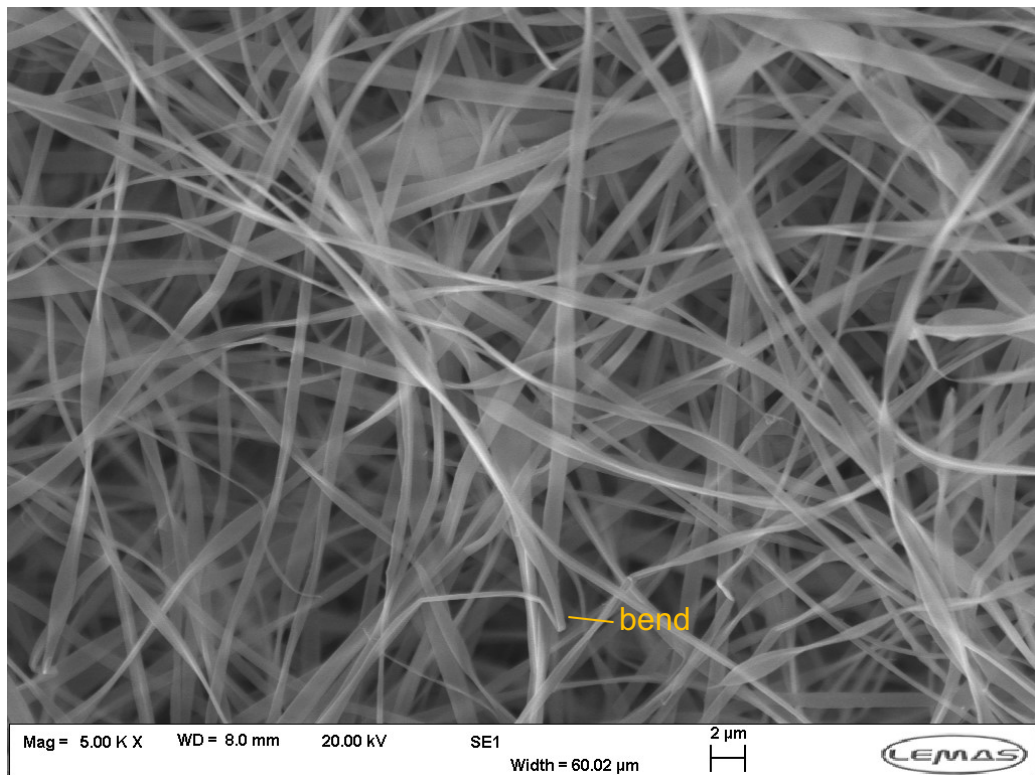
### 4.3.3 Scanning electron microscopy (SEM)

The surface morphology of zein-based films containing plant extracts of CAE, GATE, and GGE was analysed using SEM. SEM is a widely utilised two-dimensional imaging technique for examining the surface morphology of materials, with a resolution between 1 and 20 nm and image magnification from 500 to 10,000X. Furthermore, SEM analysis is important for assessing the fibre diameter distributions in electrospun fibre (Andrady, 2008). In this experiment, the surface morphologies of Neat zein, Ze-CAE, Ze-GATE, and Ze-GGE were observed at 500X, 1000X, 2000X, and 5000X magnifications, however the results in this thesis were mostly presented at 5000X magnification, as the observation of fibre morphologies was more evident at this magnification. The comparison between surface morphologies of films is illustrated in Figure 4.5. Figures 4.6, 4.9, 4.12, and 4.14 display the SEM micrographs at 5000X magnification for Neat zein, Ze-CAE, Ze-GATE, and Ze-GGE, respectively.

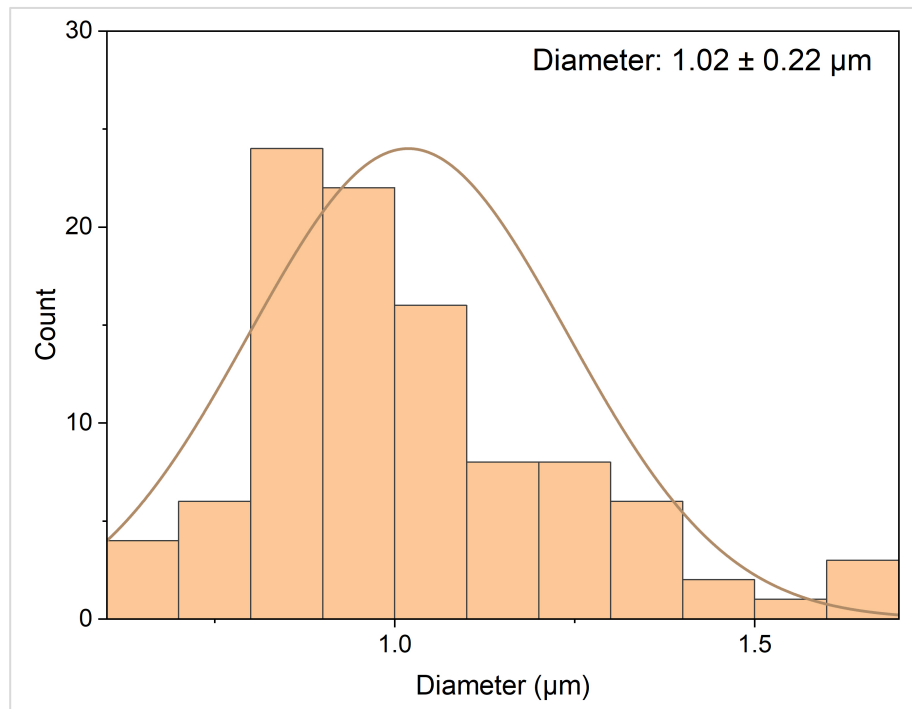


**Figure 4.5** Comparison of SEM micrographs of films at 5000X magnification.

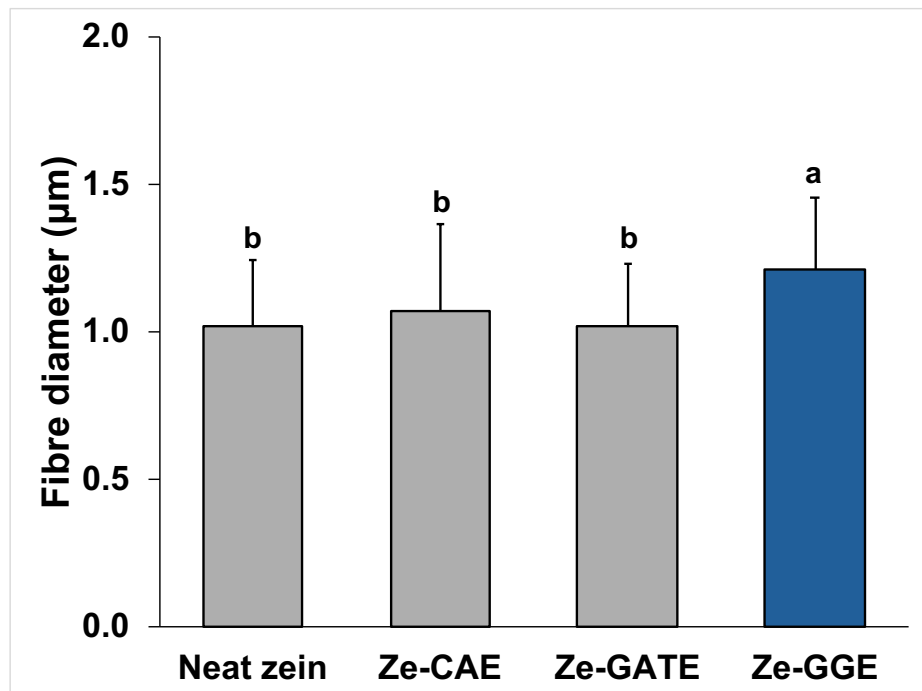
For Neat zein, it can be seen from Figure 4.6 that the micrograph shows a bead-free morphology, and the formation of fibres characterised by flat ribbon-like structures. A thin polymer skin typically forms on the liquid jet during the electrospinning process. The rapid vaporisation of the solvent at the jet's surface, influenced by atmospheric pressure, led to the collapse of the tube formed by the skin, ultimately resulting in the formation of ribbon-like structures. The flat ribbon-like morphology observed can be attributed to the stiffness of the polymer skin and the electrostatic self-repulsion of charges on the individual tubes (Kooombhongse et al., 2001). Table 4.2 and Figure 4.7 show the average fibre diameter for Neat zein, which was measured at  $1.02\pm 0.22\ \mu\text{m}$  and the comparison of fibre diameter data with other zein-based films is illustrated in Figure 4.8.



**Figure 4.6** SEM micrograph of Neat zein at 5000X magnification showing fibres with flat ribbon-like morphology and bend formation.



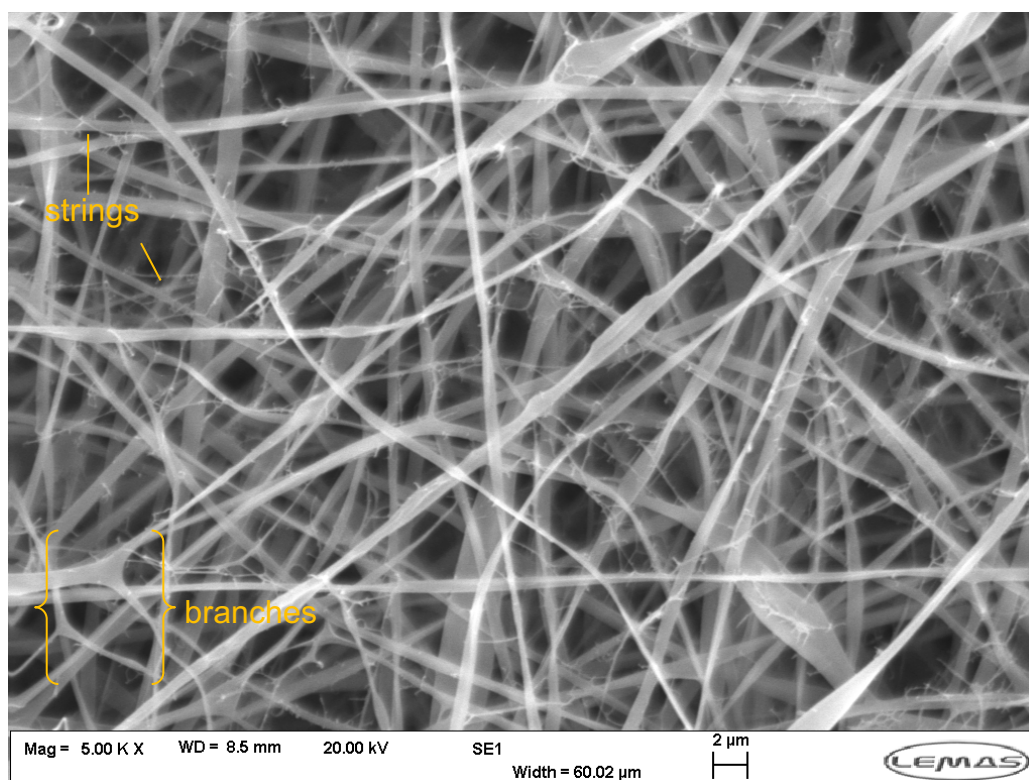
**Figure 4.7** Histogram showing the average fibre diameter distribution based on 100 randomly selected fibres from the SEM micrograph of Neat zein.



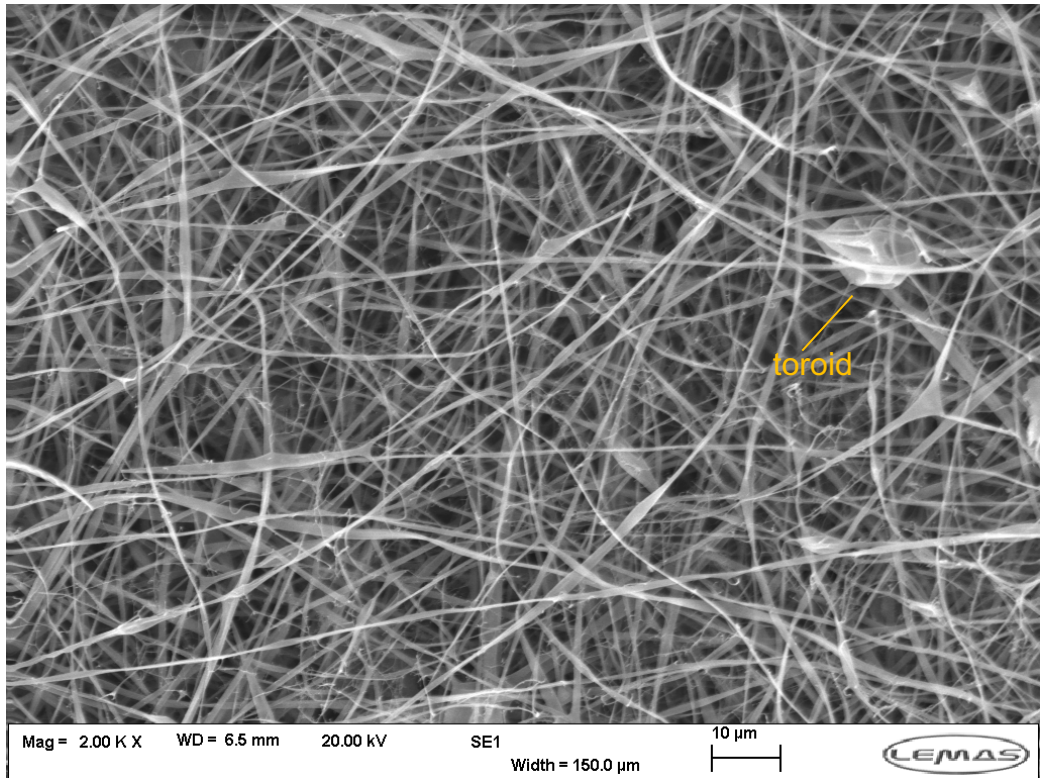
**Figure 4.8** The average fibre diameter ( $\mu\text{m}$ ) between Neat zein, Ze-CAE, Ze-GATE and Ze-GGE films.

Bar graph represents the means of average fibre diameter. Error bars represent the sample standard deviation (mean  $\pm$  SD,  $n = 100$ ). Means sharing the same letter indicate that the average fibre diameter is not significantly different, while means with different letters indicate a statistically significant difference in average fibre diameter (Tukey's pairwise comparisons,  $p < 0.05$ ).

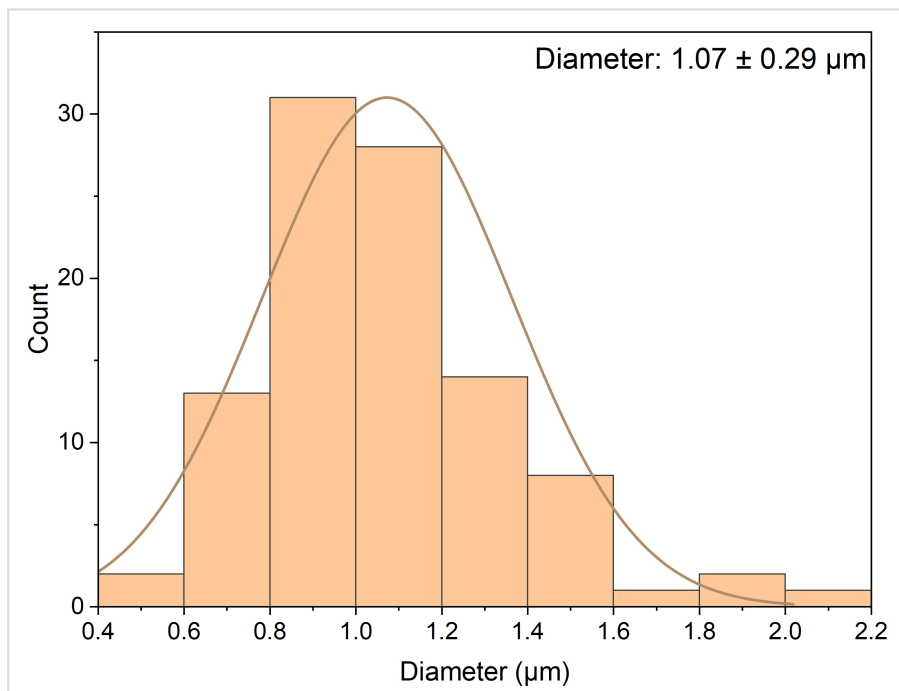
In comparison to Neat zein, Ze-CAE revealed a similar appearance on a macroscopic level but differs on a microscopic level. SEM micrograph in Figure 4.9 demonstrates that Ze-CAE exhibits flat ribbon-like morphologies. However, additional branches were observed developing from the main jet, primarily resulting from the ejection of smaller jets on the surface of the primary jet (Koombhongse et al., 2001). The formation of strings between the jets was also observed. The strings are likely derived from the compounds in CAE, which was added into the polymer solution, indicating successful integration of plant extract during the electrospinning process (Salevic et al., 2022). It is also important to note the presence of toroid in Figure 4.10. A toroid is formed when beads develop on a jet skin, and during solvent vaporisation and the collapsing of the jet, the skin of the bead also collapses, resulting in a toroid (Koombhongse et al., 2001). Toroids or beads are common type of defect occurred to the electrospun film and could reduce the fibre's functional surface area, and affect the film's overall performance (Matabola and Moutloali, 2013). The average fibre diameter of Ze-CAE was comparable to that of Neat zein, measuring  $1.07 \pm 0.29 \mu\text{m}$  ( $p > 0.05$ ) (Table 4.2, Figures 4.8 and 4.11).



**Figure 4.9** SEM micrograph of Ze-CAE at 5000X magnification showing fibres with flat ribbon-like morphology along with strings and branches formation.

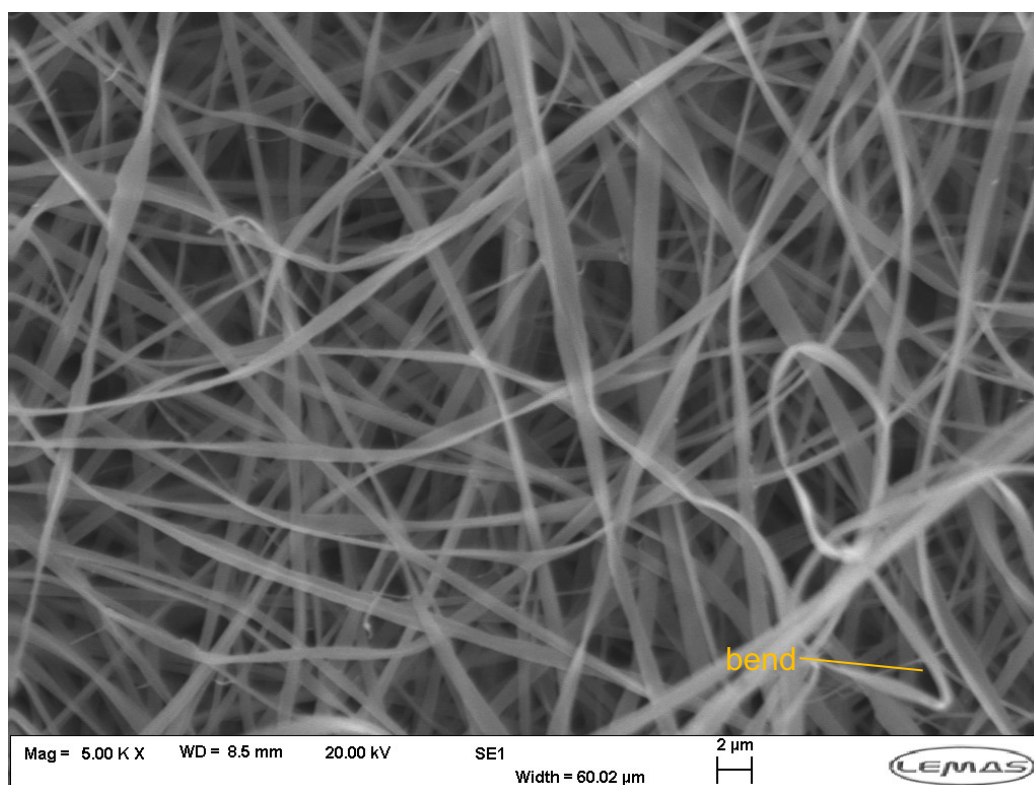


**Figure 4.10** Toroid observed in Ze-CAE fibres at 2000X magnification.

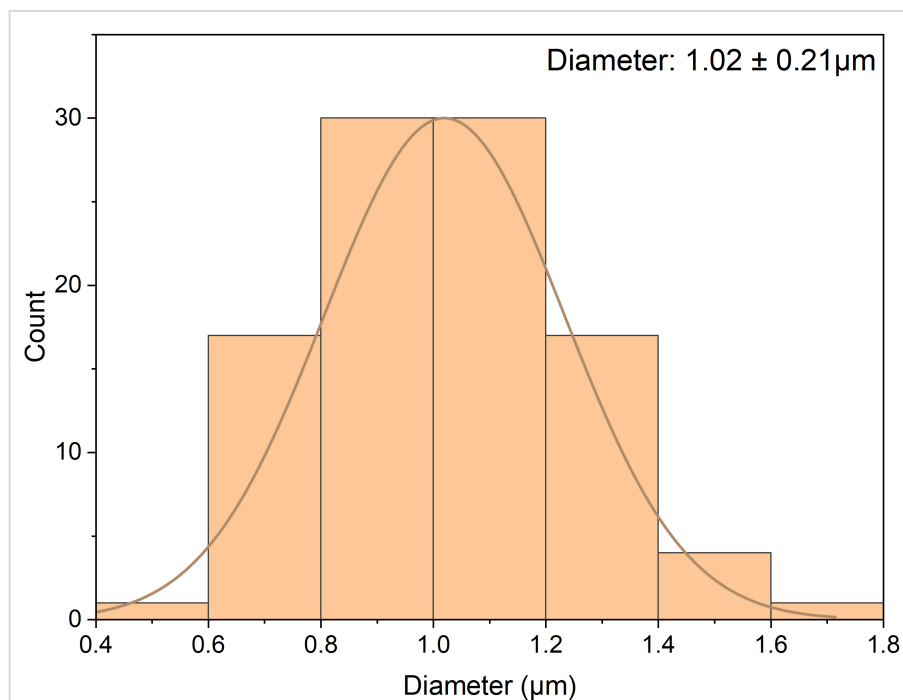


**Figure 4.11** Histogram showing the average fibre diameter distribution based on 100 randomly selected fibres from the SEM micrograph of Ze-CAE.

For Ze-GATE, the micrograph in Figure 4.12 exhibits a similar appearance as of Neat zein, with flat ribbon-like structures and the absence of beads in the fibres. Additionally, Ze-GATE fibres also displayed an apparent ribbon bend, which was caused by bending instability in the electric field and forces that occurred when the ribbon was stopped on the collector (Koombhongse et al., 2001). A similar bend was also observed in Neat zein fibres (Figure 4.6). The average fibre diameter for Ze-GATE was determined as  $1.02 \pm 0.21 \mu\text{m}$ , showing no significant difference from Neat zein ( $p > 0.05$ ) (Table 4.2, Figures 4.8 and 4.13). Interestingly, Ze-GATE fibres did not exhibit string-like structures, unlike Ze-CAE and Ze-GGE. The discrepancy is most likely due to variations in the phytochemical compositions of the extracts used in this study. CAE and GGE were obtained from leaf extracts, whereas GATE was prepared from the fruit part of the plant. Fruit extracts have previously been reported to have high levels of organic acids but as mentioned in Section 3.3.2, contain the lowest quantity of phenolic compounds (Hamidon et al., 2017; Lim et al., 2020). These phenolic compounds are known to function as cross-linking agents and encourage molecular entanglement during fibre formation, which may explain the presence of strings in Ze-CAE and Ze-GGE and the absence of string-like morphologies in Ze-GATE fibres (Gaikwad et al., 2020; Zhang, Xueqian et al., 2021; Munir et al., 2023).

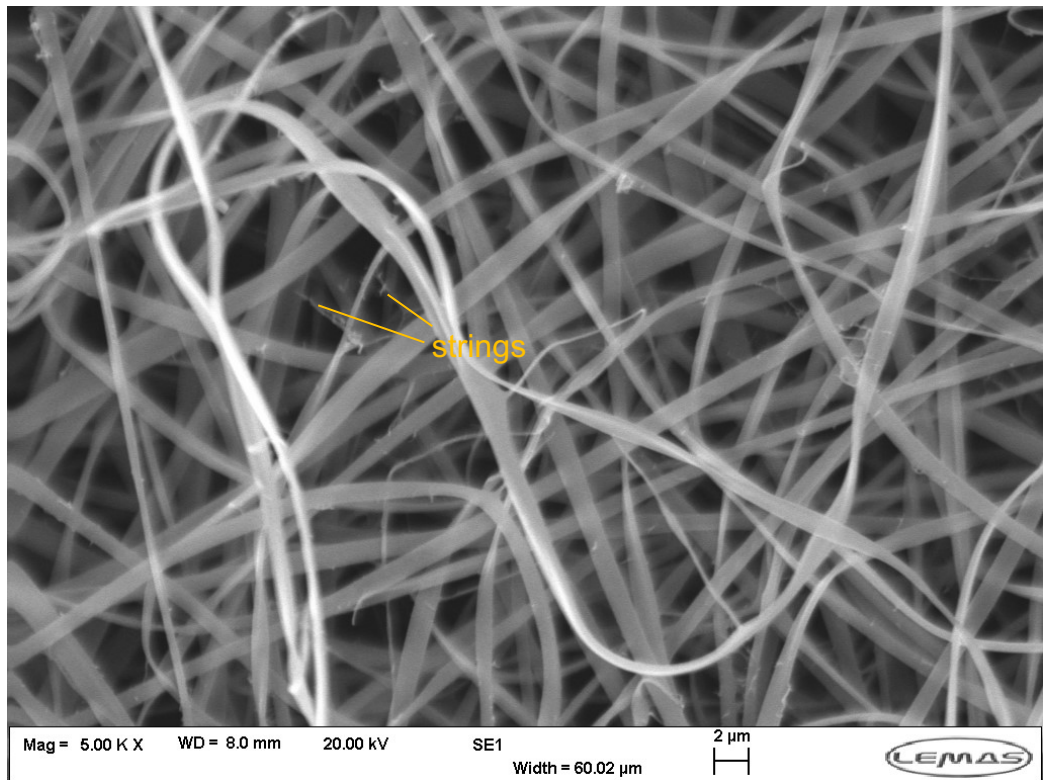


**Figure 4.12** SEM micrograph of Ze-GATE at 5000X magnification showing fibres with flat ribbon-like morphology and bend formation.

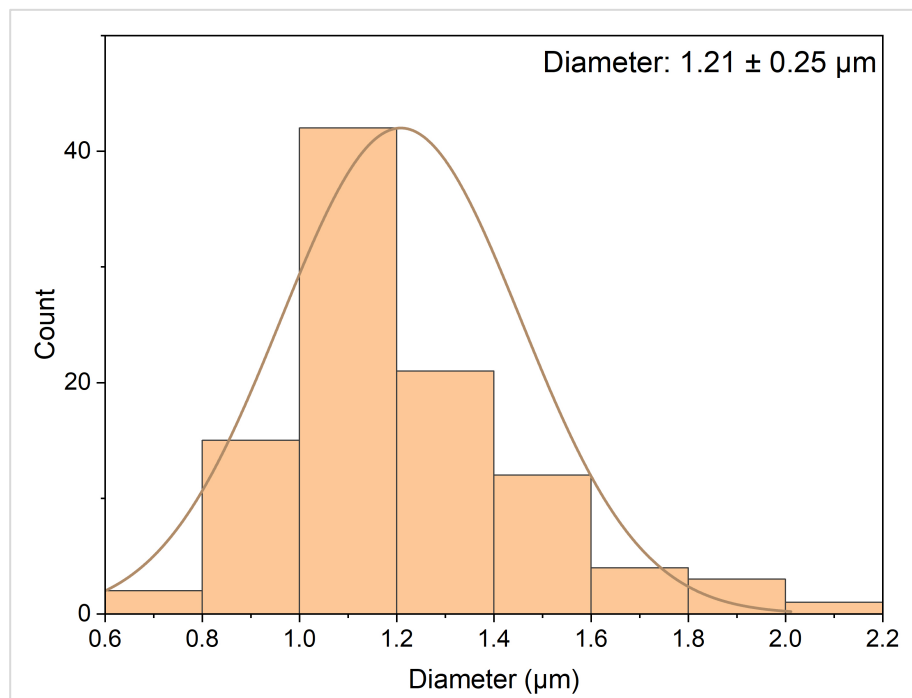


**Figure 4.13** Histogram showing the average fibre diameter distribution based on 100 randomly selected fibres from the SEM micrograph of Ze-GATE.

In the case of Ze-GGE, flat ribbon-like morphologies were observed, consistent with other zein films, during the examination of SEM micrographs presented in Figure 4.14. The formation of strings between the Ze-GGE fibres was also observed. No visible bend, branch or toroid structures were detected on Ze-GGE fibres. The average fibre diameter for Ze-GGE was significantly higher than that of Neat zein, Ze-CAE, and Ze-GATE, measured at  $1.21 \pm 0.25 \mu\text{m}$  ( $p < 0.05$ ) (Table 4.2, Figures 4.8 and 4.15). Additionally, Ze-GGE exhibited the highest viscosity at the start of the viscosity experiment in comparison to other polymer solutions (Figure 4.2). This observation aligns with prior studies indicating that an increase in the viscosity of the polymer solution leads to an increase in the fibre diameter (Yao et al., 2016; Altan et al., 2018; Wu, X. et al., 2023). A higher viscosity polymer solution is reported to reduce jet stretching, thereby decreasing jet path and resulting in the production of larger fibres (Phiriyawirut and Phaechamud, 2012). The shear thinning behaviour of high viscosity polymer solutions can increase polymer chain entanglement, leading to greater resistance against jet stretching due to electrostatic repulsive force during electrospinning, which results in larger fibre diameters (Reneker and Yarin, 2008; Kriegel et al., 2009; Bai et al., 2014).



**Figure 4.14** SEM micrograph of Ze-GGE at 5000X magnification showing flat ribbon-like morphology and strings formation.



**Figure 4.15** Histogram showing the average fibre diameter distribution based on 100 randomly selected fibres from the SEM micrograph of Ze-GGE.

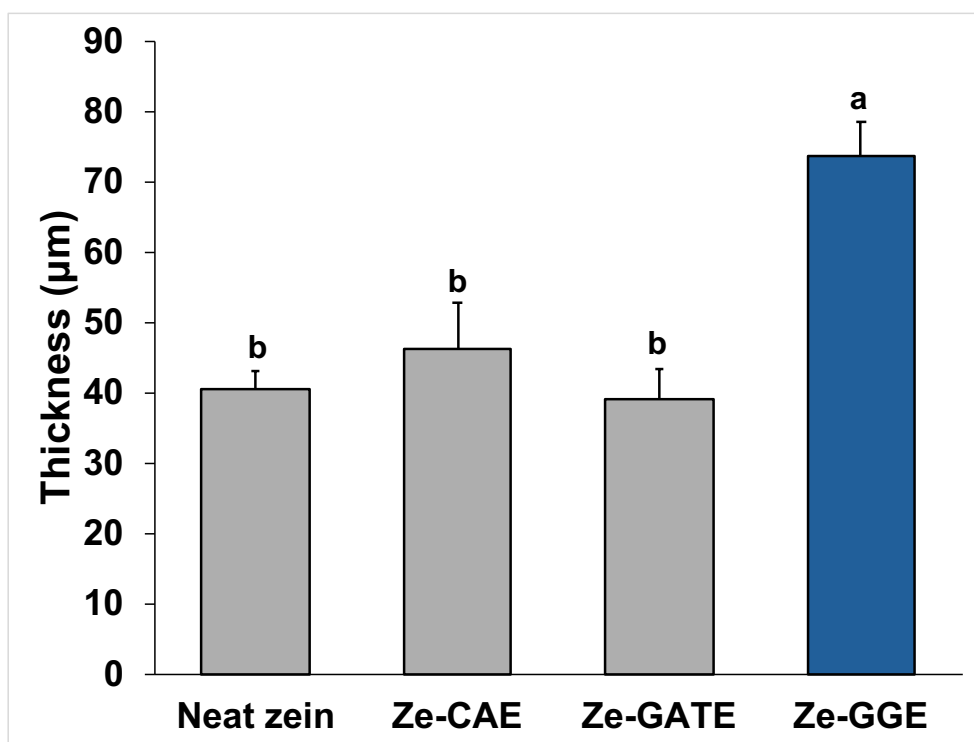
Vogt et al. (2018) reported two distinct morphologies of electrospun zein fibres incorporating poly(glycerol sebacate), specifically a ribbon-like structure and a circular cross-section, as observed through SEM analysis. The experiments were conducted at two relative humidities (RH) of 25% and 50%. The use of acetic acid as the electrospinning solvent resulted in a circular cross-section, while ethanol produced a ribbon-like morphology. This report agrees with the current study, which also observed ribbon-like morphology and utilised 75% ethanol as a solvent. The findings indicate that solvent choice influences the morphology of the electrospun fibre. In a similar study, Vogt et al. (2018) also reported no significant difference in fibre diameter across various electrospinning solvents. The average fibre diameter was measured at  $1.1\pm 0.3\ \mu\text{m}$  at 25% RH and  $0.7\pm 0.2\ \mu\text{m}$  at 50% RH for Neat zeinZ30AA (using acetic acid as solvent), while for Z26E (using ethanol as solvent), the measurements were  $0.8\pm 0.2\ \mu\text{m}$  at 25% RH and  $0.6\pm 0.3\ \mu\text{m}$  at 50% RH.

Overall, a variety of morphologies were observed, primarily flat ribbon-like, along with branch, bend, and toroid structures across all films, with significant strings formation observed in Ze-CAE and Ze-GGE films. The incorporation of GGE resulted in an increased of average fibre diameter in Ze-GGE film compared to Neat zein film, whereas Ze-CAE and Ze-GATE films exhibited similar average fibre diameters to Neat zein film. The heterogeneity in fibre diameter was observed in Ze-CAE film, as shown in the SEM micrograph (Figure 4.9), where fibres displayed variation in sizes. However, based on measurements of the average diameter from 100 fibre samples, a significantly larger fibre diameter was observed only in the Ze-GGE film, indicating that the size variation observed in Ze-CAE film was not statistically significant. It can be concluded that solution parameters, such as solvent type and viscosity, as well as ambient conditions and electrospinning process parameters, can influence the morphology and size of electrospun nanofibres. Nevertheless, even under controlled conditions, some degree of fibre diameter distribution is expected (Hohman et al., 2001).

#### **4.3.4 Film thickness**

In this experiment, the thickness of Neat zein, Ze-CAE, Ze-GATE, and Ze-GGE films was determined using a digital micrometre with five measurements taken for each film sample, and the results are presented in Table 4.2 and Figure 4.16. The American Society for Testing and Materials (ASTM) standard states that the plastic film's thickness should be less than or equal to 0.25 mm (ASTM, 2004). All developed zein-based films met the thickness criteria established by ASTM, exhibiting thickness below 0.25 mm, specifically ranging from  $39.20\pm 4.38$  to

73.60±4.93  $\mu\text{m}$ . The thickness of Neat zein was measured at 40.60±2.51  $\mu\text{m}$ , comparable to Ze-CAE and Ze-GATE films ( $p > 0.05$ ). The Ze-GGE film exhibited a significantly greater thickness than the other three films, measuring 73.60±4.93  $\mu\text{m}$  ( $p < 0.05$ ) (Table 4.2 and Figure 4.16).



**Figure 4.16** The film thickness ( $\mu\text{m}$ ) of Neat zein, Ze-CAE, Ze-GATE and Ze-GGE films.

Bar graph represents the means of film thickness. Error bars represent the sample standard deviation (mean  $\pm$  SD,  $n = 5$ ). Means sharing the same letter indicate that the film thickness is not significantly different, while means with different letters indicate a statistically significant difference in film thickness (Tukey's pairwise comparisons,  $p < 0.05$ ).

The film thickness is influenced by various factors. In this study, the observed differences in thickness are likely attributed to the type of plant extracts and the viscosity of the polymer solution. The data suggest that the incorporation of plant extract from CAE and GATE did not alter the zein matrix, as evidenced by the comparable thickness of Ze-CAE and Ze-GATE films relative to the Neat zein film. The incorporation of GGE significantly altered the Ze-GGE film matrix, as evidenced by the increased fibre thickness of the Ze-GGE film. The possible explanation is that GGE contains a greater number of bioactive compounds, such as phenolics, which may interact with zein chains and potentially alter the film structure (Santoso et al., 2010; Suksanga et al., 2023; Intawongse and Pranprawit, 2024). This aligns with the findings presented in Section 3.3.2, which indicated that GGE exhibited the highest phenolic content relative to CAE and GATE. As highlighted in Section 4.33, Ze-GGE exhibited the highest average fibre diameter. The increase in viscosity has been associated with an increase in

fibre diameter, ultimately leading to thicker fibres (Kameoka et al., 2003). The thickness data correspond with the viscosity data presented in Section 4.3.1, indicating that Ze-GGE exhibited higher viscosity than Ze-CAE and Ze-GATE at the beginning of viscosity measurement. Increased solution viscosity correlates with higher solid content, leading to the deposition of thicker fibres on the plate collector (Kameoka et al., 2003).

In a previous study, various concentrations of *G. atroviridis* leaf extract (GAL) between 1% and 5% were incorporated into gelatine and starch films prepared using film casting, and the thickness of the films was measured. The thickness of the films with 1%, 3%, and 5% extract incorporation was measured at  $0.098 \pm 0.007$ ,  $0.100 \pm 0.006$ , and  $0.101 \pm 0.002$  mm, respectively and these values were not significantly different from the control film, measured at  $0.094 \pm 0.001$  mm ( $p > 0.05$ ) (Nur Amila Najwa et al., 2020). In comparison to the present study, the films produced by film casting possessed thicker film compared to the electrospinning method, as shown in the thickness data of this present study. To date, no data have been reported on the thickness of films incorporated with *C. asiatica* and *G. gnemon*, either from film casting or electrospinning. The thickness measurements for the electrospun zein films in this study are consistent with those reported in previous research, which documented thicknesses between  $21.7 \pm 2.1$   $\mu\text{m}$  and 0.23 mm (Radusin et al., 2019; Valizadeh et al., 2024).

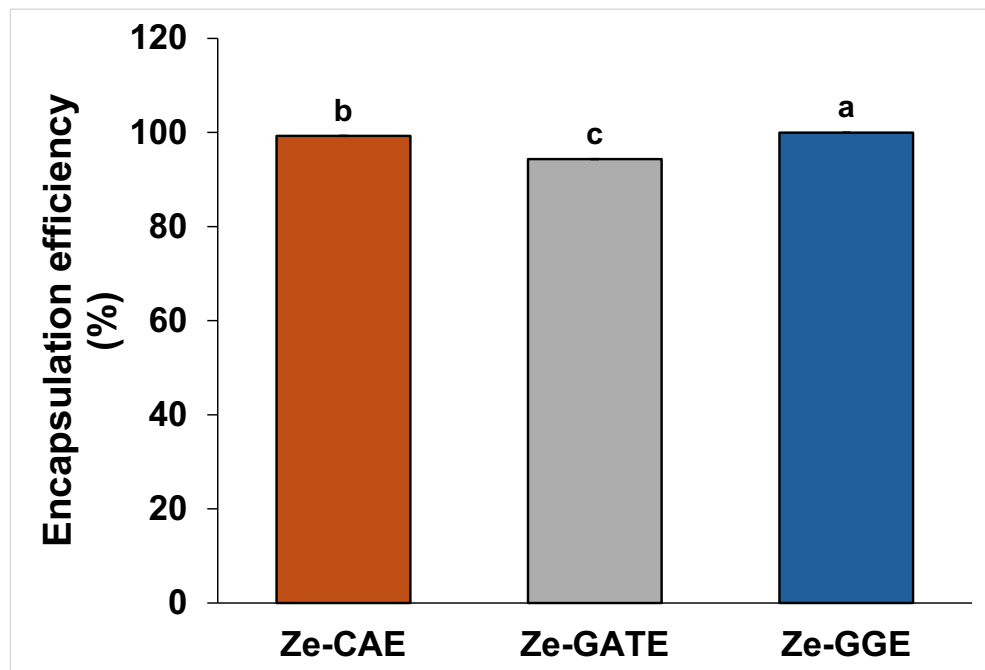
The data regarding film thickness is crucial for subsequent film characterisation, including aspects like water vapour permeability and mechanical properties. While this current study did not measure these two properties, the current findings may offer valuable insights into the film thickness produced by electrospinning with Ze-CAE, Ze-GATE, and Ze-GGE for future research.

#### **4.3.5 Encapsulation efficiency**

Encapsulation efficiency refers to the amount of material incorporated within nanoparticles or nanofibers, or adhered to their surface, relative to the amount introduced during the preparation of these materials (FDA, 2018; Marques and Segundo, 2024). In this present work context, the material is the active plant extract, and a similar encapsulation efficiency strategy was applied. The findings indicated that CAE exhibited a maximum wavelength of 267 nm, GATE 322 nm, GGE 666 nm, and zein 444 nm. Therefore, the encapsulation test for Ze-CAE, Ze-GATE, and Ze-GGE was performed at a wavelength of 267, 322, and 666 nm, respectively. Subsequently, the calibration curves for each plant extract were established, resulting in the following equations: for CAE ( $y = 3.731x + 0.0388$ ,

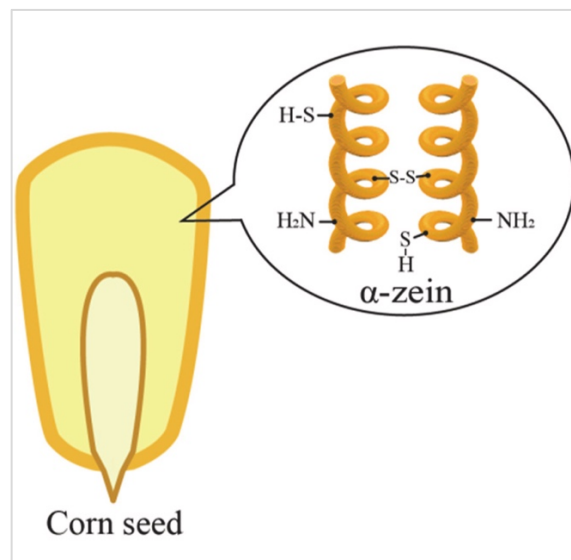
$R^2 = 0.9995$ ), for GATE ( $y = 0.2405x + 0.0213$ ,  $R^2 = 0.9977$ ), and for GGE ( $y = 0.2081x + 0.0034$ ,  $R^2 = 0.9985$ ) (Appendix A Supplementary Materials 3). The encapsulation efficiency test was conducted following the experimental procedures outlined in Section 2.6.3. The percentage of encapsulation efficiency was determined using the free extract concentration value derived from the calibration curve equation.

The encapsulation efficiency percentage of zein-based films is presented in Table 4.2 and Figure 4.17. The data indicated that Ze-GGE films achieved the highest encapsulation efficiency at  $99.97 \pm 0.01\%$ , which was significantly different from Ze-CAE at  $99.25 \pm 0.02\%$ , and Ze-GATE at  $94.35 \pm 0.00\%$  ( $p < 0.05$ ). In general, all zein-based films demonstrated encapsulation efficiency exceeding 90%. The findings align with the earlier studies which reported high encapsulation efficiencies in electrospun zein materials, approaching 100% (Wang, H. et al., 2017; Khalafi et al., 2023). This could correspond to the molecular structure of zein. The structure of  $\alpha$ -zein, the predominant class of zein, features glutamine-rich bridges that connect the linear stacks of rod-shaped helical repeat units of zein (Figure 4.18). These bridges exhibit hydrophilic properties, which facilitate the interaction with bioactive molecules through hydrogen bonding (Lai et al., 1999; Zhang, Xinrui et al., 2021). These findings also align with the results from Section 4.3.3, where SEM micrographs of zein-based films, particularly Ze-CAE and Ze-GGE films revealed the formation of string-like structures between the ribbon-shaped fibres. This morphological feature indicates intermolecular interactions, likely hydrogen bonding between zein and the plant extracts, suggesting successful encapsulation within the zein matrix and supporting the films' high encapsulation efficiency. The encapsulation of bioactive compounds, including phenolic compounds, vitamins, and essential oils within zein offers several advantages. It stabilises sensitive ingredients, enhances bioavailability, preserves the bioactivity of the compounds, provides stability and structural integrity to zein-based materials, and improves their functional properties (Gonnet et al., 2010; Huang et al., 2010; Luo, Y. et al., 2012). The findings from this study indicate that the electrospun films of Ze-CAE, Ze-GATE, and Ze-GGE exhibit high encapsulation efficiency, thus rendering them suitable for use as active packaging films. Further research on the characterisation is required to evaluate the other film's properties.



**Figure 4.17** Encapsulation efficiency (%) of Ze-CAE, Ze-GATE, and Ze-GGE films.

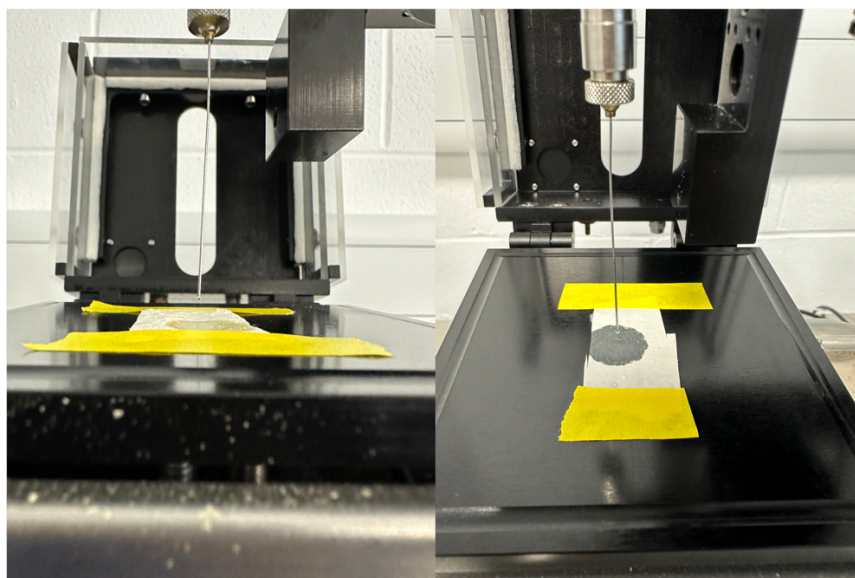
Bar graph represents the means of encapsulation efficiency. Error bars represent the sample standard deviation (mean  $\pm$  SD, n = 3). Means sharing the same letter indicate that the encapsulation efficiency is not significantly different, while means with different letters indicate a statistically significant difference in encapsulation efficiency (Tukey's pairwise comparisons,  $p < 0.05$ ).



**Figure 4.18** The  $\alpha$ -zein structure that comprises of glutamine-rich bridges that connect the linear stacks of rod-shaped helical repeat units of zein. Adapted from (Sun et al., 2023, p.2)

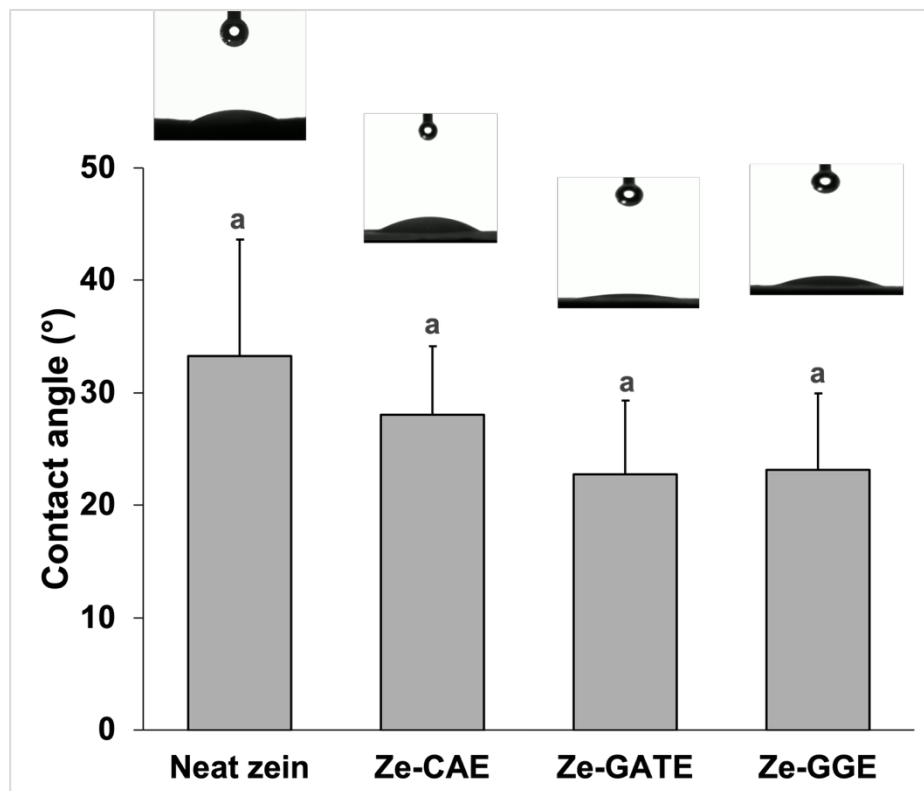
#### 4.3.6 Water contact angle ( $\theta$ )

Wetting refers to the spontaneous dispersion of a liquid across solid surfaces or other liquids, the saturation of porous materials and powders, and the stretching of the liquid interface upon interaction with a solid. Wettability refers to the susceptibility to wetting, and the wettability of solids by liquids is often measured by a contact angle ( $\theta$ ) (Young, 1805, Padday and Uffindell, 1968, Zimon, 1974, cited in Beketov and Shynkarenko, 2022, p. 4-5). The contact angle is the angle formed at the three-phase boundary, where a liquid, gas (or vapour), and solid meet. It is measured between the tangent of the liquid-vapour interface and the solid surface (Huhtamaki et al., 2018; Beketov and Shynkarenko, 2022). Water contact angle is used to determine the hydrophobicity or hydrophilicity of the surface material (Dong et al., 2013). According to the literature, a contact angle between 0 and 90° is considered hydrophilic and wetting, while a contact angle above 90° is regarded as hydrophobic and non-wetting (Blossey, 2003). In this current study, the measurement of contact angle was performed by using a drop shape tensiometer and the sessile drop method. This strategy is the most widely approached method to measure the surface wettability, performed by recording a video of a water drop on a solid surface and analysing the shape of the drop by the measurement of the angle between the surfaces of the liquid drop and the solid phase at the point where they meet (Law and Zhao, 2015; Huhtamaki et al., 2018). The selection of the sessile drop method is due to the simplicity and robustness of the process, as well as the smaller sample size and volume of water required (Huhtamaki et al., 2018). The representative photos of contact angle measurement by the sessile drop method are presented in Figure 4.19.



**Figure 4.19** Measurement of water contact angle by sessile drop method at  $20 \pm 2$  °C using drop shape tensiometer with 3  $\mu\text{L}$  of water droplet deposited on the surface of the film (20 x 40 mm).

The experiment aimed to measure the contact angle at 2 seconds, identified as the optimal time for analysing the contact angle of the films in this study. Extended exposure resulted in the films exhibiting complete wetting (data not shown), which impeded the measurement of contact angle. The selected drop volume of 3  $\mu\text{L}$  aligns with guidelines from the literature review, indicating that volumes lower than 3  $\mu\text{L}$  may disrupt the needle and lead to errors (Huhtamaki et al., 2018). Table 4.2 and Figure 4.20 present the water contact angle measurements taken 2 seconds after a water droplet was placed on the surfaces of Neat zein, Ze-CAE, Ze-GATE, and Ze-GGE films. The data indicated that the films displayed a contact angle of less than  $90^\circ$  (between  $20^\circ$  to  $35^\circ$ ), demonstrating hydrophilic and wetting characteristics. The incorporation of CAE, GATE, and GGE into Ze-CAE, Ze-GATE, and Ze-GGE films, respectively led to a minor reduction in water contact angle, however, this change was not statistically significant when compared to the control film, Neat zein ( $p > 0.05$ ).



**Figure 4.20** The water contact angle (°) of Neat zein, Ze-CAE, Ze-GATE, and Ze-GGE films. The figures above the bar graph shows the different shapes of water droplet observed after 2 seconds of exposure to films; contact angle of  $33.26 \pm 10.37^\circ$  for Neat zein,  $28.04 \pm 6.11^\circ$  for Ze-CAE,  $22.74 \pm 6.55^\circ$  for Ze-GATE, and  $23.18 \pm 6.79^\circ$  for Ze-GGE.

Bar graph represents the means of water contact angle. Error bars represent the sample standard deviation (mean  $\pm$  SD, n = 3). Means sharing the same letter indicate that the water contact angle is not significantly different, while means with different letters indicate a statistically significant difference in water contact angle (Tukey's pairwise comparisons,  $p < 0.05$ ).

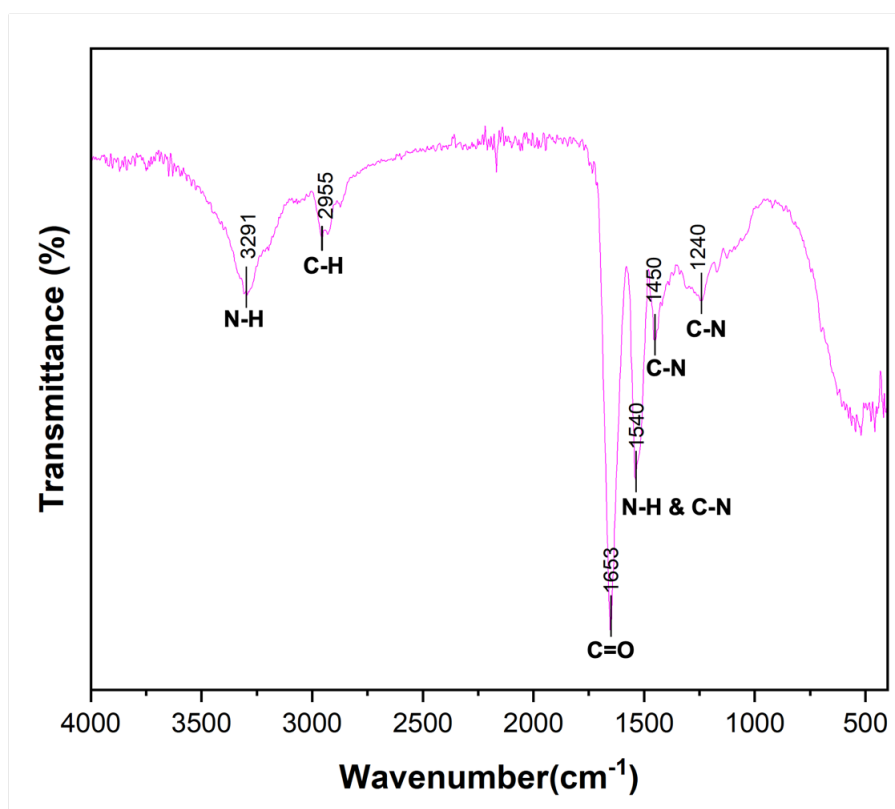
The hydrophilic characteristics of Ze-CAE, Ze-GATE, Ze-GGE, and Neat zein films may be attributed to the morphology of the films, which are produced through electrospinning. The electrospun fibres exhibit a high surface-to-volume ratio and porosity, which enhance water penetration and dissolution (Fang et al., 2008; De Schoenmaker et al., 2011). Ali et al. (2014) reported comparable findings of low contact angle values for electrospun zein, observing contact angles between 4° and 6° after 1.0 second of contact between a water drop and zein/cellulose acetate nanofibres. The research indicated that both pH and zein concentration also influenced the water contact angle, with increases in pH and zein concentration leading to a reduction in the contact angle (Luo, S. et al., 2021; Wu, Y. et al., 2023). Although zein films produced via film casting are frequently reported to have higher contact angles than those produced by electrospinning, the electrospinning technique demonstrates superior performance in terms of encapsulation efficiency, biopolymer compatibility, and bioactive stability (Gonnet et al., 2010; Huang et al., 2010; Luo, Y. et al., 2012; Luis et al., 2019; Qazanfarzadeh et al., 2021). It is also important to note that the film prepared by film casting often depends on the plasticiser to achieve flexibility and functional integrity, which is not required for the films prepared by electrospinning (Luis et al., 2019; Qazanfarzadeh et al., 2021). In summary, the zein-based films derived from CAE, GATE, and GGE exhibited relatively low contact angles, indicating hydrophilic surface properties likely due to the morphological characteristics of the films. In terms of the application of these films as active food packaging, this characteristic would become a limitation to certain range of foods, where the hydrophobicity property is essential.

#### 4.3.7 Attenuated total reflectance-Fourier transform infrared spectroscopy (ATR-FTIR)

Infrared (IR) spectroscopy is a method that employs infrared radiation to measure the fraction of incident radiation that is absorbed at designated wavelengths (Griffiths, 1983; Carden and Morris, 2000; Thompson, T.J.U. et al., 2009). Infrared light interaction with a sample lead to molecular energy absorption, causing transitions to higher vibrational states. Some wavelengths are absorbed, whereas others transmit through the sample without alteration. The wavelengths absorbed are influenced by the molecular structure of the sample, with these absorbed energies corresponding to the vibrations of atomic bonds, detectable and reflected in a spectral output. The Fourier transform (FT) is the tool used to generate this spectrum. This algorithm transforms the raw data obtained from the detector into a readable IR spectrum, with each peak representing a distinct bond vibration within a molecular group (Krishnan and Ferraro, 1990; Beasley et al., 2014). In contrast to the earlier FTIR method, ATR-FTIR represents an improvement in the FTIR technique, as it assesses the changes that take place in an internally reflected infrared beam when it interacts with the sample via a crystal, usually made of zinc selenide or diamond. When a sample is in contact with the ATR crystal, it interacts with an evanescent wave produced by the internal reflection before it is attenuated in the IR spectrum regions, where the sample absorbs energy (Bruno, 1999). The sample is placed on the sampling plate and secured by a micrometre-controlled clamp to ensure good contact between the sample and the crystal (Beasley et al., 2014). ATR-FTIR has become a preferred technique because it is fast, requires little or no sample preparation, and eliminates variations caused by traditional methods such as potassium bromide (KBr) grinding and differences in particle size (Thompson, T.J.U. et al., 2009).

In this present work, ATR-FTIR analysis was performed at the range of 4000 to 400  $\text{cm}^{-1}$  to examine the potential interactions between functional groups of CAE, GATE, and GGE with zein. The absorption band for zein-based films as well as for Neat zein and crude plant extracts of CAE, GATE, and GGE was analysed using OriginPro software by manually selecting the major bands, and the results were compared. Figure 4.21 shows that Neat zein displays a broad absorption band at 3291  $\text{cm}^{-1}$ , corresponding to the N-H stretching vibration of Amide A (Magoshi et al., 1992; Forato et al., 1998; Mohammed-Ziegler and Billes, 2002). Another observed peak occurred at 2955  $\text{cm}^{-1}$ , signifying the presence of the C-H stretching bands from the methyl ( $\text{CH}_3$ ) and methylene ( $\text{CH}_2$ ) aliphatic groups of zein (Nagarajan et al., 2013; Khalafi et al., 2023). A band at 1653  $\text{cm}^{-1}$  was

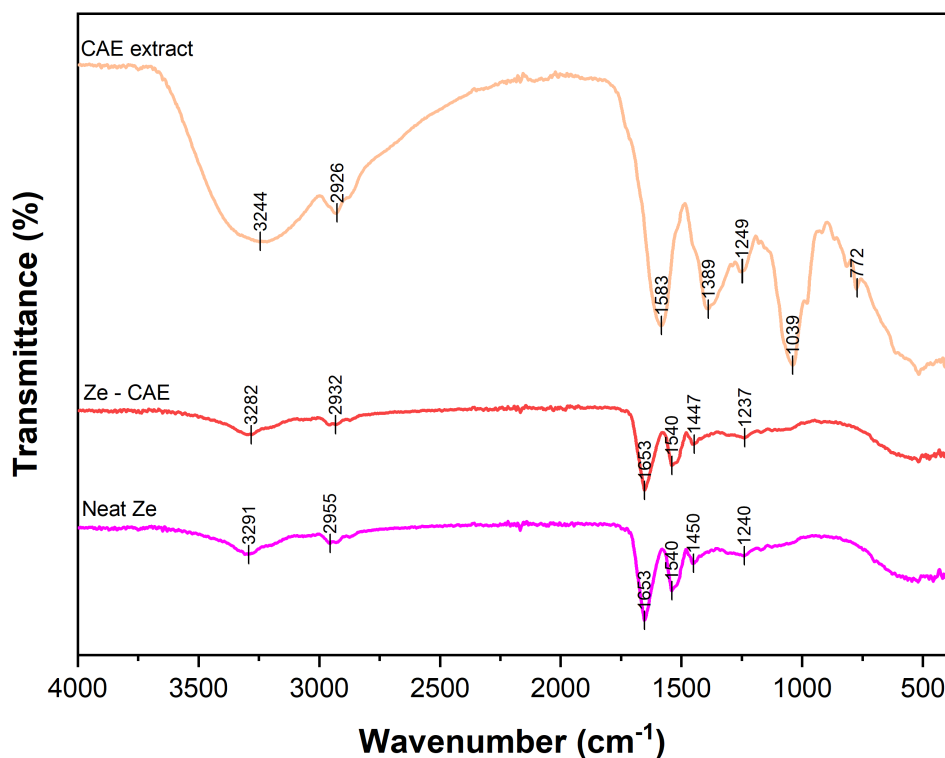
identified as amide I, corresponding to the stretching vibration of the carbonyl double bond (C=O) (Magoshi et al., 1992; Forato et al., 1998; Mohammed-Ziegler and Billes, 2002). The Amide I region, spanning 1600 to 1700  $\text{cm}^{-1}$  provides valuable information on the secondary structure of proteins such as  $\alpha$ -helix,  $\beta$ -sheet,  $\beta$ -turn, and random coil. The strong signal of 1653  $\text{cm}^{-1}$  observed in the Amide I associated with the presence of a predominant  $\alpha$ -helix structure in the Neat zein film (Forato et al., 1998; Forato et al., 2003). No other significant secondary protein signals ( $\beta$ -sheet: 1620-1640  $\text{cm}^{-1}$ , 1675-1700  $\text{cm}^{-1}$ ,  $\beta$ -turn: 1660-1675  $\text{cm}^{-1}$ , random coil: 1640-1648  $\text{cm}^{-1}$ ) were observed aside from  $\alpha$ -helix, suggesting that the conformation of the Neat zein film consisted of  $\alpha$ -helical structure (Krimm and Bandekar, 1986; Bandekar, 1992; Meng and Ma, 2002; Zhao et al., 2008). A distinct band was observed at 1540  $\text{cm}^{-1}$ , corresponding to amide II, which arises from the stretching vibrations of C-N and N-H bending (Forato et al., 2003). Additional bands identified at 1450, and 1240  $\text{cm}^{-1}$  were characterised by C-N axial deformation vibrations of amide III (Magoshi et al., 1992; Forato et al., 1998; Barth, 2007; Khalafi et al., 2023).



**Figure 4.21** FTIR spectrum for Neat zein at the range of 4000 to 400  $\text{cm}^{-1}$ . Diverse absorption bands related to zein are evidenced such as Amide A (N-H: 3291  $\text{cm}^{-1}$ ), methyl ( $\text{CH}_3$ ) and methylene ( $\text{CH}_2$ ) aliphatic groups (C-H: 2955  $\text{cm}^{-1}$ ), Amide I (C=O: 1653  $\text{cm}^{-1}$ ), Amide II (C-N & N-H: 1540  $\text{cm}^{-1}$ ), Amide III (C-N: 1450 & 1240  $\text{cm}^{-1}$ ).

The addition of 5% (w/w) plant extracts of CAE, GATE, and GGE with respect to zein content resulted in FTIR spectra as presented in Figures 4.22 to 4.24. Figure 4.22 illustrates the spectrum of crude plant extract from *C. asiatica*, which exhibits a broad absorption band at  $3244\text{ cm}^{-1}$ . This band corresponds to the absorption signal of the hydroxyl (O-H) group, a characteristic feature of phenolic compounds (Coates, 2006; Tang, Y. et al., 2021). The band at  $2926\text{ cm}^{-1}$  is attributed to C-H stretching vibrations of aliphatic groups. The band at  $1583\text{ cm}^{-1}$  is likely linked to carbon double bonds (C=C) and carbonyl groups (C=O) conjugated to aromatic systems, a characteristic feature of flavonoids (Krysa et al., 2022). The band at  $1389\text{ cm}^{-1}$  indicates C-H bending associated with the  $\text{CH}_3$  group. The band at  $1249\text{ cm}^{-1}$  corresponds to C-O stretching in alcohols or ethers and may suggest the presence of tannins or phenolic structures. Two bands at  $1039\text{ cm}^{-1}$  and  $772\text{ cm}^{-1}$  are assigned to aromatic in-plane C-H bending and out-of-plane C-H bending, respectively (Coates, 2006; Fernandez and Agosin, 2007). The data indicate the presence of functional groups, including phenolics, flavonoids, glycosides, and triterpene acids in the CAE (Lee, S.-S. et al., 2000; Nik Hairiah et al., 2013; Sangsopha et al., 2018). After electrospinning, the spectrum for Ze-CAE film showed similar major bands to Neat zein film but demonstrated some band shifting. The characteristic band of the N-H stretching vibration of Ze-CAE at  $3291\text{ cm}^{-1}$  was shifted to a lower frequency of  $3282\text{ cm}^{-1}$ , overlapping with the O-H band. The characteristic band of C-H stretching of Neat zein at  $2955\text{ cm}^{-1}$  was observed to shift progressively to  $2932\text{ cm}^{-1}$  for Ze-CAE (Figure 4.22). The observed shifts to lower frequencies may result from the interaction between the functional groups of CAE and zein, suggesting the formation of intermolecular hydrogen bonds following electrospinning (Ratajczak, 1972; Coleman et al., 1988; Mattia and Painter, 2007; McDowell, 2025). This finding is further supported by previous SEM micrographs presented in Section 4.3.3, which show strings formation in Ze-CAE, demonstrating successful cross-linking of compounds from CAE into zein fibres. No shifts in the bands were observed for C=O, N-H, and C-N bonds at  $1653\text{ cm}^{-1}$  and  $1540\text{ cm}^{-1}$ , indicating that the incorporation of CAE into zein fibres did not significantly alter the molecular structure of the functional groups. On the other hand, minimal band shifting was observed for the C-N vibrations ( $1450\rightarrow 1447\text{ cm}^{-1}$  and  $1240\rightarrow 1237\text{ cm}^{-1}$ ) (Figure 4.22). No new band was observed in the Ze-CAE spectrum, further confirming the incorporation of CAE into the zein fibres and assuming that the CAE signals overlapped with zein signals. The data is also supported by the higher encapsulation efficiency results presented whin Section 4.3.5. The disappearance of bands at  $1389$ ,  $1039$ , and  $772\text{ cm}^{-1}$  in the CAE spectrum of the Ze-CAE film might be attributed to the lower concentration of CAE incorporated

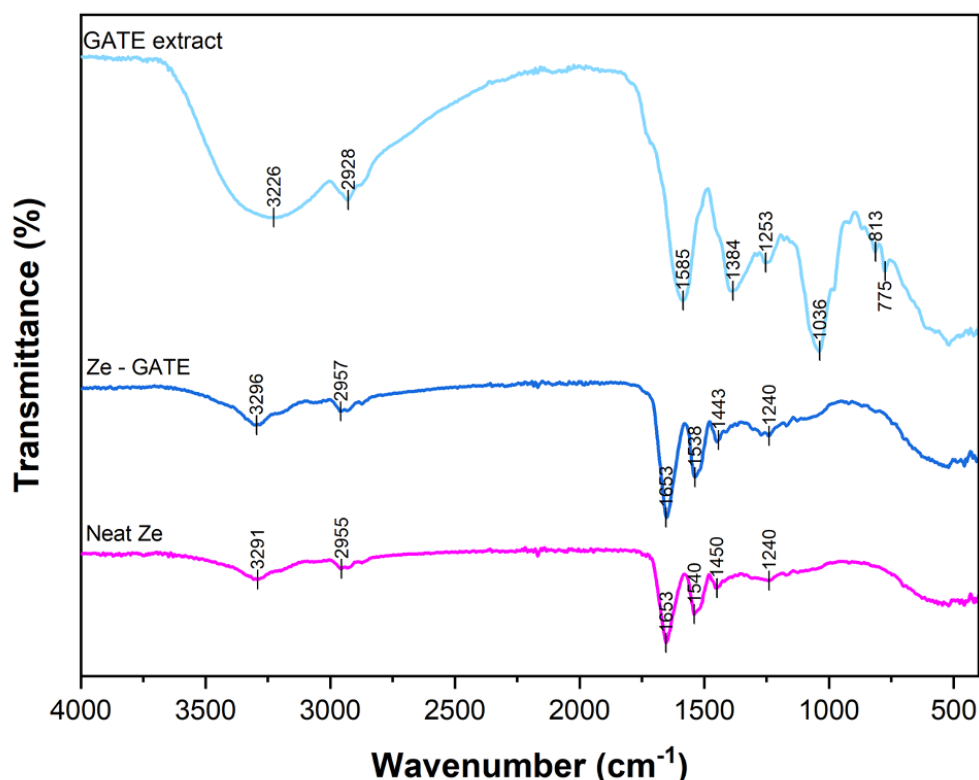
(5% w/w) into the Ze-CAE film when compared to zein concentration (30% w/v), thus resulting in reduced signal intensity.



**Figure 4.22** Comparison of FTIR spectra between Neat zein film, Ze-CAE film and CAE extract at the range of 4000 to 400  $\text{cm}^{-1}$ . Absorption bands related to CAE extract are phenolics (O-H: 3244  $\text{cm}^{-1}$ ), aliphatic groups (C-H: 2926  $\text{cm}^{-1}$ ), flavonoids (C=C & C=O: 1583  $\text{cm}^{-1}$ ), methyl group (C-H: 1389  $\text{cm}^{-1}$ ), tannins or phenolic structures (C-O: 1249  $\text{cm}^{-1}$ ), aromatic groups (C-H: 1039 & 772  $\text{cm}^{-1}$ ). Absorption bands related to Ze-CAE showed similar major bands to Neat zein with several band shifting, including (N-H overlapping with O-H: 3291 $\rightarrow$ 3282  $\text{cm}^{-1}$ ), (C-H: 2955 $\rightarrow$ 2932  $\text{cm}^{-1}$ ), (C-N: 1450 $\rightarrow$ 1447  $\text{cm}^{-1}$ , 1240 $\rightarrow$ 1237  $\text{cm}^{-1}$ ). The disappearance of bands of 1389, 1039, and 772  $\text{cm}^{-1}$  from CAE extract in the Ze-CAE spectrum might be attributed to the lower concentration of CAE incorporated into the Ze-CAE film, resulting in reduced signal intensity.

The examination of the spectrum for GATE in Figure 4.23 shows similar broad absorption band at 3226  $\text{cm}^{-1}$  (O-H stretching), followed by 2928  $\text{cm}^{-1}$  (C-H stretching), 1585  $\text{cm}^{-1}$  (C=O and C=C stretching), 1384  $\text{cm}^{-1}$  (C-H bending), and 1253  $\text{cm}^{-1}$  (C-O stretching). Three additional signals observed at 1036, 813, and 775  $\text{cm}^{-1}$  are associated with the aromatic in-plane and out-of-plane C-H bending vibrations (Figure 4.23) (Coates, 2006; Tan, W.-N. et al., 2016; Zulkifli et al., 2020). These bands propose the presence of organic acids, flavonoids, and phenolics in GATE (Kosin et al., 1998; Permana et al., 2001; Jena et al., 2002; Mackeen et al., 2002; Permana et al., 2003; Permana et al., 2005). Following electrospinning, Ze-GATE film, compared against Neat zein showed the shifting

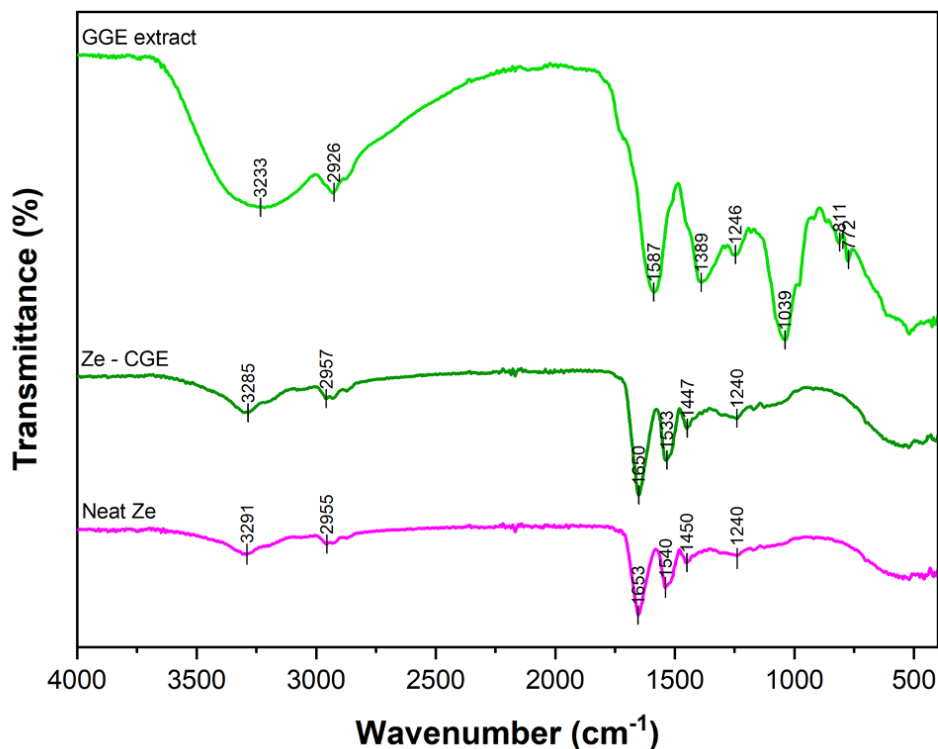
of the bands to higher frequencies at the higher IR region; 3291→3296  $\text{cm}^{-1}$  (N-H and O-H stretching) and 2955→2957  $\text{cm}^{-1}$  (C-H stretching) and lower frequencies at the lower region; 1540→1538  $\text{cm}^{-1}$  (N-H and C-N stretching) and 1450→1443  $\text{cm}^{-1}$  (C-N stretching). It can be speculated that free (non-bonded) O-H and N-H groups were present in Ze-GATE, which allowed them to vibrate at higher wavenumbers (Figure 4.23) (Coleman et al., 1988; Mattia and Painter, 2007). The shift in C-H stretching vibrations to higher frequencies can be linked to the occurrence of 'improper' hydrogen bonding, where hydrogen bonds lead to the strengthening and shortening of C-H bonds, instead of the weakening effect. This indicates that the interaction between zein and GATE involved fewer hydrogen bonds, leading to weakened intermolecular interactions and the formation of stronger C-H bonds (Hobza and Havlas, 2002; Joseph and Jemmis, 2007). This finding is supported by the SEM results presented in Section 4.3.3, which show no string formation in GATE film micrographs after electrospinning. Even further formation of hydrogen bonds occurred at the lower region; no prominent effect was observed, as shown in the SEM micrographs (no string formation). The C=O band for amide I and the C-N band for amide III remain unchanged. Three signals at the lower frequency region (1036, 813, and 775  $\text{cm}^{-1}$ ) disappeared, likely attributed to the similar reason discussed for the Ze-CAE above (lower concentration of extract). Overall, no new bands were observed with the incorporation of GATE into zein fibres. It is assumed that the majority of the significant GATE signals overlapped with zein signals, resulting in similar spectra for Neat zein and Ze-GATE.



**Figure 4.23** Comparison of FTIR spectra between Neat zein film, Ze-GATE film, and GATE extract at the range of 4000 to 400  $\text{cm}^{-1}$ . Absorption bands related to GATE extract are (O-H: 3226  $\text{cm}^{-1}$ ), (C-H: 2928  $\text{cm}^{-1}$ ), (C=O & C=C: 1585  $\text{cm}^{-1}$ ), (C-H: 1384  $\text{cm}^{-1}$ ), (C-O: 1253  $\text{cm}^{-1}$ ), (C-H: 1036, 813, & 775  $\text{cm}^{-1}$ ). Absorption bands related to Ze-GATE showed similar major bands to Neat zein with several band shifting, including (N-H & O-H: 3291 $\rightarrow$ 3296  $\text{cm}^{-1}$ ), (C-H: 2955 $\rightarrow$ 2957  $\text{cm}^{-1}$ ), (N-H & C-N: 1540 $\rightarrow$ 1538  $\text{cm}^{-1}$ ), (C-N: 1450 $\rightarrow$ 1443  $\text{cm}^{-1}$ ). The disappearance of bands of 1036, 813, and 775  $\text{cm}^{-1}$  from GATE extract in the Ze-GATE spectrum might be attributed to the lower concentration of GATE incorporated into the Ze-GATE film, resulting in reduced signal intensity.

As for Ze-GGE, the spectrum in Figure 4.24 exhibits a broad absorption band at 3233  $\text{cm}^{-1}$ , indicative of O-H stretching, characteristic of phenolics. The band at 2926  $\text{cm}^{-1}$  associates with C-H stretching bands from the  $\text{CH}_3$  and  $\text{CH}_2$  aliphatic groups. The characteristic band at 1587  $\text{cm}^{-1}$  is attributed to the C=O or C=C stretching vibrations, which are typically associated with carboxylic acid or alkene groups. The band at 1389  $\text{cm}^{-1}$  corresponds to C-H bending related to the  $\text{CH}_3$  group, whereas C-O stretching indicative of phenolic structures, is observed at 1246  $\text{cm}^{-1}$ . Three bands at 1039  $\text{cm}^{-1}$ , 811  $\text{cm}^{-1}$ , and 772  $\text{cm}^{-1}$  correspond to the aromatic in-plane C-H bending and out-of-plane C-H bending (Figure 4.24) (Coates, 2006; Dutta et al., 2018; Le, T.H. et al., 2021). The data suggest the presence of fatty acids, phenolics, and terpenoids (Dutta et al., 2018; Le, T.H. et al., 2021; Trisha et al., 2024). The FTIR spectrum analysis following the addition of GGE into zein, resulting in the Ze-GGE film after electrospinning, indicated that most bands shifted to lower frequencies (3291 $\rightarrow$ 3285  $\text{cm}^{-1}$ ; 1653 $\rightarrow$ 1650  $\text{cm}^{-1}$ ;

1540→1533  $\text{cm}^{-1}$ ; and 1450→1447  $\text{cm}^{-1}$ ) except for the signal at 1240, which did not change and at 2955  $\text{cm}^{-1}$  which shifted to a higher frequency, 2957  $\text{cm}^{-1}$  (compared to Neat zein) (Figure 4.24). It can be suggested that the functional groups from GGE interact with zein through the formation of hydrogen bonds, as indicated by the observed shifts to lower frequencies in most bands (Ratajczak, 1972; Coleman et al., 1988; Mattia and Painter, 2007; McDowell, 2025). The SEM micrographs from Section 4.3.3 show the interaction between GGE and zein, highlighting the formation of strings between zein fibres. The observed shift to higher frequency may be attributed to weakened hydrogen bonds due to fewer intermolecular interactions between zein and C-H bonds from aliphatic groups, which make the C-H bonds stronger and shorter (Hobza and Havlas, 2002; Joseph and Jemmis, 2007). Most GGE bands are presumed to be integrated into zein fibres, with their signals overlapping those of the major zein bands, therefore, no distinct spectral were observed between Neat zein and Ze-GGE. The low concentration of GGE added (5% w/w) to the Ze-GGE film likely resulted in a reduction of signal intensity within the region between 1039 and 772  $\text{cm}^{-1}$ , leading to the absence of these bands in the Ze-GGE spectrum.



**Figure 4.24** Comparison of FTIR spectra between Neat zein film, Ze-GGE film, and GGE extract at the range of 4000 to 400  $\text{cm}^{-1}$ . Absorption bands related to GGE extract are phenolics (O-H: 3233  $\text{cm}^{-1}$ ), methyl & methylene aliphatic groups (C-H: 2926  $\text{cm}^{-1}$ ), carboxylic acid/ alkene (C=O/C=C: 1587  $\text{cm}^{-1}$ ), methyl group (C-H: 1389  $\text{cm}^{-1}$ ), phenolics (C-O: 1246  $\text{cm}^{-1}$ ), aromatic groups (C-H: 1039, 811, & 772  $\text{cm}^{-1}$ ). Absorption bands related to Ze-GGE showed similar major bands to Neat zein with several band shifting, including (N-H & O-H: 3291 $\rightarrow$ 3285  $\text{cm}^{-1}$ ), (C-H: 2955 $\rightarrow$ 2957  $\text{cm}^{-1}$ ), (C=O: 1653 $\rightarrow$ 1650  $\text{cm}^{-1}$ ), (N-H & C-N: 1540 $\rightarrow$ 1533  $\text{cm}^{-1}$ ), (C-N: 1450 $\rightarrow$ 1447  $\text{cm}^{-1}$ ). The disappearance of bands of 1039, 811, and 772  $\text{cm}^{-1}$  from GGE extract in the Ze-GGE spectrum might be attributed to the lower concentration of GGE incorporated into the Ze-GGE film, resulting in reduced signal intensity.

Overall, the analysis of the spectra of Ze-CAE, Ze-GATE, and Ze-GGE films showed similar spectra with the control film of Neat zein with some band shifts observed. The bands shifted to lower frequencies are indicative of hydrogen bond formation and were more pronounced in Ze-CAE and Ze-GGE, and less evident in Ze-GATE. The FTIR spectra of Ze-CAE, Ze-GATE, and Ze-GGE indicated that the addition of these plant extracts (5% w/w) to zein fibres did not result in the emergence of new peaks, suggesting successful encapsulation of the extracts within the zein fibres without significantly altering their structural integrity. It is important to mention that the FTIR interpretation was performed using manual peak selection in OriginPro, which may introduce minor variations in the band assignment. As such, the spectral analysis should be interpreted with caution.

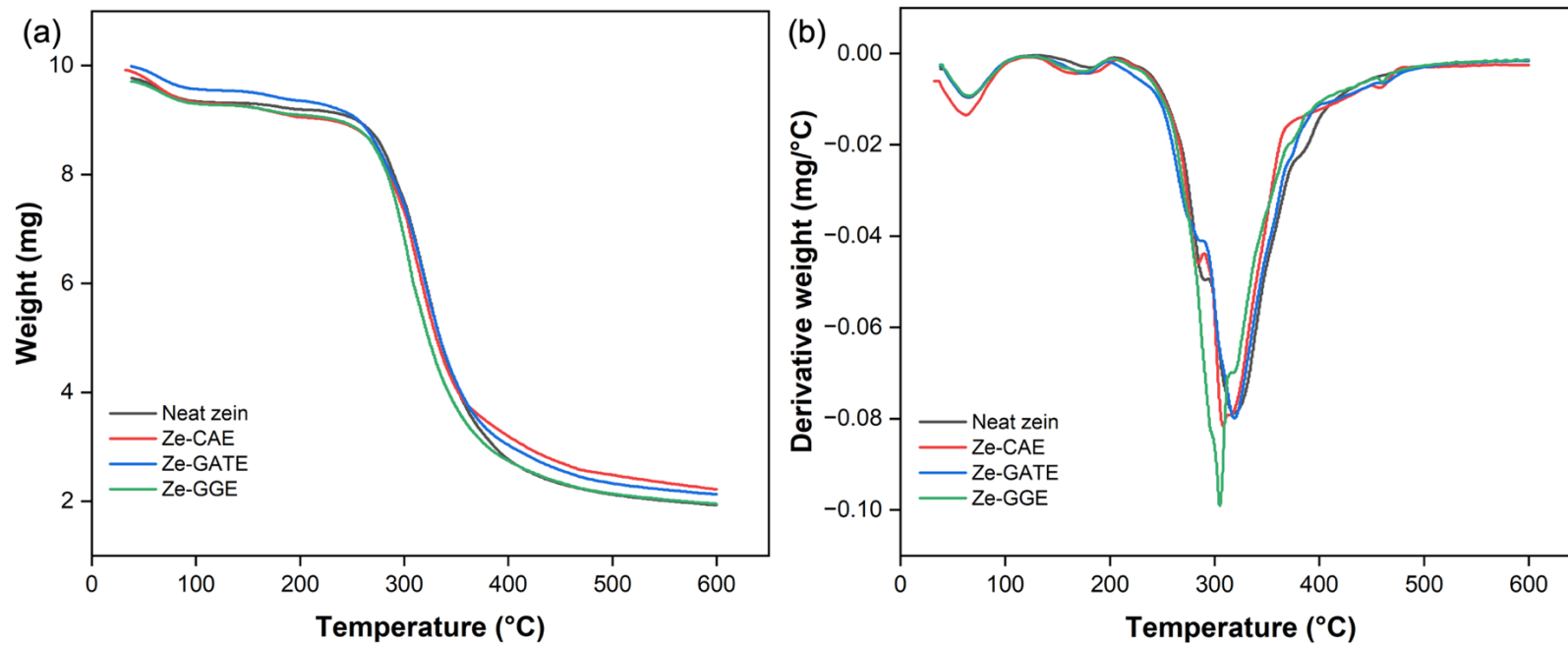
#### 4.3.8 Thermal properties

Thermogravimetric analysis (TGA) is a technique to measure the weight of a substance relative to temperature or time, performed in a controlled temperature and atmosphere with a thermogravimetric analyser, while the weight change data is captured by computer software (Earnest, 1988; Losic et al., 2024). In this present work, the sample was fixed to a pan that is held up by a precision balance within a furnace and heated from 30 to 600 °C under a nitrogen atmosphere at a heating rate of 10 °C/min. TGA data was analysed using OriginPro software, and the results were presented as TGA and Derivative thermogravimetry (DTG) curves. The DTG curve is the first derivative of the TGA curve with regard to temperature or time (Bottom, 2008). While the TGA curve provides information such as the rate of weight loss, number of decomposition steps, and remaining residue, DTG presents the maximum rate of weight loss shown by peak temperature. Each peak in DTG also represents a separate thermal event (Prime et al., 2014). In brief, TGA was performed to assess the thermal stability, decomposition stages, and residue as well as the impact of the incorporation of plant extract on the thermal behaviour of zein-based films. Neat zein served as the reference material for comparison. The data on the decomposition of packaging materials is critical, as it provides insights on their resistance to environmental stresses as well as their disposal potential through incineration (Alizadeh-Sani et al., 2021).

Thermal stability data for the developed zein-based films (Ze-CAE, Ze-GATE, and Ze-GGE) are detailed in Table 4.3 and presented in Figures 4.25 to 4.27. Figure 4.25(a) illustrates the comparison for TGA curves for all zein-based films produced, which shows the film's sample weight as a function of temperature, while Figure 4.25(b) shows the derivative weight as a function of temperature. Based on the inspection of the TGA and DTG curves, all zein-based films followed a fairly similar decomposition trend, involving multi-stages of weight loss during heating from 30 to 600 °C. Further analysis of TGA/DTG curves will be explained in greater detail for each of the zein samples in the following paragraphs.

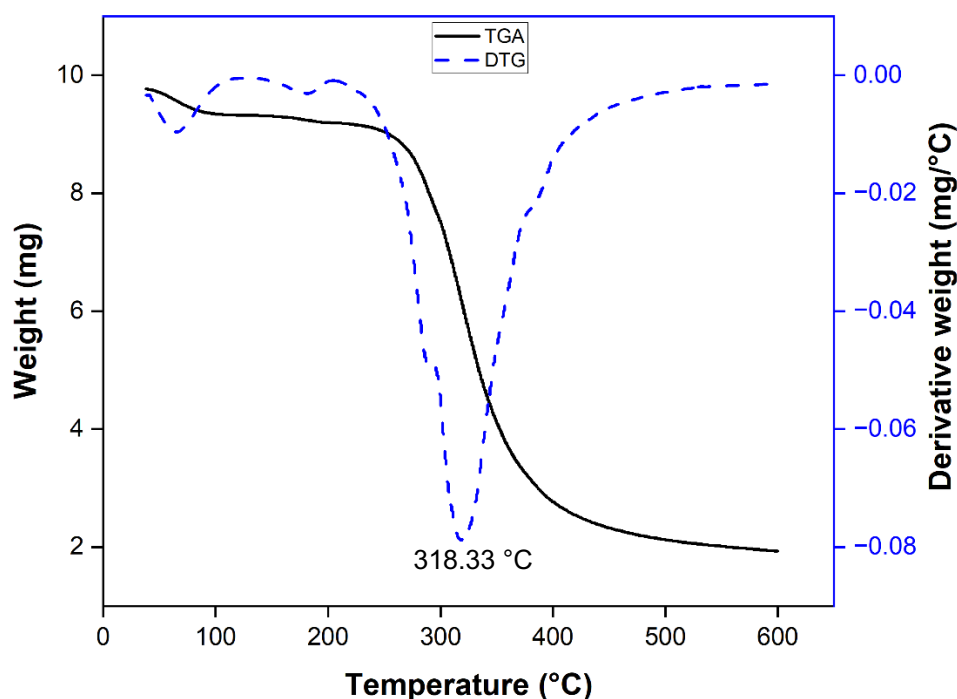
**Table 4.3** TGA profile of zein-based films at the temperature between 30 and 600 °C.

Film	Neat zein		Ze-CAE		Ze-GATE		Ze-GGE	
	Temp. (°C)	Weight loss (mg/ %)	Temp. (°C)	Weight loss (mg/ %)	Temp. (°C)	Weight loss (mg/ %)	Temp. (°C)	Weight loss (mg/ %)
Stage 1	36.12-99.89	-0.45/ -4.54	36.12-97.67	-0.63/ -6.31	37.97-100.19	-0.44/ -4.37	30.01-97.99	-0.43/ -4.38
Stage 2	144.78-195.14	-0.13/ -1.27	129.99-170.06	-0.25/ -2.55	137.44-186.14	-0.18/ -1.83	133.74-202.90	-0.19/ -1.93
Stage 3	259.40-293.11	-1.38/ -13.91	258.92-287.30	-1.22/ -12.34	243.62-287.32	-1.35/ -13.36	277.55-309.17	-3.58/ -36.31
Stage 4	302.13-376.39	-5.88/ -59.19	301.84-395.45	-5.10/ -51.43	300.26-378.23	-5.49/ -54.29	365.59-434.08	-3.58/ -36.11
Stage 5	-	-	452.71-482.27	-0.49/ -4.96	458.93-499.74	-0.40/ -3.91	-	-
Residue	1.93 mg/ 19.43%		2.22 mg/ 22.35%		2.13 mg/ 21.64%		1.95 mg/ 19.83%	



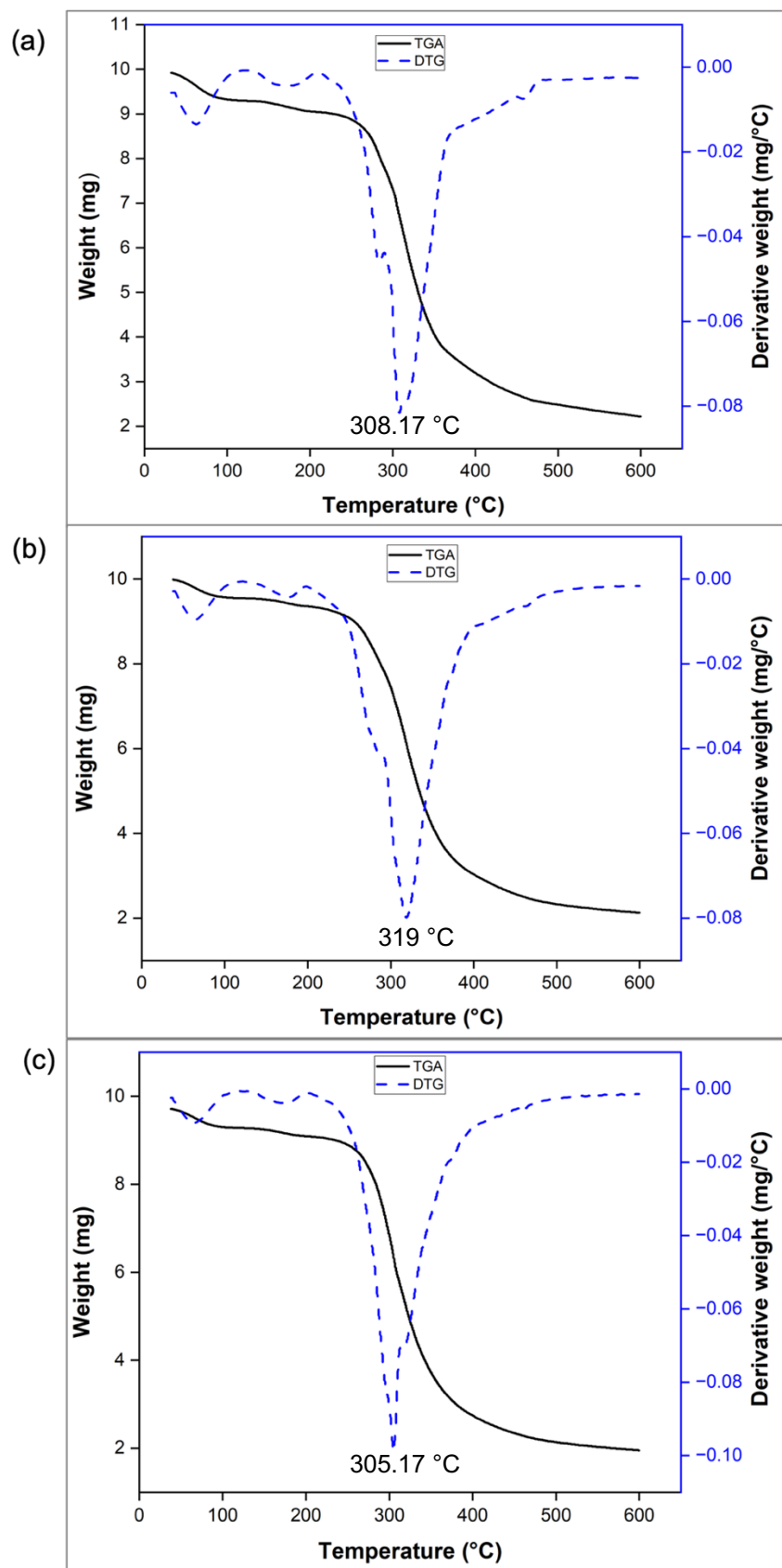
**Figure 4.25** Comparison of (a) TGA and (b) DTG curves for zein-based films.

The TGA/DTG data for Neat zein film displayed a four-stage decomposition process (Table 4.3 and Figure 4.26). The first stage occurred from 36.12 to 99.89 °C, with a weight loss of 0.45 mg (4.54%), primarily due to the evaporation of water and residual ethanol solvent (Torres-Giner and Lagaron, 2010; Neo et al., 2013). The second stage occurred around 144.78 to 195.14 °C, involved a 0.13 mg (1.27%) weight loss, likely due to the decomposition of low molecular weight components of zein (Shukla and Cheryan, 2001; Prime et al., 2014). The third stage of decomposition process occurred at 259.40 to 293.11 °C, which resulted in 1.38 mg (13.91%) of weight loss, likely attributed to the initial degradation of amino acids, such as proline (Schaberg et al., 2018). The same author indicated that most amino acids required two to four decomposition steps, with proline loss it's 99.5% mass between 220 and 290 °C (Schaberg et al., 2018). A subsequent weight loss of 5.88 mg (59.19%) occurred between 302.13 and 376.39 °C, mainly attributed to thermal degradation of the major protein backbone (Magoshi et al., 1992; Torres-Giner and Lagaron, 2010). A 1.93 mg (19.43%) residue remained at 600 °C. The DTG profile indicated a maximum decomposition rate at 318.33 °C, consistent with the finding of Magoshi et al. (1992), which was reported at 320 °C. The number of decomposition stages of Neat zein in this study differ slightly from previous research, likely due to different sources (e.g., different  $\alpha$ -,  $\beta$ -,  $\gamma$ -, and  $\delta$ -zein content) and experimental protocols for electrospinning and thermal analysis (Torres-Giner and Lagaron, 2010; Neo et al., 2013).



**Figure 4.26** TGA/DTG curve of Neat zein showing four-stage decomposition process with maximum decomposition rate temperature at 318.33 °C.

The TGA/DTG data for Ze-CAE and Ze-GATE films revealed five decomposition stages of weight loss during heating. In contrast, Ze-GGE involved only four stages of weight loss, similar to that of Neat zein (Table 4.3 and Figure 4.27(a-c)). The initial stage of weight loss of 4.37 to 6.31% occurred around 30 to 100 °C, which is correlated to the moisture evaporation and volatilisation of residual solvent (Torres-Giner and Lagaron, 2010; Neo et al., 2013). This initial decomposition stage was consistent across all film samples. The first decomposition stage is also probably due to chlorophyll, as it was previously reported that chlorophyll decomposition begins at 70 °C, and it especially influenced the decomposition stages for Ze-CAE and Ze-GGE films, as these two extracts were derived from the leaf part (Martinez-Mendoza et al., 2016). The second stage occurred around 130 to 200 °C, which involved 1.83 to 2.55% of weight loss corresponding to the decomposition of low molecular weight components of zein (Shukla and Cheryan, 2001; Prime et al., 2014). The decomposition of fatty acids from GGE, such as oleic acid, also occurred in this stage (Peters et al., 2022). The third stage started around 240 to 300 °C and exhibited 12.34% to 36.31% of weight loss, mainly representing the initial decomposition of amino acids (Schaberg et al., 2018). Weight loss due to carbohydrates, organic acids, and other organic compounds in plant extracts also occurred in the second and third stages (Araujo et al., 2006; Martinez-Mendoza et al., 2016; Varol and Mutlu, 2023). In the fourth stage, major weight loss of 36.11 to 54.29% occurred around 300 to 430 °C, primarily due to the decomposition of the protein backbone as well as the phenolic compounds from the extracts (Magoshi et al., 1992; Torres-Giner and Lagaron, 2010; Cheng et al., 2014). It can be observed that Ze-GGE had a slightly higher decomposition temperature compared to Ze-CAE and Ze-GATE during the third and fourth stages, probably due to the combined thermal events of decomposition, carbonisation of polymeric materials, and ash formation occurred during the fourth stage, resulting in a higher decomposition temperature. The fifth stage, which only occurred for Ze-CAE and Ze-GATE, occurred around 450 to 500 °C due to carbonisation of polymeric materials and ash formation with 3.91 to 4.96% of weight loss (Torres-Giner and Lagaron, 2010; Varol and Mutlu, 2023).



**Figure 4.27** TGA/DTG curves of (a) Ze-CAE showing five-stage decomposition process with maximum decomposition rate temperature at 308.17 °C, (b) Ze-GATE showing five-stage decomposition process with maximum decomposition rate temperature at 319 °C, and (c) Ze-GGE showing four-stage decomposition process with maximum decomposition rate temperature at 305.17 °C.

A residue of 22.35%, 21.64%, and 19.83% was observed at 600 °C for Ze-CAE, Ze-GATE, and Ze-GGE, respectively. Compared to Neat zein, Ze-CAE and Ze-GATE had a higher amount of residue, while Ze-GGE had a comparable amount of residue. In addition, the DTG data demonstrate that the incorporation of CAE led to a decrease in the thermal decomposition rate of Ze-CAE compared to Neat zein, from 318.33 to 308.17 °C (↓10.16 °C). The peak decomposition rate temperature for Ze-GATE was recorded at 319 °C, which is an almost similar temperature to Neat zein. The maximum decomposition rate temperature for Ze-GGE was recorded at 305.17 °C, which was lower than Neat zein (↓13.16 °C). The DTG curve in Figure 4.27(c) also shows that Ze-GGE exhibits the sharpest DTG curve, indicating that Ze-GGE had the highest thermal decomposition rate compared to other films. Based on the findings, it can be suggested that the addition of CAE and GGE decreased the thermal stability of Ze-CAE and Ze-GGE film, respectively. This effect is likely due to the addition of these extracts, which reduced the protein-protein bonds in the film matrix. In other words, the presence of bioactive compounds such as phenolics in CAE and GGE lowers the thermal stability of the overall film by interacting with zein, thereby reducing protein-protein interactions (Altan et al., 2018). In contrast, the addition of GATE did not influence the maximum decomposition rate temperature of Ze-GATE film. Other studies reported the decomposition rate temperature of zein-based films with the addition of other bioactive compounds or polymer blends. The peak decomposition rate temperatures were reported to be 329 °C, 330 °C, and 326 °C for carvacrol-loaded zein fibres at 5%, 10%, and 20% carvacrol concentration (Altan et al., 2018). Other research also reported higher thermal stability for zein-cellulose acetate blend nanofibres compared to the pure zein nanofibres (Ali et al., 2014). These findings imply that the maximum rate of decomposition temperature and residue depend on the organic and inorganic compounds present in samples, resulting in distinctive thermal decomposition curves.

In brief, the thermal analysis of zein-based films revealed that incorporating various plant extracts significantly influenced their thermal behaviour. The zein-based films displayed either four or five decomposition stages, indicating similar or more complex degradation pathways influenced by the presence of bioactive compounds such as phenolics, organic acids, fatty acids, and terpenoids. Ze-CAE showed reduced thermal stability and more decomposition stages, suggesting a more complex degradation profile. Ze-GATE exhibited a maximum decomposition rate temperature comparable to that of Neat zein, but with a higher number of decomposition stages, indicating better thermal resistance. Ze-GGE demonstrated a similar number of decomposition stages to Neat zein, but it displayed the lowest thermal stability, indicating a significant interaction between

GGE and the zein matrix. From this study, all zein-based films exhibited lower or similar thermal stability compared to Neat zein, and Ze-GATE appeared to be the most thermally stable among the zein-based films, while Ze-CAE and Ze-GGE demonstrated higher interaction between plant extract and the zein matrix, altering their thermal behaviour.




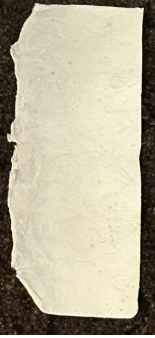


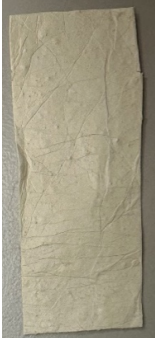





### 4.3.9 Biodegradation study

Biodegradation refers to the breakdown of macromolecular components into smaller fragments through the activity of microorganisms. In general, the initial step of polymer biodegradation includes the depolymerisation or chain cleavage of polymer materials, which converts polymer chains into lower molecular weight oligomeric fragments through the activity of bacteria, fungi, and algae. These fragments are subsequently converted into biomass, minerals, water, and gases such as CO<sub>2</sub> and methane (CH<sub>4</sub>) (Robertson, G., 2013c). This process causes weight loss in the polymer matrix, which is evaluated by measuring the sample's weight throughout degradation study (Azevedo and Reis, 2005).

In the present study, a soil burial test was performed, in which film samples were buried in soil for a total of 12 days, with the initial films' weight varying from 10 to 63 mg (20 x 50 mm). The films were recovered at 6-day intervals, dried, and weighed, and the rate of weight loss was measured. A control film was kept inside a box without the soil. It is important to acknowledge that the weight loss data obtained from the soil burial test serve only as an indicator of biodegradability and do not constitute the sole evidence of the material's biodegradability. The weight loss indicates the initial phase of microbial activity, as it converting the polymer to smaller molecular weight fragments (Mohee et al., 2008). The soil burial approach was chosen, due to its simplicity and cost-effectiveness as well as its ability to simulate natural environmental conditions (Zafar et al., 2013; Oprea, 2015; Badia et al., 2017; Tai et al., 2019). Furthermore, time constraints for this project favours the selection of soil burial test method, as standard ASTM D5988 and International Organization for Standardization (ISO) 17556 methodologies require a longer study duration. According to standard protocols, biodegradation test is performed by measuring the rate of CO<sub>2</sub> evolution or oxygen consumption, generally conducted between 6 to 12 months (ASTM, 2012; ISO, 2019).

Although the initial aim was to quantify the weight loss after the film was buried in soil, this method somehow was impractical for zein-based films produced in this present work, due to the difficulty of separating the soil residues that attached to the degraded films without damaging the samples. Therefore, the assessment of the biodegradation behaviour of zein-based films was performed through a visual inspection of their physical appearance using photographs taken every 6 days, for a total of 12 days. The results are demonstrated in Table 4.4, where the film's appearance before and after soil burial was compared.

**Table 4.4** Physical appearance of Neat zein, Ze-CAE, Ze-GATE, and Ze-GGE films before and after soil burial test conducted for 12 days.

Film	Before soil burial	After 6 Days	After 12 Days
Neat zein			
Ze-CAE			
Ze-GATE			
Ze-GGE			

From Table 4.4, it can be observed that at the beginning of the experiment, all films had an intact and uniform rectangular shape which was cut to a size of approximately 20 x 50 mm. After 6 days, all the films showed some degree of degradation, in which they were disintegrated into smaller fragments and lost their original shape, except for Ze-CAE, in which the rectangular shape could still be observed. After 12 days, similar fragments were observed for Neat zein, suggesting no changes in the biodegradation process. In contrast, Ze-CAE showed more progression in the degradation process, where the film degraded into smaller fragments, similar to that of Neat zein. More distinct fragmentation also occurred to Ze-GATE and Ze-GGE, with the smaller films' fragments being difficult to distinguish from soil. Based on the findings, it is imperative to mention that all zein-based films exhibited indicators of rapid biodegradation process, with most of the films substantially degraded after 12 days of burial in soil. In addition, the incorporation of CAE, GATE, and GGE did not significantly affect the biodegradability of zein-based films. As for the control film, there were no changes in the films' weight except for Ze-CAE control, where 3.17% of weight loss was recorded after 12 days (data not shown).

A report on other zein-based film biodegradation studies revealed weight loss of zein films with/without the addition of liquorice (*Glycyrrhiza glabra* L.) essential oils at almost half of the original weight, reported around 45 to 60% only after 10 days of burial in soil. The film produced in this study was prepared via film casting with the addition of glycerol as a plasticiser (Luis et al., 2019). In addition, Wei et al. (2019) found increasing the zein concentration from 10 to 25% resulted in the enhanced biodegradability (over 26 and 53% of weight loss) of poly(butylene adipate-terephthalate) (PBAT)/ zein blend materials, compared to pure PBAT film. They followed a comparable soil burial test method with a longer study duration of 30 days, and the film was produced via compression moulding (Wei et al., 2019). The most recent study from Pleva et al. (2025), who assessed the biodegradability of zein/polyethylene glycol (PEG) nanofibres via an aerobic composting test, discovered that all zein-based nanofibres were fully mineralised after 29 days. These results suggest that zein films have a higher biodegradation rate, which is supported by current and past research using different biodegradation test procedures, such as soil burial and aerobic composting biodegradation methods. The extent of biodegradation may be related to the composition of material used. The usage of zein, which is high in protein, offers an excellent carbon source for microbial growth and serves as a substrate for enzymatic hydrolysis throughout the biodegradation process (Mikkelsen, 1994; Imam and Gordon, 2002).

In summary, Ze-CAE, Ze-GATE, and Ze-GGE films demonstrated indicators of a rapid biodegradation process, with significant degradation observed after 12 days of soil burial. Furthermore, the addition of CAE, GATE, and GGE into zein films did not influence the biodegradability of zein-based films. Thus, this study highlights the potential of zein-based films, specifically Ze-CAE, Ze-GATE, and Ze-GGE, as biodegradable packaging films. Further research, however, is recommended to further assess the biodegradation of zein-based films, particularly the biodegradation of zein-based films under composting environments.

## 4.4 Conclusion

Novel biodegradable films with 30% zein incorporated with 5% (w/w) active extracts of CAE, GATE, and GGE were prepared by electrospinning. A Neat zein film was produced via similar protocols. The films appeared as light cream-coloured, opaque, smooth and thin films, with the Ze-GATE and Ze-GGE films had an additional granular-like appearance on the surfaces. The electrospun films of Ze-CAE and Ze-GGE demonstrated cross-linking of active compounds with zein fibres, evident from the examination of surface morphologies of SEM micrographs. However, no cross-linking was observed in the Ze-GATE film. The addition of the plant extracts did not significantly influence the fibre diameter and film thickness, except for Ze-GGE film. All zein-based films demonstrated high encapsulation efficiency, exceeding 90%, with Ze-GGE exhibiting the significantly higher encapsulation efficiency, rendering the suitability of all films in the application as active packaging film. The structural analysis of the FTIR spectra of Ze-CAE, Ze-GATE, and Ze-GGE films indicated that the addition of plant extracts into zein fibres did not result in the emergence of new peaks, suggesting successful encapsulation of the extracts within the zein fibres without significantly altering their structural integrity. The data from FTIR spectra also highlighted the formation of hydrogen bonds between zein and the plant extracts, with most bands shifting to lower frequencies in the Ze-CAE and Ze-GGE films, and some bands showing similar shifts to lower frequencies in the Ze-GATE film. The zein-based films showed a hydrophilic surface characteristic via water contact angle investigation. Addition of CAE, GATE, and GGE to the zein-based films showed similar or reduced thermal properties, with the control film of Neat zein having the maximum decomposition rate at 318.33 °C, with 4 stages of decomposition process. Ze-GATE appeared to be the most thermally stable among the zein-based films, while Ze-CAE and Ze-GGE demonstrated higher interaction between plant extract and the zein matrix, altering their thermal behaviour. All zein-based films exhibited a high degree of biodegradability indicator, as shown by the visual inspection of films. It can be concluded that the developed zein-based films encapsulated with active extract from CAE, GATE, and GGE could be used as sustainable and biodegradable packaging to enhance the shelf life of food, albeit some aspect of improvement on its properties such as films morphology and hydrophobicity would be required depending on the type of foods.

## **Chapter 5**

### **Storage Study of Zein-Based Films on Beef**

#### **5.1 Introduction**

As zein-based films of Ze-CAE, Ze-GATE, and Ze-GGE, along with Neat zein were successfully produced, characterised, and assessed for their properties as previously detailed in Chapter 4, further evaluation of their functionality as active packaging materials is crucial to determine their effectiveness to reduce the growth of foodborne pathogens and spoilage microorganisms on foods. In this study, beef was selected as the sample to determine the effectiveness of the packaging films, particularly due to its perishable nature and high nutritional value. Beef is recognised as a rich source of essential nutrients, including proteins and micronutrients such as vitamins B6 and B12, zinc, magnesium, selenium, and iron (Williams, 2007). Although the results in Section 4.3.6 showed that these films possess hydrophilic surface properties, which are undesirable for wrapping highly perishable foods, particularly beef, they were still selected for this study. This is because beef serves as an ideal food sample to assess the effectiveness of these films due to its short shelf-life, likely due to microbial growth. Therefore, the effectiveness of these films on beef would imply greater effectiveness against other food products.

In general, consumers' preferences and purchasing decisions for food products are heavily influenced by the visual appearance of both the food itself and its packaging (Gidlof et al., 2017). In terms of packaging aesthetics, transparency plays a significant role in the decision-making process. Transparent packaging elements are associated with greater consumer trust and stronger purchase intentions (Billeter et al., 2012). This is because consumers can use intrinsic visual cues such as for meat, the colour, fat content, marbling, and drip loss to assess the freshness and quality of the product, aligning these observations with their quality expectations (Bredahl et al., 1998; Verbeke et al., 2005; Banovic et al., 2009). With regards to food products, certain items are only perceived as acceptable if they fall within a specific colour range (Schwartz et al., 2007, cited in Robertson, G., 2013d, p.296). For instance, in the case of red meat, a red-purple colour is typically associated with freshness and high quality, whereas a brownish colour is commonly perceived as a sign of lower quality (Faustman and Cassens, 1990; Issanchou, 1996; Carpenter et al., 2001).

When discussing meat, it is generally categorised into two types: red meat and white meat. In brief, the red colour observed on the surface of meat is primarily due to a pigment called myoglobin, which accounts for more than 90% of the total pigment content in the muscle tissue of red meat animals (Warriss and Rhodes, 1977). In the absence of oxygen ( $O_2$ ), myoglobin exists in the form of deoxymyoglobin (Mb), which imparts a dull, purplish hue to the meat. When exposed to  $O_2$ , myoglobin is converted into oxymyoglobin ( $O_2$ Mb), resulting in a bright red colour that typically appears when the muscle is freshly cut and exposed to air, an appearance generally preferred by consumers (Giddings, 1977, cited in Gill and Gill, 2009, p. 260). However, when meat is exposed to air for an extended period or when the oxygen concentration drops to between 0.5% and 1.0%, myoglobin is oxidised to metmyoglobin (MetMb), which gives the meat a brownish colour (Robertson, G., 2013e). The various forms of myoglobin and their associated colours are interconvertible and reversible, depending on the partial pressure of oxygen and the oxidation state of the iron atom within the myoglobin molecule (Giddings, 1977, Wallace et al., 1982, cited in Gill and Gill, 2009, p. 260). In addition to the chemical and physical state of myoglobin, the colour of meat is also affected by microbial activity (Robertson, G., 2013e). Aerobic bacteria in the logarithmic growth phase have a high  $O_2$  demand, which reduces the  $O_2$  tension on the meat surface. This also leads to the formation of metmyoglobin (MetMb) (Robertson, G., 2013e). Typically, the surface of meat hosts facultative anaerobes, obligate anaerobes, and microaerophilic bacteria, including *Aeromonas hydrophila*, *Campylobacter* spp., *C. botulinum*, verotoxigenic *E. coli*, *Salmonella*, and *L. monocytogenes* (Gill and Gill, 2009). Among these, *Pseudomonas* and *Lactobacillus* are predominant in meat stored at chilled temperatures. These bacteria are classified as psychrotrophs, meaning they thrive at low temperatures, with optimal growth below 15 °C (Robertson, G., 2013d; Robertson, G., 2013e). Although fungi (e.g., *Candida* spp., *Cryptococcus* spp., and *Rhodotorula* spp.) can also be found in meat, bacteria generally grow faster. As a result, when conditions are favourable for both groups, bacteria usually outcompete fungi (Dillon and Board, 1991; Robertson, G., 2013d).

Food packaging is therefore essential to maintain the safety and quality of meat. At present, the commonly used films for meat wrapping are PVC and modified atmosphere packaging (MAP). PVC is a transparent and inert plastic that is highly permeable to oxygen and moisture and functions to maintain the red colour of meat (Lavieri and Williams, 2014). In contrast, MAP provides modifications of atmospheric gas concentrations using different proportions of  $O_2$ ,  $CO_2$ , and nitrogen. This method effectively preserves the bright red colour of fresh meat and minimises microbial spoilage (Slavica et al., 2010). In summary, food

packaging plays a crucial role in maintaining meat quality, as it influences attributes such as colour, flavour, texture, appearance, and safety. While the use of both PVC and MAP as film wrapping for meat are effective, however, it also raises concerns regarding the reliance to the plastic materials, suggesting the need of sustainable alternatives. As discussed in Section 4.3.2, the newly developed films of Neat Zein, Ze-CAE, Ze-GATE, and Ze-GGE have limitations in packaging aesthetics. These films lack transparency, and their appearance is dominated by the natural yellow colour of zein. Figure 5.1 shows a representative photo of beef wrapped with commercial film (transparent) compared to Ze-CAE film (opaque) at the beginning of the storage period (day 0). Even though it is generally mentioned in the earlier part of the introduction, where the transparent element plays an important role in the decision-making process, several studies reported mixed responses to the acceptance of the non-transparent packaging materials. Both the study by Sabo et al. (2017) and Simmonds et al. (2018) reported on the people's preference for transparent packaging, while Taylor et al. (2024) reported contradictory findings where the participants were willing to spend more to purchase sustainable alternatives regardless of their appearance. Based on these findings, people's acceptance of the transparency of packaging materials varied and has been changing over the years. Therefore, even though the transparency element could not be achieved in this current research, it is still important to determine the safety and quality parameters, such as microbiological activity, water activity ( $a_w$ ), and colour, and compare the findings with those of a commercially available film.



**Figure 5.1** Representative photo of beef (left) wrapped with commercial film and (right) zein-based films on day 0 of storage.

Films produced from biobased and biodegradable polymer films, with the incorporation of active plant extracts might preserve the quality and safety for beef, as well as offering greener alternative compared to plastic film (Ahmed et al., 2017). Therefore, this chapter focuses on evaluating the quality and safety of beef stored at 4 °C over a five-day period using newly developed biobased and biodegradable zein-based films. For this study, beef samples were prepared by cutting them into portions weighing  $5.0 \pm 1.0$  g, with approximate surface dimensions of 2.3 x 2.3 cm. Three key parameters for beef were evaluated: microbiological activity,  $a_w$ , and colour. The study duration was set at 5 days, aligning with the USDA-FSIS recommendation for storing chilled (4 °C) steak meat, which is typically between 3 to 5 days. Hence, the maximum storage duration of 5 days was selected for this experiment (USDA-FSIS, 2024). To the best of the author's knowledge, this is the first study to assess beef quality using electrospun zein-based films added with plant extracts from *Colubrina asiatica*, *Garcinia atroviridis*, and *Gnetum gnemon*.

## 5.2 Aim of the chapter

The aim of the work presented in this chapter was to evaluate the quality and safety attributes of beef wrapped with zein-based films incorporated with active antimicrobial plant extracts (Neat zein, Ze-CAE, Ze-GATE, and Ze-GGE) stored under chilled conditions at 4 °C. This evaluation involved the assessment of microbiological activity in term of total plate count, water activity ( $a_w$ ), and colour of beef after stored with Neat zein, Ze-CAE, Ze-GATE, and Ze-GGE films. For comparison purposes, the same tests were also conducted on beef samples wrapped using commercial packaging film (Buffalo cling film, China), in order to benchmark the performance of the newly developed zein-based films against an existing commercial alternative, with the aim of providing a more environmentally friendly option for beef wrapping.

### 5.3 Results and Discussion

The investigation of quality and safety attributes of beef in terms of microbiological activity,  $a_w$ , and colour analysis was conducted in accordance with the literature by Rotronic (2011), Rollini et al. (2016) and Arezoo et al. (2020). Shortly after purchasing, all beef samples were cut to a weight of  $5.0 \pm 1.0$  g and a size of approximately  $2.3 \times 2.3$  cm in surface dimensions. For microbiological activity analysis, 6 pieces of cut beef samples were placed on a food tray and wrapped with all test films before storage at  $4^\circ\text{C}$  in the Microbiology Laboratory (x2 trays were prepared for duplicate measurement). For microbiological activity, at 24-hour interval, a piece of stored beef was taken out from  $4^\circ\text{C}$  storage, homogenised, and serial dilution was performed. The diluted solution was plated on plate count agar, and the bacteria colonies were counted after a 24-hour of incubation period. The results were expressed as log CFU/g of beef. A similar preparation step was performed for beef samples for measurement of  $a_w$  and colour analyses, with the samples stored at  $4^\circ\text{C}$  in the Food Technology Laboratory. However, the beef samples from the same tray were used to conduct the  $a_w$  and colour tests, with  $a_w$  measured first, followed by colour analysis. A whole piece of beef was placed in the  $a_w$  device, and the result was recorded at the end of measurement. Subsequently, a colorimeter was used to measure beef colour once per sample at each time point, with the measurement location selected randomly.

Overall, the results presented in this chapter exhibited some fluctuations, with large error bars observed in several tests, especially for the colour analysis. Several factors may explain these observations. Firstly, the same beef sample was used for both  $a_w$  and colour tests due to the scarcity of zein-based film samples. The films were available in limited quantities due to the malfunctioning of the electrospinning at the University of Leeds therefore, the film production was constrained. Furthermore, the availability of plant extracts was also limited. Consequently, the same beef samples had to be used for multiple tests. Considering the above factors also resulted in the use of only two replications of samples for each test in Chapter 5. The low number of sample replications therefore would likely affect the standard deviation values and power of overall statistical analysis.

Another important factor that might influence the findings was the beef sample itself. As the beef was purchased from a local supermarket, the batch of beef also differs every time of purchase. As the test was performed for a duration of approximately one month with the beef purchased on every Monday, the

availability of beef was inconsistent. Some of the tests were using samples from beef rump steak, while the other part of the tests was using samples of beef fillet steak (Figure 5.2a). The different batches of beef samples that varied in extrinsic and intrinsic factors and the heterogeneity of beef parts are therefore expected to affect the findings, especially for the  $a_w$  and colour analyses data. The inherent diversity of the purchased beef samples resulted in the variability of data even on day 0. The statistical analyses were performed on day 0 for all test data (data not shown). Even at the beginning of the storage study (day 0), significant variation was observed for  $a_w$  and yellow/blue ( $b^*$ ) colour values, proving that different beef batches/parts played a role for the diversity of data. Nevertheless, in the context of using different beef batches, which could be one of the determining factors for the observed fluctuations and large error bars, the results still provide a valuable general indication of the films' effectiveness on beef overall. Regardless of the specific beef cuts used, the findings from the use of films on different beef parts can be considered beneficial, as they provide relevant and applicable data on the films' performance across different range of beef samples.

On the other hand, based on Figure 5.2(b), each beef sample was prepared to a weight of  $5.0 \pm 1.0$  g and size of approximately 2.3 x 2.3 cm in surface dimensions, although the thickness varied between samples. Therefore, even though the best effort was made to ensure uniformity of size, it was quite challenging to obtain precise similarity in the sample sizes of beef. In addition, the experimental design, which involved storing the beef in the same tray throughout the study period (five days) and repeatedly opening and closing the packaging film, is also believed to have influenced the results. Given these constraints, the findings presented in this chapter should be interpreted with caution, considering the aforementioned factors that likely affect the results.



**Figure 5.2** (a) Different beef samples utilised; British beef rump steak and British beef fillet steak, (b) the beef was cut to  $5.0 \pm 1.0$  g, approximately 2.3 x 2.3 cm in surface dimensions.

### 5.3.1 Microbiological activity analysis

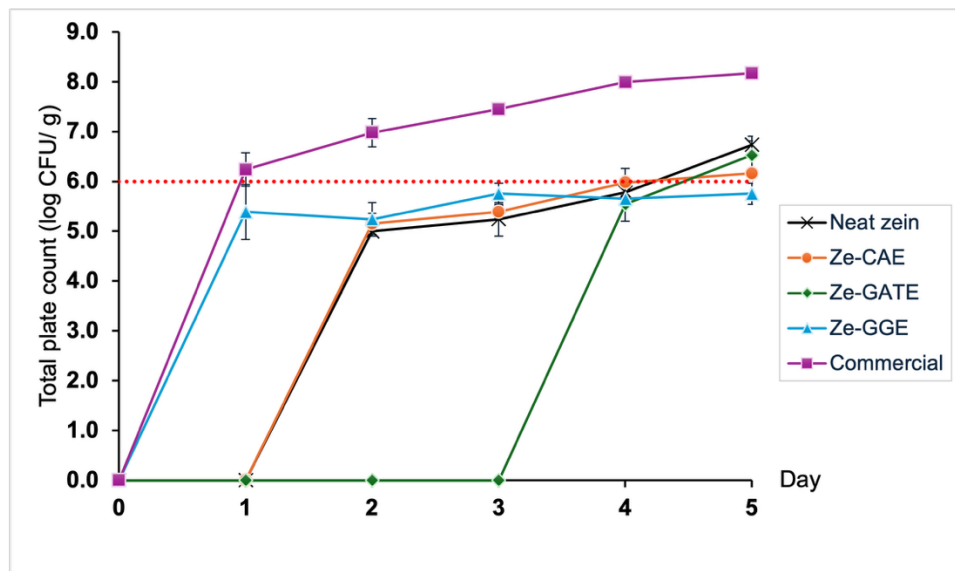
Red meat is highly susceptible to spoilage due to its rich protein content, optimum pH, and high water activity ( $a_w$ ), which create an ideal environment for microbial growth. This microbial proliferation leads to deteriorative reactions that compromise meat quality and safety (Dillon and Board, 1991; Robertson, G., 2013d). Therefore, preventing microbial growth is essential to minimise spoilage and extend shelf life. In this study, the effect of an extrinsic factor was investigated by employing various newly developed zein-based films to wrap beef samples. A similar test was performed on the commercial wrapping film purchased from a supermarket and the results were compared. The total bacterial counts on raw beef wrapped with zein-based films and commercial film were monitored over five days of storage at 4 °C, with results presented in Table 5.1 and Figure 5.3. Statistical analysis of an applied general linear model and multiple pairwise comparisons indicated that both the different types of films and storage days

significantly influenced the total bacterial counts on beef samples ( $p < 0.05$ ). The red dotted line in Figure 5.3 represents the microbial safety threshold for chilled beef, set at log 6.0 CFU/g. A bacterial count reaching log 7.0 CFU/g is considered indicative of spoilage and renders the product unsafe for consumption (Foods, 1986).

**Table 5.1** Bacterial growth observed on beef wrapped with different packaging films of Neat zein, Ze-CAE, Ze-GATE, Ze-GGE and commercial films.

Storage at 4 °C (Day)	Total plate count (log CFU/g)				
	Neat zein	Ze-CAE	Ze-GATE	Ze-GGE	Commercial
0	0.0± 0.0 <sup>j</sup>	0.0± 0.0 <sup>j</sup>	0.0± 0.0 <sup>j</sup>	0.0± 0.0 <sup>j</sup>	0.0± 0.0 <sup>j</sup>
1	0.0± 0.0 <sup>j</sup>	0.0± 0.0 <sup>j</sup>	0.0± 0.0 <sup>j</sup>	5.4± 0.6 <sup>ghi</sup>	6.2± 0.3 <sup>cdef</sup>
2	5.0± 0.0 <sup>i</sup>	5.2± 0.2 <sup>hi</sup>	0.0± 0.0 <sup>j</sup>	5.2± 0.3 <sup>hi</sup>	7.0± 0.3 <sup>bc</sup>
3	5.2± 0.3 <sup>hi</sup>	5.4± 0.1 <sup>ghi</sup>	0.0± 0.0 <sup>j</sup>	5.8± 0.2 <sup>efghi</sup>	7.4± 0.1 <sup>ab</sup>
4	5.8± 0.2 <sup>efghi</sup>	6.0± 0.3 <sup>defgh</sup>	5.5± 0.3 <sup>fghi</sup>	5.7± 0.1 <sup>fghi</sup>	8.0± 0.1 <sup>a</sup>
5	6.7± 0.2 <sup>bcd</sup>	6.2± 0.0 <sup>cdefg</sup>	6.5± 0.3 <sup>cde</sup>	5.8± 0.2 <sup>efghi</sup>	8.2± 0.0 <sup>a</sup>

Bacterial growth (mean ± SD, n = 2). Different superscript letters (a-j) indicate significant differences among means across both rows and columns (Tukey's pairwise comparisons,  $p < 0.05$ ).



**Figure 5.3** Bacterial growth observed on beef wrapped with different packaging films of Neat zein, Ze-CAE, Ze-GATE, Ze-GGE and commercial films during five days of storage at 4 °C. The red dotted line represents the microbial safety threshold for chilled beef, set at log 6.0 CFU/g.

Based on Table 5.1 and Figure 5.3, on day 0, no bacterial colonies were detected on any beef samples, regardless of film types. However, from day 1 onwards, bacterial growth was observed in samples wrapped with the commercial film, with the total colony count increasing progressively over the storage period. On day 1, bacterial growth was absent in beef samples wrapped with Neat zein, Ze-CAE, and Ze-GATE films, while minimal growth was detected on Ze-GGE-wrapped beef ( $\log 5.4 \pm 0.6$  CFU/g). From days 2 to 3, there were no statistically significant differences in bacterial counts among Neat zein, Ze-CAE, and Ze-GGE films ( $p > 0.05$ ). Notably, the Ze-GATE film effectively inhibited bacterial growth until day 3. By day 4, bacterial loads among all zein-based films showed no significant differences ( $p > 0.05$ ). On the final storage day, the commercial film exhibited the highest bacterial load, reaching  $\log 8.2 \pm 0.0$  CFU/g, significantly higher than the counts observed for all zein-based films ( $p < 0.05$ ). The total counts for Neat zein, Ze-CAE, Ze-GATE, and Ze-GGE on day 5 were  $\log 6.7 \pm 0.2$  CFU/g,  $\log 6.2 \pm 0.0$  CFU/g,  $\log 6.5 \pm 0.3$  CFU/g, and  $\log 5.8 \pm 0.2$  CFU/g, respectively.

The findings of this study demonstrated that zein-based films were more effective at inhibiting bacterial growth on chilled beef compared to existing commercial film options. Bacterial counts on beef wrapped in commercial film increased progressively during storage, exceeding the microbial safety limit of  $\log 6.0$  CFU/g only after one day of storage and reaching  $\log 8.2$  CFU/g by day 5. These results indicated that commercial packaging was insufficient for maintaining microbial safety during extended chilled storage. In contrast, all zein-based films maintained bacterial levels below the safety limit up to four days storage period.

Among the zein-based films, Ze-GATE showed the strongest antibacterial performance during the early storage period, completely inhibiting bacterial growth until day 3. This suggests the presence of potent antimicrobial compounds in the plant extract used for Ze-GATE, such as organic acids (Mackeen et al., 2000; Tan et al., 2013; Lim et al., 2020). The findings from the investigation of antimicrobial activity in Chapter 3 also highlighted that GATE exhibited the highest antibacterial activity when subjected to the minimum inhibitory concentration (MIC) and minimum bactericidal concentration (MBC) tests, which supports the performance observed for the Ze-GATE film in this section. However, its bacterial count increased by day 5, indicating that its effectiveness may decrease over time, and it is recommended to use this film only up to three storage days.

Ze-GGE was the only zein-based film to show bacterial growth on day 1 ( $\log 5.4 \pm 0.6$  CFU/g), but by day 5, it had a significantly lower bacterial count ( $\log 5.8 \pm 0.2$  CFU/g) compared to Neat zein ( $\log 6.7 \pm 0.2$  CFU/g) and commercial film ( $\log 8.2 \pm 0.0$  CFU/g) ( $p < 0.05$ ). This observation suggests that the Ze-GGE film may exhibit a delayed or sustained antimicrobial effect. Previous studies have demonstrated that zein-based films are capable of controlled release of active compounds, with the release kinetics influenced by the presence of specific functional groups such as phenolics, flavonoids, and the overall hydrophobicity of the incorporated compounds (Ouattara et al., 2000; Ozdemir and Floros, 2003; Arcan and Yemenicioglu, 2011; Arcan and Yemenicioglu, 2013). Notably, *G. gnemon* leaves are known to be rich in hydrophobic bioactive constituents, including phytol, oleic acid, 2,3-dihydroxypropyl icosanoate, and cis,cis,cis-7,10,13-hexadecatrienal. It is therefore plausible that the hydrophobic nature of these compounds contributes to a slower release profile, thereby accounting for the delayed or sustained antimicrobial activity observed in the Ze-GGE film (Dutta et al., 2018; Trisha et al., 2024). It could be proposed that the observed lower antimicrobial activity shown in Chapter 3 for GGE is due to this delayed or sustained antimicrobial activity, as the antimicrobial tests in Chapter 3 were limited to a 24-hour (bacteria)/ 48-hour (fungi) period, whereas the current storage study assessed the bacterial growth over a five-day duration.

Neat zein, which did not contain any added plant extract, still demonstrated antimicrobial activity. This suggests that zein may possess inherent antibacterial properties. However, as Neat zein was not tested in earlier antimicrobial screenings (Chapter 3), direct comparisons are not possible, and further research is needed to evaluate its standalone antibacterial efficacy and potential functional groups responsible for microbial inhibition. Overall, zein-based films containing

plant extracts (Ze-CAE, Ze-GATE, and Ze-GGE) were more effective than commercial film in controlling bacterial growth. These results support the potential of zein-based films as active packaging materials to improve the microbiological safety and extend the shelf life of chilled beef. The effectiveness of each film appears to depend on the specific extract used and its antimicrobial properties, which was consistent with the findings of antimicrobial activities demonstrated for CAE, GATE, and GGE against five foodborne pathogens, as discussed in Chapter 3.

The findings of the antimicrobial effects of plant extract-based films from this study, particularly those incorporating *G. atroviridis* are in agreement with the previous studies, where the films successfully reduced microbial loads in perishable food products. For example, Sivanasvaran et al. (2021) investigated the microbiological quality of chicken meat wrapped in a chitosan film containing 5% (v/v) *G. atroviridis* extract and stored at 4 °C for 15 days. The results showed a significant reduction in total colony counts, with the treated sample exhibiting log 6.10 CFU/g compared to log 8.17 CFU/g in the control. Similarly, Zaman et al. (2018), reported that wrapping Indian mackerel in a chitosan-*G. atroviridis* film extended its shelf life by approximately 3.5 days compared to unwrapped samples under refrigerated storage (4 °C) over a 6-day period. Although storage studies using film applications for *C. asiatica* and *G. gnemon* are limited, several investigations have confirmed their antimicrobial properties. Raunsai et al. (2021) reported that the minimum inhibitory concentration (MIC) of *C. asiatica* leaf extract exceeded 512 µg/mL against both *S. aureus* and *E. coli*. Additionally, Desai et al. (2015) observed antimicrobial activity of *C. asiatica* extract against *E. coli*, *S. aureus*, and *Streptococcus pneumoniae*, with inhibition zones of 8 mm, 9 mm, and 10 mm, respectively. The preservative potential of *G. gnemon* was demonstrated in a study by Kato, E. et al. (2009), in which powdered *G. gnemon* extract was incorporated into potato salad stored at 20 °C for three days. The bacterial cells were significantly reduced, with bacterial counts decreasing from  $2.0 \times 10^5$  in the control to  $7.9 \times 10^3$  in the sample treated with 0.2% extract.

In summary, both types of films and storage days influenced the growth of bacteria on beef samples. Zein-based films were more effective at controlling the bacterial growth on the stored beef samples compared to commercial film. Among the zein-based films, Ze-GATE showed the strongest inhibition of bacterial growth up to the first three days of storage. In addition, Ze-GGE consistently exhibited lower bacterial growth over a five-day period (below log 6.0 CFU/g), with significantly reduced bacteria growth than Neat zein and commercial film on day 5, suggesting its potential for extending beef storage life. It is important to

mention that this study solely focused on bacterial growth, further investigation into fungal growth could provide valuable insights into other spoilage microorganisms in beef.

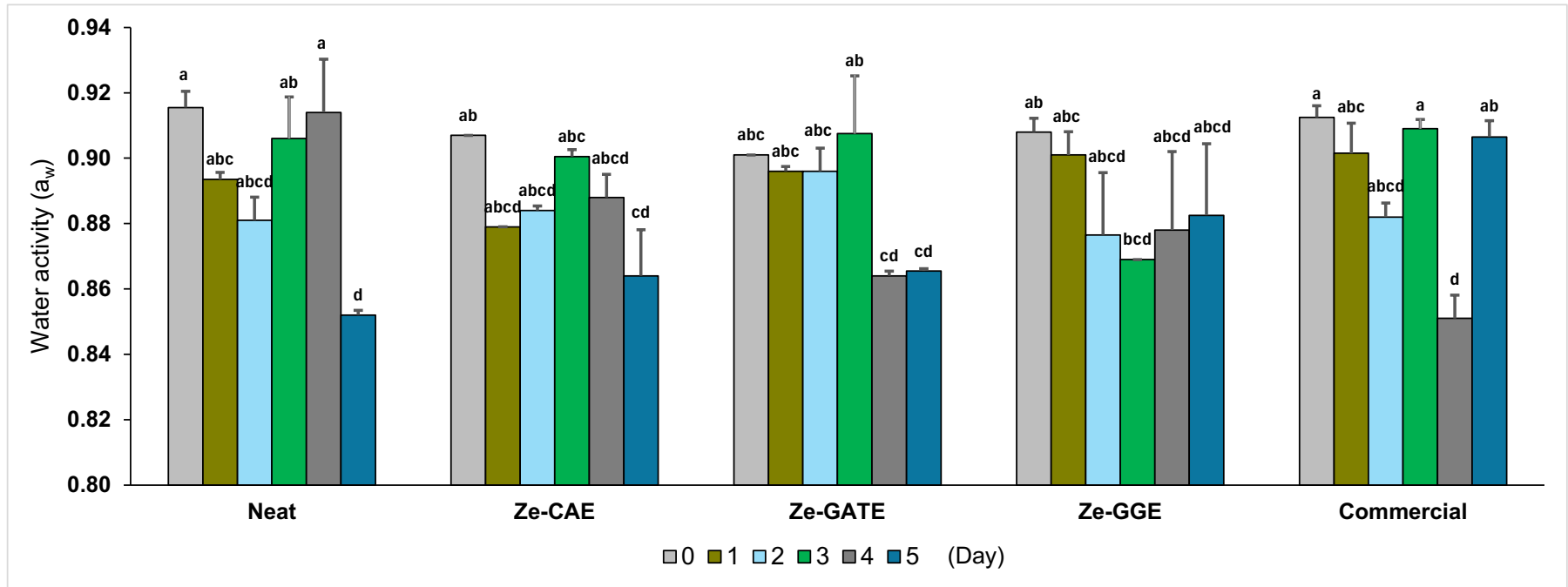
### 5.3.2 Water activity ( $a_w$ )

Water activity ( $a_w$ ) is a key intrinsic property of food that influences its stability, safety, and quality. It plays a critical role in the occurrence of deteriorative reactions in foods, such as microbial growth, alteration in enzymatic activity, and chemical changes including lipid oxidation and Maillard browning (Labuza et al., 1977; Robertson, G., 2013d). By definition,  $a_w$  is the ratio of the water vapour pressure of a substance to the vapour pressure of pure water at the same temperature (Labuza et al., 1977). Certain microorganisms, such as bacteria, yeasts, and moulds, have minimum  $a_w$  levels below which they are unable to grow. Most bacteria need a higher  $a_w$  than moulds or yeasts (Robertson, G., 2013d). On the other hand, preserving the  $a_w$  of food relates to the quality attribute of foods, therefore, it is essential to study the  $a_w$  to further understand its role in food preservation, packaging, and formulation. In this study, the  $a_w$  of beef samples wrapped with commercial and zein-based films during five days of storage at 4 °C was measured, and the data is presented in Table 5.2 and Figure 5.4. Statistical analysis of the applied general linear model showed that only storage duration influences the  $a_w$  of the beef samples ( $p < 0.05$ ). However, subsequent investigation of multiple pairwise comparisons found there was a significant influence of different packaging films versus storage time on the  $a_w$  values observed on certain storage day and packaging film ( $p < 0.05$ ).

**Table 5.2** Water activity of beef wrapped with different packaging films of Neat zein, Ze-CAE, Ze-GATE, Ze-GGE and commercial films.

Storage at 4 °C (Day)	Water activity ( $a_w$ )				
	Neat zein	Ze-CAE	Ze-GATE	Ze-GGE	Commercial
0	0.916± 0.005 <sup>a</sup>	0.907± 0.000 <sup>ab</sup>	0.901± 0.000 <sup>abc</sup>	0.908± 0.004 <sup>ab</sup>	0.913± 0.004 <sup>a</sup>
1	0.894± 0.002 <sup>abc</sup>	0.879± 0.000 <sup>abcd</sup>	0.896± 0.001 <sup>abc</sup>	0.901± 0.007 <sup>abc</sup>	0.902± 0.009 <sup>abc</sup>
2	0.881± 0.007 <sup>abcd</sup>	0.884± 0.001 <sup>abcd</sup>	0.896± 0.007 <sup>abc</sup>	0.877± 0.019 <sup>abcd</sup>	0.882± 0.004 <sup>abcd</sup>
3	0.906± 0.013 <sup>ab</sup>	0.901± 0.002 <sup>abc</sup>	0.908± 0.018 <sup>ab</sup>	0.869± 0.000 <sup>bcd</sup>	0.909± 0.003 <sup>a</sup>
4	0.914± 0.016 <sup>a</sup>	0.888± 0.007 <sup>abcd</sup>	0.864± 0.001 <sup>cd</sup>	0.878± 0.024 <sup>abcd</sup>	0.851± 0.007 <sup>d</sup>
5	0.852± 0.001 <sup>d</sup>	0.864± 0.014 <sup>cd</sup>	0.866± 0.001 <sup>cd</sup>	0.883± 0.022 <sup>abcd</sup>	0.907± 0.005 <sup>ab</sup>

Water activity ( $a_w$ ) (mean ± SD, n = 2). Different superscript letters (a-d) indicate significant differences among means across both rows and columns (Tukey's pairwise comparisons,  $p < 0.05$ ).



**Figure 5.4** Water activity of beef wrapped with different packaging films of Neat zein, Ze-CAE, Ze-GATE, Ze-GGE and commercial films during five days of storage.

Data represent means of  $n = 2$ , (mean  $\pm$  SD,  $n = 2$ ). Different superscript letters indicate significant differences among means across both days and type of films (Tukey's pairwise comparisons,  $p < 0.05$ ). The different bar colours represent the different storage day; light grey- Day 0, olive green- Day 1, blue- Day 2, green- Day 3, dark grey- Day 4, dark blue- Day 5.

Based on Table 5.2 and Figure 5.4, the  $a_w$  of beef using Neat zein, Ze-CAE, Ze-GATE, Ze-GGE, and commercial film showed high values and remained relatively stable during the first two days, with no significant differences observed among samples ( $p > 0.05$ ). On day 3, a noticeable decrease in  $a_w$  was observed for beef wrapped with Ze-GGE ( $0.869 \pm 0.000$ ) compared to the commercial film ( $0.909 \pm 0.003$ ) ( $p < 0.05$ ), however, this difference was not significant when compared to Ze-GGE on day 0 ( $p > 0.05$ ). On the next storage day (day 4), more pronounced differences were observed where the  $a_w$  of beef wrapped with two other films, Ze-GATE ( $0.864 \pm 0.001$ ) and commercial film ( $0.851 \pm 0.007$ ) had significantly decreased in  $a_w$  compared to their respective values on day 0 ( $p < 0.05$ ). On the final day of storage, only the beef wrapped with Ze-GATE ( $0.866 \pm 0.001$ ), Ze-GGE ( $0.883 \pm 0.022$ ), and commercial film ( $0.907 \pm 0.005$ ) maintained  $a_w$  values similar to those recorded on day 0 ( $p > 0.05$ ). The findings from this study showed the  $a_w$  values of beef samples measured at above 0.850 throughout the study duration with slight decreases observed over time. The Neat zein and zein-based films, particularly Ze-CAE showed significantly reduced  $a_w$ . This observation is considered a normal occurrence when utilising packaging materials that are derived from biodegradable packaging materials such as zein, as the produced film has high water vapour permeability owing to the hydrophilic nature of film, and the prolonged exposure to moisture will further increase the water vapour permeability of the film (Parris et al., 1997; Chen, C. et al., 2020).

In brief, the  $a_w$  for all beef samples suggests that during the first two days, all the packaging films were effective in retaining the  $a_w$  of all beef samples. This indicates that the beef maintained its quality from the day of purchase. The significant decline in  $a_w$  observed in Neat zein and Ze-CAE on the last storage day, indicated lower  $a_w$  of beef on day 5 compared to day 0. The decline in the  $a_w$  of beef wrapped with Neat zein is expected, as previous study have reported higher water vapour permeability of Neat zein film, without the addition of bioactive compounds, thereby allowing greater moisture transfer from food products to the surrounding atmosphere (Escamilla-Garcia et al., 2017). However, the use of Ze-CAE also resulted in a reduction in  $a_w$  on day 5, indicating higher water vapour permeability, which contradicts to the findings obtained by Escamilla-Garcia et al. (2017), who observed that the addition of active constituents such as essential oils significantly decreased the water vapour permeability of the film compared to the control zein film. This discrepancy could be attributed to the different substances incorporated into the film materials and the use of different primary polymers, including a blend of zein and chitosan in their study. The different substances may have different chemical structures and polar groups, as water vapour permeability is dependent on the number of polar

groups the polymer contains (Higushi and Aguiar, 1959, cited in Gontard et al., 1992, p. 194). The author also observed that the previous report employed the film casting method for film preparation, which differs from the method used in this study, which may affect the overall water vapour permeability property. From this study, Ze-GATE and Ze-GGE showed a slight reduction in  $a_w$  of the beef compared to day 0, however they did not significantly influence the  $a_w$  over five days of storage. This indicates the better potential of these two films in preserving the  $a_w$  in wrapped beef samples, as well as maintaining their juiciness, rendering them acceptable to customers. In contrast, commercial film exhibited consistently higher  $a_w$  (except for day 4), demonstrating better retention of juiciness, but speeds up spoilage due to microbial growth. The findings from Section 5.3.1 on the microbiological analysis support the fact that  $a_w$  is responsible for the microbial growth, as the microbial growth data for beef wrapped in commercial film show the highest bacterial growth after five days of storage, compared to beef wrapped in zein-based films of Ze-GATE and Ze-GGE, which show a reduction in microbial growth. These results suggest that the commercial film (absence of active antimicrobial compounds), compared to Ze-GATE and Ze-GGE films, promotes microbial growth by allowing microorganisms to utilise unbound, free water present in the beef to carry out enzymatic reactions, synthesise cellular materials, and participate in other biochemical processes (Lulietto et al., 2015). This observation also aligns with the concept of hurdle technology, where the combination of two or more preservation parameters acts synergistically to control microbial growth (Singh and Shalini, 2016). In the present study, the incorporation of plant extracts into zein-based films, particularly in Ze-GATE and Ze-GGE may provide an additional antimicrobial hurdle that limits microbial proliferation, even when water activity remains relatively favourable for microbial growth. Further investigation into hurdle technology for the preservation of beef would be valuable for future research, and future work are therefore recommended.

While direct comparative data on the  $a_w$  of zein-based films produced in this study with the previous literature is limited, indirect comparison, such as the rate of water loss in food products can be performed. A recent study by Wang, X. et al. (2024) reported that strawberries coated with zein and gum Arabic with the addition of trans-cinnamaldehyde did not result in significant weight loss of strawberries over 7 days of storage at 4 °C. A separate study also reported a significantly lower weight loss percentage of strawberries wrapped with multilayer zein film (between  $6.30\pm 0.54\%$  and  $7.02\pm 0.22\%$ ) compared to the control film ( $8.34\pm 0.74\%$ ) (Moradinezhad et al., 2024). These data are consistent with the present study, which indicates that zein-based films, particularly with the addition

of active extracts such as Ze-GATE and Ze-GGE, have the potential to effectively preserve perishable food products. In summary, different storage days had a greater influence on the  $a_w$  of beef samples compared to the different packaging films. Overall, the trend showed a decrease in  $a_w$  over time when using Neat zein and Ze-CAE and the preservative ability of  $a_w$  when Ze-GATE, Ze-GGE, and commercial films were used. However, several fluctuations in the  $a_w$  values were observed across samples, for instance in commercial film, as the  $a_w$  decreased on day 4 and increased back again on day 5. The possible explanation could be due to the factors discussed earlier in the results and discussion part, such as the effects of low sample size ( $n = 2$ ), different batches of beef with different beef parts, the beef cut into 2.3 x 2.3 cm in surface dimensions, and the opening and closing of the beef packaging every day, which likely influence the results.

### 5.3.3 Colour analysis

Colour is one of the primary factors that influence an individual's decision for the selection of food products. In this study, colour measurements were carried out to determine the variation in the colour of the beef surface wrapped with different zein-based films during a five-day storage period at 4 °C, as per CIELAB colour space. The beef samples were assessed for three colour indexes, which are lightness ( $L^*$ ), red/green ( $a^*$ ), and yellow/blue ( $b^*$ ). The  $L^*$  scale ranges from 0 to 100, with the lowest value corresponding to the white colour and the highest value equivalent to black. Meanwhile, positive  $a^*$  indicates the red colour spectrum, and negative  $a^*$  denotes the green colour. For  $b^*$ , positive  $b^*$  represents yellow colour, and negative  $b^*$  indicates blue colour (Viscarra Rossel et al., 2006). The colour data of beef samples is presented in Tables 5.3 to 5.5 and Figures 5.5 to 5.8.

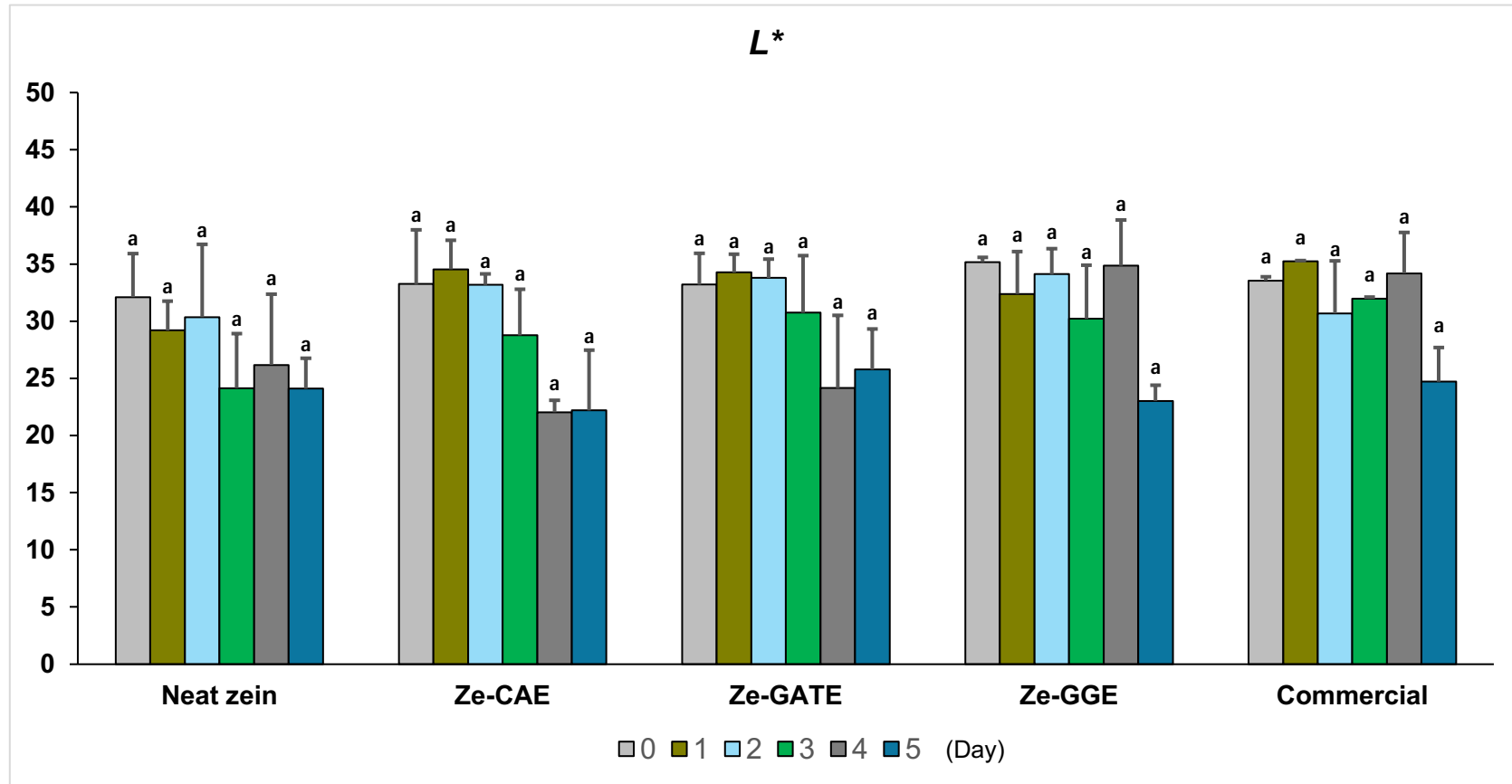
The  $L^*$  values of beef wrapped with zein-based films are shown in Table 5.3 and Figure 5.5. Statistical analysis of the applied general linear model showed that storage duration had a greater influence on the  $L^*$  values of the beef samples compared to the type of films ( $p < 0.05$ ). In general, a decreasing trend was observed for all beef samples wrapped with most of the films over the five-day storage period. However, further statistical analysis of multiple pairwise comparisons found no significant decline in  $L^*$  values of beef samples during a 5-day storage duration using different packaging films ( $p > 0.05$ ). The discrepancy between the general observation and statistical data could be due to high variability among the samples, as observed in relatively large error bars for most of the samples. Since the statistical analysis was intended to observe the interaction of means of  $L^*$ ,  $a^*$ , and  $b^*$  across both days and type of films, the analysis of a large set of data resulted in large error bars in some of the samples. In addition, the difference could be due to the heterogeneity of the beef samples, which resulted in variable  $L^*$  values (as discussed in the earlier part of the discussion). According to literature, the  $L^*$  value of meat is associated with the light scattering, a process in which the light is diffused or deflected by collisions with particles of the medium that it traverses. In the case of meat, the light can be scattered by a medium such as connective tissue, muscle fibre structures and any intracellular and extracellular fluids. Therefore, the extent of light scattering is influenced by the structural attributes of meat, which consequently affect the  $L^*$  value. A high  $L^*$  value indicates high light scattering, which can be observed in low pH or light-coloured meat, while a low  $L^*$  value demonstrates less scattering at the meat surface and greater light absorption by the medium, commonly observed in high pH or dark-coloured meat (Hughes et al., 2014). A recent study by Hu et al. (2023) reported an increase in  $L^*$  values up to 4 days of storage and

a declining trend thereafter up to 12 days of storage at 4 °C for beef wrapped with allicin-zein gelatin films with varying allicin concentrations. In contrast, the present study observed consistent  $L^*$  over five days. The discrepancy may be due to the difference in storage duration of beef (5 days versus 12 days), as a longer storage period generally leads to greater surface water loss in beef, resulting in a darker surface appearance. Reduced surface water results in the reduction of surface reflectivity, thereby reducing the  $L^*$  value (Hughes et al., 2014; Hu et al., 2023). In brief, the data obtained from this study suggest that the lightness of beef samples remained consistent over the course of five days of storage, although slight declines in  $L^*$  values were observed, they were not statistically meaningful, suggesting that zein-based films preserved the lightness and structural integrity of beef during 5 days of storage.

**Table 5.3** Colour of beef wrapped with different packaging films of Neat zein, Ze-CAE, Ze-GATE, Ze-GGE and commercial films: ( $L^*$ ).

Storage at 4 °C (Day)	Lightness ( $L^*$ )				
	Neat zein	Ze-CAE	Ze-GATE	Ze-GGE	Commercial
0	32.11± 3.81 <sup>a</sup>	33.26± 4.74 <sup>a</sup>	33.21± 2.73 <sup>a</sup>	35.17± 0.42 <sup>a</sup>	33.55± 0.34 <sup>a</sup>
1	29.21± 2.55 <sup>a</sup>	34.54± 2.55 <sup>a</sup>	34.27± 1.58 <sup>a</sup>	32.39± 3.71 <sup>a</sup>	35.24± 0.07 <sup>a</sup>
2	30.36± 6.38 <sup>a</sup>	33.18± 0.96 <sup>a</sup>	33.79± 1.64 <sup>a</sup>	34.13± 2.23 <sup>a</sup>	30.69± 4.58 <sup>a</sup>
3	24.14± 4.77 <sup>a</sup>	28.78± 4.02 <sup>a</sup>	30.75± 4.98 <sup>a</sup>	30.22± 4.67 <sup>a</sup>	31.96± 0.14 <sup>a</sup>
4	26.18± 6.20 <sup>a</sup>	22.03± 1.06 <sup>a</sup>	24.16± 6.36 <sup>a</sup>	34.86± 4.01 <sup>a</sup>	34.18± 3.59 <sup>a</sup>
5	24.11± 2.67 <sup>a</sup>	22.20± 5.28 <sup>a</sup>	25.78± 3.56 <sup>a</sup>	23.03± 1.36 <sup>a</sup>	24.71± 2.98 <sup>a</sup>

Colorimeter values (mean ± SD, n = 2). Different superscript letters indicate significant differences among means across both rows and columns (Tukey's pairwise comparisons,  $p < 0.05$ ).



**Figure 5.5** Lightness ( $L^*$ ) of beef wrapped with different packaging films of Neat zein, Ze-CAE, Ze-GATE, Ze-GGE and commercial films.

Data represent means of  $n = 2$ , (mean  $\pm$  SD,  $n = 2$ ). Different superscript letters indicate significant differences among means across both days and type of films (Tukey's pairwise comparisons,  $p < 0.05$ ). The different bar colours represent the different storage day; light grey- Day 0, olive green- Day 1, blue- Day 2, green- Day 3, dark grey- Day 4, dark blue- Day 5.

The  $a^*$  values of beef samples are elaborated in Table 5.4 and illustrated in Figure 5.6. Statistical analysis of the general linear model showed that both the different types of films and storage days significantly influenced the  $a^*$  values of the beef samples ( $p < 0.05$ ). A general observation of the data showed the decreasing trend in  $a^*$  values, indicating the shift of red beef colour towards green colour. Further statistical analysis of multiple pairwise comparisons revealed that significant decline occurred only on certain  $a^*$  values of storage day and packaging film ( $p < 0.05$ ). For example, the  $a^*$  value of beef wrapped with Ze-GGE on day 5 ( $9.77 \pm 2.33$ ) was significantly lower than that of beef wrapped with Ze-GGE on day 0 ( $26.29 \pm 1.07$ ) ( $p < 0.05$ ). There was no significant difference in  $a^*$  values of beef samples between day 0 and day 5 observed for Neat zein, Ze-CAE, and Ze-GATE, as well as for commercial film ( $p > 0.05$ ). The data suggests that Neat zein, Ze-CAE, Ze-GATE, and commercial films retained the red colour of the beef samples after five days of storage. The significant decline in the  $a^*$  values for Ze-GGE could be justified as the faster formation of metmyoglobin (MetMb) on the surface of beef wrapped with Ze-GGE. As the beef was freshly cut to  $5.0 \pm 1.0$  g on day 0, the new surface exposed to  $O_2$  resulted in the bright red colour observed, indicating the formation of oxymyoglobin ( $O_2Mb$ ) (Giddings, 1977, cited in Gill and Gill, 2009, p. 260). As the storage day increased, and the beef surface was exposed to the air for a prolonged period of time, the  $O_2Mb$  will be oxidised to MetMb, which gives the beef a darker red colour, as seen in Figure 5.7 on day 5 (Robertson, G., 2013e). It can be speculated that MetMb formation occurred at a faster rate in beef wrapped with Ze-GGE compared to other zein films. This  $a^*$  value indicated the beef on day 5 has undergone discolouration, where its original red colour was shifted due to the exposure to oxygen for an extended period of time and the formation of MetMb.

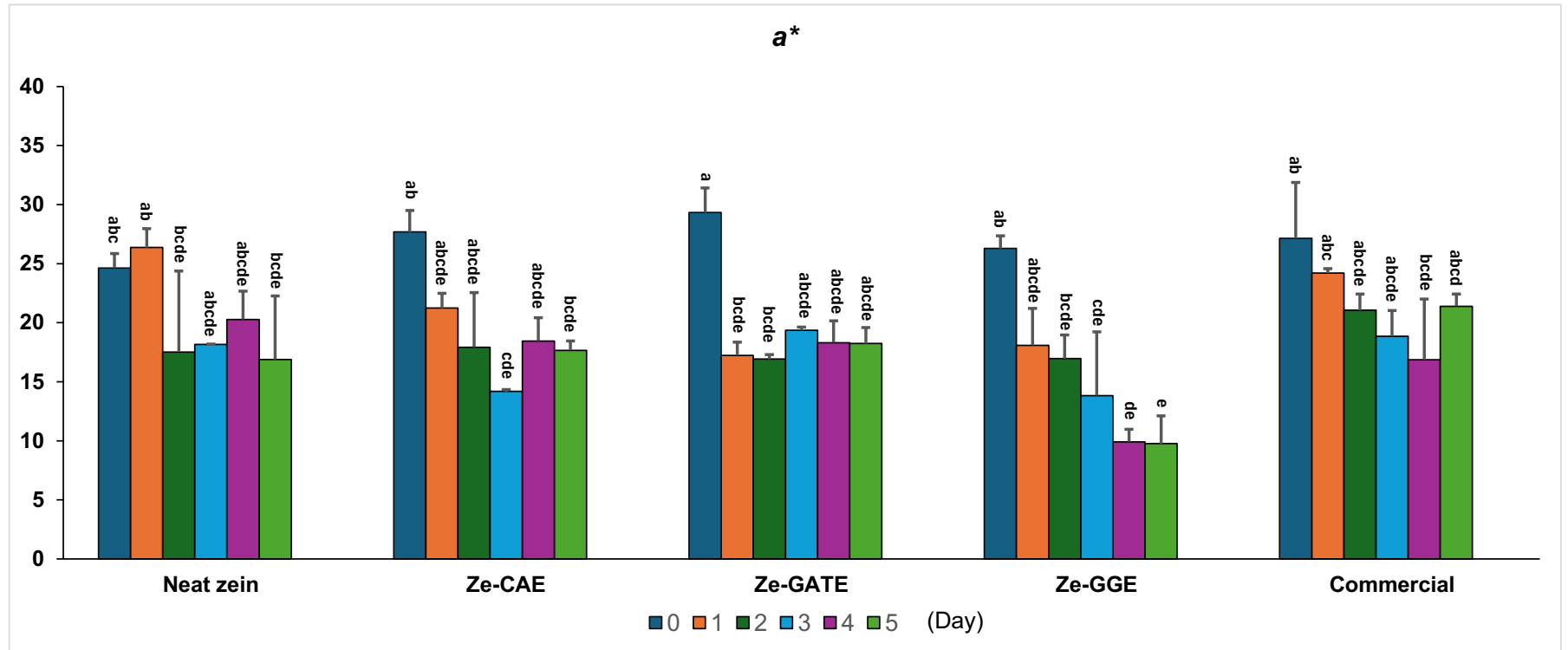
It is important to acknowledge that there was a fluctuation in data for Ze-CAE, where on day 3 ( $14.18 \pm 0.16$ ), beef wrapped with Ze-CAE had a significantly lower  $a^*$  value compared to day 0 ( $27.69 \pm 1.82$ ), and the value increased again on days 4 ( $18.46 \pm 1.96$ ) and 5 ( $17.67 \pm 0.80$ ). A similar trend was observed in the beef that was wrapped with Ze-GATE. The  $a^*$  values were substantially reduced on day 1 ( $17.23 \pm 1.12$ ) and day 2 ( $16.93 \pm 0.37$ ), but then regained the similar  $a^*$  as on day 0 ( $29.33 \pm 2.09$ ) from day 3 onwards. These fluctuations may be attributed to the influencing factors of this present work, which are previously addressed in the earlier part of discussion, such as different beef parts with varying structural characteristics, e.g., the presence of fat strands, which likely influence the colour analysis data. Previous studies by Hu et al. (2023) and Unalan et al. (2011) showed a reduction in  $a^*$  values during the storage study when zein-based films were employed on beef and ground beef patties, respectively. The  $a^*$  value for

beef on day 12 (~6.11) was significantly lower than that of day 0 (>10) (Hu et al., 2023). The  $a^*/b^*$  index of beef patties also significantly reduced after 7 days of storage, recorded below 1.0 (Unalan et al., 2011). In general, these findings imply that the reduction of  $a^*$  values in beef is expected after some period of storage as the biochemical process of MetMb formation. Preserving the red colour of beef is important, as it is closely associated to freshness and acceptability of consumer. Based on these findings, Neat zein, Ze-CAE, Ze-GATE, and commercial films were effective in maintaining the redness of the beef samples after five days of storage.

**Table 5.4** Colour of beef wrapped with different packaging films of Neat zein, Ze-CAE, Ze-GATE, Ze-GGE and commercial films: ( $a^*$ ).

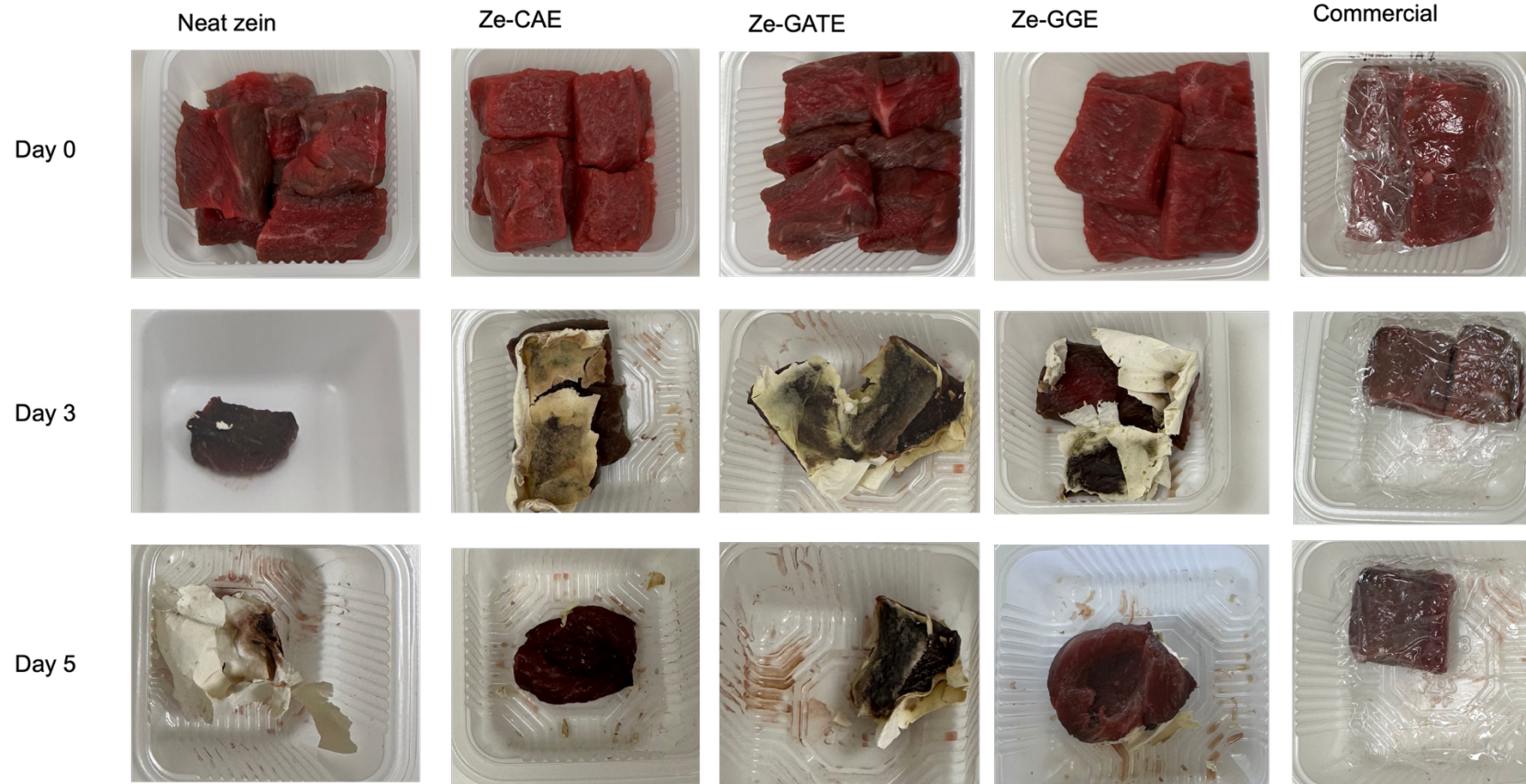
Storage at 4 °C (Day)	red/green ( $a^*$ )				
	Neat zein	Ze-CAE	Ze-GATE	Ze-GGE	Commercial
0	24.64± 1.22 <sup>abc</sup>	27.69± 1.82 <sup>ab</sup>	29.33± 2.09 <sup>a</sup>	26.29± 1.07 <sup>ab</sup>	27.15± 4.72 <sup>ab</sup>
1	26.37± 1.60 <sup>ab</sup>	21.24± 1.26 <sup>abcde</sup>	17.23± 1.12 <sup>bcde</sup>	18.09± 3.12 <sup>abcde</sup>	24.21± 0.37 <sup>abc</sup>
2	17.52± 6.87 <sup>bcde</sup>	17.92± 4.62 <sup>abcde</sup>	16.93± 0.37 <sup>bcde</sup>	16.96± 2.01 <sup>bcde</sup>	21.06± 1.38 <sup>abcde</sup>
3	18.17± 0.04 <sup>abcde</sup>	14.18± 0.16 <sup>cde</sup>	19.36± 0.28 <sup>abcde</sup>	13.83± 5.39 <sup>cde</sup>	18.86± 2.16 <sup>abcde</sup>
4	20.28± 2.40 <sup>abcde</sup>	18.46± 1.96 <sup>abcde</sup>	18.31± 1.84 <sup>abcde</sup>	9.92± 1.05 <sup>de</sup>	16.87± 5.13 <sup>bcde</sup>
5	16.89± 5.38 <sup>bcde</sup>	17.67± 0.80 <sup>bcde</sup>	18.24± 1.34 <sup>abcde</sup>	9.77± 2.33 <sup>e</sup>	21.39± 1.04 <sup>abcd</sup>

Colorimeter values (mean ± SD, n = 2). Different superscript letters (a-e) indicate significant differences among means across both rows and columns (Tukey's pairwise comparisons,  $p < 0.05$ ).



**Figure 5.6** Red/green opponent colours ( $a^*$ ) of beef wrapped with different packaging films of Neat zein, Ze-CAE, Ze-GATE, Ze-GGE and commercial films.

Data represent means of  $n = 2$ , (mean  $\pm$  SD,  $n = 2$ ). Different superscript letters indicate significant differences among means across both days and type of films (Tukey's pairwise comparisons,  $p < 0.05$ ). The different bar colours represent the different storage day; dark blue- Day 0, orange- Day 1, dark green- Day 2, blue- Day 3, purple- Day 4, green- Day 5.



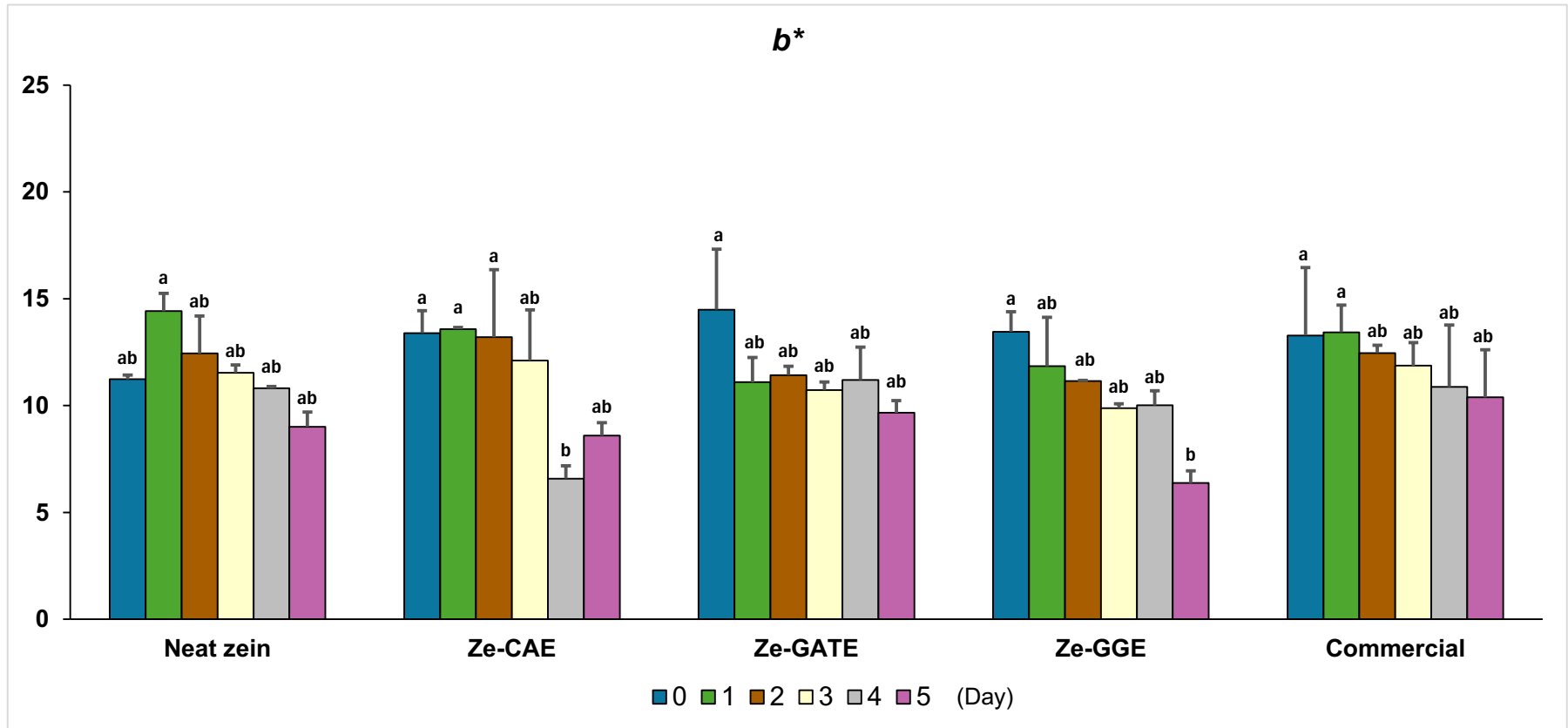
**Figure 5.7** The comparison of beef colours over a five-day storage period using different films of Neat zein, Ze-CAE, Ze-GATE, Ze-GGE, and commercial films. The beef colour gradually progressed from a bright red colour, with a moist and tender appearance (Day 0), to the darker colour, stale, and dry appearance (Day 5).

Additionally, the values for  $b^*$  were measured, and the data are presented in Table 5.5 and Figure 5.8. A general linear model analysis showed that storage days significantly influenced the  $b^*$  values of the beef samples ( $p < 0.05$ ). Subsequent analysis of multiple pairwise comparisons revealed significant influence of different packaging films versus storage time only occurred on certain  $b^*$  values of storage day and packaging film ( $p < 0.05$ ). Similar to the  $a^*$  value, the  $b^*$  value of beef wrapped with Ze-GGE on day 5 ( $6.38 \pm 0.57$ ) was significantly lower than that of beef wrapped with Ze-GGE on day 0 ( $13.46 \pm 0.93$ ) ( $p < 0.05$ ). There was no significant difference in  $b^*$  values observed between day 0 and day 5 for Neat zein, Ze-CAE, Ze-GATE, and commercial film ( $p > 0.05$ ). The data suggest that all zein-based films possessed a similar ability to preserve the  $b^*$  values (yellowness) of beef on day 5, with no significant alterations from day 0, with the exception of samples wrapped with Ze-GGE. Generally, the reduction of  $b^*$  values indicates that the colour shifted away from yellow to blue. This shift is associated with the decrease of  $O_2Mb$  content due to oxygen consumption by microorganisms in beef, suggesting loss of freshness (Bozkurt, 2007). Therefore, according to these findings, the beef wrapped with Ze-GGE on day 5 showed a significant reduction in freshness compared to the beef on day 0. It can be observed that some fluctuations in  $b^*$  values occurred in the beef wrapped with zein-based films, compared to commercial film, even though the effect was not significant. For instance, the fluctuation in the  $b^*$  values between day 0 and 3. This fluctuation is likely due to the interference of the zein film itself, which is dominated by the yellow zein colour, which has been previously highlighted in Chapter 4. Sometimes, a small piece of film attached to the beef samples, and despite efforts to remove it, some film debris remained on the surface of the beef, likely contributing to variability in the  $b^*$  values. The findings of water contact angle presented in Chapter 4 also indicate that all zein-based films exhibit hydrophilic and wetting properties, which may explain the ease of attachment of the film debris to the beef. A previous study reported an overall significant decline in  $b^*$  values of beef samples, however the zein film with the addition of the active antimicrobial substance of allicin showed better preservation of beef colour for 12 days of storage duration (Hu et al., 2023). When comparing the previous data with the current findings, the colour preservation of zein films is dependent on the types of active substances added. As for this study, the zein-based films of Ze-CAE and Ze-GATE showed better colour preservative ability compared to Ze-GGE during five storage days.

**Table 5.5** Colour of beef wrapped with different packaging films of Neat zein, Ze-CAE, Ze-GATE, Ze-GGE and commercial films: (*b\**).

Storage at 4 °C (Day)	yellow/blue ( <i>b*</i> )				
	Neat zein	Ze-CAE	Ze-GATE	Ze-GGE	Commercial
0	11.24± 0.19 <sup>ab</sup>	13.40± 1.05 <sup>a</sup>	14.49± 2.83 <sup>a</sup>	13.46± 0.93 <sup>a</sup>	13.29± 3.17 <sup>a</sup>
1	14.43± 0.83 <sup>a</sup>	13.58± 0.08 <sup>a</sup>	11.10± 1.15 <sup>ab</sup>	11.85± 2.28 <sup>ab</sup>	13.44± 1.27 <sup>a</sup>
2	12.45± 1.75 <sup>ab</sup>	13.21± 3.16 <sup>a</sup>	11.43± 0.41 <sup>ab</sup>	11.15± 0.04 <sup>ab</sup>	12.46± 0.37 <sup>ab</sup>
3	11.54± 0.37 <sup>ab</sup>	12.11± 2.38 <sup>ab</sup>	10.73± 0.38 <sup>ab</sup>	9.89± 0.21 <sup>ab</sup>	11.87± 1.07 <sup>ab</sup>
4	10.82± 0.07 <sup>ab</sup>	6.59± 0.60 <sup>b</sup>	11.20± 1.55 <sup>ab</sup>	10.02± 0.69 <sup>ab</sup>	10.88± 2.89 <sup>ab</sup>
5	9.02± 0.69 <sup>ab</sup>	8.60± 0.60 <sup>ab</sup>	9.67± 0.57 <sup>ab</sup>	6.38± 0.57 <sup>b</sup>	10.39± 2.22 <sup>ab</sup>

Colorimeter values (mean ± SD, n = 2). Different superscript letters (a-b) indicate significant differences among means across both rows and columns (Tukey's pairwise comparisons,  $p < 0.05$ ).



**Figure 5.8** Yellow/blue opponent colours ( $b^*$ ) of beef wrapped with different packaging films of Neat zein, Ze-CAE, Ze-GATE, Ze-GGE and commercial films.

Data represent means of  $n = 2$ , (mean  $\pm$  SD,  $n = 2$ ). Different superscript letters indicate significant differences among means across both days and type of films (Tukey's pairwise comparisons,  $p < 0.05$ ). The different bar colours represent the different storage day; dark blue- Day 0, green- Day 1, brown- Day 2, light yellow- Day 3, light grey- Day 4, pink- Day 5.

In brief, the author found that the results for colour analysis were quite ambiguous. Based on the results of the overall colour analysis, the data demonstrated similar or little variation in colour. However, visual observations (as shown in the photos in Figure 5.7) appeared to contradict the colour measurements obtained from the colorimeter, suggesting a discrepancy between perceived and instrumentally measured colour attributes. The visual inspection showed the beef colour gradually progressed from a bright red colour, with a moist and tender appearance, to the darker colour, stale, and dry appearance over the five storage days. As such, the results were expected to have some significant influence on the  $L^*$ ,  $a^*$  and  $b^*$  values. However, the data indicated results that were contrary to expectations. The possible explanation for the discrepancy may be due to large error bar values that made the overall colour analysis not significantly differ. In addition, it could be speculated that the experiment using a colorimeter measured at only certain random spots, in which the samples might appear differently when observed visually as a whole beef sample. Thus, this might explain the difference between the data obtained by the colorimeter and the perceived beef colour by the naked eye. As the visual inspection of beef is the critical factor in decision-making for beef purchases, therefore, these results highlighted further work needed, such as sensory analysis performed by trained sensory panellists. In addition, the author cannot rule out the possible influence of the factors mentioned at the start of the discussion part, such as the effects of low sample size ( $n = 2$ ), different batches of beef with different beef parts, the beef cut into 2.3 x 2.3 cm in surface dimensions, and the opening and closing of the beef packaging every day, which likely influence the colour analysis results.

To summarise, storage duration had more effect on the colour of beef than the type of packaging film. In general, the  $L^*$  values of beef wrapped with zein-based films were consistent throughout the study period, showing values that were comparable to those of commercial film. On day 5, the  $a^*$  value of beef wrapped with Ze-GGE was significantly lower compared to day 0, meanwhile the  $a^*$  values in beef wrapped with Neat zein, Ze-CAE, and Ze-GATE between day 0 and day 5 retained, which were similar to those observed with commercial film. As for the  $b^*$  values, the beef wrapped with Ze-GGE on day 5 had a significantly lower value when compared to day 0. However, no significant difference in  $b^*$  values was observed across various packaging films, including for commercial film on day 5. Visual observation, however, found contradictory findings, as the author's observed some significant colour changes to the beef samples over the storage period. Therefore, future study of sensory analysis performed by trained sensory panellists is recommended.

## 5.4 Conclusion

This chapter presents the findings of the storage study of beef wrapped with zein-based films (Neat zein, Ze-CAE, Ze-GATE, and Ze-GGE) and their comparison with commercially available film. This study examined quality and safety attributes through the assessment of three parameters, which are microbiological activity,  $a_w$ , and colour analysis. In addition, this chapter also presents a statistical analysis for a comparison of different types of packaging films and storage durations on the quality and safety aspects of beef.

The microbiological analysis demonstrated that the newly developed zein-based films were more effective at controlling the bacterial growth on the stored beef samples compared to commercial film. Among the zein-based films, Ze-GATE showed better bacterial-controlling ability for the first three days of storage, however by the fifth day, it showed similar activity with Ze-CAE and Ze-GGE. In addition, Ze-GGE consistently exhibited lower bacterial growth over a five-day period (below log 6.0 CFU/g) and recorded significantly lower bacterial growth compared to Neat zein and commercial film on day 5, suggesting its potential for extending beef storage life. The growth of bacteria on beef samples was influenced by both film types and storage duration. In the case of  $a_w$ , the beef wrapped with Neat zein, and Ze-CAE showed a reduction in  $a_w$  after 5 days of storage, meanwhile the one wrapped with Ze-GATE and Ze-GGE maintained similar  $a_w$  as of day 0. Ze-GGE had a comparable  $a_w$  on day 5, similar to those of commercial film. Different storage days had a greater influence on the  $a_w$  of beef samples compared to the different packaging films. In the colour analysis, the  $L^*$  values of beef remained stable across all films. Only beef wrapped with Ze-GGE showed a significant decrease in  $a^*$  and  $b^*$  values by day 5, while other films maintained consistent  $a^*$  and  $b^*$  values, similar to those observed in commercial film. The analysis showed that storage duration had a greater impact on the beef's colour than the type of packaging film. The colour analysis, however, exhibited quite ambiguous results because the visual observation contradicted the experimental data. Therefore, future study of sensory analysis performed by trained panellists is recommended.

In brief, all zein-based films demonstrated superior performance compared to the commercial film regarding the inhibition of microbial growth on beef. Ze-GATE film was useful for beef storage up to 3 days, while Ze-GGE film exhibited potential for a longer storage period of up to five days. The  $a_w$  of beef samples reduced over the storage period when using Neat zein and Ze-CAE films,

however, the use of Ze-GATE, Ze-GGE, and commercial films showed the preservative ability of  $a_w$ . The colour analysis of the beef samples resulted in ambiguous results, and sensory analysis is recommended for future work. The factors such as low sample size ( $n = 2$ ), different batches of beef with different beef parts, the beef cut into 2.3 x 2.3 cm in surface dimensions, and the opening and closing of the beef packaging every day should be considered during the analysis of the findings from this chapter.

Overall, the newly developed zein-based films, especially Ze-GATE and Ze-GGE exhibited antibacterial properties, indicating their potential as active antimicrobial food packaging. The ability of these films to inhibit bacterial growth is particularly valuable in food safety and preservation. However, their hydrophilic nature presents a significant drawback, especially for wrapping perishable foods such as beef, as it results in moisture absorption, alters the structural integrity of the packaging, and affects the properties of beef, including colour. Due to this limitation, zein-based films may not be suitable for direct application with beef unless further modifications are made to improve their hydrophilic properties. They could be effectively utilised for packaging of semi-perishable foods such as dried fruits, nuts, and bakery items. The hydrophilic characteristics of the films would not adversely affect these applications, and they would benefit from their antimicrobial functionality. Therefore, while existing formulations may not be suitable for beef packaging, the films may exhibit promising potential for use in alternative food packaging applications.

## Chapter 6 General Discussion

### 6.1 Summary of the research

The demand for biodegradable materials has been growing over the past few years, particularly in the packaging industry. Single-use plastics contribute to the generation of plastic waste, which later accumulates in landfills and pollutes both terrestrial and marine environments (Thompson et al., 2009; IUCN, 2024). Zein is a corn by-product, high in protein, that attracts ongoing interest among researchers owing to its properties. In particular, zein recognised as GRAS, has good film-forming properties and high biocompatibility and is a biobased and biodegradable product (Shukla and Cheryan, 2001; Corradini et al., 2014; FDA, 2024). In addition, Malaysia hosts many varieties of flora, most of which are still underutilised, including *C. asiatica*, *G. atroviridis*, and *G. gnemon*. These three plants have been consistently researched for their biological potential, such as antioxidant, antimicrobial, antiobesity, and anti-inflammatory potential (Ramlan, 2003, cited in Tan, T.Y.C. et al., 2020, p. 1; Shahrul, 2023). However, there is a lack of knowledge about the application of these plants after evaluating their activities. Therefore, this PhD study seeks to contribute to the knowledge on the application of the active extracts from these plants for the development of active antimicrobial packaging films, utilising zein as primary packaging material.

This thesis addressed three key areas. Firstly, the extraction and evaluation of the biological potential of *C. asiatica* extract (CAE), *G. atroviridis* extract (GATE), and *G. gnemon* extract (GGE) using varying ethanol ratios and two different extraction methods. Secondly, the development of active antimicrobial packaging film utilising zein and active extracts, followed by an investigation into the quality and safety of beef stored with the developed films for a duration of five days. Primarily, this study proposed a suitable solvent ratio and extraction method with respect to the biological activities tested, along with comparative data on the total phenolic content, antioxidant capacity, and antimicrobial activity of various processed extracts. Secondly, a novel workflow for developing active antimicrobial zein-based films incorporating CAE, GATE, and GGE was suggested. Finally, the assessment of beef safety and quality following storage with newly developed films under chiller conditions was conducted and compared across different films.

## 6.2 Discussion points and contribution of the thesis

### 6.2.1 Effect of different ethanol ratios and extraction methods on yield and biological activities

Traditionally, medicinal plants are extracted through the solvent extraction method. Recent research has led to the development of many new techniques, such as Soxhlet extraction, microwave-assisted extraction (MAE), ultrasound-assisted extraction (UAE), accelerated solvent extraction (ASE), and supercritical fluid extraction (SFE), as discussed in **Chapter 1**. The extraction of CAE, GATE, and GGE is commonly performed by solvent extraction, as reported in the previous studies (Kato, E. et al., 2009; Desai and Gaikwad, 2014; Desai et al., 2015; Lim et al., 2020; Irma et al., 2021). Limited data is available for the extraction of these extracts using other extraction methods. In addition, there are no universal reports on the evaluation of the biological activities of these three plant extracts using different extraction methods and ethanol ratios. Therefore, the present study aimed to address the gap in the extraction efficiency by using different solvent ratios of ethanol-to-water and two different extraction methods and how they influence the recovery of yield, total phenolic content, antioxidant activities, and antimicrobial properties. The detailed parameters used for solvent extraction and MAE, and the different ethanol ratios were elaborated in **Chapter 2**.

The effects of different ethanol ratios and extraction methods on yield and biological activities were detailed in **Chapter 3** and summarised in Table 6.1. The findings highlighted that the different ethanol ratios had a more significant impact on the extraction yield and bioactivities than the extraction methods, albeit the effect of the extraction method was apparent in certain tests as well. Based on Table 6.1, the influence of ethanol ratio and extraction method varied between tests, making it challenging to establish only one best/optimal ethanol ratio and extraction method. The use of the aqueous ethanol ratio consistently showed a higher activity for most of the tests, as the combination of water and organic solvent may facilitate the recovery of bioactive phytoconstituents that are soluble in water and/or organic solvents (Do et al., 2014; Hikmawanti et al., 2021). The reason for the varying ethanol-to-water ratios used is that different ratios result in changes in the ethanol concentration, which lead to the alteration of the physical properties of the solvent, such as density, dynamic viscosity, and dielectric constant. The change would result in the modification of the solubilities of compounds that further influence the yield and the biological activity (Frank et al., 1999, cited in Cacace and Mazza, 2003, p. 243). This section provides a valuable insight into the suitable ethanol ratio and extraction method for maximising yield

and biological activities of CAE, GATE, and GGE. The findings can guide the choice of extraction method, whether conventional solvent extraction or MAE, based on the available resources, and the option for a sustainable extraction procedure by selecting a lower ethanol ratio without compromising the biological activity.

**Table 6.1** The influence of ethanol ratio and extraction method.

Test	General linear model		Tukey's pairwise comparisons
	Influence of ethanol ratio	Influence of extraction method	Results with higher yield/ activity
Extraction yield	YES	NO	<ul style="list-style-type: none"> <li>• CAE: 0-50 ethanol, solvent</li> <li>• CAE: 0-75 ethanol, MAE</li> <li>• GATE: 0-75 ethanol, solvent</li> <li>• GATE: 0-50 ethanol, MAE</li> <li>• GGE: 0-75 ethanol, solvent &amp; MAE</li> </ul>
Total phenolic content	YES	YES	<ul style="list-style-type: none"> <li>• CAE: 0-50 ethanol, solvent</li> <li>• CAE: 0-75 ethanol, MAE</li> <li>• GATE: 50-100 ethanol, MAE</li> <li>• GGE: 0-75 ethanol, solvent</li> <li>• GGE: 0-100 ethanol, MAE</li> </ul>
Antioxidant: DPPH	YES	YES to GATE	<ul style="list-style-type: none"> <li>• CAE: 25-75 ethanol, solvent</li> <li>• CAE: 0-75 ethanol, MAE</li> <li>• GATE: 0, 75-100 ethanol, solvent</li> <li>• GATE: 75-100 ethanol, MAE</li> <li>• GGE: 50-75 ethanol, solvent</li> <li>• GGE: 75 ethanol, MAE</li> </ul>
Antioxidant: FRAP	YES to CAE & GGE	YES to GGE	<ul style="list-style-type: none"> <li>• CAE: 0 ethanol, solvent</li> <li>• GATE: 50-75 ethanol, solvent</li> <li>• GATE: 0 &amp; 100 ethanol, MAE</li> <li>• GGE: 0, 50, 100 ethanol, solvent</li> <li>• GGE: 100 ethanol, MAE</li> </ul>
Test	Highest activity		
Antimicrobial 10 mg/mL	No analysis for MBC		<ul style="list-style-type: none"> <li>• GGE100-S lowest MBC against <i>B. cereus</i></li> </ul>
Antimicrobial 50 mg/mL	No analysis for MBC		<ul style="list-style-type: none"> <li>• GATE50-S/M lowest MBC against all bacteria tested</li> <li>• CAE50-M lowest MFC against <i>C. albicans</i></li> </ul>

## 6.2.2 Comparison of the biological activities of CAE, GATE, and GGE and their potential as active antimicrobial agents

The consumption of CAE, GATE, and GGE is associated with various biological activities, such as antioxidant, antimicrobial, antiobesity, and anti-inflammatory effects. Previous studies on the biological activities of these plants are elaborated in **Chapter 1**. While previous studies have documented the individual biological properties of these plants, no prior research has focused on a comparative analysis using various ethanol ratios and the MAE procedure. Since these plants are widely used in traditional medicine and as a food source, it is important to scientifically assess their potential. Therefore, this study evaluated and compared the biological potential of CAE, GATE, and GGE based on total phenolic content, antioxidant capacity, and antimicrobial activity, as discussed in **Chapter 3**. The experimental protocols used for these assessments are outlined in **Chapter 2**.

The results of the present study indicated that all plant extracts exhibited varying degrees of extraction yield and biological activities. GATE had the highest extraction yield; however, it exhibited the lowest biological activities of total phenolic content and antioxidant activity. The higher yield observed in GATE could be due to the extract which was derived from fruit that contained a higher level of soluble phytoconstituents compared to CAE and GGE, which were obtained from leaves (Jena et al., 2002; Desai and Gaikwad, 2014; Shahid et al., 2022; Siripongvutikorn et al., 2023). Although GATE demonstrated the lowest phenolic content and antioxidant capacity, antimicrobial tests against five foodborne pathogens at starting concentration of 50 mg/mL of GATE exhibited that GATE had the lowest MBC values, indicating higher antibacterial activity than CAE and GGE. Meanwhile, for a test at a similar starting concentration, CAE exhibited higher antifungal activity against *C. albicans*. The finding of the antibacterial activity of GATE is in agreement with the results reported by Mackeen et al. (2000), who found that GATE possessed antibacterial activity but not antifungal activity. The antifungal activity of the methanol fraction of CAE was also previously reported by (Irma et al., 2021). In addition, Pearson correlation analysis demonstrated that a significant correlation between total phenolic content and DPPH and FRAP was observed only in CAE, but not in GATE and GGE. Therefore, it is suggested that the biological activity of CAE is predominantly due to phenolic compounds such as flavonoids and saponins (Mat-Ali, 2008; Desai and Gaikwad, 2014; Irma et al., 2021). Meanwhile, a higher antibacterial activity exhibited by GATE might be due to compounds other than phenolics. Hydroxycitric acid (HCA) was reported to be the main organic acid found in GATE, which may contribute to the observed activity (Jena et al., 2002). In the case of GGE, the activity is possibly derived from diterpene alcohol,

monoacylglycerols and triterpenoids (Dutta et al., 2018; Trisha et al., 2024). The general rank order of the biological activity of the plant extracts of CAE, GATE, and GGE is summarised in Table 6.2.

**Table 6.2** The rank of biological activity of the plant extract.

Test	Rank order/ highest activity
Extraction yield	GATE > CAE > GGE
Total phenolic content	GGE > CAE > GATE
Antioxidant: DPPH	CAE > GGE > GATE
Antioxidant: FRAP	GGE > CAE > GATE
Antimicrobial 10 mg/mL	GGE > GATE > CAE
Antimicrobial 50 mg/mL	antibacterial: GATE antifungal: CAE

A diverse range of data on the biological activities of CAE, GATE, and GGE was obtained from this current and previous studies. The discrepancies might be due to different geographical locations, processing, transportation, and storage conditions of the samples prior to analysis, and those conditions can affect the availability and stability of bioactive compounds present in the sample. In addition, the extraction parameters, solvents, and concentrations might have influenced the data. Additionally, differences in data analysis methods across studies, such as differences in the reporting units, make it challenging to compare results, as they are only comparable when presented in a consistent format.

Overall, the findings presented in **Chapter 3** demonstrated the suitability of these extracts for the formulation of active antimicrobial films. Among all *C. asiatica* extracts, the extract of CAE50-S was selected for future research because it produced a higher yield and phenolic content, along with stronger antioxidant and antimicrobial activities, especially against *B. cereus* at lower concentrations. As for *G. atroviridis*, GATE100-M was selected due to its stronger antimicrobial performance, showing a larger inhibition zone and a lower minimum bactericidal concentration (MBC), compared to other GATE samples. For *G. gnemon*, GGE50-M was chosen for its higher bioactivity, and it was available in sufficient quantity for further testing. Based on their biological activities and extract availability, three extracts of CAE50-S, GATE100-M, and GGE50-M were selected for the development of biodegradable packaging films, utilising zein as the primary packaging material.

### 6.2.3 Electrospinning as a novel approach to develop zein-based films incorporated with CAE, GATE, and GGE

The approach of using electrospinning for the development of packaging film is due to the inherent advantages, such as its non-thermal process and its ability to produce materials with a high surface-to-volume ratio, tailored morphology, and high encapsulation efficiency (Anu Bhushani and Anandharamakrishnan, 2014). The details on the electrospinning concept are elaborated in **Chapter 1**, and the electrospinning parameters used are detailed in **Chapter 2**. The results and discussion on the development of active antimicrobial zein-based films and their characterisation are presented in **Chapter 4**. Prior to the production of the Neat zein film, a preliminary study was conducted to determine the optimal zein concentration for electrospinning, as outlined in **Supplementary Materials 2**. The preliminary experimental data indicated that a 30% zein concentration was the most suitable for producing fibres with a smooth film following electrospinning. Therefore, 30% zein was selected for the development of active antimicrobial zein-based film. To the best of author's knowledge, this is the first study to report the production and characterisation of Ze-CAE, Ze-GATE, and Ze-GGE films employing the electrospinning method.

The main findings in this section were related to the development of active antimicrobial films from zein and CAE, GATE, and GGE and the characterisations of the films. Neat zein, Ze-CAE, Ze-GATE, and Ze-GGE films were successfully prepared using 30% (w/v) zein as a primary polymer material and incorporated with 5% (w/w) of active plant extracts via electrospinning. All zein-based film solutions exhibited viscosities ranging from 0.1377 to 0.1790 Pa.s, aligning with the optimal range for electrospinning (0.1 to 2.0 Pa.s) (Fong et al., 1999). Viscosity is the crucial factor that determines the suitability of polymer solution for electrospinning, as it affects both the fibre diameter and morphology (Demir et al., 2002; Zong et al., 2002). In short, the solutions of Ze-CAE, Ze-GATE, and Ze-GGE demonstrated superior shear thinning properties compared to Neat zein at shear rates ranging from 0.1 to 1.0 s<sup>-1</sup>, indicating better pseudoplastic behaviour. The addition of CAE, GATE, and GGE did not influence the viscosity of the zein polymer solution at a shear rate of 100 s<sup>-1</sup>.

The resulting films were light cream-coloured, opaque, smooth, and thin films, with the Ze-GATE and Ze-GGE films exhibited an additional granular-like appearance on their surfaces. An examination using SEM at magnifications of 5000X revealed the formation of fibres, predominantly appearing as flat ribbon-like structures, with apparent string formation on Ze-CAE and Ze-GGE. The strings' formation suggests the successful incorporation of CAE and GGE into the

zein polymer matrix during the electrospinning process (Salevic et al., 2022). As the string formation is associated with the cross-linking of phenolics, the absence of string in the Ze-GATE film could be explained by its lower amount of phenolic content, as mentioned in **Chapter 3**, and thereby supports the results of this section (Gaikwad et al., 2020; Zhang, Xueqian et al., 2021; Munir et al., 2023). The analysis of fibre diameter and film thickness found that Ze-GGE exhibited significantly higher fibre diameter and thickness compared to other films, likely due to the higher viscosity of Ze-GGE relative to other zein solutions. A high viscosity solution is linked with reduced jet stretching, which leads to a shorter jet path and the formation of larger fibres during electrospinning. It is also correlated to a higher solid content, as shown by the highest phenolic amount in GGE, leading to the deposition of thicker fibres on the plate collector (Kameoka et al., 2003; Phiriyawirut and Phaechamud, 2012).

The encapsulation efficiency data showed the rate of encapsulation of CAE, GATE, and GGE exceeded 90%, demonstrating a high level of encapsulation of these extracts within the zein polymer matrix. This corresponds to the structure of  $\alpha$ -zein, the primary class of zein, characterised by glutamine-rich bridges that enhance interactions with bioactive molecules through hydrogen bonding (Lai et al., 1999; Zhang, Xinrui et al., 2021). The water contact angle of films measured between 20° and 35° after 2 seconds, demonstrating hydrophilic and wetting characteristics. In comparison to the control film of Neat zein, the incorporation of CAE, GATE, and GGE into Ze-CAE, Ze-GATE, and Ze-GGE films, respectively, did not significantly affect the water contact angle. The FTIR spectra of Ze-CAE, Ze-GATE, and Ze-GGE indicated that the addition of the plant extracts to zein fibres did not produce new peaks, suggesting successful encapsulation of the extracts within the zein fibres without significantly altering their structural integrity. The spectra also highlighted the formation of hydrogen bonds between zein and the plant extracts, evidenced by a majority of bands shifting to lower frequencies in the Ze-CAE and Ze-GGE films, while some bands exhibit similar shifts in the Ze-GATE film (Ratajczak, 1972; Coleman et al., 1988; Mattia and Painter, 2007; McDowell, 2025).

The incorporation of zein-based films with CAE, GATE, and GGE showed comparable or reduced thermal properties. Neat zein demonstrated the maximum decomposition rate at 318.33 °C, with four stages of decomposition and a residue of 19.43%. Ze-GATE appeared to be the most thermally stable among the zein-based films, exhibiting a temperature of maximum decomposition rate of 319 °C, with five decomposition stages and a residue of 21.64%. Ze-CAE and Ze-GGE demonstrated higher interaction between plant extract and the zein

matrix, observed from the reduced maximum decomposition rate temperature to 308.17 °C and 305.17 °C, respectively. This suggests the interaction of these two extracts with the zein matrix, results in reduced protein-protein interactions of zein. All zein-based films exhibited a high degree of biodegradability indicator, as shown by the breakdown of films into smaller fragments under visual inspection after 12 days of burial in soil. Overall, it could be concluded that Ze-CAE, Ze-GATE, and Ze-GGE films can be used as sustainable and biodegradable packaging film, with necessary improvement on the hydrophobicity property required depending on the type of foods.

#### **6.2.4 The quality of beef stored with newly developed zein-based films**

Foods, especially fresh produce, poultry, and raw meat are frequently subjected to foodborne pathogens and food spoilage microorganisms. These contaminants can be introduced in any stages of food supply chain including production, processing, storage and transportation (Thakali and MacRae, 2021). Foodborne pathogens are responsible for foodborne illness, which can, in severe instances, result in fatality. In contrast, spoilage microorganisms lead to food contamination and quality deterioration (Linscott, 2011; Amit et al., 2017; Wessner et al., 2020). The details of the common foodborne pathogens and food spoilage microorganisms are outlined in **Chapter 1**. This present study focuses on the role of active antimicrobial packaging films to minimise the growth of foodborne pathogens and food spoilage microorganisms. The use of biobased and biodegradable packaging film offers a greener alternative compared to plastic film. In addition, the antimicrobial potential of extracts would enhance the function of films to preserve the quality and safety of raw beef. **Chapter 2** elaborated on the experimental procedures used to analyse the beef quality and safety for 5 days of storage at 4 °C.

Based on the results in **Chapter 5**, statistical analysis revealed that both types of film and storage days significantly influenced the growth of bacteria on beef samples. The total plate count results showed that Neat zein and zein-based films of Ze-CAE, Ze-GATE, and Ze-GGE were more effective in inhibiting bacterial growth on chilled beef compared to commercial film after 5 days of storage at 4 °C. The total plate count values ranged from 5.8±0.2 to 6.7±0.2 log CFU/g, which were lower than commercial film's value of 8.2±0.0 log CFU/g. Overall, the data suggest that Ze-GATE is more suitable for the shorter duration of beef storage up to 3 days, while Ze-GGE is more effective for longer storage duration of up to five days, as indicated by the consistently low log CFU/g value of beef wrapped

with Ze-GGE (below log 6.0 CFU/g) compared to other films throughout the study duration. The findings for the Ze-GATE are in agreement with the antimicrobial results in **Chapter 3**, which reported that it had the highest antimicrobial activity as compared to CAE and GGE. For GGE, it is assumed that the hydrophobic compounds in GGE exert a delayed or sustained antimicrobial effect, as shown by the maintained log CFU/g value of bacteria for the beef wrapped with Ze-GGE over five days of storage (Dutta et al., 2018; Trisha et al., 2024).

As for water activity ( $a_w$ ), storage days had a pronounced effect on the  $a_w$  compared to the different film types. The data revealed a downward trend in  $a_w$  over time when using Neat zein and Ze-CAE. Ze-GATE and Ze-GGE were considered better films to wrap beef, as they showed moderately lower  $a_w$  but did not significantly affect the overall  $a_w$  during the five-day storage period. This finding suggests the capability of these two films to preserve the  $a_w$  in wrapped beef samples and maintain their juiciness, thereby ensuring consumer acceptability. Commercial film exhibited higher  $a_w$ , demonstrating better retention of juiciness, however, this also increases the risk of faster spoilage due to microbial growth. Colour analysis showed no significant variation in lightness ( $L^*$ ) values of beef across different films and storage duration. This evidence suggests that all zein-based films helped maintain the  $L^*$  values of beef, thereby preserving the muscle structure integrity of the beef (Hughes et al., 2014). A significant variation in red/green ( $a^*$ ) and yellow/blue ( $b^*$ ) was only observed on day 5 for Ze-GGE, which was statistically significant different compared to the same film on day 0. This variation in  $a^*$  and  $b^*$  for the beef wrapped with Ze-GGE indicates a faster rate of MetMb formation occurred in Ze-GGE film compared to other zein films (Robertson, G., 2013e). The colour analysis, however, exhibited quite ambiguous results, as visual observations contradicted the instrumental data. Therefore, future studies involving sensory analysis by trained panellists are recommended. The findings from this section should be interpreted with a caution due to several influencing factors, such as low sample size ( $n = 2$ ), different batches of beef with different beef parts, the beef cut into 2.3 x 2.3 cm in surface dimensions, and the opening and closing of the beef packaging every day, as discussed in the earlier results and discussion part of **Chapter 5**.

Overall, the newly developed zein-based films, particularly Ze-GATE and Ze-GGE demonstrated antibacterial properties, suggesting their potential application as active antimicrobial food packaging especially for the food items that are highly susceptible to bacterial spoilage. These films effectively reduced bacterial growth, which is crucial for food safety and preservation. Nonetheless, the hydrophilic characteristics present a considerable limitation, particularly in the

context of wrapping perishable items like beef, as they lead to moisture absorption, compromise the structural integrity of the packaging, and influence the properties of beef, including its colour. Zein-based films may be unsuitable for direct application with beef due to this limitation, unless modifications are implemented to improve their hydrophilic properties. However, they may be effectively utilised for packaging of semi-perishable foods, where the hydrophilic nature of the films is less likely to cause adverse effects, and their antimicrobial functionality will provide advantages. Thus, although the current formulations are not ideal for beef packaging, the films demonstrate significant potential for other food packaging applications.

### 6.3 Research limitations

The author acknowledges the following limitations of the current research, as detailed below:

**Covid-19 impact:** Due to the Covid-19 pandemic, the access to the laboratories was restricted. It was not possible to commence the lab work until 9 months after enrolment in the PhD study. Thus, this impacted the overall progress of the project, which limited the scope and duration of the study.

**Data collection and research:** The electrospinning machine, essential for producing film samples, was out of operation from July 2024. As a result, the author could not produce more films for subsequent biodegradation and storage studies, thus hindering the overall timeline of the research. In November 2024, the author received an update that the electrospinning machine could not be repaired, leading to the decision to outsource the subsequent film production to an electrospinning company in Italy. Given the constraints related to cost and availability of plant extracts, only sufficient Ze-CAE, Ze-GATE, and Ze-GGE films were produced for application in the storage studies. Therefore, in Chapter 5, the experiment was performed with only two replicates of samples.

Another limitation of this study is the lack of information regarding the phytochemical composition of the plant materials used. For *C. asiatica* and *G. gnemon* leaves, although the plant materials were freshly collected, the stage of growth of the leaves at the time of collection was unknown. As for *G. atroviridis* fruits, the samples were purchased from a local market in Terengganu, Malaysia where information regarding factors such as the stage of fruit maturity during harvest, processing conditions, and the location of collection was not available. Since these factors can significantly influence the phytochemical profile, and

consequently, the bioactivity of plant extracts, these gaps in information are acknowledged as study limitations.

In addition, for the evaluation of antimicrobial activity in Chapter 3 and the microbiological assay conducted during the storage study in Chapter 5, the plant extracts and zein-based films were assessed for their ability to reduce microbial growth. However, there remains a risk of beef contamination that may lead to foodborne diseases caused by bacterial toxins, (e.g., Shiga toxin-producing *E. coli* O157:H7 or botulinum toxin from *Clostridium botulinum*) where even at very low doses can cause the disease. These toxin-related risks were not evaluated in the present study. Furthermore, this study focused only on contamination occurring on the surface of packaged foods, using beef cuts as the model food samples. In a broader context, contamination can also occur inside of beef, such as in minced or ground beef, which was beyond the scope of this present work.

In term of experimental approaches, the limitations of the selected assays in Chapter 3 were also acknowledged. For example, in the total phenolic content assay, non-phenolic reducing agents (e.g., reducing sugar and certain amino acids) present in the system may also reduce the Folin-Ciocalteu reagent. This could consequently lead to an overestimation of the total phenolic content (Blasco et al., 2005; Munteanu and Apetrei, 2021). In the evaluation of the antioxidant activity of the plant extracts using the DPPH inhibition assay, the method measured absorbance values, where antioxidant activity is indicated by a decrease in absorbance over time. However, the plant extracts themselves exhibited inherent colours (e.g., dark green, dark brown, and yellow), which may potentially interfere with DPPH absorbance readings. These methodological limitations, which were not included in the earlier discussion sections, are therefore acknowledged in this section.

**Timeframe of study:** This study was funded by Majlis Amanah Rakyat, Malaysia, for only four years. Therefore, all the experimental design, data analysis, and thesis writing were structured to be completed within this four-year timeframe.

## 6.4 Future directions

This research has established a detailed workflow for investigating the biological activities of CAE, GATE, and GGE, followed by the development of active packaging films from zein and incorporated with the active plant extracts using electrospinning. The three selected active extracts of CAE, GATE, and GGE were incorporated into zein film to assess their efficacy as wrapping film for beef. Further studies should be initiated to explore the other potential of these packaging films. Some of the suggestions for future work directly related to research are addressed as follows:

- The incidence of food contamination and spoilage results from the proliferation of microbial flora, encompassing a range of bacterial and fungal strains. In this present study, the initial antimicrobial screening of the plant extracts involved five strains of foodborne pathogens and only one fungal strain. The subsequent investigation into microbiological analysis of total plate count using zein-based films focused mainly on bacterial growth. In order to fully explore the antimicrobial potential of these plants (CAE, GATE, and GGE), whether in the form of crude extract or as a film, it is recommended that the antimicrobial testing include a broader range of fungal species and the evaluation of the total plate count for fungi also be performed.
- The film casting is a traditional method to produce biodegradable films. As this current study employed an advanced electrospinning method, there is a gap in knowledge regarding the Ze-CAE, Ze-GATE, and Ze-GGE films produced using the traditional method, as no prior research has been conducted on film casting with these plant extracts and zein as packaging materials. Future research on this aspect could bridge the findings from the current study and provide a comparison of the films' properties and applications produced by two different procedures.
- The film produced is commonly evaluated for its physical, mechanical and barrier properties to ensure it can be successfully used as packaging material. While physical properties such as thickness, SEM, wetting and thermal properties were successfully evaluated in this present study, other mechanical and barrier properties were not assessed. The mechanical properties of packaging materials are essential for preserving food quality throughout handling and storage in the supply chain, as the quality of packaging materials directly impacts these processes (Murrieta-Martinez

et al., 2018). Barrier properties are critical in assessing the shelf life of food products. These properties assess the interaction of water, gases, and light with packaging materials, which are key factors in the physical and chemical degradation of food products (Miller and Krochta, 1997; Germain, 1997, cited in Siracusa et al., 2008, p. 636). In this context, there is a need for future studies to assess films' mechanical and barrier properties, such as tensile strength, gas permeability, and water vapour permeability.

- Among the very essential aspects of this present work is the biodegradability of the films. Although the soil burial test was performed to study the biodegradability of the films, this test was acted only as an indicator of biodegradability, as the results only involved the visual observation of the breakdown of films upon burial in soil after 12 days of burial, indicating the initial microbial activity of converting polymer to smaller molecular weight fragments (Mohee et al., 2008). The ultimate biodegradation of film is when the microorganism converts these fragments into biomass, minerals, water, and gases, which can be measured by carbon dioxide evolved or biochemical oxygen demand (BOD). Therefore, it is imperative to perform a biodegradation test study according to ASTM or ISO standard procedures, as these two standard protocols measure the conversion of the small fragments into biomass, minerals, and gases, and finally are able to explore the full biodegradability potential of films (ASTM, 2012; ISO, 2019).
- The testing of the quality of stored food using various packaging materials often involves the measurement of their ability to inhibit microbial growth,  $a_w$ , colour and texture analysis of food products. While the first three aspects were determined in this study, the texture analysis could not be completed due to the scarcity of film samples. Although a preliminary study on the texture profile analysis was conducted, comprehensive data were not available. In this study context, the texture determination of beef via texture profile analysis is important, as it correlates to perceived sensory attributes, and the data will provide information such as the beef's tenderness, springiness, and chewiness, which are all related to overall beef quality. Therefore, it is suggested that future studies include the texture profile analysis of beef wrapped with the film samples to examine its textural attributes over the storage period.
- In addition to the instrumental analysis on beef, utilising tools such as colorimeter and Texture analyser, it is advisable to conduct sensory

analysis. As previously mentioned in the discussion of colour analysis in Chapter 5, the colour analysis results from the colorimeter were inconsistent with the visual observations. Therefore, it is recommended to perform sensory evaluation by trained sensory panellists to assess the quality attributes of beef samples, as visual inspection plays a crucial role in the decision-making process for beef purchases.

- In this study, the active extracts were selected for the development of active antimicrobial films of Ze-CAE, Ze-GATE, and Ze-GGE. The knowledge of the specific compound responsible for the biological activities would be advantageous in terms of future work. Therefore, it would be interesting to identify the active compounds from these extracts via GCMS, HPLC or NMR equipment, as these instruments could identify volatile and non-volatile bioactive compounds and give detailed structural information of the identified compounds.

## 6.5 Conclusion

This study aimed to examine and compare the biological potential of extracts from underutilised medicinal plants of *C. asiatica*, *G. atroviridis*, and *G. gnemon* as active antimicrobial agents. The focus was on their application as biobased and biodegradable film packaging, particularly for use as wrapping film, with raw beef was selected as a food sample representing typical microbial risks in foods. Current reports on these plants are limited due to the native nature of the plants (Southeast Asia), where most of the research has been conducted by local researchers. There is a gap in the knowledge on the development of active packaging film incorporated with these plant extracts, employing biobased and biodegradable materials. Many studies have focused on the evaluation of the biological activities alone, and no further research was conducted following the investigation. Reports on the development and characterisation of film packaging using these plant extracts, especially employing the electrospinning method, are still scarce, highlighting the importance of this study.

In this study, a new scope of knowledge was successfully established, providing a comparison of the biological activities between CAE, GATE, and GGE using different extraction methods and ethanol ratios. The findings indicated that the ethanol ratio had a more significant effect on the extraction yield and biological activities than the extraction method. Following the evaluation of biological activities, the active extracts of CAE50-S, GATE100-M, and GGE50-M were selected for the development of biodegradable packaging films. Novel zein-based films of Ze-CAE, Ze-GATE, and Ze-GGE were successfully produced using electrospinning, with zein as the primary polymer at 30% concentration and 5% (w/w) of the selected active extracts. All the beef samples wrapped with the zein-based films, particularly Ze-GATE and Ze-GGE, exhibited reduced bacterial growth over a five-day storage period, indicating a higher antibacterial activity than the commercial film tested in this study. However, the hydrophilic nature of films posed a limitation for beef packaging, indicating the need for further work to improve their properties as well as their application across a broader range of food products. The outcomes of this research contribute to the knowledge for the development of active antimicrobial films developed from biobased and biodegradable materials, aiming to reduce the reliance on plastic packaging in the food industry and giving major players from the industry an option for the sustainable alternative. Importantly, this research also provides valuable data on three underutilised medicinal plants from Malaysia, making it accessible to the global scientific community and encouraging further research.

## List of References

- Abdul-Mutalib, N.A., Syafinaz, A.N., Sakai, K. and Shirai, Y. 2015. An overview of foodborne illness and food safety in Malaysia. *International Food Research Journal*. **22**(3), pp.896-901. Available from: <Go to ISI>://WOS:000422948700003
- Abdullahi, M.G., Toriman, M.E., Gasim, M.B. and Juahir, H. 2014. Rainfall dynamics of Terengganu Malaysia and its recent trends analysis using the Mann-Kendall Test. *Journal of Advances in Biotechnology*. **4**(2), pp.372-381. Available from: <https://doi.org/10.24297/jbt.v4i2.1620>
- Abebe, E., Gugsu, G. and Ahmed, M. 2020. Review on major food-borne zoonotic bacterial pathogens. *Journal of Tropical Medicine*. **2020**, p19 article no: 4674235 [no pagination]. Available from: <https://doi.org/10.1155/2020/4674235>
- Acheson, P., Bell, V., Gibson, J., Gorton, R. and Inns, T. 2016. Enforcement of science—using a *Clostridium perfringens* outbreak investigation to take legal action. *Journal of Public Health*. **38**(3), pp.511-515. Available from: <https://doi.org/10.1093/pubmed/fdv060>
- Addgene. 2021. *Creating bacterial glycerol stocks for long-term storage of plasmids*. [Online]. [Accessed 15 January 2021]. Available from: <https://www.addgene.org/protocols/create-glycerol-stock/>
- Ahmed, I., Lin, H., Zou, L., Brody, A. L., Li, Z., Qazi, I. M., Pavase, T. R. and Lv, L. 2017. A comprehensive review on the application of active packaging technologies to muscle foods. *Food Control*. **82**, pp.163-178. Available from: <https://doi.org/10.1016/j.foodcont.2017.06.009>
- Ajila, C.M., Brar, S.K., Verma, M., Tyagi, R.D., Godbout, S. and Valero, J.R. 2011. Extraction and analysis of polyphenols: Recent trends. *Critical Reviews in Biotechnology*. **31**(3), pp.227-249. Available from: <https://doi.org/10.3109/07388551.2010.513677>
- Al-Mansoub, M.A., Asmawi, M.Z. and Murugaiyah, V. 2014. Effect of extraction solvents and plant parts used on the antihyperlipidemic and antioxidant effects of *Garcinia atroviridis*: a comparative study. *Journal of the Science of Food and Agriculture*. **94**(8), pp.1552-1558. Available from: <https://doi.org/10.1002/jsfa.6456>
- Ali, S., Khatri, Z., Oh, K.W., Kim, I.-S. and Kim, S.H. 2014. Zein/cellulose acetate hybrid nanofibers: Electrospinning and characterization. *Macromolecular Research*. **22**(9), pp.971-977. Available from: <https://doi.org/10.1007/s13233-014-2136-4>
- Alizadeh-Sani, M., Tavassoli, M., McClements, D.J. and Hamishehkar, H. 2021. Multifunctional halochromic packaging materials: Saffron petal anthocyanin loaded-chitosan nanofiber/methyl cellulose matrices. *Food Hydrocolloids*. **111**, p106237. Available from: <https://doi.org/10.1016/j.foodhyd.2020.106237>

Allkin, B. 2017. *Useful Plants – Medicines: at least 28,187 plant species are currently recorded as being of medicinal use* London, UK: Royal Botanic Gardens, Kew.

Altan, A., Aytac, Z. and Uyar, T. 2018. Carvacrol loaded electrospun fibrous films from zein and poly(lactic acid) for active food packaging. *Food Hydrocolloids*. **81**, pp.48-59. Available from: <https://doi.org/10.1016/j.foodhyd.2018.02.028>

Altomare, R. E. and Ghossi, P. 1986. An analysis of residence time distribution patterns in a twin screw cooking extruder. *Biotechnology Progress*. **2**(3), pp.157-163. Available from: <https://doi.org/10.1002/btpr.5420020310>

Amit, S.K., Uddin, M.M., Rahman, R., Islam, S.M.R. and Khan, M.S. 2017. A review on mechanisms and commercial aspects of food preservation and processing. *Agriculture & Food Security*. **6**(1), p51. Available from: <https://doi.org/10.1186/s40066-017-0130-8>

Anand, U., Jacobo-Herrera, N., Altemimi, A. and Lakhssassi, N. 2019. A comprehensive review on medicinal plants as antimicrobial therapeutics: Potential avenues of biocompatible drug discovery. *Metabolites*. **9**(11). Available from: <https://doi.org/10.3390/metabo9110258>

Andrady, A.L. 2008. *Science and technology of polymer nanofibers*. [Online]. New Jersey, USA: John Wiley & Sons, Inc. [Accessed 19 June 2025]. Available from: <https://ereader.perlego.com/1/book/2774721/6>

Anderson, T.J. and Lamsa, B.P. 2011. Zein extraction from corn, corn products, and coproducts and modifications for various applications: A review. *Cereal Chemistry*. **88**(2), pp.159-173. Available from: <https://doi.org/10.1094/CCHEM-06-10-0091>

Anisong, N., Siripongvutikorn, S., Wichienchot, S. and Puttarak, P. 2022. A comprehensive review on nutritional contents and functional properties of *Gnetum gnemon* Linn. *Food Science and Technology*. **42**. Available from: <https://doi.org/10.1590/fst.100121>

Ansarifar, E. and Moradinezhad, F. 2021. Preservation of strawberry fruit quality via the use of active packaging with encapsulated thyme essential oil in zein nanofiber film. *International Journal of Food Science and Technology*. **56**(9), pp.4239-4247. Available from: <https://doi.org/10.1111/ijfs.15130>

Ansarifar, E. and Moradinezhad, F. 2022. Encapsulation of thyme essential oil using electrospun zein fiber for strawberry preservation. *Chemical and Biological Technologies in Agriculture*. **9**(1), p2. Available from: <https://doi.org/10.1186/s40538-021-00267-y>

Anu Bhushani, J. and Anandharamakrishnan, C. 2014. Electrospinning and electro spraying techniques: Potential food based applications. *Trends in Food Science & Technology*. **38**(1), pp.21-33. Available from: <https://doi.org/10.1016/j.tifs.2014.03.004>

Anwar, S., Mohammad, T., Shamsi, A., Queen, A., Parveen, S., Luqman, S., Hasan, G.M., Alamry, K.A., Azum, N., Asiri, A.M. and Hassan, M.I. 2020.

- Discovery of hordenine as a potential inhibitor of pyruvate dehydrogenase kinase 3: Implication in lung cancer therapy. *Biomedicines*. [Online]. **8**(5). Available from: <https://doi.org/10.3390/biomedicines8050119>
- Araujo, A.A.S., Mercuri, L.P., Seixas, S.R.S., Storpirtis, S. and Matos, J.R. 2006. Determination of moisture and ash contents of commercial guarana samples using conventional methods and thermal analysis. *Brazilian Journal of Pharmaceutical*. **42**(2), p[no pagination]. Available from: <https://doi.org/10.1590/S1516-93322006000200013>
- Arcan, I. and Yemenicioglu, A. 2011. Incorporating phenolic compounds opens a new perspective to use zein films as flexible bioactive packaging materials. *Food Research International*. **44**(2), pp.550-556. Available from: <https://doi.org/10.1016/j.foodres.2010.11.034>
- Arcan, I. and Yemenicioglu, A. 2013. Development of flexible zein–wax composite and zein–fatty acid blend films for controlled release of lysozyme. *Food Research International*. **51**(1), pp.208-216. Available from: <https://doi.org/10.1016/j.foodres.2012.12.011>
- Arezoo, E., Mohammadreza, E., Maryam, M. and Abdorreza, M.N. 2020. The synergistic effects of cinnamon essential oil and nano TiO<sub>2</sub> on antimicrobial and functional properties of sago starch films. *International Journal of Biological Macromolecules*. **157**, pp.743-751. Available from: <https://doi.org/10.1016/j.ijbiomac.2019.11.244>
- ASTM. 2004. *Standard Guide for Determination of Thickness of Plastic Film Test Specimens*. Pennsylvania, USA: ASTM International.
- ASTM. 2010. *D882 Standard test method for tensile properties of thin plastic sheeting*. Pennsylvania, USA: ASTM International.
- ASTM. 2012. *D5988-12 Standard test method for determining aerobic biodegradation of plastic materials in soil*. Pennsylvania, United States: ASTM International.
- ATCC. 2021. *Reviving freeze-dried microorganisms instructional guide*. [Leaflet]. Virginia, USA: American Type Culture Collection.
- Atun, S., Arianingrum, R. and Masatake, N. 2007. Some phenolic compounds from stem bark of Melinjo (*Gnetum gnemon*) and their activity test antioxidant and UV-B protection. In: *JSChem-ITB-UKM-2007*: JSChem-ITB-UKM-2007.
- Ayivi, R.D. and Ibrahim, S.A. 2022. Lactic acid bacteria: an essential probiotic and starter culture for the production of yoghurt. *International Journal of Food Science & Technology*. **57**(11), pp.7008-7025. Available from: <https://doi.org/10.1111/ijfs.16076>
- Azevedo, H.S. and Reis, R.L. 2005. Understanding the enzymatic degradation of biodegradable polymers and strategies to control their degradation rate. In: Reis, R.L. and Roman, J.S. eds. *Biodegradable systems in tissue engineering and regenerative medicine*. [Online]. CRC Press LLC, pp.177-201.

- Azwanida, N.N. 2015. A review on the extraction methods use in medicinal plants, principle, strength and limitation. *Medicinal & Aromatic Plants*. **04**(03). Available from: <https://doi.org/10.4172/2167-0412.1000196>
- Badia, J.D., Stromberg, E., Kittikorn, T., Ek, M., Karlsson, S. and Ribes-Greus, A. 2017. Relevant factors for the eco-design of polylactide/sisal biocomposites to control biodegradation in soil in an end-of-life scenario. *Polymer Degradation and Stability*. **143**, pp.9-19. Available from: <https://doi.org/10.1016/j.polymdegradstab.2017.06.004>
- Bailly, C. and Vergoten, G. 2020. Glycyrrhizin: An alternative drug for the treatment of COVID-19 infection and the associated respiratory syndrome? *Pharmacology & Therapeutics*. **214**, p107618. Available from: <https://doi.org/10.1016/j.pharmthera.2020.107618>
- Bai, Y., Huang, Z.-H. and Kang, F. 2014. Electrospun preparation of microporous carbon ultrafine fibers with tuned diameter, pore structure and hydrophobicity from phenolic resin. *Carbon*. **66**, pp.705-712. Available from: <https://doi.org/10.1016/j.carbon.2013.09.074>
- Bakkali, F., Averbeck, S., Averbeck, D., Zhiri, A., Baudoux, D. and Idaomar, M. 2006. Antigenotoxic effects of three essential oils in diploid yeast (*Saccharomyces cerevisiae*) after treatments with UVC radiation, 8-MOP plus UVA and MMS. *Mutation Research*. **606**(1-2), pp.27-38. Available from: <https://doi.org/10.1016/j.mrgentox.2006.02.005>
- Bandekar, J. 1992. Amide modes and protein conformation. *Biochimica et Biophysica Acta (BBA) - Protein Structure and Molecular Enzymology*. **1120**(2), pp.123-143. Available from: [https://doi.org/10.1016/0167-4838\(92\)90261-B](https://doi.org/10.1016/0167-4838(92)90261-B)
- Banovic, M., Grunert, K.G., Barreira, M.M. and Fontes, M.A. 2009. Beef quality perception at the point of purchase: A study from Portugal. *Food Quality and Preference*. **20**(4), pp.335-342. Available from: <https://doi.org/10.1016/j.foodqual.2009.02.009>
- Barish, J. A. and Goddard, J. M. 2011. Polyethylene glycol grafted polyethylene: A versatile platform for nonmigratory active packaging applications. *Journal of Food Science*. **76**(9), pp.586-591. Available from: <https://doi.org/10.1111/j.1750-3841.2011.02396.x>
- Barth, A. 2007. Infrared spectroscopy of proteins. *Biochimica et Biophysica Acta (BBA) - Bioenergetics*. **1767**(9), pp.1073-1101. Available from: <https://doi.org/10.1016/j.bbabi.2007.06.004>
- Barua, C.C., Haloi, P. and Barua, I.C. 2015. *Gnetum gnemon* linn.: A comprehensive review on its biological, pharmacological and pharmacognostical potentials. *International Journal of Pharmacognosy and Phytochemical Research*. **7**(3), pp.531-539. Available from: [https://www.researchgate.net/publication/281759358\\_Gnetum\\_gnemon\\_linn\\_A\\_comprehensive\\_review\\_on\\_its\\_biological\\_pharmacological\\_and\\_pharmacognostical\\_potentials](https://www.researchgate.net/publication/281759358_Gnetum_gnemon_linn_A_comprehensive_review_on_its_biological_pharmacological_and_pharmacognostical_potentials)
- Basri, D.F., Raziye, S., Paden, M. and Jalifah, L. 2005. Evaluation of antimicrobial activities of the crude extracts from *Garcinia atroviridis* and

*Solanum torvum*. *Malaysian Journal of Science*. **24**, pp.233-238. Available from: <https://www.semanticscholar.org/paper/Evaluation-of-antimicrobial-activities-of-the-crude-D.F-Sharif/354a12a327598a15c1008f06bfd623ef8ef6fb99>

Beasley, M.M., Bartelink, E.J., Taylor, L. and Miller, R.M. 2014. Comparison of transmission FTIR, ATR, and DRIFT spectra: implications for assessment of bone bioapatite diagenesis. *Journal of Archaeological Science*. **46**, pp.16-22. Available from: <https://doi.org/10.1016/j.jas.2014.03.008>

Beketov, G. and Shynkarenko, O. 2022. Surface wetting and contact angle: basics and characterisation. *Himia, Fizika ta Tehnologija Poverhni*. **13**, pp.3-35. Available from: <https://doi.org/10.15407/hftp13.01.003>

Benzie, I.F.F. and Strain, J.J. 1999. Ferric reducing/antioxidant power assay: Direct measure of total antioxidant activity of biological fluids and modified version for simultaneous measurement of total antioxidant power and ascorbic acid concentration. *Methods in Enzymology*. [Online]. **299**, pp.15-27. [Accessed 1999/01/01/]. Available from: [https://doi.org/10.1016/S0076-6879\(99\)99005-5](https://doi.org/10.1016/S0076-6879(99)99005-5)

Bhat, R. and Yahya, N.b. 2014. Evaluating belinjau (*Gnetum gnemon* L.) seed flour quality as a base for development of novel food products and food formulations. *Food Chemistry*. **156**, pp.42-49. Available from: <https://doi.org/10.1016/j.foodchem.2014.01.063>

Billeter, D., Zhu, M. and Inman, J.J. 2012. Transparent packaging and consumer purchase decisions. *ACR North American Advances*.

Bintsis, T. 2017. Foodborne pathogens. *AIMS Microbiology*. **3**(3), pp.529-563. Available from: <https://doi.org/10.3934/microbiol.2017.3.529>

Biorender.com. 2024a. *Basic electrospinning set-up*. Biorender.

Biorender.com. 2024b. *Solvent extraction process for medicinal plants*. Biorender.

Bitwell, C., Indra, S.S., Luke, C. and Kakoma, M.K. 2023. A review of modern and conventional extraction techniques and their applications for extracting phytochemicals from plants. *Scientific African*. **19**, pe01585. Available from: <https://doi.org/10.1016/j.sciaf.2023.e01585>

Blasco, A. J., Rogerio, M. C., Gonzalez, M. C. and Escarpa, A. 2005. "Electrochemical Index" as a screening method to determine "total polyphenolics" in foods: A proposal. *Analytica Chimica Acta*. **539**(1-2), pp.237-244. Available from: <https://doi.org/10.1016/j.aca.2005.02.056>

Blossey, R. 2003. Self-cleaning surfaces — virtual realities. *Nature Materials*. **2**(5), pp.301-306. Available from: <https://doi.org/10.1038/nmat856>

Bottom, R. 2008. Thermogravimetric analysis. In: Paul, G. ed. *Principles and applications of thermal analysis*. Oxford, UK: Blackwell Publishing, pp.87-118.

Bozkurt, H. 2007. Comparison of the effects of sesame and *Thymbra spicata* oil during the manufacturing of Turkish dry-fermented sausage. *Food Control*.

- 18**(2), pp.149-156. Available from:  
<https://doi.org/10.1016/j.foodcont.2005.09.009>
- Bredahl, L., Grunert, K.G. and Fertin, C. 1998. Relating consumer perceptions of pork quality to physical product characteristics. *Food Quality and Preference*. **9**(4), pp.273-281. Available from: [https://doi.org/10.1016/S0950-3293\(98\)00007-X](https://doi.org/10.1016/S0950-3293(98)00007-X)
- Bruno, T.J. 1999. Sampling accessories for infrared spectrometry. *Applied Spectroscopy Reviews*. **34**(1-2), pp.91-120. Available from:  
<https://doi.org/10.1081/ASR-100100840>
- Bubonja-Sonje, M., Giacometti, J. and Abram, M. 2011. Antioxidant and antilisterial activity of olive oil, cocoa and rosemary extract polyphenols. *Food Chemistry*. **127**(4), pp.1821-1827. Available from:  
<https://doi.org/10.1016/j.foodchem.2011.02.071>
- Burt, S. 2004. Essential oils: their antibacterial properties and potential applications in foods—a review. *International Journal of Food Microbiology*. **94**(3), pp.223-253. Available from:  
<https://doi.org/10.1016/j.ijfoodmicro.2004.03.022>
- Cacace, J.E. and Mazza, G. 2003. Optimization of extraction of anthocyanins from black currants with aqueous ethanol. *Journal of Food Science*. **68**(1), pp.240-248. Available from: <https://doi.org/10.1111/j.1365-2621.2003.tb14146.x>
- Camel, V. 2001. Recent extraction techniques for solid matrices—supercritical fluid extraction, pressurized fluid extraction and microwave-assisted extraction: their potential and pitfalls. *Analyst*. **126**(7), pp.1182-1193. Available from:  
<https://doi.org/10.1039/B008243K>
- Carden, A. and Morris, M.D. 2000. Application of vibrational spectroscopy to the study of mineralized tissues (review). *Journal of Biomedical Optics*. **5**(3), pp.259-268. Available from: <https://doi.org/10.1117/1.429994>
- Carpenter, C.E., Cornforth, D.P. and Whittier, D. 2001. Consumer preferences for beef color and packaging did not affect eating satisfaction. *Meat Science*. **57**(4), pp.359-363. Available from: [https://doi.org/10.1016/S0309-1740\(00\)00111-X](https://doi.org/10.1016/S0309-1740(00)00111-X)
- CDC. 2012. *2012 Salmonella outbreak associated with a raw scraped ground tuna product*. [Online]. [Accessed 6 December 2024]. Available from:  
[https://archive.cdc.gov/www\\_cdc\\_gov/salmonella/bareilly-04-12/index.html#:~:text=A%20total%20of%20425%20persons%20infected%20with%20the,persons%20were%20hospitalized%2C%20and%20no%20deaths%20were%20reported.](https://archive.cdc.gov/www_cdc_gov/salmonella/bareilly-04-12/index.html#:~:text=A%20total%20of%20425%20persons%20infected%20with%20the,persons%20were%20hospitalized%2C%20and%20no%20deaths%20were%20reported.)
- CDC. 2021a. *Outbreaks of E. coli infections*. [Online]. [Accessed 18 December]. Available from: <https://www.cdc.gov/ecoli/outbreaks/index.html>
- CDC. 2021b. *Salmonella*. [Online]. [Accessed 21 July]. Available from:  
<https://www.cdc.gov/salmonella/>

- Chahyadi, A. and Elfahmi. 2020. The influence of extraction methods on rutin yield of cassava leaves (*Manihot esculenta* Crantz). *Saudi Pharmaceutical Journal*. **28**(11), pp.1466-1473. Available from: <https://doi.org/10.1016/j.jsps.2020.09.012>
- Chan, C.-H., Yusoff, R., Ngoh, G.-C. and Kung, F.W.-L. 2011. Microwave-assisted extractions of active ingredients from plants. *Journal of Chromatography A*. **1218**(37), pp.6213-6225. Available from: <https://doi.org/10.1016/j.chroma.2011.07.040>
- Cheesman, M.J., Shivashekaregowda, N.K.H. and Cock, I.E. 2023. Bacterial foodborne illness in Malaysia: *Terminalia* spp. as a potential resource for treating infections and countering antibiotic resistance. *Malays Journal of Medical Sciences*. **30**(2), pp.42-54. Available from: <https://doi.org/10.21315/mjms2023.30.2.4>
- Chen, C., Du, Y., Zuo, G., Chen, F., Liu, K. and Zhang, L. 2020. Effect of storage condition on the physico-chemical properties of corn–wheat starch/zein edible bilayer films. *Royal Society Open Science*. **7**(2), p191777. Available from: <https://doi.org/10.1098/rsos.191777>
- Chen, J., Zhang, R., Qi, X., Zhou, B., Wang, J., Chen, Y. and Zhang, H. 2017. Epidemiology of foodborne disease outbreaks caused by *Vibrio parahaemolyticus* during 2010–2014 in Zhejiang Province, China. *Food Control*. **77**, pp.110-115. Available from: <https://doi.org/10.1016/j.foodcont.2017.02.004>
- Cheng, Y., Xu, Q., Liu, J., Zhao, C., Xue, F. and Zhao, Y. 2014. Decomposition of five phenolic compounds in high temperature water. *Journal of the Brazilian Chemical Society*. **25**. Available from: <https://doi.org/10.5935/0103-5053.20140201>
- Chew, Y.-L. and Lim, Y.-Y. 2018. Evaluation and comparison of antioxidant activity of leaves, pericarps and pulps of three *Garcinia* species in Malaysia. *Free Radicals and Antioxidants*. **8**(2), pp.130-134. Available from: <https://doi.org/10.5530/fra.2018.2.19>
- Chuaijit, S., Punsawad, C., Winoto, V., Plaingam, W., Kongkaew, I., Phetcharat, A., Ichikawa, T., Kubo, M., Kawakami, F., Tedasen, A. and Chatatikun, M. 2024. Leaf extract of *Garcinia atroviridis* promotes anti-heat stress and antioxidant effects in *Caenorhabditis elegans*. *Frontiers in Pharmacology*. **15**. Available from: <https://doi.org/10.3389/fphar.2024.1331627>
- CLSI. 2012a. *Performance Standards for Antimicrobial Disk Susceptibility Tests; Approved Standard—Eleventh Edition*. Pennsylvania, USA: Clinical and Laboratory Standards Institute.
- CLSI. 2012b. *Methods for Dilution Antimicrobial Susceptibility Tests for Bacteria That Grow Aerobically; Approved Standard—Ninth Edition*. Pennsylvania, USA: Clinical and Laboratory Standards Institute.
- Coates, J. 2006. Interpretation of infrared spectra, A practical approach. *Encyclopedia of Analytical Chemistry*.

- Cockell, C.S. and Knowland, J. 1999. Ultraviolet radiation screening compounds. *Biological Reviews*. **74**(3), pp.311-345. Available from: <https://doi.org/10.1111/j.1469-185X.1999.tb00189.x>
- Coleman, M.M., Skrovanek, D.J., Hu, J. and Painter, P.C. 1988. Hydrogen bonding in polymer blends. 1. FTIR studies of urethane-ether blends. *Macromolecules*. **21**(1), pp.59-65. Available from: <https://doi.org/10.1021/ma00179a014>
- Conde-Hernandez, L.A., Espinosa-Victoria, J.R., Trejo, A. and Guerrero-Beltran, J.A. 2017. CO<sub>2</sub>-supercritical extraction, hydrodistillation and steam distillation of essential oil of rosemary (*Rosmarinus officinalis*). *Journal of Food Engineering*. **200**, pp.81-86. Available from: <https://doi.org/10.1016/j.jfoodeng.2016.12.022>
- Corradini, E., Curti, P.S., Meniqueti, A.B., Martins, A.F., Rubira, A.F. and Muniz, E.C. 2014. Recent advances in food-packing, pharmaceutical and biomedical applications of zein and zein-based materials. *International Journal of Molecular Sciences*. [Online]. **15**(12), pp.22438-22470. Available from: <https://doi.org/10.3390/ijms151222438>
- Croteau, R., Kutchan, T.M. and Lewis, N.G. 2000. Natural products (secondary metabolites). In: Buchanan, B., Gruissem, W. and Jones, R. eds. *Biochemistry & molecular biology of plants*. American Society of Plant Physiologists, pp.1250-1318.
- D'Almeida, A.R. and Dias, M.L. 1997. Comparative study of shear degradation of carboxymethylcellulose and poly(ethylene oxide) in aqueous solution. *Polymer Degradation and Stability*. **56**(3), pp.331-337. Available from: [https://doi.org/10.1016/S0141-3910\(96\)00187-5](https://doi.org/10.1016/S0141-3910(96)00187-5)
- Dai, J. and Mumper, R.J. 2010. Plant phenolics: Extraction, analysis and their antioxidant and anticancer properties. *Molecules*. [Online]. **15**(10), pp.7313-7352. Available from: <https://doi.org/10.3390/molecules15107313>
- Daniel, N., Casadevall, N., Sun, P., Sugden, D. and Aldin, V. 2020. *The Burden of Foodborne Disease in the UK 2018*. Food Standards Agency.
- Dankowska, A. and Kowalewski, W. 2019. Tea types classification with data fusion of UV-Vis, synchronous fluorescence and NIR spectroscopies and chemometric analysis. *Spectrochimica Acta Part A: Molecular and Biomolecular Spectroscopy*. **211**, pp.195-202. Available from: <https://doi.org/10.1016/j.saa.2018.11.063>
- Debeaufort, F., Quezada-Gallo, J.-A. and Voilley, A. 1998. Edible films and coatings: Tomorrow's packagings: A review. *Critical Reviews in Food Science and Nutrition*. **38**(4), pp.299-313. Available from: <https://doi.org/10.1080/10408699891274219>
- Delazar, A., Nahar, L., Hamedeyazdan, S. and Sarker, S.D. 2012. Microwave-assisted extraction in natural products isolation. In: Sarker, S.D. and Nahar, L. eds. *Natural Products Isolation Methods and Protocols*. [Online]. Third ed. Humana Press, pp.89-115. Available from: <https://doi.org/10.1007/978-1-61779-624-1>

- De Schoenmaker, B., Van der Schueren, L., De Vrieze, S., Westbroek, P. and De Clerck, K. 2011. Wicking properties of various polyamide nanofibrous structures with an optimized method. *Journal of Applied Polymer Science*. **120**(1), pp.305-310. Available from: <https://doi.org/10.1002/app.33117>
- Demir, M.M., Yilgor, I., Yilgor, E. and Erman, B. 2002. Electrospinning of polyurethane fibers. *Polymer*. **43**(11), pp.3303-3309. Available from: [https://doi.org/10.1016/S0032-3861\(02\)00136-2](https://doi.org/10.1016/S0032-3861(02)00136-2)
- Desai, N. and Gaikwad, D.K. 2014. Essential oil composition and antibacterial activity of *Colubrina asiatica* (L.) Brong. *Asian Journal of Pharmaceutical Research and Development*. **2**(4), pp.13-17. Available from: <https://ajprd.com/index.php/journal/article/view/206>
- Desai, N., Dethé, U.L. and Gaikwad, D.K. 2015. In vitro antioxidant activities and antimicrobial efficacy of Asian snakewood; *Colubrina asiatica* (L.) Brong. *Research Journal of Medicinal Plant*. **9**, pp.307-320. Available from: <https://doi.org/10.3923/rjmp.2015.307.320>
- Dhumal, C.V. and Sarkar, P. 2018. Composite edible films and coatings from food-grade biopolymers. *J Food Sci Technol*. **55**(11), pp.4369-4383. Available from: <https://doi.org/10.1007/s13197-018-3402-9>
- di Franco, C.R., Cyras, V.P., Busalmen, J.P., Ruseckaite, R.A. and Vázquez, A. 2004. Degradation of polycaprolactone/starch blends and composites with sisal fibre. *Polymer Degradation and Stability*. **86**(1), pp.95-103. Available from: <https://doi.org/10.1016/j.polymdegradstab.2004.02.009>
- Dillon, V.M. and Board, R.G. 1991. Yeasts associated with red meats. *Journal of Applied Bacteriology*. **71**(2), pp.93-108. Available from: <https://doi.org/10.1111/j.1365-2672.1991.tb02962.x>
- Do, Q.D., Angkawijaya, A.E., Tran-Nguyen, P.L., Huynh, L.H., Soetaredjo, F.E., Ismadji, S. and Ju, Y.-H. 2014. Effect of extraction solvent on total phenol content, total flavonoid content, and antioxidant activity of *Limnophila aromatica*. *Journal of Food and Drug Analysis*. **22**(3), pp.296-302. Available from: <https://doi.org/10.1016/j.jfda.2013.11.001>
- Dobson, P. and Yadav, A. 2012. *Packaging in a market economy: The economic and commercial role of packaging communication*. [Online]. University of East Anglia. [Accessed 27 February 2026]. Available from: <http://www.packagingfedn.co.uk/images/reports/Packaging%20in%20a%20Market%20Economy.pdf>
- Dong, F., Padua, G.W. and Wang, Y. 2013. Controlled formation of hydrophobic surfaces by self-assembly of an amphiphilic natural protein from aqueous solutions. *Soft Matter*. **9**(25), pp.5933-5941. Available from: <https://doi.org/10.1039/C3SM50667C>
- Doshi, J. and Reneker, D.H. 1995. Electrospinning process and applications of electrospun fibers. *Journal of Electrostatics*. **35**(2), pp.151-160. Available from: [https://doi.org/10.1016/0304-3886\(95\)00041-8](https://doi.org/10.1016/0304-3886(95)00041-8)

- Drago, E., Franco, P., Campardelli, R., De Marco, I. and Perego, P. 2022. Zein electrospun fibers purification and vanillin impregnation in a one-step supercritical process to produce safe active packaging. *Food Hydrocolloids*. **122**, p107082. Available from: <https://doi.org/10.1016/j.foodhyd.2021.107082>
- Dutta, P.P., Bordoloi, M., Roy, S., Narzary, B., Gogoi, K., Bhattacharyya, D.R., Mohapatra, P.K. and Mazumder, B. 2018. Antiplasmodial activity of *Gnetum gnemon* leaves and compounds isolated from them. *Natural Product Communications*. **13**(10), p1934578X1801301007. Available from: <https://doi.org/10.1177/1934578X1801301007>
- Earnest, C.M. 1988. *Compositional Analysis by Thermogravimetry*, ASTM STP 997. Philadelphia: ASTM International.
- Eldesouky, A., Pulido, A.F. and Mesias, F.J. 2015. The role of packaging and presentation format in consumers' preferences for food: an application of projective techniques. *Journal of Sensory Studies*. **30**(5), pp.360-369. Available from: <https://doi.org/10.1111/joss.12162>
- Escamilla-Garcia, M., Calderon-Dominguez, G., Chanona-Perez, J.J., Mendoza-Madriral, A.G., Di Pierro, P., Garcia-Almendarez, B.E., Amaro-Reyes, A. and Regalado-Gonzalez, C. 2017. Physical, structural, barrier, and antifungal characterization of chitosan-zein edible films with added essential oils. *International Journal of Molecular Sciences*. **18**(11). Available from: <https://doi.org/10.3390/ijms18112370>
- Esen, A. 1987. A proposed nomenclature for the alcohol-soluble proteins (zeins) of maize (*Zea mays* L.). *Journal of Cereal Science*. **5**(2), pp.117-128. Available from: [https://doi.org/10.1016/S0733-5210\(87\)80015-2](https://doi.org/10.1016/S0733-5210(87)80015-2)
- European-Bioplastics. 2024. Bioplastics market development update 2024. Berlin, Germany: European Bioplastics.
- Fang, J., Niu, H., Lin, T. and Wang, X. 2008. Applications of electrospun nanofibers. *Chinese Science Bulletin*. **53**, pp.2265-2286. Available from: <https://doi.org/10.1007/s11434-008-0319-0>
- FAO. 2019. *Moving forward on food loss and waste reduction*. Rome, Italy: Food and Agriculture Organization (FAO).
- Farnsworth, N.R., Akerele, O., Bingel, A.S., Soejarto, D.D. and Guo, Z. 1985. Medicinal plants in therapy. *Bulletin of the World Health Organization*. **63**(6), p16.
- Faustman, C. and Cassens, R.G. 1990. The biochemical basis for discoloration in fresh meat: A review. *Journal of Muscle Foods*. **1**(3), pp.217-243. Available from: <https://doi.org/10.1111/j.1745-4573.1990.tb00366.x>
- FDA. 2018. FDA-2016-D-2817. *Liposome drug products chemistry, manufacturing, and controls; human pharmacokinetics and bioavailability; and labeling documentation - guidance for industry*. USA: U.S. Department of Health and Human Services Food and Drug Administration Center for Drug Evaluation and Research.

*Food and drugs-listing of specific substances affirmed as GRAS 2024.* (Sec. 184.1984 Zein). Silver Spring, MD, USA: U.S. Food and Drug Administration.

Federici, E., Selling, G.W., Campanella, O.H. and Jones, O.G. 2020. Incorporation of plasticizers and co-proteins in zein electrospun fibers. *Journal of Agricultural and Food Chemistry*. **68**(49), pp.14610-14619. Available from: <https://doi.org/10.1021/acs.jafc.0c03532>

Fernandez, K. and Agosin, E. 2007. Quantitative analysis of red wine tannins using Fourier-transform mid-infrared spectrometry. *Journal of Agricultural and Food Chemistry*. **55**(18), pp.7294-7300. Available from: <https://doi.org/10.1021/jf071193d>

Fidrianny, I., Ayu, D. and Hartati, R. 2015. Antioxidant capacities, phenolic, flavonoid and carotenoid content of various polarities extracts from three organs of *Sechium edule* (Jacq.) Swartz. **7**, pp.914-920.

Flora-Fauna-Web. 2023. *Colubrina asiatica* (L.) Brongn. [Online]. [Accessed 18 December 2024]. Available from: <https://www.nparks.gov.sg/florafaunaweb/flora/3/6/3679#>

Fong, H., Chun, I. and Reneker, D.H. 1999. Beaded nanofibers formed during electrospinning. *Polymer*. **40**(16), pp.4585-4592. Available from: [https://doi.org/10.1016/S0032-3861\(99\)00068-3](https://doi.org/10.1016/S0032-3861(99)00068-3)

Foods, I.C.o.M.S.f. 1986. *Microorganisms in foods 2: Sampling for microbiological analysis: Principles and specific applications*. Toronto, Canada: University of Toronto Press.

Food Standards Agency (FSA). 2022. *Irradiated food*. [Online]. [Accessed 27 February 2026]. Available from: <https://www.food.gov.uk/safety-hygiene/irradiated-food>

Forato, L.A., Bernardes-Filho, R. and Colnago, L.A. 1998. Protein structure in KBr pellets by Infrared spectroscopy. *Analytical Biochemistry*. **259**(1), pp.136-141. Available from: <https://doi.org/10.1006/abio.1998.2599>

Forato, L.A., Bicudo, T.D.C. and Colnago, L.A. 2003. Conformation of  $\alpha$  zeins in solid state by Fourier transform IR. *Biopolymers*. **72**(6), pp.421-426. Available from: <https://doi.org/10.1002/bip.10481>

Fortier, C.A., Cintron, M.S., Peralta, D., Hoven, T.V., Fontenot, K., Rodgers, J.E. and Delhom, C. 2019. A comparison of the accelerated solvent extraction method to the Soxhlet method in the extraction of cotton fiber wax. *AATCC Journal of Research*. **6**(1), pp.15-20. Available from: <https://doi.org/10.14504/ajr.6.1.3>

Foti, M.C. 2015. Use and Abuse of the DPPH• Radical. *Journal of Agricultural and Food Chemistry*. **63**(40), pp.8765-8776. Available from: <https://doi.org/10.1021/acs.jafc.5b03839>

Fracassetti, D., Del Bo', C., Simonetti, P., Gardana, C., Klimis-Zacas, D. and Ciappellano, S. 2013. Effect of time and storage temperature on anthocyanin decay and antioxidant Activity in wild blueberry (*Vaccinium angustifolium*)

powder. *Journal of Agricultural and Food Chemistry*. **61**(12), pp.2999-3005. Available from: <https://doi.org/10.1021/jf3048884>

Frank, L., Wenig, M., Ghirardo, A., van der Krol, A., Vlot, A.C., Schnitzler, J.-P. and Rosenkranz, M. 2021. Isoprene and  $\beta$ -caryophyllene confer plant resistance via different plant internal signalling pathways. *Plant, Cell & Environment*. **44**(4), pp.1151-1164. Available from: <https://doi.org/10.1111/pce.14010>

FSA-Ireland. 2022. *Validation of product shelf-life (Revision 5)*. Dublin, Ireland: Food Safety Authority of Ireland.

Gaikwad, A., Hlushko, H., Karimineghlani, P., Selin, V. and Sukhishvili, S.A. 2020. Hydrogen-bonded, mechanically strong nanofibers with tunable antioxidant activity. *ACS Applied Materials & Interfaces*. **12**(9), pp.11026-11035. Available from: <https://doi.org/10.1021/acsami.9b23212>

Garcia-Garcia, R. and Searle, S.S. 2016. Preservatives: food use. In: Caballero, B., Finglas, P.M. and Toldra, F. eds. *Encyclopedia of Food and Health*. Oxford: Academic Press, pp.505-509.

Garnier, L., Valence, F. and Mounier, J. 2017. Diversity and control of spoilage fungi in dairy products: an update. *Microorganisms*. **5**(3). Available from: <https://doi.org/10.3390/microorganisms5030042>

Gerassimidou, S., Geueke, B., Groh, K.J., Muncke, J., Hahladakis, J.N., Martin, O.V. and Iacovidou, E. 2023. Unpacking the complexity of the polyethylene food contact articles value chain: A chemicals perspective. *Journal of Hazardous Materials*. **454**, p131422. Available from: <https://doi.org/10.1016/j.jhazmat.2023.131422>

Ghannoum, M.A. and Rice, L.B. 1999. Antifungal agents: mode of action, mechanisms of resistance, and correlation of these mechanisms with bacterial resistance. *Clin Microbiol Rev*. **12**(4), pp.501-517. Available from: <https://doi.org/10.1128/cmr.12.4.501>

Ghenabzia, I., Hemmami, H., Ben Amor, I., Zeghoud, S., Ben Seghir, B. and Hammoudi, R. 2023. Different methods of extraction of bioactive compounds and their effect on biological activity: A review. *International Journal of Secondary Metabolite*. **10**(4), pp.469-494. Available from: <https://doi.org/10.21448/ijsm.1225936>

Gidlof, K., Anikin, A., Lingonblad, M. and Wallin, A. 2017. Looking is buying. How visual attention and choice are affected by consumer preferences and properties of the supermarket shelf. *Appetite*. **116**, pp.29-38. Available from: <https://doi.org/10.1016/j.appet.2017.04.020>

Gil, M.I., Tomas-Barberan, F.A., Hess-Pierce, B. and Kader, A.A. 2002. Antioxidant capacities, phenolic compounds, carotenoids, and vitamin C contents of nectarine, peach, and plum cultivars from California. *Journal of Agricultural and Food Chemistry*. **50**(17), pp.4976-4982. Available from: <https://doi.org/10.1021/jf020136b>

Gill, A.O. and Gill, C.O. 2009. Packaging and the shelf life of fresh red and poultry meats. In: Robertson, G.L. ed. *Food packaging and shelf life*. [Online]. Boca Raton, USA: CRC Press, pp.259-277. [Accessed 16 April 2025]. Available from: <https://ereader.perlego.com/1/book/1696500/295>

Goksen, G., Fabra, M.J., Ekiz, H.I. and Lopez-Rubio, A. 2020. Phytochemical-loaded electrospun nanofibers as novel active edible films: Characterization and antibacterial efficiency in cheese slices. *Food Control*. **112**, p107133. Available from: <https://doi.org/10.1016/j.foodcont.2020.107133>

Gonnet, M., Lethuaut, L. and Boury, F. 2010. New trends in encapsulation of liposoluble vitamins. *Journal of Controlled Release*. **146**(3), pp.276-290. Available from: <https://doi.org/10.1016/j.jconrel.2010.01.037>

Gontard, N., Guilbert, S. and Cuq, J.-L. 1992. Edible wheat gluten films: Influence of the main process variables on film properties using response surface methodology. *Journal of Food Science*. **57**(1), pp.190-195. Available from: <https://doi.org/10.1111/j.1365-2621.1992.tb05453.x>

Griffiths, P.R. 1983. Fourier transform infrared spectrometry. *Science*. **222**(4621), pp.297-302. Available from: <https://doi.org/10.1126/science.6623077>

Gustafson, J.E., Liew, Y.C., Chew, S., Markham, J., Bell, H.C., Wyllie, S.G. and Warmington, J.R. 1998. Effects of tea tree oil on *Escherichia coli*. *Letters in Applied Microbiology*. **26**(3), pp.194-198. Available from: <https://doi.org/10.1046/j.1472-765X.1998.00317.x>

Gutierrez-Grijalva, E.P., Lopez- Martinez, L.X., Contreras-Angulo, L.A., Elizalde-Romero, C.A. and Heredia, J.B. 2020. Plant alkaloids: structures and bioactive properties. In: Swamy, M.K. ed. *Plant alkaloids: structures and bioactive properties*. Mexico: Springer Nature Singapore Pte Ltd, pp.85-117.

Halliwell, B. and Gutteridge, J.M.C. 1985. Free radicals in biology and medicine. In.

Hamidon, H., Susanti, D., Taher, M. and Zakaria, Z.A. 2017. *Garcinia atroviridis* - a review on phytochemicals and pharmacological properties. *Marmara Pharmaceutical Journal*. **21**, pp.38-47. Available from: <https://doi.org/10.12991/marupj.259879>

Handa, S.S. 2008. An overview of extraction techniques for medicinal and aromatic plants. In: Handa, S.S., Khanuja, S.P.S., Longo, G. and Rakesh, D.D. eds. *Extraction technologies for medicinal and aromatic plants*. Trieste, Italy: United Nations Industrial Development Organization and the International Centre for Science and High Technology, pp.21-54.

Hedberg, C.W., Levine, W.C., White, K.E., Carlson, R.H., Winsor, D.K., Cameron, D.N., MacDonald, K.L. and Osterholm, M.T. 1992. An international foodborne outbreak of Shigellosis associated with a commercial airline. *JAMA*. **268**(22), pp.3208-3212. Available from: <https://doi.org/10.1001/jama.1992.03490220052027>

Helander, I.M., Alakomi, H.-L., Latva-Kala, K., Mattila-Sandholm, T., Pol, I., Smid, E.J., Gorris, L.G. and von Wright, A. 1998. Characterization of the action

of selected essential oil components on Gram-negative bacteria. *Journal of Agricultural and Food Chemistry*. **46**(9), pp.3590-3595.

Hernandez, V., Ibarra, D., Triana, J. F., Martinez-Soto, B., Faundez, M., Vasco, D. A., Gordillo, L., Herrera, F., Garcia-Herrera, C. and Garmulewicz, A. 2022. Agar biopolymer films for biodegradable packaging: A reference dataset for exploring the limits of mechanical performance. *Materials*. **15**(11), p.17. Available from: <https://doi.org/10.3390/ma15113954>

Hikmawanti, E.N.P., Fatmawati, S. and Asri, A.W. 2021. The effect of ethanol concentrations as the extraction solvent on antioxidant activity of Katuk (*Sauropus androgynus* (L.) Merr.) leaves extracts. *IOP Conference Series: Earth and Environmental Science*. **755**(1), p012060. Available from: <https://doi.org/10.1088/1755-1315/755/1/012060>

Hobza, P. and Havlas, Z. 2002. Improper, blue-shifting hydrogen bond. *Theoretical Chemistry Accounts*. **108**(6), pp.325-334. Available from: <https://doi.org/10.1007/s00214-002-0367-5>

Hohman, M., Shin, M., Rutledge, G. and Brenner, M. 2001. Electrospinning and electrically forced jets. I. Stability theory. *Physics of Fluids*. **13**(8), pp.2201-2220. Available from: <https://doi.org/10.1063/1.1383791>

Hu, L., Zhao, P., Wei, Y., Guo, X., Deng, X. and Zhang, J. 2023. Properties of allicin–zein composite nanoparticle gelatin film and their effects on the quality of cold, fresh beef during storage. *Foods*. [Online]. **12**(19). Available from: <https://doi.org/10.3390/foods12193713>

Huang, Q., Yu, H. and Ru, Q. 2010. Bioavailability and delivery of nutraceuticals using nanotechnology. *Journal of Food Science*. **75**(1), pp.R50-R57. Available from: <https://doi.org/10.1111/j.1750-3841.2009.01457.x>

Hughes, J.M., Oiseth, S.K., Purslow, P.P. and Warner, R.D. 2014. A structural approach to understanding the interactions between colour, water-holding capacity and tenderness. *Meat Science*. **98**(3), pp.520-532. Available from: <https://doi.org/10.1016/j.meatsci.2014.05.022>

Huhtamaki, T., Tian, X., Korhonen, J.T. and Ras, R.H.A. 2018. Surface-wetting characterization using contact-angle measurements. *Nature Protocols*. **13**(7), pp.1521-1538. Available from: <https://doi.org/10.1038/s41596-018-0003-z>

Iliya, I., Ali, Z., Tanaka, T., Iinuma, M., Furusawa, M., Nakaya, K., Murata, J., Darnaedi, D., Matsuura, N. and Ubukata, M. 2003. Stilbene derivatives from *Gnetum gnemon* Linn. *Phytochemistry*. **62**, p5. Available from: [https://doi.org/10.1016/s0031-9422\(02\)00670-2](https://doi.org/10.1016/s0031-9422(02)00670-2)

Imam, S.H. and Gordon, S.H. 2002. Biodegradation of coproducts from industrially processed corn in a compost environment. *Journal of Polymers and the Environment*. **10**(4), pp.147-154. Available from: <https://doi.org/10.1023/A:1021144104458>

Ingram, L. 2011. *Small-flower opium poppy (Papaver somniferum ssp. setigerum (DC.) Corb.)*. USDA National Institute of Food and Agriculture. Available from: <https://www.invasive.org/browse/detail.cfm?imgnum=5402139>

Intawongse, M. and Pranprawit, A. 2024. Nutritional value, bioactive compounds, and antioxidant activity of Phak-liang (*Gnetum gnemon* Linn. var. *tenerum* Markgr.) in Surat Thani province, Thailand. *Suan Sunandha Science and Technology Journal*. **11**(2), pp.53-60. Available from: <https://doi.org/10.53848/ssstj.v11i2.816>

Irma, S., Risa, N. and Y, Y. 2021. Antifungal active fraction of *Peria pantai* (*Colubrina asiatica* (L.) Brong) leaf against fluconazole-resistance *Candida albicans*. *Asian Journal of Pharmaceutical Research and Development*. **9**(2), pp.1-5. Available from: <https://doi.org/10.22270/ajprd.v9i2.936>

ISO. 2019. *ISO 17556 Plastic- Determination of the ultimate aerobic biodegradability of plastic materials in soil by measuring the oxygen demand in a respirometer or the amount of carbon dioxide evolved*. Geneva, Switzerland: ISO.

Issanchou, S. 1996. Consumer expectations and perceptions of meat and meat product quality. *Meat Science*. **43**, pp.5-19. Available from: [https://doi.org/10.1016/0309-1740\(96\)00051-4](https://doi.org/10.1016/0309-1740(96)00051-4)

IUCN. 2024. *Plastic pollution*. [Online]. [Accessed 10 December 2024]. Available from: <https://iucn.org/resources/issues-brief/plastic-pollution>

Iulietto, M.F., Sechi, P., Borgogni, E. and Cenci-Goga, B.T. 2015. Meat spoilage: A critical review of a neglected alteration due to rosy slime producing bacteria. *Italian Journal of Animal Science*. **14**(3), pp.316-326. Available from: <https://doi.org/10.4081/ijas.2015.4011>

Jaakkola, J. J. and Knight, T. L. 2008. The role of exposure to phthalates from polyvinyl chloride products in the development of asthma and allergies: a systematic review and meta-analysis. *Environmental Health Perspectives*. **116**(7), pp.845-853. Available from: <https://doi.org/10.1289/ehp.10846>

Jambeck, J.R., Geyer, R., Wilcox, C., Siegler, T.R., Perryman, M., Andrady, A., Narayan, R. and Law, K.L. 2015. *Plastic waste inputs from land into the ocean*. USA.

Jamila, N., Khan, N., Hwang, I.M., Nho, E.Y., Choi, J.Y., Atlas, A., Khan, S.N., Amin, F., Javed, F. and Kim, K.S. 2020. Application of phytochemical and elemental profiling, chemometric multivariate analyses, and biological activities for characterization and discrimination of fruits of four *Garcinia* species. *Analytical Letters*. **53**(1), pp.122-139. Available from: <https://doi.org/10.1080/00032719.2019.1640244>

Jamiuddin, A., Kamariah Abu, S., Linda, B.L.L. and Abdalla Mohamed, J. 2019. Evaluation of antioxidant activity and phytochemical screening of leaves, barks, stems and fruits of *Alphitonia philippinensis* (Rhamnaceae) from Brunei Darussalam. *Pharmacognosy Journal*. **11**(5). Available from: <https://doi.org/10.5530/pj.2019.11.151>

Jena, B.S., Jayaprakasha, G.K., Singh, R.P. and Sakariah, K.K. 2002. Chemistry and biochemistry of (-)-hydroxycitric acid from *Garcinia*. *J Agric Food Chem*. **50**(1), pp.10-22. Available from: <https://doi.org/10.1021/jf010753k>

Jeon, Y.J., Jang, J.Y., Shim, J.H., Myung, P.K. and Chae, J.I. 2015. Esculetin, a coumarin derivative, exhibits anti-proliferative and pro-apoptotic activity in G361 human malignant melanoma. *Journal of Cancer Prevention*. **20**(2), pp.106-112. Available from: <https://doi.org/10.15430/jcp.2015.20.2.106>

Joseph, J. and Jemmis, E.D. 2007. Red-, blue-, or no-shift in hydrogen bonds: A unified explanation. *Journal of the American Chemical Society*. **129**(15), pp.4620-4632. Available from: <https://doi.org/10.1021/ja067545z>

Juven, B.J., Kanner, J., Schved, F. and Weisslowicz, H. 1994. Factors that interact with the antibacterial action of thyme essential oil and its active constituents. *Journal of Applied Bacteriology*. **76**(6), pp.626-631. Available from: <https://doi.org/10.1111/j.1365-2672.1994.tb01661.x>

Kabubii, Z.N., Mbaria, J.M., Mathiu, M.P., Wanjohi, J.M. and Nyaboga, E.N. 2023. Evaluation of seasonal variation, effect of extraction solvent on phytochemicals and antioxidant activity on *Rosmarinus officinalis* grown in different agro-ecological zones of Kiambu County, Kenya. *CABI Agriculture and Bioscience*. **4**(1), p1. Available from: <https://doi.org/10.1186/s43170-023-00141-x>

Kameoka, J., Reid, O., Yanou, Y., David, C., Robert, M., Geoffrey, W.C. and Craighead, H.G. 2003. A scanning tip electrospinning source for deposition of oriented nanofibres. *Nanotechnology*. **14**(10), p1124. Available from: <https://doi.org/10.1088/0957-4484/14/10/310>

Karatas, M. and Arslan, N. 2016. Flow behaviours of cellulose and carboxymethyl cellulose from grapefruit peel. *Food Hydrocolloids*. **58**, pp.235-245. Available from: <https://doi.org/10.1016/j.foodhyd.2016.02.035>

Kato, E., Tokunaga, Y. and Sakan, F. 2009. Stilbenoids isolated from the seeds of melinjo (*Gnetum gnemon* L.) and their biological activity. *Journal of Agricultural and Food Chemistry*. **57**(6), pp.2544-2549. Available from: <https://doi.org/10.1021/jf803077p>

Kato, H., Samizo, M., Kawabata, R., Takano, F. and Ohta, T. 2011. Stilbenoids from the melinjo (*Gnetum gnemon* L.) fruit modulate cytokine production in murine Peyer's patch cells ex vivo. *Planta Medica*. **77**(10), pp.1027-1034. Available from: <https://doi.org/10.1055/s-0030-1250742>

Kaufmann, B. and Christen, P. 2002. Recent extraction techniques for natural products: microwave-assisted extraction and pressurised solvent extraction. *Phytochemical Analysis*. **13**(2), pp.105-113. Available from: <https://doi.org/10.1002/pca.631>

Kavoosi, G., Rahmatollahi, A., Mohammad Mahdi Dadfar, S. and Mohammadi Purfard, A. 2014. Effects of essential oil on the water binding capacity, physico-mechanical properties, antioxidant and antibacterial activity of gelatin films. *LWT - Food Science and Technology*. **57**(2), pp.556-561. Available from: <https://doi.org/10.1016/j.lwt.2014.02.008>

Keukens, E.A.J., de Vrije, T., van den Boom, C., de Waard, P., Plasman, H.H., Thiel, F., Chupin, V., Jongen, W.M.F. and de Kruijff, B. 1995. Molecular basis of glycoalkaloid induced membrane disruption. *Biochimica et Biophysica Acta*

(BBA) - *Biomembranes*. **1240**(2), pp.216-228. Available from: [https://doi.org/10.1016/0005-2736\(95\)00186-7](https://doi.org/10.1016/0005-2736(95)00186-7)

Khalafi, N., Gharachorloo, M., Ganjloo, A. and Yousefi, S. 2023. Electrospun zein nanofibers containing anthocyanins extracted from red cabbage (*Brassica oleracea* L.). *Journal of Food Science*. **88**(11), pp.4620-4629. Available from: <https://doi.org/10.1111/1750-3841.16780>

Khameneh, B., Iranshahy, M., Soheili, V. and Fazly Bazzaz, B.S. 2019. Review on plant antimicrobials: a mechanistic viewpoint. *Antimicrobial Resistance & Infection Control*. **8**(1), p118. Available from: <https://doi.org/10.1186/s13756-019-0559-6>

Kim, H.S. and Chin, K.B. 2017. Evaluation of antioxidative activity of various levels of ethanol extracted tomato powder and application to pork patties. *Korean Journal for Food Science and Animal Resources*. **37**(2), pp.242-253. Available from: <https://doi.org/10.5851/kosfa.2017.37.2.242>

King, T., Dykes, G. and Kristianti, R. 2008. Comparative evaluation of methods commonly used to determine antimicrobial susceptibility to plant extracts and phenolic compounds. *J AOAC Int*. **91**(6), pp.1423-1429.

Kiss, A., Papp, V.A., Pál, A., Prokisch, J., Mirani, S., Toth, B.E. and Alshaal, T. 2025. Comparative study on antioxidant capacity of diverse food matrices: Applicability, suitability and inter-correlation of multiple assays to assess polyphenol and antioxidant status. *Antioxidants*. [Online]. **14**(3). Available from: <https://doi.org/10.3390/antiox14030317>

Klinchongkon, K., Intim, B., Milasing, N. and Khuwijitjaru, P. 2022. Effect of ethanol concentration and temperature on solubility of fructose. *Food Science and Technology Research*. **28**(1), pp.105-109. Available from: <https://doi.org/10.3136/fstr.FSTR-D-21-00191>

Knobloch, K., Alexander, P., Bernard, I., Hildegunde, W. and Weis, N. 1989. Antibacterial and antifungal properties of essential oil components. *Journal of Essential Oil Research*. **1**(3), pp.119-128. Available from: <https://doi.org/10.1080/10412905.1989.9697767>

Kong, L. and Ziegler, G.R. 2014. Fabrication of pure starch fibers by electrospinning. *Food Hydrocolloids*. **36**, pp.20-25. Available from: <https://doi.org/10.1016/j.foodhyd.2013.08.021>

Kong, Y., Zu, Y.-G., Fu, Y.-J., Liu, W., Chang, F.-R., Li, J., Chen, Y.-H., Zhang, S. and Gu, C.-B. 2010. Optimization of microwave-assisted extraction of cajaninstilbene acid and pinostrobin from pigeonpea leaves followed by RP-HPLC-DAD determination. *Journal of Food Composition and Analysis*. **23**(4), pp.382-388. Available from: <https://doi.org/10.1016/j.jfca.2009.12.009>

Koombhongse, S., Liu, W. and Reneker, D.H. 2001. Flat polymer ribbons and other shapes by electrospinning. *Journal of Polymer Science Part B: Polymer Physics*. **39**(21), pp.2598-2606. Available from: <https://doi.org/10.1002/polb.10015>

- Kosin, J., Ruangrunsi, N., Ito, C. and Furukawa, H. 1998. A xanthone from *Garcinia atroviridis*. *Phytochemistry*. **47**(6), pp.1167-1168. Available from: [https://doi.org/10.1016/S0031-9422\(98\)80095-2](https://doi.org/10.1016/S0031-9422(98)80095-2)
- Kriegel, C., Arecchi, A., Kit, K., McClements, D.J. and Weiss, J. 2008. Fabrication, functionalization, and application of electrospun biopolymer nanofibers. *Critical Reviews in Food Science and Nutrition*. **48**(8), pp.775-797. Available from: <https://doi.org/10.1080/10408390802241325>
- Kriegel, C., Kit, K.M., McClements, D.J. and Weiss, J. 2009. Electrospinning of chitosan–poly(ethylene oxide) blend nanofibers in the presence of micellar surfactant solutions. *Polymer*. **50**(1), pp.189-200. Available from: <https://doi.org/10.1016/j.polymer.2008.09.041>
- Krimm, S. and Bandekar, J. 1986. Vibrational spectroscopy and conformation of peptides, polypeptides, and proteins. In: Anfinsen, C.B., Edsall, J.T. and Richards, F.M. eds. *Advances in Protein Chemistry*. Academic Press, pp.181-364.
- Krishnan, K. and Ferraro, J.R. 1990. *Practical Fourier transform infrared spectroscopy : Industrial and laboratory chemical analysis*. San Diego: Academic Press.
- Krysa, M., Szymanska-Chargot, M. and Zdunek, A. 2022. FT-IR and FT-Raman fingerprints of flavonoids – A review. *Food Chemistry*. **393**, p133430. Available from: <https://doi.org/10.1016/j.foodchem.2022.133430>
- Kumar, S., Yadav, A., Yadav, M. and Yadav, J.P. 2017. Effect of climate change on phytochemical diversity, total phenolic content and in vitro antioxidant activity of *Aloe vera* (L.) Burm.f. *BMC Research Notes*. **10**(1), p60. Available from: <https://doi.org/10.1186/s13104-017-2385-3>
- Kunimasa, K., Ohta, T., Tani, H., Kato, E., Eguchi, R., Kaji, K., Ikeda, K., Mori, H., Mori, M., Tatefuji, T. and Yamori, Y. 2011. Resveratrol derivative-rich melinjo (*Gnetum gnemon* L.) seed extract suppresses multiple angiogenesis-related endothelial cell functions and tumor angiogenesis. *Molecular Nutrition and Food Research*. **55**(11), pp.1730-1734. Available from: <https://doi.org/10.1002/mnfr.201100098>
- Labuza, T.P., Warren, R.M. and Warmbier, H.C. 1977. The physical aspects with respect to water and non-enzymatic browning. *Advances in Experimental Medicine and Biology*. **86B**, pp.379-418. Available from: [https://doi.org/10.1007/978-1-4757-9113-6\\_25](https://doi.org/10.1007/978-1-4757-9113-6_25)
- Lagrouh, F., Dakka, N. and Bakri, Y. 2017. The antifungal activity of Moroccan plants and the mechanism of action of secondary metabolites from plants. *Journal de Mycologie Médicale*. **27**(3), pp.303-311. Available from: <https://doi.org/10.1016/j.mycmed.2017.04.008>
- Lahti, E., Lofdahl, M., Agren, J., Hansson, I. and Olsson Engvall, E. 2017. Confirmation of a Campylobacteriosis outbreak associated with chicken liver pate using PFGE and WGS. *Zoonoses and Public Health*. **64**(1), pp.14-20. Available from: <https://doi.org/10.1111/zph.12272>

- Lai, H.M., Geil, P.H. and Padua, G.W. 1999. X-ray diffraction characterization of the structure of zein–Oleic acid films. *Journal of Applied Polymer Science*. **71**(8), pp.1267-1281. Available from: [https://doi.org/10.1002/\(SICI\)1097-4628\(19990222\)71:8<1267::AID-APP7>3.0.CO;2-O](https://doi.org/10.1002/(SICI)1097-4628(19990222)71:8<1267::AID-APP7>3.0.CO;2-O)
- Lavieri, N. and Williams, S.K. 2014. Effects of packaging systems and fat concentrations on microbiology, sensory and physical properties of ground beef stored at 4±1°C for 25 days. *Meat Science*. **97**(4), pp.534-541. Available from: <https://doi.org/10.1016/j.meatsci.2014.02.014>
- Law, K.Y. and Zhao, H. 2015. *Surface wetting: Characterization, contact angle, and fundamentals*.
- Le, H.H.T., Dalsgaard, A., Andersen, P.S., Nguyen, H.M., Ta, Y.T. and Nguyen, T.T. 2021. Large-scale *Staphylococcus aureus* foodborne disease poisoning outbreak among primary school children. *Microbiology Research*. [Online]. **12**(1), pp.43-52. Available from: <https://doi.org/10.3390/microbiolres12010005>
- Le, T.H., Van Do, T.N., Nguyen, H.X., Dang, P.H., Nguyen, N.T. and Nguyen, M.T.T. 2021. A new phenylheptanoid from the leaves of *Gnetum gnemon* L. *Natural Product Research*. **35**(21), pp.3999-4004. Available from: <https://doi.org/10.1080/14786419.2020.1753055>
- Ledenbach, L.H. and Marshall, R.T. 2009. Microbiological spoilage of dairy products. In: *Compendium of the microbiological spoilage of foods and beverages, New York, USA*. Springer, pp.41-67.
- Lee, S.-S., Chen, W.-C. and Chen, C.-H. 2000. New jujubogenin glycosides from *Colubrina asiatica*. *Journal of Natural Products*. **63**(11), pp.1580-1583. Available from: <https://doi.org/10.1021/np000225n>
- Lee, W., Woo, E.-R. and Lee, D.G. 2016. Phytol has antibacterial property by inducing oxidative stress response in *Pseudomonas aeruginosa*. *Free Radical Research*. **50**(12), pp.1309-1318. Available from: <https://doi.org/10.1080/10715762.2016.1241395>
- Lewis, Y.S. 1969. [77] Isolation and properties of hydroxycitric acid. *Methods in Enzymology*. Academic Press, pp.613-619.
- Li, H., Pordesimo, L. and Weiss, J. 2004. High intensity ultrasound-assisted extraction of oil from soybeans. *Food Research International*. **37**(7), pp.731-738. Available from: <https://doi.org/10.1016/j.foodres.2004.02.016>
- LibreTexts. 2024. *1.2A Types of Microorganisms*. [Online]. LibreTexts. [Accessed 27 February 2026]. Available from: <https://bio.libretexts.org/@go/page/8771>
- Lim, W.F., Nasir, S.M., Teh, L.K., James, R.J., Izhar, M.H.M. and Salleh, M.Z. 2020. The methanolic extract of *Garcinia atroviridis* (MeGa) reduces body weight and food intake, and improves lipid profiles by altering the lipid metabolism: a rat model. *Turkish Journal of Biology*. **44**(6), pp.437-448. Available from: <https://doi.org/10.3906/biy-2005-2>

- Linscott, A.J. 2011. Food-Borne Illnesses. *Clinical Microbiology Newsletter*. **33**(6), pp.41-45. Available from: <https://doi.org/10.1016j.clinmicnews.2011.02.004>
- Liu, A., Shen, L., Tan, Y., Zeng, Z., Liu, Y. and Li, C. 2018. Food integrity in China: Insights from the national food spot check data in 2016. *Food Control*. **84**, pp.403-407. Available from: <https://doi.org/10.1016/j.foodcont.2017.08.033>
- Liu, H., Xie, F., Yu, L., Chen, L. and Li, L. 2009. Thermal processing of starch-based polymers. *Progress in Polymer Science (Oxford)*. **34**(12), pp.1348-1368. Available from: <https://doi.org/10.1016/j.progpolymsci.2009.07.001>
- Liu, J., Wang, W., Zhu, J., Li, Y., Luo, L., Huang, Y. and Zhang, W. 2018. Di(2-ethylhexyl) phthalate (DEHP) influences follicular development in mice between the weaning period and maturity by interfering with ovarian development factors and microRNAs. *Environmental Toxicology*. **33**(5), pp.535-544. Available from: <https://doi.org/10.1002/tox.22540>
- Losic, D., Farivar, F. and Yap, P.L. 2024. Refining and validating thermogravimetric analysis (TGA) for robust characterization and quality assurance of graphene-related two-dimensional materials (GR2Ms). *C*. [Online]. **10**(2). Available from: <https://doi.org/10.3390/c10020030>
- Louisiana-State-University. 2024. *Dielectric constant*. [Online]. [Accessed 13 November 2024]. Available from: <https://macro.lsu.edu/HowTo/solvents/Dielectric%20Constant%20.htm>
- Lu, Y. and Luthria, D. 2014. Influence of postharvest storage, processing, and extraction methods on the analysis of phenolic phytochemicals. *Instrumental Methods for the Analysis and Identification of Bioactive Molecules*. American Chemical Society, pp.3-31.
- Luis, A., Domingues, F. and Ramos, A. 2019. Production of hydrophobic zein-based films bioinspired by the lotus leaf surface: Characterization and bioactive properties. *Microorganisms*. [Online]. **7**(8). Available from: <https://doi.org/10.3390/microorganisms7080267>
- Luo, S., Saadi, A., Fu, K., Taxipalati, M. and Deng, L. 2021. Fabrication and characterization of dextran/zein hybrid electrospun fibers with tailored properties for controlled release of curcumin. *Journal of the Science of Food and Agriculture*. **101**(15), pp.6355-6367. Available from: <https://doi.org/10.1002/jsfa.11306>
- Luo, Y., Teng, Z. and Wang, Q. 2012. Development of zein nanoparticles coated with carboxymethyl chitosan for encapsulation and controlled release of vitamin D3. *Journal of Agricultural and Food Chemistry*. **60**(3), pp.836-843. Available from: <https://doi.org/10.1021/jf204194z>
- Luque de Castro, M.D. and Garcia-Ayuso, L.E. 1998. Soxhlet extraction of solid materials: an outdated technique with a promising innovative future. *Analytica Chimica Acta*. **369**(1), pp.1-10. Available from: [https://doi.org/10.1016/S0003-2670\(98\)00233-5](https://doi.org/10.1016/S0003-2670(98)00233-5)

Ma, Z., Ginsberg, A. M. and Spigelman, M. 2007. 7.24 - Antimycobacterium agents. In: Taylor, J. B. and Triggler, D. J. eds. *Comprehensive Medicinal Chemistry II*. [Online]. USA: Elsevier, 2007, pp.699-730. [Accessed 25 February 2026]. Available from: <https://doi.org/10.1016/B0-08-045044-X/00224-8>

Mackeen, M.M., Ali, A.M., Lajis, N.H., Kawazu, K., Hassan, Z., Amran, M., Habsah, M., Mooi, L.Y. and Mohamed, S.M. 2000. Antimicrobial, antioxidant, antitumour-promoting and cytotoxic activities of different plant part extracts of *Garcinia atroviridis* Griff. ex T. Anders. *Journal of Ethnopharmacology*. **72**(3), pp.395-402. Available from: [https://doi.org/10.1016/S0378-8741\(00\)00245-2](https://doi.org/10.1016/S0378-8741(00)00245-2)

Mackeen, M.M., Ali, A.M., Lajis, N.H., Kawazu, K., Kikuzaki, H. and Nakatani, N. 2002. Antifungal garcinia acid esters from the fruits of *Garcinia atroviridis*. **57**(3-4), pp.291-295. Available from: <https://doi.org/10.1515/znc-2002-3-416>

Magoshi, J., Nakamura, S. and Murakami, K.I. 1992. Structure and physical-properties of seed proteins. 1. Glass-transition and crystallization of zein protein from corn. *Journal of Applied Polymer Science*. **45**, pp.2043-2048.

Mahardika, R.G. and Roanisca, O. 2020. Microwave-assisted extraction of polyphenol content from leaves of *Tristanopsis merguensis* Griff. *ASEAN Journal of Chemical Engineering*. **19**, p110. Available from: <https://doi.org/10.22146/ajche.50448>

Majrashi, T.A., Alshehri, S.A., Alsayari, A., Muhsinah, A.B., Alrouji, M., Alshahrani, A.M., Shamsi, A. and Atiya, A. 2023. Insight into the biological roles and mechanisms of phytochemicals in different types of cancer: Targeting cancer therapeutics. *Nutrients*. **15**(7). Available from: <https://doi.org/10.3390/nu15071704>

Malaysia. 2024. [Online database]. International Commission on Irrigation & Drainage. Available from: [https://www.icid.org/i\\_d\\_malaysia.pdf](https://www.icid.org/i_d_malaysia.pdf)

Marques, S.S. and Segundo, M.A. 2024. Nanometrics goes beyond the size: Assessment of nanoparticle concentration and encapsulation efficiency in nanocarriers. *TrAC Trends in Analytical Chemistry*. **174**, p117672. Available from: <https://doi.org/10.1016/j.trac.2024.117672>

Marsh, K. and Bugusu, B. 2007. Food packaging-roles, materials, and environmental issues. *Journal of Food Science*. **72**(3), pp.R39-55. Available from: <https://doi.org/10.1111/j.1750-3841.2007.00301.x>

Martinez-Mendoza, J., Espericueta-Gonzalez, E., Gonzalez, D.E., Ortega-Zarzosa, G. and Guerrero, A.L. 2016. Thermo-Stability of natural products based on chlorophyll species embedded in silica xerogel. *American Journal of Analytical Chemistry*. **07**, pp.356-362. Available from: <https://doi.org/10.4236/ajac.2016.74034>

Martins-Noguerol, R., Matías, L., Pérez-Ramos, I.M., Moreira, X., Francisco, M., Pedroche, J., DeAndrés-Gil, C., Gutiérrez, E., Salas, J.J., Moreno-Pérez, A.J., Davy, A.J., Muñoz-Vallés, S., Figueroa, M.E. and Cambrollé, J. 2023. Soil physicochemical properties associated with the yield and phytochemical composition of the edible halophyte *Crithmum maritimum*. *Science of The Total*

*Environment*. **869**, p161806. Available from:  
<https://doi.org/10.1016/j.scitotenv.2023.161806>

Mastromatteo, M., Mastromatteo, M., Conte, A. and Del Nobile, M. A. 2010. Advances in controlled release devices for food packaging applications. *Trends in Food Science & Technology*. **21**(12), pp.591-598. Available from:  
<https://doi.org/10.1016/j.tifs.2010.07.010>

Mat-Ali, M.S. 2008. *Analysis of phenolics and other phytochemicals in selected Malaysian traditional vegetables and their activities in vitro*. Doctor of Philosophy thesis, University of Glasgow.

Matabola, K.P. and Moutloali, R.M. 2013. The influence of electrospinning parameters on the morphology and diameter of poly(vinylidene fluoride) nanofibers- effect of sodium chloride. *Journal of Materials Science*. **48**(16), pp.5475-5482. Available from: <https://doi.org/10.1007/s10853-013-7341-6>

Mattia, J. and Painter, P. 2007. A comparison of hydrogen bonding and order in a polyurethane and poly(urethane-urea) and their blends with poly(ethylene glycol). *Macromolecules*. **40**(5), pp.1546-1554. Available from:  
<https://doi.org/10.1021/ma0626362>

Matuschek, E., Brown, D.F. and Kahlmeter, G. 2014. Development of the EUCAST disk diffusion antimicrobial susceptibility testing method and its implementation in routine microbiology laboratories. *Clinical Microbiology and Infection*. **20**(4), pp.O255-266. Available from: <https://doi.org/10.1111/1469-0691.12373>

Maxwell, A. 1997. DNA gyrase as a drug target. *Trends in Microbiology*. **5**(3), pp.102-109. Available from: [https://doi.org/10.1016/S0966-842X\(96\)10085-8](https://doi.org/10.1016/S0966-842X(96)10085-8)

McCollum, J., T., Cronquist, A., B., Silk, B., J., Jackson, K., A., O'Connor, K., A., Cosgrove, S., Gossack, J., P., Parachini, S., S., Jain, N., S., Ettestad, P., Ibraheem, M., Cantu, V., Joshi, M., DuVernoy, T., Fogg, N., W., Gorny, J., R., Mogen, K., M., Spires, C., Teitell, P., Joseph, L., A., Tarr, C., L., Imanishi, M., Neil Karen, P., Tauxe Robert, V. and Mahon, B., E. 2013. Multistate outbreak of Listeriosis associated with cantaloupe. *New England Journal of Medicine*. **369**(10), pp.944-953. Available from: <https://doi.org/10.1056/NEJMoa1215837>

McDowell, S.A.C. 2025. Comparative computational study of frequency shifts and infrared intensity changes in model binary complexes with red- and blue-shifting hydrogen bonds. *Molecules*. [Online]. **30**(1). Available from:  
<https://doi.org/10.3390/molecules30010106>

McKee, M., Wilkes, G., Colby, R. and Long, T. 2004. Correlations of solution rheology with electrospun fiber formation of linear and branched polyesters. *Macromolecules*. **37**. Available from: <https://doi.org/10.1021/ma035689h>

McKee, M.G., Park, T., Unal, S., Yilgor, I. and Long, T.E. 2005. Electrospinning of linear and highly branched segmented poly(urethane urea)s. *Polymer*. **46**(7), pp.2011-2015. Available from: <https://doi.org/10.1016/j.polymer.2005.01.028>

Meng, G. and Ma, C.-Y. 2002. Characterization of globulin from *Phaseolus angularis* (red bean). *International Journal of Food Science & Technology*.

37(6), pp.687-695. Available from: <https://doi.org/10.1046/j.1365-2621.2002.00601.x>

Merck. 2019. *Technical data sheet plate count agar*. [Leaflet]. Germany: Merck KGaA.

Mikkelsen, R.L. 1994. Using hydrophilic polymers to control nutrient release. *Fertilizer research*. **38**(1), pp.53-59. Available from: <https://doi.org/10.1007/BF00750062>

Milanda, T., Safrudin, A.D., Samudra, G., Sumiwi, S.A. and Muchtaridi, M. 2019. Sub-chronic toxicity of *Garcinia atroviridis* Griff fruit's ethanol extract on Wistar rats (*Ratus norvegicus*). *Journal of Advanced Pharmaceutical Technology & Research*. **10**(4), pp.178-183. Available from: [https://doi.org/10.4103/japtr.JAPTR\\_70\\_19](https://doi.org/10.4103/japtr.JAPTR_70_19)

Miller, K.S. and Krochta, J.M. 1997. Oxygen and aroma barrier properties of edible films: A review. *Trends in Food Science & Technology*. **8**(7), pp.228-237. Available from: [https://doi.org/10.1016/S0924-2244\(97\)01051-0](https://doi.org/10.1016/S0924-2244(97)01051-0)

Minelli, C., Wywijas, M., Bartczak, D., Cuello-Nunez, S., Infante, H.G., Deumer, J., Gollwitzer, C., Krumrey, M., Murphy, K.E., Johnson, M.E., Montoro Bustos, A.R., Strenge, I.H., Faure, B., Høghøj, P., Tong, V., Burr, L., Norling, K., Höök, F., Roeslein, M., Kocic, J., Hendriks, L., Kestens, V., Ramaye, Y., Contreras Lopez, M.C., Auclair, G., Mehn, D., Gilliland, D., Potthoff, A., Oelschlägel, K., Tentschert, J., Jungnickel, H., Krause, B.C., Hachenberger, Y.U., Reichardt, P., Luch, A., Whittaker, T.E., Stevens, M.M., Gupta, S., Singh, A., Lin, F.-h., Liu, Y.-H., Costa, A.L., Baldisserri, C., Jawad, R., Andaloussi, S.E.L., Holme, M.N., Lee, T.G., Kwak, M., Kim, J., Ziebel, J., Guignard, C., Cambier, S., Contal, S., Gutleb, A.C., "Kuba" Tatarkiewicz, J., Jankiewicz, B.J., Bartosewicz, B., Wu, X., Fagan, J.A., Elje, E., Rundén-Pran, E., Dusinska, M., Kaur, I.P., Price, D., Nesbitt, I., O' Reilly, S., Peters, R.J.B., Bucher, G., Coleman, D., Harrison, A.J., Ghanem, A., Gering, A., McCarron, E., Fitzgerald, N., Cornelis, G., Tuoriniemi, J., Sakai, M., Tsuchida, H., Maguire, C., Prina-Mello, A., Lawlor, A.J., Adams, J., Schultz, C.L., Constantin, D., Thanh, N.T.K., Tung, L.D., Panariello, L., Damilos, S., Gavriilidis, A., Lynch, I., Fryer, B., Carrasco Quevedo, A., Guggenheim, E., Briffa, S., Valsami-Jones, E., Huang, Y., Keller, A.A., Kinnunen, V.-T., Perämäki, S., Krpetic, Z., Greenwood, M. and Shard, A.G. 2022. Versailles project on advanced materials and standards (VAMAS) interlaboratory study on measuring the number concentration of colloidal gold nanoparticles. *Nanoscale*. **14**(12), pp.4690-4704. Available from: <https://doi.org/10.1039/D1NR07775A>

Ministry of Health. 2024. *Annual Report 2024*. [Online]. Malaysia: Ministry of Health. [Accessed 25 February 2026]. Available from: [https://www.moh.gov.my/images/04-penerbitan/laporan-tahunan/MOH\\_Annual\\_Report2024.pdf](https://www.moh.gov.my/images/04-penerbitan/laporan-tahunan/MOH_Annual_Report2024.pdf)

Mohammed-Ziegler, I. and Billes, F. 2002. Vibrational spectroscopic calculations on pyrogallol and gallic acid. *Journal of Molecular Structure: THEOCHEM*. **618**(3), pp.259-265. Available from: [https://doi.org/10.1016/S0166-1280\(02\)00547-X](https://doi.org/10.1016/S0166-1280(02)00547-X)

- Mohee, R., Unmar, G.D., Mudhoo, A. and Khadoo, P. 2008. Biodegradability of biodegradable/degradable plastic materials under aerobic and anaerobic conditions. *Waste Management*. **28**(9), pp.1624-1629. Available from: <https://doi.org/10.1016/j.wasman.2007.07.003>
- Mokhtar, N., Siddiqui, Y. and Ali, N.S. 2018. In vitro utilization of bio-active components from the underutilized fruits of *Garcinia atroviridis* for the suppression of *Colletotrichum capsici*. *International Journal of Agriculture and Biology*. **20**, pp.1809-1817. Available from: <https://doi.org/10.17957/IJAB/15.0696>
- Molyneux, P. 2004. The use of the stable free radical diphenylpicrylhydrazyl (DPPH) for estimating antioxidant activity. *Songklanakar J. sci. technol.* **26**(2), pp.211-219. Available from: [https://scholar.googleusercontent.com/scholar?q=cache:1UTNU\\_YI3vQJ:scholar.google.com/&hl=en&as\\_sdt=0,5](https://scholar.googleusercontent.com/scholar?q=cache:1UTNU_YI3vQJ:scholar.google.com/&hl=en&as_sdt=0,5)
- Moradinezhad, F., Aliabadi, M. and Ansarifard, E. 2024. Zein multilayer electrospun nanofibers contain essential oil: Release kinetic, functional effectiveness, and application to fruit preservation. *Foods*. [Online]. **13**(5). Available from: <https://doi.org/10.3390/foods13050700>
- Mostafavi, F. S. and Zaeim, D. 2020. Agar-based edible films for food packaging applications - A review. *International Journal of Biological Macromolecules*. **159**, pp.1165-1176. Available from: <https://doi.org/10.1016/j.ijbiomac.2020.05.123>
- Munir, S., Yue, W., Li, J., Yu, X., Ying, T., Liu, R., You, J., Xiong, S. and Hu, Y. 2023. Effects of phenolics on the physicochemical and structural properties of collagen hydrogel. *Polymers*. [Online]. **15**(24). Available from: <https://doi.org/10.3390/polym15244647>
- Munteanu, I.G. and Apetrei, C. 2021. Analytical methods used in determining antioxidant activity: A Review. *International Journal of Molecular Sciences*. [Online]. **22**(7), p.3380. Available from: <https://doi.org/10.3390/ijms22073380>
- Murrieta-Martinez, C.L., Soto-Valdez, H., Pacheco-Aguilar, R., Torres-Arreola, W., Rodriguez-Felix, F. and Marquez Rios, E. 2018. Edible protein films: Sources and behavior. *Packaging Technology and Science*. **31**(3), pp.113-122. Available from: <https://doi.org/10.1002/pts.2360>
- Nagarajan, M., Benjakul, S., Prodpran, T., Songtipya, P. and Nuthong, P. 2013. Film forming ability of gelatins from splendid squid (*Loligo formosana*) skin bleached with hydrogen peroxide. *Food Chemistry*. **138**(2), pp.1101-1108. Available from: <https://doi.org/10.1016/j.foodchem.2012.11.069>
- Nahar, L. and Sarker, S.D. 2012. Supercritical fluid extraction in natural products analyses. In: Sarker, S.D. and Nahar, L. eds. *Natural Products Isolation Methods and Protocols*. [Online]. Third ed. Humana Press, pp.42-74. Available from: <https://doi.org/10.1007/978-1-61779-624-1>
- Nayak, B., Dahmoune, F., Moussi, K., Remini, H., Dairi, S., Aoun, O. and Khodir, M. 2015a. Comparison of microwave, ultrasound and accelerated-assisted solvent extraction for recovery of polyphenols from *Citrus sinensis*

- peels. *Food Chemistry*. **187**, pp.507-516. Available from: <https://doi.org/10.1016/j.foodchem.2015.04.081>
- Nayak, B., Liu, R.H. and Tang, J. 2015b. Effect of processing on phenolic antioxidants of fruits, vegetables, and grains—A Review. *Critical Reviews in Food Science and Nutrition*. **55**(7), pp.887-918. Available from: <https://doi.org/10.1080/10408398.2011.654142>
- Nazari, M., Majdi, H., Milani, M., Abbaspour-Ravasjani, S., Hamishehkar, H. and Lim, L.-T. 2019. Cinnamon nanophytosomes embedded electrospun nanofiber: Its effects on microbial quality and shelf-life of shrimp as a novel packaging. *Food Packaging and Shelf Life*. **21**, p100349. Available from: <https://doi.org/10.1016/j.fpsl.2019.100349>
- NCCLS. 2004. *Method for Antifungal Disk Diffusion Susceptibility Testing of Yeasts; Approved Guideline*. Pennsylvania, USA: National Committee for Clinical Laboratory Standards.
- Neo, Y.P., Ray, S., Jin, J., Gizdavic-Nikolaidis, M., Nieuwoudt, M.K., Liu, D. and Quek, S.Y. 2013. Encapsulation of food grade antioxidant in natural biopolymer by electrospinning technique: A physicochemical study based on zein–gallic acid system. *Food Chemistry*. **136**(2), pp.1013-1021. Available from: <https://doi.org/10.1016/j.foodchem.2012.09.010>
- Nicoletti, M. and Serrone, P.D. 2017. Intelligent and smart Packaging. In: Heimo, M. ed. *Future Foods*. [Online]. Rijeka: IntechOpen, p.[no pagination]. [Accessed 2024-12-10]. Available from: <https://doi.org/10.5772/intechopen.68773>
- Nik Hairiah, N.M.R., Nor Azila, M., Husna Hawa, M.H. and Maryana, M.N. 2013. Phytochemicals screening and antioxidant activities of aqueous leaves extract of *Euodia ridleyi* and *Colubrina asiatica*. *International Journal of Science and Research*. **5**(4), pp.2004-2007. Available from: <https://www.ijsr.net/archive/v5i4/NOV163034.pdf>
- Nikaido, H. 1994. Prevention of drug access to bacterial targets: permeability barriers and active efflux. *Science*. **264**(5157), pp.382-388. Available from: <https://doi.org/10.1126/science.8153625>
- North, E.J. and Halden, R.U. 2013. Plastics and environmental health: The road ahead. *Reviews on Environmental Health*. **28**(1), pp.1-8. Available from: <https://doi.org/10.1515/reveh-2012-0030>
- Nowak, D. and Jakubczyk, E. 2020. The freeze-drying of foods -The characteristic of the process course and the effect of its parameters on the physical properties of food materials. *Foods (Basel, Switzerland)*. **9**(10), p.1488. Available from: <https://doi.org/10.3390/foods9101488>
- Nur Amila Najwa, I.S., Guerrero, P., de la Caba, K. and Nur Hanani, Z.A. 2020. Physical and antioxidant properties of starch/gelatin films incorporated with *Garcinia atroviridis* leaves. *Food Packaging and Shelf Life*. **26**, p100583. Available from: <https://doi.org/10.1016/j.fpsl.2020.100583>

- Nursakinah, I., Zulkhairi, H.A., Norhafizah, M., Hasnah, B., Zamree, M.S., Farrah, S.I., Razif, D. and Hamzah, F.H. 2012. Nutritional content and in vitro antioxidant potential of *Garcinia atroviridis* (Asam gelugor) leaves and fruits. *Malays J Nutr.* **18**(3), pp.363-371.
- Oommen, A. 2018. *Poison hemlock (Conium maculatum L.)*. New York, USA: USDA National Institute of Food and Agriculture. Available from: <https://www.invasive.org/browse/detail.cfm?imgnum=5589146#>
- Oosterhaven, K., Poolman, B. and Smid, E.J. 1995. S-carvone as a natural potato sprout inhibiting, fungistatic and bacteristatic compound. *Industrial Crops and Products.* **4**(1), pp.23-31. Available from: [https://doi.org/10.1016/0926-6690\(95\)00007-Y](https://doi.org/10.1016/0926-6690(95)00007-Y)
- Oprea, S. 2015. Effects of introducing crude and modified soybean oil into polyurethane structures on the soil-burial biodegradation process. *Polymer-Plastics Technology and Engineering.* **54**(4), pp.342-349. Available from: <https://doi.org/10.1080/03602559.2014.935411>
- Ota, H., Akishita, M., Tani, H., Tatefuji, T., Ogawa, S., Iijima, K., Eto, M., Shirasawa, T. and Ouchi, Y. 2013. Trans-resveratrol in *Gnetum gnemon* protects against oxidative-stress-induced endothelial senescence. *Journal of Natural Products.* **76**(7), pp.1242-1247. Available from: <https://doi.org/10.1021/np300841v>
- Othman, M., Loh, H.S., Wiart, C., Khoo, T.J., Lim, K.H. and Ting, K.N. 2011. Optimal methods for evaluating antimicrobial activities from plant extracts. *Journal of Microbiological Methods.* **84**(2), pp.161-166. Available from: <https://doi.org/10.1016/j.mimet.2010.11.008>
- Ouattara, B., Simard, R.E., Piette, G., Begin, A. and Holley, R.A. 2000. Diffusion of acetic and propionic acids from chitosan-based antimicrobial packaging films. *Journal of Food Science.* **65**(5), pp.768-773. Available from: <https://doi.org/10.1111/j.1365-2621.2000.tb13584.x>
- Ozdemir, M. and Floros, J.D. 2003. Film composition effects on diffusion of potassium sorbate through whey protein films. *Journal of Food Science.* **68**(2), pp.511-516. Available from: <https://doi.org/10.1111/j.1365-2621.2003.tb05703.x>
- Ozdemir, M. and Floros, J.D. 2004. Active food packaging technologies. *Critical Reviews in Food Science and Nutrition.* **44**(3), pp.185-193. Available from: <https://doi.org/10.1080/10408690490441578>
- Parhusip, A.J.N. and Sitanggang, A.B. 2011. Antimicrobial activity of Melinjo seed and peel extract (*Gnetum gnemon*) against selected pathogenic bacteria. *Microbiology Indonesia.* **5**(2), pp.103-112. Available from: <https://doi.org/10.5454/mi.5.3.2>
- Parris, N., Dickey, L.C., Kurantz, M.J., Moten, R.O. and Craig, J.C. 1997. Water vapor permeability and solubility of zein/starch hydrophilic films prepared from dry milled corn extract. *Journal of Food Engineering.* **32**(2), pp.199-207. Available from: [https://doi.org/10.1016/S0260-8774\(97\)00015-0](https://doi.org/10.1016/S0260-8774(97)00015-0)

- Peanparkdee, M. and Iwamoto, S. 2019. Bioactive compounds from by-products of rice cultivation and rice processing: Extraction and application in the food and pharmaceutical industries. *Trends in Food Science & Technology*. **86**, pp.109-117. Available from: <https://doi.org/10.1016/j.tifs.2019.02.041>
- Permana, D., Abas, F., Maulidiani, F., Shaari, K., Stanslas, J., Ali, A.M. and Lajis, N.H. 2005. Atrovirisidone B, a new prenylated depsidone with cytotoxic property from the roots of *Garcinia atroviridis*. **60**(7-8), pp.523-526. Available from: <https://doi.org/10.1515/znc-2005-7-802>
- Permana, D., Lajis, N.H., Mackeen, M.M., Ali, A.M., Aimi, N., Kitajima, M. and Takayama, H. 2001. Isolation and bioactivities of constituents of the roots of *Garcinia atroviridis*. *Journal of Natural Products*. **64**(7), pp.976-979. Available from: <https://doi.org/10.1021/np000563o>
- Permana, D., Lajis, N.H., Shaari, K., Ali, A.M., Mackeen, M.M., Kitajima, M., Takayama, H. and Aimi, N. 2003. A new prenylated hydroquinone from the roots of *Garcinia atroviridis* Griff ex T. Anders (Guttiferae). **58**(4), pp.332-335. Available from: <https://doi.org/10.1515/znb-2003-0414>
- Peters, M., Alves, C., Wang, J. and Onwudili, J. 2022. Subcritical water hydrolysis of fresh and waste cooking oils to fatty acids followed by esterification to fatty acid methyl esters: Detailed characterization of feedstocks and products. *ACS Omega*. **7**. Available from: <https://doi.org/10.1021/acsomega.2c05972>
- Phiriyawirut, M. and Phaechamud, T. 2012. Gallic acid-loaded cellulose acetate electrospun nanofibers: Thermal properties, mechanical properties, and drug release behavior. *Open Journal of Polymer Chemistry*. **2**, pp.21-29. Available from: <https://doi.org/10.4236/ojpcem.2012.21004>
- Pires, J.R., Souza, V.G., Fucinos, P., Pastrana, L. and Fernando, A.L. 2022. Methodologies to assess the biodegradability of bio-based polymers—Current knowledge and existing gaps. *Polymers*. [Online]. **14**(7). Available from: <https://doi.org/10.3390/polym14071359>
- Pleva, P., Bartošová, L., Janalíková, M., Polášková, M., Šišková, A.O., Matošková, L., Krejčí, O. and Sedlaříková, J. 2025. Biodegradable zein/PEG nanofibers incorporated with natural antimicrobial compounds for eco-friendly food packaging. *New Biotechnology*. **88**, pp.12-21. Available from: <https://doi.org/10.1016/j.nbt.2025.03.005>
- Poverty-Pollution-Persecution. 2019. *Amount of food wasted by Malaysians enough to feed 12 million people a day*. [Online]. [Accessed 16 November 2022]. Available from: <https://ppppp.my/malaysian-food-waste.html>
- Prabhudev, S.H., Ravindra, K.N., Supreetha, B.H., Nithyanandha, K.R., Deepdarshan, U., Dharmappa, K.K. and Giresha, A.S. 2023. Effect of soil pH on plants growth, phytochemical contents and their antioxidant activity. *Journal Of Advanced Applied Scientific Research*. **5**(5). Available from: <https://joaasr.com/index.php/joaasr/article/view/687>

Prentice, J.H. 1968. Dimensional problem of the Power Law in rheology. *Nature*. **217**(5124), pp.157-157. Available from: <https://doi.org/10.1038/217157a0>

Prenzler, P., Ryan, D., Robards, K., Prenzler, P., Ryan, D. and Robards, K. 2021. *Handbook of Antioxidant Methodology [Online]*. [Online]. First edition ed. Royal Society of Chemistry. [Accessed 11 February 2025]. Available from: <https://www.perlego.com/book/3043283>.

Prime, R.B., Bair, H.E., Vyazovkin, S., Gallagher, P.K. and Riga, A. 2014. Thermal analysis of polymers Fundamental s and Applications. In: Menczel, J.D. and Prime, R.B. eds. *Thermogravimetric analysis*. [Online]. New Jersey: John Wiley & Sons, Inc. [Accessed 1 August 2025]. Available from: <https://www.perlego.com/book/1009137>

Qaderi, M.M., Martel, A.B. and Strugnell, C.A. 2023. Environmental factors regulate plant secondary metabolites. *Plants*. [Online]. **12**(3). Available from: <https://doi.org/10.3390/plants12030447>

Qazanfarzadeh, Z., Kadivar, M., Shekarchizadeh, H. and Porta, R. 2021. Rye secalin characterisation and use to improve zein-based film performance. *International Journal of Food Science & Technology*. **56**(2), pp.742-752. Available from: <https://doi.org/10.1111/ijfs.14718>

Qin, P., Li, T., Liu, C., Liang, Y., Sun, H., Chai, Y., Yang, T., Gong, X. and Wu, Z. 2023. Extraction and utilization of active substances from edible fungi substrate and residue: A review. *Food Chemistry*. **398**, p133872. Available from: <https://doi.org/10.1016/j.foodchem.2022.133872>

Qiu, L., Zhang, M., Chitrakar, B. and Bhandari, B. 2020. Application of power ultrasound in freezing and thawing processes: Effect on process efficiency and product quality. *Ultrasonics Sonochemistry*. **68**, p105230. Available from: <https://doi.org/10.1016/j.ultsonch.2020.105230>

Quintavalla, S. and Vicini, L. 2002. Antimicrobial food packaging in meat industry. *Meat Science*. **62**(3), pp.373-380. Available from: [https://doi.org/10.1016/S0309-1740\(02\)00121-3](https://doi.org/10.1016/S0309-1740(02)00121-3)

Radusin, T., Torres-Giner, S., Stupar, A., Ristic, I., Miletic, A., Novakovic, A. and Lagaron, J.M. 2019. Preparation, characterization and antimicrobial properties of electrospun polylactide films containing *Allium ursinum* L. extract. *Food Packaging and Shelf Life*. **21**, p100357. Available from: <https://doi.org/10.1016/j.fpsl.2019.100357>

Raghu, A. and Velayudhannair, K. 2023. Phytochemical analysis and antibacterial potential of *Stevia rebaudiana* (Bertoni, 1899) leaf extracts against *Aeromonas* species: Influence of extraction methods and solvents in aquaculture applications. *Journal of Pure and Applied Microbiology*. **17**(4), pp.2352-2366. Available from: <https://doi.org/10.22207/jpam.17.4.31>

Ratajczak, H. 1972. Charge-transfer properties of the hydrogen bond. I. Theory of the enhancement of dipole moment of hydrogen-bonded systems. *The Journal of Physical Chemistry*. **76**(21), pp.3000-3004. Available from: <https://doi.org/10.1021/j100665a013>

- Raunsai, M.M., Palupi, K.D., Fathoni, A. and Agusta, A. 2021. Bioactivities of plant extracts collected in Halmahera, Indonesia: A bioprospection study of underexplored plant species. *Indonesian Journal of Pharmacy*. **32**(3). Available from: <https://doi.org/10.22146/ijp.1774>
- Reneker, D.H. and Yarin, A.L. 2008. Electrospinning jets and polymer nanofibers. *Polymer*. **49**(10), pp.2387-2425. Available from: <https://doi.org/10.1016/j.polymer.2008.02.002>
- Reshi, Z.A., Ahmad, W., Lukatkin, A.S. and Javed, S.B. 2023. From nature to lab: A review of secondary metabolite biosynthetic pathways, environmental influences, and in vitro approaches. *Metabolites*. **13**(8). Available from: <https://doi.org/10.3390/metabo13080895>
- Rezaei, A., Nasirpour, A. and Fathi, M. 2015. Application of cellulosic nanofibers in food science using electrospinning and its potential risk. *Comprehensive Reviews in Food Science and Food Safety*. **14**(3), pp.269-284. Available from: <https://doi.org/10.1111/1541-4337.12128>
- Rezaei, S., Rezaei, K., Haghghi, M. and Labbafi, M. 2013. Solvent and solvent to sample ratio as main parameters in the microwave-assisted extraction of polyphenolic compounds from apple pomace. *Food Science and Biotechnology*. **22**, pp.1269-1274. Available from: <https://doi.org/10.1007/s10068-013-0212-8>
- Rhim, J.W., Mohanty, K.A., Singh, S.P. and Ng, P.K.W. 2006. Preparation and properties of biodegradable multilayer films based on soy protein isolate and poly(lactide). *Industrial & Engineering Chemistry Research*. **45**(9), pp.3059-3066. Available from: <https://doi.org/10.1021/ie051207+>
- Ribeiro, A.M., Estevinho, B.N. and Rocha, F. 2021. Preparation and incorporation of functional ingredients in edible films and coatings. *Food and Bioprocess Technology*. **14**(2), pp.209-231. Available from: <https://doi.org/10.1007/s11947-020-02528-4>
- Rice-Evans, C.A., Miller, N.J. and Paganga, G. 1996. Structure-antioxidant activity relationships of flavonoids and phenolic acids. *Free Radical Biology and Medicine*. **20**(7), pp.933-956. Available from: [https://doi.org/10.1016/0891-5849\(95\)02227-9](https://doi.org/10.1016/0891-5849(95)02227-9)
- Richter, B.E., Jones, B.A., Ezzell, J.L., Porter, N.L., Avdalovic, N. and Pohl, C. 1996. Accelerated solvent extraction: A technique for sample preparation. *Analytical Chemistry*. **68**(6), pp.1033-1039. Available from: <https://doi.org/10.1021/ac9508199>
- Rind, F.M.A., Mughal, U.R., Memon, A.H., Almani, F., Laghari, M.G.H., Maheshwari, M.L., Khuhawar, M.Y., Memon, N. and Dayo, A. 2010. Spectrophotometric analysis of vanillin from natural and synthetic sources. *Asian Journal of Chemistry*. **21**(4), pp.2849-2856. Available from: <https://asianpubs.org/index.php/ajchem/article/view/12394>
- Robertson, G. 2013a. Introduction to food packaging. *Food packaging: principles and practise*. [Online]. Second ed. Boca Raton, USA: CRC Press, pp.1-9. [Accessed 10 December 2024]. Available from:

<https://www.taylorfrancis.com/books/mono/10.1201/9781420056150/food-packaging-gordon-robertson>

Robertson, G. 2013b. Active and intelligent packaging. *Food packaging: principles and practise*. [Online]. Second ed. Boca Raton, USA: CRC Press, pp.399-427. [Accessed 10 December 2024]. Available from: <https://www.taylorfrancis.com/books/mono/10.1201/9781420056150/food-packaging-gordon-robertson>

Robertson, G. 2013c. Edible, biobased and biodegradable food packaging materials. *Food packaging: principles and practise*. [Online]. Second ed. Boca Raton, USA: CRC Press, pp.49-89. [Accessed 10 December 2024]. Available from: <https://www.taylorfrancis.com/books/mono/10.1201/9781420056150/food-packaging-gordon-robertson>

Robertson, G. 2013d. Deteriorative reactions in foods. *Food packaging: principles and practise*. [Online]. Second ed. Boca Raton, USA: CRC Press, pp.194-224. [Accessed 15 December 2024]. Available from: <https://www.taylorfrancis.com/books/mono/10.1201/9781420056150/food-packaging-gordon-robertson>

Robertson, G. 2013e. Packaging of flesh foods. *Food packaging: principles and practise*. [Online]. Second ed. Boca Raton, USA: CRC Press, pp.445-476. [Accessed 15 April 2025]. Available from: <https://www.taylorfrancis.com/books/mono/10.1201/9781420056150/food-packaging-gordon-robertson>

Robertson, K., Green, A., Allen, L., Ihry, T., White, P., Chen, W.-S., Douris, A. and Levine, J. 2016. Foodborne outbreaks reported to the U.S. Food Safety and Inspection Service, fiscal years 2007 through 2012. *Journal of Food Protection*. **79**(3), pp.442-447. Available from: <https://doi.org/10.4315/0362-028X.JFP-15-376>

Rodriguez-Rojo, S., Visentin, A., Maestri, D. and Cocero, M.J. 2012. Assisted extraction of rosemary antioxidants with green solvents. *Journal of Food Engineering*. **109**(1), pp.98-103. Available from: <https://doi.org/10.1016/j.jfoodeng.2011.09.029>

Rollini, M., Nielsen, T., Musatti, A., Limbo, S., Piergiovanni, L., Hernandez Munoz, P. and Gavara, R. 2016. Antimicrobial performance of two different packaging materials on the microbiological quality of fresh salmon. *Coatings*. [Online]. **6**(1), pp.1-7. Available from: <https://doi.org/10.3390/coatings6010006>

Royal-Botanic-Gardens-Kew. 2023. *Garcinia atroviridis* Griff. ex T.Anderson. [Online]. [Accessed 18 December 2024]. Available from: <https://powo.science.kew.org/taxon/urn:lsid:ipni.org:names:427811-1#distributions>

Rukayadi, Y. and Hwang, J.K. 2007. In vitro antimycotic activity of xanthorrhizol isolated from *Curcuma xanthorrhiza* Roxb. against opportunistic filamentous fungi. *Phytotherapy Research*. **21**(5), pp.434-438. Available from: <https://doi.org/10.1002/ptr.2092>

Rukayadi, Y., Lau, K.Y., Zainin, N.S., Zakaria, M. and Abas, F. 2013. Screening antimicrobial activity of tropical edible medicinal plant extracts against five standard microorganisms for natural food preservative. *International Food Research Journal*. **20**, pp.2905-2910.

Rotronic. 2011. *HygroLab C1 bench-top indicator user guide*. [Online]. Available from: [https://www.instrumart.com/assets/Rotronic\\_HygroLabC1\\_manual.pdf](https://www.instrumart.com/assets/Rotronic_HygroLabC1_manual.pdf)

Sabo, B., Becica, T., Keles, N., Kovacevic, D. and Brozovic, M. 2017. The impact of packaging transparency on product attractiveness. *Journal of Graphic Engineering and Design*. **8**, pp.5-9. Available from: <https://doi.org/10.24867/JGED-2017-2-005>

Saha, S., Singh, J., Paul, A., Sarkar, R., Khan, Z. and Banerjee, K. 2020. Anthocyanin profiling using UV-Vis spectroscopy and liquid chromatography mass spectrometry. *Journal of AOAC INTERNATIONAL*. **103**(1), pp.23-39. Available from: <https://doi.org/10.5740/jaoacint.19-0201>

Saini, R.K. and Keum, Y.-S. 2018. Carotenoid extraction methods: A review of recent developments. *Food Chemistry*. **240**, pp.90-103. Available from: <https://doi.org/10.1016/j.foodchem.2017.07.099>

Salam, U., Ullah, S., Tang, Z.-H., Elateeq, A.A., Khan, Y., Khan, J., Khan, A. and Ali, S. 2023. Plant metabolomics: An overview of the role of primary and secondary metabolites against different environmental stress factors. *Life*. [Online]. **13**(3). Available from: <https://doi.org/10.3390/life13030706>

Salevic, A., Stojanovic, D., Levic, S., Pantic, M., Dordevic, V., Pesic, R., Bugarski, B., Pavlovic, V., Uskokovic, P. and Nedovic, V. 2022. The structuring of sage (*Salvia officinalis* L.) extract-Incorporating edible zein-based materials with antioxidant and antibacterial functionality by solvent casting versus electrospinning. *Foods*. **11**(3), p18 article no: 390 [no pagination]. Available from: <https://doi.org/10.3390/foods11030390>

Samsonowicz, M., Kalinowska, M. and Gryko, K. 2021. Enhanced antioxidant activity of ursolic acid by complexation with copper (II): Experimental and theoretical study. *Materials*. [Online]. **14**(2). Available from: <https://doi.org/10.3390/ma14020264>

Sanchez-Camargo, A.d.P., Gutierrez, L.-F., Vargas, S.M., Martinez-Correa, H.A., Parada-Alfonso, F. and Narvaez-Cuenca, C.-E. 2019. Valorisation of mango peel: Proximate composition, supercritical fluid extraction of carotenoids, and application as an antioxidant additive for an edible oil. *The Journal of Supercritical Fluids*. **152**, p104574. Available from: <https://doi.org/10.1016/j.supflu.2019.104574>

Sangsopha, W., Kanokmedhakul, K., Lekphrom, R. and Kanokmedhakul, S. 2018. Chemical constituents and biological activities from branches of *Colubrina asiatica*. *Natural Product Research*. **32**(10), pp.1176-1179. Available from: <https://doi.org/10.1080/14786419.2017.1320787>

Sangsopha, W., Lekphrom, R., Schevenels, F.T., Kanokmedhakul, K. and Kanokmedhakul, S. 2020. Two new bioactive triterpenoids from the roots of

*Colubrina asiatica*. *Natural Product Research*. **34**(4), pp.482-488. Available from: <https://doi.org/10.1080/14786419.2018.1489385>

Santoso, M., Naka, Y., Angkawidjaja, C., Yamaguchi, T., Matoba, T. and Takamura, H. 2010. Antioxidant and DNA damage prevention activities of the edible parts of *Gnetum gnemon* and their changes upon heat treatment. *Food Science and Technology Research*. **16**, pp.549-556. Available from: <https://doi.org/10.3136/fstr.16.549>

Sarker, S.D. and Nahar, L. 2012. An introduction to natural products isolation. In: Sarker, S.D. and Nahar, L. eds. *Natural Products Isolation Methods and Protocols*. [Online]. Third ed. Humana Press, pp.1-25. Available from: <https://doi.org/10.1007/978-1-61779-624-1>

Saxena, M. and Saxena, J. 2012. Evaluation of phytoconstituents of *Acorus calamus* by FTIR and UV-VIS spectroscopic analysis. *International Journal of Biological & Pharmaceutical Research*. **3**, pp.498-501.

Schaberg, A., Wroblowski, R. and Goertz, R. 2018. Comparative study of the thermal decomposition behaviour of different amino acids and peptides. *Journal of Physics: Conference Series*. **1107**(3), p032013. Available from: <https://doi.org/10.1088/1742-6596/1107/3/032013>

Schneider, T. and Sahl, H.-G. 2010. An oldie but a goodie – Cell wall biosynthesis as antibiotic target pathway. *International Journal of Medical Microbiology*. **300**(2), pp.161-169. Available from: <https://doi.org/10.1016/j.ijmm.2009.10.005>

Seidel, V. 2012. Initial and bulk extraction of natural products isolation. In: Sarker, S.D. and Nahar, L. eds. *Natural Products Isolation Methods and Protocols*. [Online]. Third ed. Humana Press, pp.27- 42. Available from: <https://doi.org/10.1007/978-1-61779-624-1>

Senturk Parreidt, T., Muller, K. and Schmid, M. 2018. Alginate-based edible films and coatings for food packaging applications. *Foods*. [Online]. **7**(10). Available from: <https://doi.org/10.3390/foods7100170>

Shahid, M., Fazry, S., Azfaralariff, A., Najm, A.A.K., Law, D. and Mackeen, M.M. 2023. Bioactive compound identification and in vitro evaluation of antidiabetic and cytotoxic potential of *Garcinia atroviridis* fruit extract. *Food Bioscience*. **51**, p102285. Available from: <https://doi.org/10.1016/j.fbio.2022.102285>

Shahid, M., Law, D., Azfaralariff, A., Mackeen, M.M., Chong, T.F. and Fazry, S. 2022. Phytochemicals and biological activities of *Garcinia atroviridis*: A critical review. *Toxics*. [Online]. **10**(11). Available from: <https://doi.org/10.3390/toxics10110656>

Shahrul. 2023. *Article 2: Biodiversity of flora in Malaysia*. [Online]. [Accessed 18 December 2024]. Available from: <https://globinmed.com/conservation/article-2-biodiversity-of-flora-in-malaysia/>

Shang, A., Luo, M., Gan, R.Y., Xu, X.Y., Xia, Y., Guo, H., Liu, Y. and Li, H.B. 2020. Effects of microwave-assisted extraction conditions on antioxidant

capacity of sweet tea (*Lithocarpus polystachyus* Rehd.). *Antioxidants (Basel)*. **9**(8). Available from: <https://doi.org/10.3390/antiox9080678>

Sharif, N., Fabra, M.J. and Lopez-Rubio, A. 2019. Nanostructures of zein for encapsulation of food ingredients. *Biopolymer Nanostructures for Food Encapsulation Purposes*. Elsevier, pp.217-245.

Sharifi-Rad, J., Sureda, A., Tenore, G.C., Daglia, M., Sharifi-Rad, M., Valussi, M., Tundis, R., Sharifi-Rad, M., Loizzo, M.R., Ademiluyi, A.O., Sharifi-Rad, R., Ayatollahi, S.A. and Iriti, M. 2017. Biological activities of essential oils: From plant chemoecology to traditional healing systems. *Molecules*. **22**(1). Available from: <https://doi.org/10.3390/molecules22010070>

Sharma, P. and Singh, R.P. 2013. Evaluation of antioxidant activity in foods with special reference to TEAC method. *American Journal of Food Technology*. **8**, p18. Available from: <https://doi.org/10.3923/ajft.2013.83.101>

Shen, L., Pang, S., Zhong, M., Sun, Y., Qayum, A., Liu, Y., Rashid, A., Xu, B., Liang, Q., Ma, H. and Ren, X. 2023. A comprehensive review of ultrasonic assisted extraction (UAE) for bioactive components: Principles, advantages, equipment, and combined technologies. *Ultrasonics Sonochemistry*. **101**, p106646. Available from: <https://doi.org/10.1016/j.ultsonch.2023.106646>

Shenoy, S.L., Bates, W.D., Frisch, H.L. and Wnek, G.E. 2005. Role of chain entanglements on fiber formation during electrospinning of polymer solutions: good solvent, non-specific polymer–polymer interaction limit. *Polymer*. **46**(10), pp.3372-3384. Available from: <https://doi.org/10.1016/j.polymer.2005.03.011>

Shi, T., Wu, G., Jin, Q. and Wang, X. 2025. <sup>1</sup>H NMR and chemical analysis to characterize camellia oil obtained by different extraction methods: A comparative study using chemometrics. *Journal of Food Composition and Analysis*. **137**, p106926. Available from: <https://doi.org/10.1016/j.jfca.2024.106926>

Shukla, R. and Cheryan, M. 2001. Zein: the industrial protein from corn. *Industrial Crops and Products*. **13**(3), p21. Available from: [https://doi.org/10.1016/S0926-6690\(00\)00064-9](https://doi.org/10.1016/S0926-6690(00)00064-9)

Shukri, M., Alan, C., Mat-Ali, M.S. and Crozier, A. 2011. Polyphenols and antioxidant activities of selected traditional vegetables. *Journal of Tropical Agriculture and Food Science*. **39**, pp.69-83.

Sikkema, J., De Bont, J.A.M. and Poolman, B. 1994. Interactions of cyclic hydrocarbons with biological membranes. *Journal of Biological Chemistry*. **269**(11), pp.8022-8028. Available from: [https://doi.org/10.1016/s0021-9258\(17\)37154-5](https://doi.org/10.1016/s0021-9258(17)37154-5)

Sikkema, J., De Bont, J.A.M. and Poolman, B. 1995. Mechanisms of membrane toxicity of hydrocarbons. *Microbiological Reviews*. **59**(2), pp.201-222. Available from: <https://doi.org/10.1128/membr.59.2.201-222.1995>

Simmonds, G., Woods, A.T. and Spence, C. 2018. ‘Show me the goods’: Assessing the effectiveness of transparent packaging vs. product imagery on

- product evaluation. *Food Quality and Preference*. **63**, pp.18-27. Available from: <https://doi.org/10.1016/j.foodqual.2017.07.015>
- Singh, S. and Shalini, R. 2016. Effect of hurdle technology in food preservation: A review. *Critical Reviews in Food Science and Nutrition*. **56**(4), pp.641–649. Available from: <https://doi.org/10.1080/10408398.2012.761594>
- Singleton, V.L., Orthofer, R. and Lamuela-Raventos, R.M. 1999. Analysis of total phenols and other oxidation substrates and antioxidants by means of Folin-Ciocalteu reagent. *Methods in Enzymology*. **299**, pp.152-178.
- Siracusa, V., Rocculi, P., Romani, S. and Rosa, M.D. 2008. Biodegradable polymers for food packaging: a review. *Trends in Food Science & Technology*. **19**(12), pp.634-643. Available from: <https://doi.org/10.1016/j.tifs.2008.07.003>
- Siripongvutikorn, S., Usawakesmanee, W., Pisuchpen, S., Khatcharin, N. and Rujirapong, C. 2023. Quality changes during storage in Thai indigenous leafy vegetable, Liang leaves (*Gnetum gnemon* var. *tenerum*) after different preparation methods. *Italian Journal of Food Science*. **35**(3), pp.1-16. Available from: <https://doi.org/10.15586/ijfs.v35i3.2346>
- Siswoyo, T.A., Mardiana, E., Lee, K.O. and Hoshokawa, K. 2011. Isolation and characterization of antioxidant protein fractions from melinjo (*Gnetum gnemon*) seeds. *J Agric Food Chem*. **59**(10), pp.5648-5656. Available from: <https://doi.org/10.1021/jf2000647>
- Sivasvaran, S.N., Kong, I., Hui ling, T. and Pui, L.P. 2021. Addition of glycerol and sodium chloride into *Garcinia atroviridis* chitosan film, and its application for wrapping of chicken meat. *Malaysian Journal of Analytical Sciences*. **25**, pp.399-414. Available from: [https://www.researchgate.net/publication/358307807\\_Addition\\_of\\_glycerol\\_and\\_sodium\\_chloride\\_into\\_garcinia\\_atroviridis\\_chitosan\\_film\\_and\\_its\\_application\\_for\\_wrapping\\_of\\_chicken\\_meat](https://www.researchgate.net/publication/358307807_Addition_of_glycerol_and_sodium_chloride_into_garcinia_atroviridis_chitosan_film_and_its_application_for_wrapping_of_chicken_meat)
- SKE-Research-Equipment. 2020. *E-Fiber EF100 Electrospinning system: User and safety manual*. [Online]. Available from: <https://www.ske.it/app/uploads/2021/07/E-Fiber-EF100-Electrospinning-system.pdf>
- Slavica, G., Radoslav, G. and Kovačić, K. 2010. Effects of modified atmosphere packaging on quality and safety of fresh meat. *Quality Of Life*. **1**, pp.121-133. Available from: <https://doi.org/10.7251/QOL1002121G>
- Sokhal, K.S., Dasoraju, G. and Bulasara, V.K. 2019. Effect of Reynolds number and concentration of biopolymer (Gum Arabic) on drag reduction of turbulent flow in circular pipe. In: *World Academy of Science, Engineering and Technology: International Scholarly and Scientific Research & Innovation*.
- Subbiah, T., Bhat, G.S., Tock, R.W., Parameswaran, S. and Ramkumar, S.S. 2005. Electrospinning of nanofibers. *Journal of Applied Polymer Science*. **96**(2), pp.557-569. Available from: <https://doi.org/10.1002/app.21481>
- Suhag, R., Kumar, N., Petkoska, A.T. and Upadhyay, A. 2020. Film formation and deposition methods of edible coating on food products: A review. *Food*

*Research International*. **136**, p109582. Available from:  
<https://doi.org/10.1016/j.foodres.2020.109582>

Suksanga, A., Siripongvutikorn, S., Leelawattana, R., Yupanqui, C.T. and Ildowu, A.O. 2023. Assessment of biological activities, acute and sub-chronic toxicity of Liang (*Gnetum gnemon* var. *tenerum*) leaves powder, a natural product. *Biological and Pharmaceutical Bulletin*. **46**(12), pp.1666-1675. Available from: <https://doi.org/10.1248/bpb.b23-00208>

Sumang, F.A., Ward, A., Errington, J. and Dashti, Y. 2024. Hibiscus acid and hydroxycitric acid dimethyl esters from Hibiscus flowers induce production of dithiolopyrrolone antibiotics by *Streptomyces* Strain MBN2-2. *Natural Products and Bioprospecting*. **14**(1), p40. Available from: <https://doi.org/10.1007/s13659-024-00460-0>

Sun, Y., Wei, Z. and Xue, C. 2023. Development of zein-based nutraceutical delivery systems: A systematic overview based on recent researches. *Food Hydrocolloids*. **137**, p108368. Available from:  
<https://doi.org/10.1016/j.foodhyd.2022.108368>

Sung, S.-Y., Sin, L.T., Tee, T.-T., Bee, S.-T., Rahmat, A.R., Rahman, W.A.W.A., Tan, A.-C. and Vikhraman, M. 2013. Antimicrobial agents for food packaging applications. *Trends in Food Science & Technology*. **33**(2), pp.110-123. Available from: <https://doi.org/10.1016/j.tifs.2013.08.001>

Tai, N.L., Adhikari, R., Shanks, R. and Adhikari, B. 2019. Aerobic biodegradation of starch–polyurethane flexible films under soil burial condition: Changes in physical structure and chemical composition. *International Biodeterioration & Biodegradation*. **145**, p104793. Available from:  
<https://doi.org/10.1016/j.ibiod.2019.104793>

Tan, T.Y.C., Lee, J.C., Mohd Yusof, N.A., Teh, B.P. and Syed Mohamed, A.F. 2020. Malaysian herbal monograph development and challenges. *Journal of Herbal Medicine*. **23**, p100380. Available from:  
<https://doi.org/10.1016/j.hermed.2020.100380>

Tan, W.-N., Khairuddean, M., Khaw, K.-Y., Murugaiyah, V., Yenn, T., Leong, C.R. and Ibrahim, D. 2019. Phytochemical screening and biological evaluations of *Garcinia atroviridis*. *Iranian Journal of Pharmaceutical Sciences*. **15**, pp.91-104.

Tan, W.-N., Khairuddean, M., Wong, K.-C., Khaw, K.-Y. and Vikneswaran, M. 2014. New cholinesterase inhibitors from *Garcinia atroviridis*. *Fitoterapia*. **97**, pp.261-267. Available from: <https://doi.org/10.1016/j.fitote.2014.06.003>

Tan, W.-N., Khairuddean, M., Wong, K.-C., Tong, W.Y. and Ibrahim, D. 2016. Antioxidant compounds from the stem bark of *Garcinia atroviridis*. *Journal of Asian Natural Products Research*. **18**(8), pp.804-811. Available from:  
<https://doi.org/10.1080/10286020.2016.1160071>

Tan, W.-N., Lim, J.-Q., Afiqah, F., Nik Mohamed Kamal, N.N.S., Abdul Aziz, F.A., Tong, W.-Y., Leong, C.-R. and Lim, J.-W. 2018. Chemical composition and cytotoxic activity of *Garcinia atroviridis* Griff. ex T. Anders. essential oils in

combination with tamoxifen. *Natural Product Research*. **32**(7), pp.854-858. Available from: <https://doi.org/10.1080/14786419.2017.1361951>

Tan, W.-N., Wong, K.-C., Khairuddean, M., Eldeen, I.M., Asmawi, M.Z. and Sulaiman, B. 2013. Volatile constituents of the fruit of *Garcinia atroviridis* and their antibacterial and anti-inflammatory activities. *Flavour and Fragrance Journal*. **28**(1), pp.2-9. Available from: <https://doi.org/10.1002/ffj.3118>

Tang, C. and Liu, H. 2008. Cellulose nanofiber reinforced poly(vinyl alcohol) composite film with high visible light transmittance. *Composites Part A: Applied Science and Manufacturing*. **39**(10), pp.1638-1643. Available from: <https://doi.org/10.1016/j.compositesa.2008.07.005>

Tang, Y., Liu, L., Han, J., Zhang, Z., Yang, S., Li, S., Fan, Z. and Zhao, H. 2021. Fabrication and characterization of multiple herbal extracts-loaded nanofibrous patches for topical treatment of acne vulgaris. *Fibers and Polymers*. **22**. Available from: <https://doi.org/10.1007/s12221-021-0156-1>

Tang, Z.-P., Chen, C.-W. and Xie, J. 2018. Development of antimicrobial active films based on poly(vinyl alcohol) containing nano-TiO<sub>2</sub> and its application in *macrobrachium rosenbergii* packaging. *Journal of Food Processing and Preservation*. **42**(8), pp.1-12. Available from: <https://doi.org/10.1111/jfpp.13702>

Taylor, S., Colonna, A., Jung, J., Gutierrez, J. and Zhao, Y. 2024. Consumer perception and acceptance of edible packaging for various food products. *Journal of Food Science*. **89**(4), pp.2423-2437. Available from: <https://doi.org/10.1111/1750-3841.16992>

Tennenhouse, E. 2017. *How to deal with solvent bumping and foaming during lab evaporation*. [Online]. [Accessed 6 February 2025]. Available from: <https://www.labmanager.com/how-to-deal-with-solvent-bumping-and-foaming-during-lab-evaporation-3219>

Teoh, E.S. 2015. Secondary metabolites of plants. *Medicinal Orchids of Asia*. pp.59-73. Available from: [https://doi.org/10.1007/978-3-319-24274-3\\_5](https://doi.org/10.1007/978-3-319-24274-3_5)

Thaikruea, L., Pataraarechachai, J., Savanpunyalert, P. and Naluponjiragul, U. 1995. An unusual outbreak of food poisoning. *The Southeast Asian Journal of Tropical Medicine and Public Health*. **26**(1), pp.78-85.

Thaipong, K., Boonprakob, U., Crosby, K., Cisneros-Zevallos, L. and Hawkins Byrne, D. 2006. Comparison of ABTS, DPPH, FRAP, and ORAC assays for estimating antioxidant activity from guava fruit extracts. *Journal of Food Composition and Analysis*. **19**(6), pp.669-675. Available from: <https://doi.org/10.1016/j.jfca.2006.01.003>

Thakali, A. and MacRae, J.D. 2021. A review of chemical and microbial contamination in food: What are the threats to a circular food system? *Environmental Research*. **194**, p110635. Available from: <https://doi.org/10.1016/j.envres.2020.110635>

The-Habitat. 2023. *10 Orchids for Every USDA Hardiness Zone*. [Online]. [Accessed 28 November 2024]. Available from: <https://thehabitat.com/home/succulent-101-faqs-for-beginners/>

- Thompson, R.C., Moore, C.J., Saal, F.S. and Swan, S.H. 2009. Plastics, the environment and human health: current consensus and future trends. *Philosophical Transactions of The Royal Society*. **364**, p13. Available from: <https://doi.org/10.1098/rstb.2009.0053>
- Thompson, T.J.U., Gauthier, M. and Islam, M. 2009. The application of a new method of Fourier transform infrared spectroscopy to the analysis of burned bone. *Journal of Archaeological Science*. **36**(3), pp.910-914. Available from: <https://doi.org/10.1016/j.jas.2008.11.013>
- Thongkham, E., Aiensaard, J. and Kaenjampa, P. 2021. Antioxidant and antimicrobial properties of ethanolic extract of asam gelugor fruit (*Garcinia atroviridis*). *Burapha Science Journal*. **26**(2), p14.
- Tiwari, B.K. 2015. Ultrasound: A clean, green extraction technology. *TrAC Trends in Analytical Chemistry*. **71**, pp.100-109. Available from: <https://doi.org/10.1016/j.trac.2015.04.013>
- Toor, R.K. and Savage, G.P. 2006. Effect of semi-drying on the antioxidant components of tomatoes. *Food Chemistry*. **94**(1), pp.90-97. Available from: <https://doi.org/10.1016/j.foodchem.2004.10.054>
- Torres-Giner, S. and Lagaron, J.M. 2010. Zein-based ultrathin fibers containing ceramic nanofillers obtained by electrospinning. I. Morphology and thermal properties. *Journal of Applied Polymer Science*. **118**(2), pp.778-789. Available from: <https://doi.org/10.1002/app.32180>
- Trisha, M.R., Deavyndra Gunawan, V., Wong, J.X., Pak Dek, M.S. and Rukayadi, Y. 2024. Antibacterial effect of ethanolic *Gnetum gnemon* L. leaf extract on food-borne pathogens and its application as a natural preservative on raw quail eggs. *Heliyon*. **10**(16), pe35691. Available from: <https://doi.org/10.1016/j.heliyon.2024.e35691>
- Unalan, I.U., Korel, F. and Yemenicioglu, A. 2011. Active packaging of ground beef patties by edible zein films incorporated with partially purified lysozyme and Na<sub>2</sub>EDTA. *International Journal of Food Science and Technology*. **46**(6), pp.1289-1295. Available from: <https://doi.org/10.1111/j.1365-2621.2011.02625.x>
- Ungchusak, K., Chunsuttiwat, S., Braden, C., Aldis, W., Ueno, K., Olsen, S. and Wiboolpolprasert, S. 2007. The need for global planned mobilization of essential medicine: lessons from a massive Thai botulism outbreak. *Bulletin of the World Health Organization*. **85**(3), pp.238-240. Available from: <https://doi.org/10.2471/blt.06.039545>
- Universiteit-Leiden. 2024. *Erythroxylum coca*. [Online]. [Accessed 28 November 2024]. Available from: <https://hortusleiden.gardenexplorer.org/taxon-7441.aspx>
- USDA-NRCS. 2024a. *Colubrina asiatica* (L.) Brongn. [Online]. [Accessed 18 December 2024]. Available from: <https://plants.usda.gov/plant-profile/COAS3>
- USDA-NRCS. 2024b. *Gnetum gnemon* L. [Online]. [Accessed 18 December 2024]. Available from: <https://plants.usda.gov/plant-profile/GNGN>

USDA-FSIS. 2024. *Keep food safe! Food safety basics*. [Online]. [Accessed 18 April 2025]. Available from: <https://www.fsis.usda.gov/food-safety/safe-food-handling-and-preparation/food-safety-basics/steps-keep-food-safe#:~:text=Check%20the%20temperature%20of%20your,within%203%20to%205%20days>.

Vaara, M. 1992. Agents that increase the permeability of the outer membrane. *Microbiological Reviews*. **56**(3), pp.395-411. Available from: <https://doi.org/10.1128/mr.56.3.395-411.1992>

Valizadeh, R., Zandi, M., Ganjloo, A. and Dardmeh, N. 2024. Bioactive multilayer film based on the sage seed gum-gelatin, TiO<sub>2</sub> and electrospun zein fibers encapsulating pomegranate peel extract. *International Journal of Biological Macromolecules*. **283**, p137826. Available from: <https://doi.org/https://doi.org/10.1016/j.ijbiomac.2024.137826>

Vardanyan, R. and Hruby, V. 2016. Chapter 12 - Adrenoblockers. In: Vardanyan, R. and Hruby, V. eds. *Synthesis of best-seller drugs*. [Online]. UK: Elsevier, 2016, pp.201-214. [Accessed 25 February 2026]. Available from: <https://doi.org/10.1016/B978-0-12-411492-0.00012-2>

van Duin, M., Machado, A.V. and Covas, J. 2001. A look inside the extruder: evolution of chemistry, morphology and rheology along the extruder axis during reactive processing and blending. *Macromolecular Symposia*. **170**(1), pp.29-40. Available from: [https://doi.org/10.1002/1521-3900\(200106\)170:1<29::AID-MASY29>3.0.CO;2-4](https://doi.org/10.1002/1521-3900(200106)170:1<29::AID-MASY29>3.0.CO;2-4)

Varol, E.A. and Mutlu, U. 2023. TGA-FTIR analysis of biomass samples based on the thermal decomposition behavior of hemicellulose, cellulose, and lignin. *Energies*. [Online]. **16**(9). Available from: <https://doi.org/10.3390/en16093674>

Verbeke, W., De Smet, S., Vackier, I., Van Oeckel, M.J., Warnants, N. and Van Kenhove, P. 2005. Role of intrinsic search cues in the formation of consumer preferences and choice for pork chops. *Meat Science*. **69**(2), pp.343-354. Available from: <https://doi.org/10.1016/j.meatsci.2004.08.005>

Vermeiren, L., Devlieghere, F., van Beest, M., de Kruijf, N. and Debevere, J. 1999. Developments in the active packaging of foods. *Trends in Food Science & Technology*. **10**(3), pp.77-86. Available from: [https://doi.org/10.1016/S0924-2244\(99\)00032-1](https://doi.org/10.1016/S0924-2244(99)00032-1)

Villareal, M. 2024. *Lemon*. Available from: <https://freepngimg.com/png/37353-lemon-hd>

Viscarra Rossel, R.A., Minasny, B., Roudier, P. and McBratney, A.B. 2006. Colour space models for soil science. *Geoderma*. **133**(3), pp.320-337. Available from: <https://doi.org/10.1016/j.geoderma.2005.07.017>

Vogt, L., Liverani, L., Roether, J.A. and Boccaccini, A.R. 2018. Electrospun zein fibers incorporating poly(glycerol sebacate) for soft tissue engineering. *Nanomaterials*. [Online]. **8**(3). Available from: <https://doi.org/10.3390/nano8030150>

- Walker, G.M. and White, N.A. 2005. Introduction to Fungal Physiology. *Fungi*. pp.1-34.
- Walsh, C. 2003. Where will new antibiotics come from? *Nature Reviews Microbiology*. **1**(1), pp.65-70. Available from: <https://doi.org/10.1038/nrmicro727>
- Wang, H., Hao, L., Wang, P., Chen, M., Jiang, S. and Jiang, S. 2017. Release kinetics and antibacterial activity of curcumin loaded zein fibers. *Food Hydrocolloids*. **63**, pp.437-446. Available from: <https://doi.org/10.1016/j.foodhyd.2016.09.028>
- Wang, Q., Chen, W., Zhu, W., McClements, D.J., Liu, X. and Liu, F. 2022. A review of multilayer and composite films and coatings for active biodegradable packaging. *npj Science of Food*. **6**(1), p18. Available from: <https://doi.org/10.1038/s41538-022-00132-8>
- Wang, X., Xue, J., Wang, Y., Zhu, H., Chen, S., Xiao, Z. and Luo, Y. 2024. Development and characterization of zein/gum Arabic nanocomposites incorporated edible films for improving strawberry preservation. *Advanced Composites and Hybrid Materials*. **7**(6), p249. Available from: <https://doi.org/10.1007/s42114-024-01051-w>
- Warriss, P.D. and Rhodes, D.N. 1977. Haemoglobin concentrations in beef. *Journal of the Science of Food and Agriculture*. **28**(10), pp.931-934. Available from: <https://doi.org/10.1002/jsfa.2740281012>
- Wazir, D., Ahmad, S., Muse, R., Mahmood, M. and Shukor, M.Y. 2011. Antioxidant activities of different parts of *Gnetum gnemon* L. *Journal of Plant Biochemistry and Biotechnology*. **20**(2), pp.234-240. Available from: <https://doi.org/10.1007/s13562-011-0051-8>
- Wei, B., Zhao, Y., Wei, Y., Yao, J., Chen, X. and Shao, Z. 2019. Morphology and properties of a new biodegradable material prepared from zein and poly(butylene adipate-terephthalate) by reactive blending. *ACS Omega*. **4**(3), pp.5609-5616. Available from: <https://doi.org/10.1021/acsomega.9b00210>
- Wen, C., Zhang, J., Zhang, H., Dzah, C.S., Zandile, M., Duan, Y., Ma, H. and Luo, X. 2018. Advances in ultrasound assisted extraction of bioactive compounds from cash crops – A review. *Ultrasonics Sonochemistry*. **48**, pp.538-549. Available from: <https://doi.org/10.1016/j.ultsonch.2018.07.018>
- Wessner, D., Dupont, C., Charles, T. and Neufeld, J. 2020. *Microbiology*. Third ed. United States: Wiley.
- WHO. 2024a. *E. coli*. [Online]. [Accessed 6 December 2024]. Available from: <https://www.who.int/news-room/fact-sheets/detail/e-coli>
- WHO. 2024b. *Food safety*. [Online]. Available from: <https://www.who.int/news-room/fact-sheets/detail/food-safety>
- WHO. 2024c. *Foodborne diseases*. [Online]. [Accessed 4 December 2024]. Available from: [https://www.who.int/health-topics/foodborne-diseases#tab=tab\\_1](https://www.who.int/health-topics/foodborne-diseases#tab=tab_1)

WHO. 2024d. *Listeriosis*. [Online]. [Accessed 6 December 2024]. Available from: <https://www.who.int/news-room/fact-sheets/detail/listeriosis>

Williams, P. 2007. Nutritional composition of red meat. *Nutrition and Dietetics*. **64**(SUPPL. 4), pp.S113-S119. Available from: <https://doi.org/10.1111/j.1747-0080.2007.00197.x>

Wilson, C.M. 1991. Multiple zeins from maize endosperms characterized by reversed-phase high performance liquid chromatography. *Plant Physiology*. **95**(3), pp.777-786. Available from: <https://doi.org/10.1104/pp.95.3.777>

Wojtunik-Kulesza, K.A., Ciesla, L.M. and Waksmundzka-Hajnos, M. 2018. Approach to determination a structure – Antioxidant activity relationship of selected common terpenoids evaluated by ABTS•+ radical cation assay. *Natural Product Communications*. **13**(3), p1934578X1801300308. Available from: <https://doi.org/10.1177/1934578X1801300308>

Wong, C.-C., Li, H.-B., Cheng, K.-W. and Chen, F. 2006. A systematic survey of antioxidant activity of 30 Chinese medicinal plants using the ferric reducing antioxidant power assay. *Food Chemistry*. **97**(4), pp.705-711. Available from: <https://doi.org/10.1016/j.foodchem.2005.05.049>

Woo, Y.-M., Hu, D.W.-N., Larkins, B.A. and Jung, R. 2001. Genomics analysis of genes expressed in maize endosperm identifies novel seed proteins and clarifies patterns of zein gene expression. *The Plant Cell*. **13**(10), pp.2297-2317. Available from: <https://doi.org/10.2307/3871509>

Wu, X., Liu, Z., He, S., Liu, J. and Shao, W. 2023. Development of an edible food packaging gelatin/zein based nanofiber film for the shelf-life extension of strawberries. *Food Chemistry*. **426**, p136652. Available from: <https://doi.org/10.1016/j.foodchem.2023.136652>

Wu, Y., Du, J., Zhang, J., Li, Y. and Gao, Z. 2023. pH Effect on the structure, rheology, and electrospinning of maize zein. *Foods*. [Online]. **12**(7). Available from: <https://doi.org/10.3390/foods12071395>

Yang, L. and Paulson, A.T. 2000. Mechanical and water vapour barrier properties of edible gellan films. *Food Research International*. **33**(7), pp.563-570. Available from: [https://doi.org/10.1016/S0963-9969\(00\)00092-2](https://doi.org/10.1016/S0963-9969(00)00092-2)

Yang, Y., Zheng, S., Liu, Q., Kong, B. and Wang, H. 2020. Fabrication and characterization of cinnamaldehyde loaded polysaccharide composite nanofiber film as potential antimicrobial packaging material. *Food Packaging and Shelf Life*. **26**, p100600. Available from: <https://doi.org/10.1016/j.fpsl.2020.100600>

Yao, Z.C., Chang, M.W., Ahmad, Z. and Li, J.S. 2016. Encapsulation of rose hip seed oil into fibrous zein films for ambient and on demand food preservation via coaxial electrospinning. *Journal of Food Engineering*. **191**, pp.115-123. Available from: <https://doi.org/10.1016/j.jfoodeng.2016.07.012>

Zafar, U., Houlden, A. and Robson Geoffrey, D. 2013. Fungal communities associated with the biodegradation of polyester polyurethane buried under compost at different temperatures. *Applied and Environmental Microbiology*. **79**(23), pp.7313-7324. Available from: <https://doi.org/10.1128/AEM.02536-13>

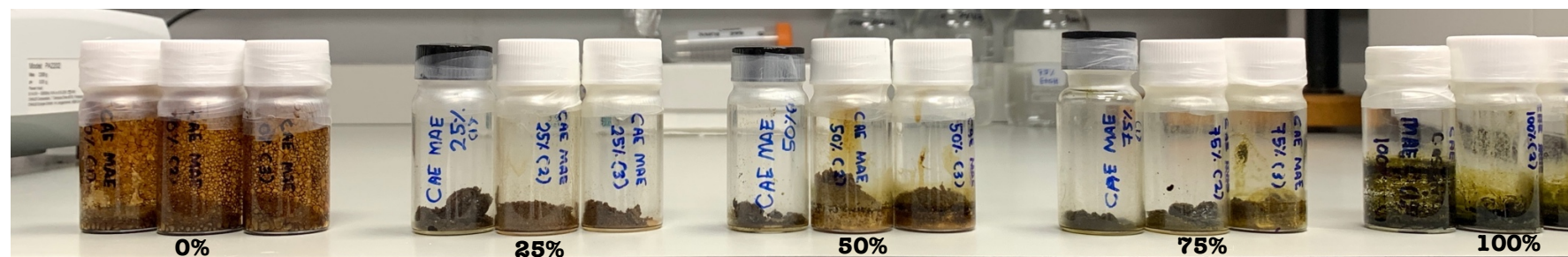
- Zainin, N.S., Lau, K.Y., Zakaria, M., Son, R., Abdull-Razis, A.F. and Rukayadi, Y. 2013. Antibacterial activity of *Boesenbergia rotunda* (L.) Mansf. A. extract against *Escherichia coli*. *International Food Research Journal*. **20**(6), p4. Available from: <https://www.cabidigitallibrary.org/doi/pdf/10.5555/20143047548>
- Zaman, N.B.K., Lin, N.K. and Phing, P.L. 2018. Chitosan film incorporated with *Garcinia atroviridis* for the packaging of Indian mackerel (*Rastrelliger kanagurta*). *Ciencia e Agrotecnologia*. **42**, pp.666-675. Available from: <https://doi.org/10.1590/1413-70542018426019918>
- Zhang, J., Onakpoya, I.J., Posadzki, P. and Eddouks, M. 2015. The safety of herbal medicine: from prejudice to evidence. *Evidence-Based Complementary and Alternative Medicine*. **2015**, p316706. Available from: <https://doi.org/10.1155/2015/316706>
- Zhang, X., Dong, C., Hu, Y., Gao, M. and Luan, G. 2021. Zein as a structural protein in gluten-free systems: an overview. *Food Science and Human Wellness*. **10**(3), pp.270-277. Available from: <https://doi.org/10.1016/j.fshw.2021.02.018>
- Zhang, X., Li, Z., Yang, P., Duan, G., Liu, X., Gu, Z. and Li, Y. 2021. Polyphenol scaffolds in tissue engineering. *Materials Horizons*. **8**(1), pp.145-167. Available from: <https://doi.org/10.1039/D0MH01317J>
- Zhang, Y.-J., Guo, J.-L., Xue, J.-c., Bai, C.-L. and Guo, Y. 2021. Phthalate metabolites: Characterization, toxicities, global distribution, and exposure assessment. *Environmental Pollution*. **291**, p.118106. Available from: <https://doi.org/10.1016/j.envpol.2021.118106>
- Zhao, X., Chen, F., Xue, W. and Lee, L. 2008. FTIR spectra studies on the secondary structures of 7S and 11S globulins from soybean proteins using AOT reverse micellar extraction. *Food Hydrocolloids*. **22**(4), pp.568-575. Available from: <https://doi.org/10.1016/j.foodhyd.2007.01.019>
- Zheng, X.-Q., Liu, X.-L., Yu, S.-F., Wang, X.-J., Ma, Y.-Q., Yang, S. and Jing, S.-S. 2014. Effects of extrusion and starch removal pretreatment on zein proteins extracted from corn gluten meal. *Cereal Chemistry*. **91**(5), pp.496-501. Available from: <https://doi.org/10.1094/CCHEM-07-13-0141-R>
- Zong, X., Kim, K., Fang, D., Ran, S., Hsiao, B.S. and Chu, B. 2002. Structure and process relationship of electrospun bioabsorbable nanofiber membranes. *Polymer*. **43**(16), pp.4403-4412. Available from: [https://doi.org/10.1016/S0032-3861\(02\)00275-6](https://doi.org/10.1016/S0032-3861(02)00275-6)
- Zulkifli, N., Muhamad, M., Mohamad Zain, N.N., Wen Nee, T., Yahaya, N., Bustami, Y., Abdul Aziz, A. and Nik Mohamed Kamal, N.N.S. 2020. A bottom-up synthesis approach to silver nanoparticles induces anti-proliferative and apoptotic activities against MCF-7, MCF-7/TAMR-1 and MCF-10A human breast cell lines. *Molecules*. **25**. Available from: <https://doi.org/10.3390/molecules25184332>

## Appendix A Supplementary Materials

### Supplementary Materials 1(a) Morphology of plant extract: CAE.

Plant extract	Ethanol ratio	Morphological of solvent extraction extracts	Morphological of MAE extracts
CAE	0%	Dark brown, coarse powder	Dark brown, coarse powder
	25%	Dark brown, coarse powder	Dark brown, coarse powder with coagulates (R1, R2), Dark brown, mixed coarse and fine powder with small coagulates (R3)
	50%	Dark brown, coarse powder with small coagulates	Dark brown, sticky coagulate (R1), Dark brown, coarse powder (R2, R3)
	75%	Dark green, coarse powder with small coagulates	Dark green, small coagulates (R1), Dark green, coarse powder with small coagulates (R2, R3)
	100%	Dark green, sticky coagulate	Dark green, sticky coagulate

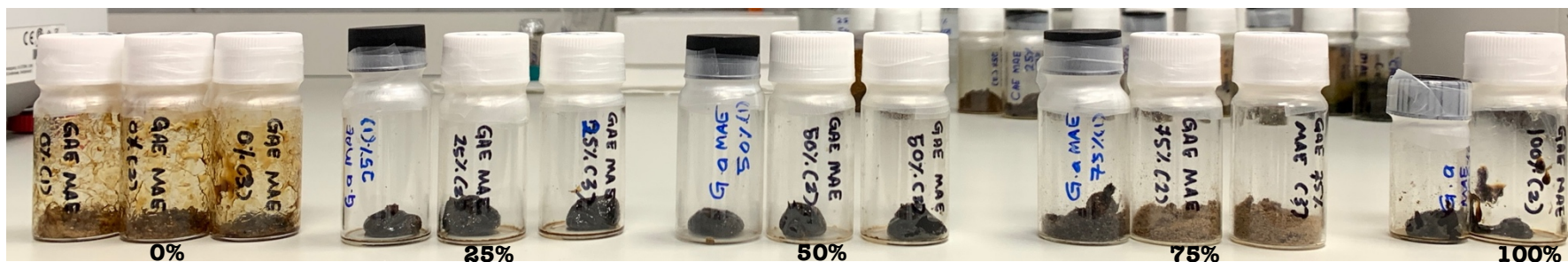
\*R1: replicate 1, R2: replicate 2, R3: replicate 3



**Supplementary Materials 1(b) Morphology of plant extract: GATE.**

Plant extract	Ethanol ratio	Morphological of solvent extraction extracts	Morphological of MAE extracts
GATE	0%	Light brown, sticky coagulate	Light brown, sticky coagulate (R1), Dark brown, small sticky coagulates (R2, R3)
	25%	Dark brown, sticky coagulate (R1, R2), Dark brown, sticky coarse powder with small coagulates (R3)	Dark brown, sticky coagulate
	50%	Dark brown, sticky coagulate	Dark brown, sticky coagulate
	75%	Mixed dark and light brown, sticky coarse powders	Mixed dark and light brown, sticky coarse powders
	100%	Dark brown, sticky coagulate	Dark brown, sticky coagulate

\*R1: replicate 1, R2: replicate 2, R3: replicate 3



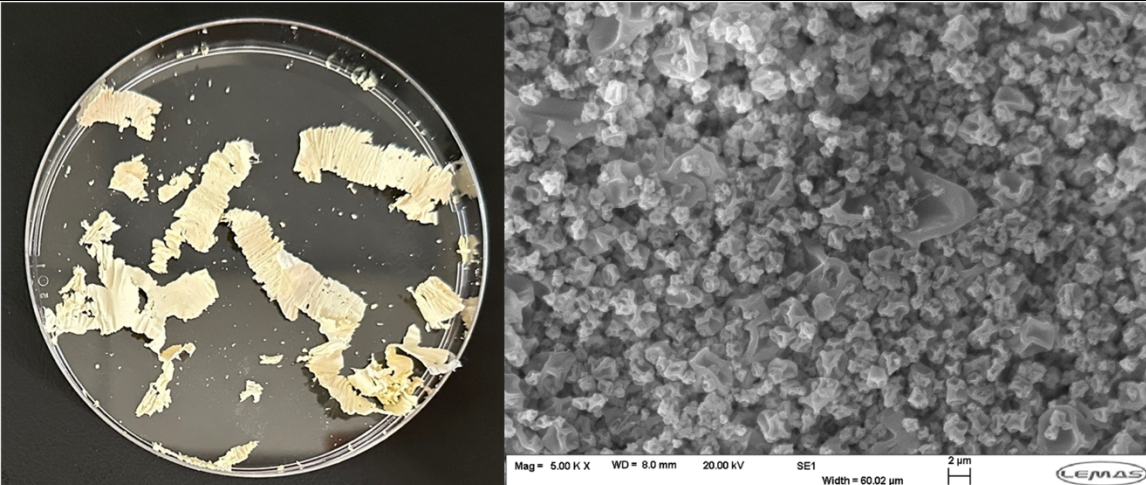
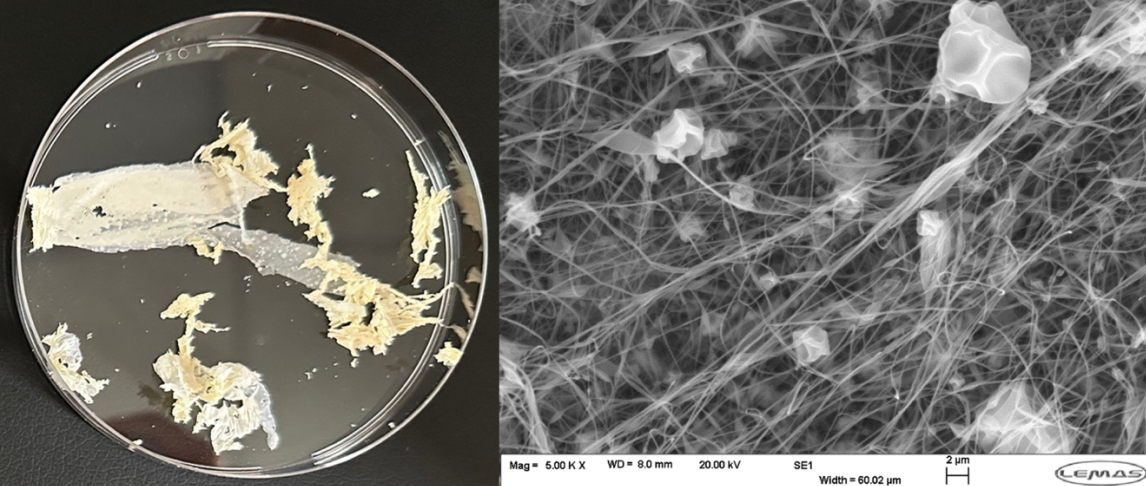
**Supplementary Materials 1(c) Morphology of plant extract: GGE.**

Plant extract	Ethanol ratio	Morphological of solvent extraction extracts	Morphological of MAE extracts
GGE	0%	Dark brown, sticky coagulate	Light brown, fine powder
	25%	Dark brown, coarse powder (R1, R2), Dark brown, big coagulate (R3)	Dark brown, coarse powder
	50%	Dark brown, sticky coagulate (R1), Dark brown, coarse powder (R2), Dark brown, coarse powder with small coagulates (R3)	Dark brown with sticky big coagulate (R1), Dark brown, coarse powder (R2, R3)
	75%	Dark green, coarse powder	Dark green, fine powder
	100%	Dark green, sticky coagulate	Dark green, sticky coagulates

\*R1: replicate 1, R2: replicate 2, R3: replicate 3



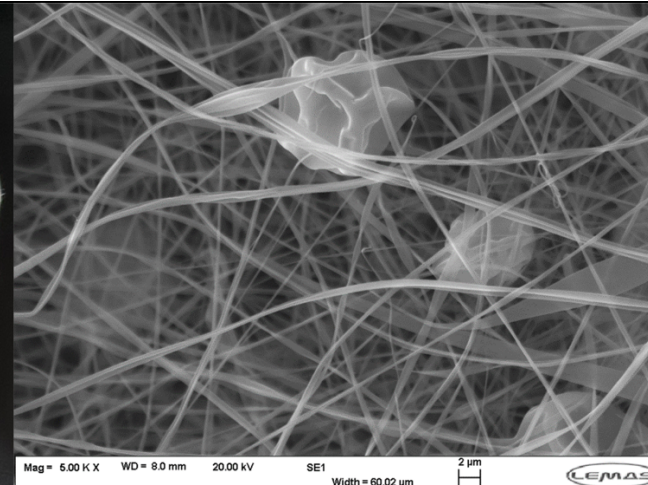
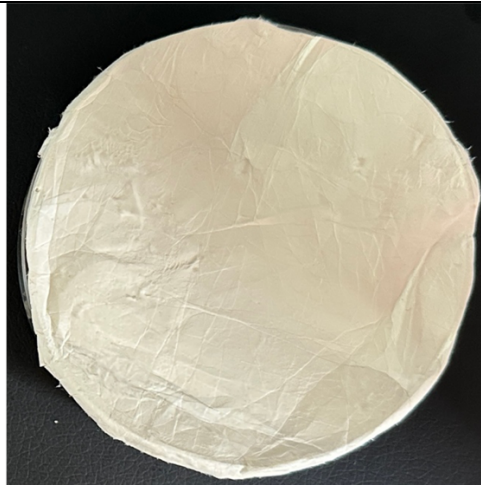
**Supplementary Materials 2 Morphology of zein-based films from 16% to 30% zein concentration.**

Zein solution concentration (%)	Viscosity (Pa.s)	Film morphology (visual and SEM)
16	0.01924-0.04675	
20	0.03539-0.2919	

Supplementary Materials 2 continued

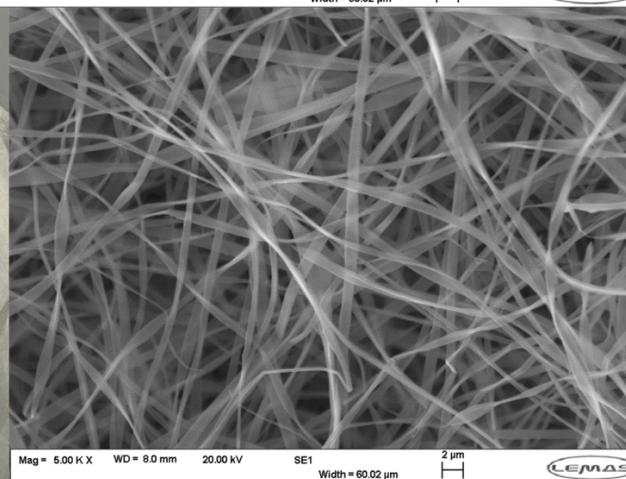
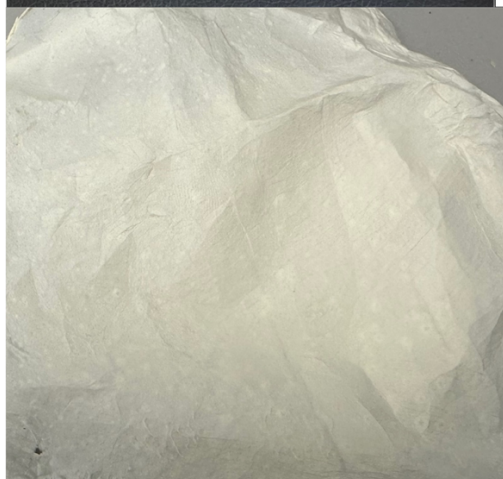
25

0.0420-  
0.1598



30

0.1605-  
0.2586



**Supplementary Materials 3 Calibration curves of the plant extracts, used for the determination of encapsulation efficiency in Section 4.3.5.**

